

ISSN 2313–5891 (Online)

ISSN 2304–974X (Print)

Ukrainian Food Journal

***Volume 13, Issue 2
2024***

Kyiv

2024

Київ

Ukrainian Food Journal is an international scientific journal that publishes articles of the specialists in the fields of food science, engineering and technology, chemistry, economics and management.

Ukrainian Food Journal – міжнародне наукове періодичне видання для публікації результатів досліджень фахівців у галузі харчової науки, техніки та технології, хімії, економіки і управління.

Ukrainian Food Journal is abstracted and indexed by scientometric databases:

Ukrainian Food Journal індексується наукометричними базами:

Index Copernicus (2012)
EBSCO (2013)
Google Scholar (2013)
UlrichsWeb (2013)
CABI full text (2014)
Online Library of University of Southern Denmark (2014)
Directory of Open Access scholarly Resources (ROAD) (2014)
European Reference Index for the Humanities and the Social Sciences (ERIH PLUS) (2014)
Directory of Open Access Journals (DOAJ) (2015)
InfoBase Index (2015)
Chemical Abstracts Service Source Index (CASSI) (2016)
FSTA (Food Science and Technology Abstracts) (2018)
Web of Science (Emerging Sources Citation Index) (2018)
Scopus (2022)

Ukrainian Food Journal включено у перелік наукових фахових видань України з технічних наук, категорія А (Наказ Міністерства освіти і науки України № 358 від 15.03.2019)

Editorial office address:

National University
of Food Technologies
68 Volodymyrska str.
Kyiv 01601, **Ukraine**

Адреса редакції:

Національний університет
харчових технологій
вул. Володимирська, 68
Київ 01601, **Україна**

e-mail: ufj_nuft@meta.ua

Ukrainian Food Journal is an open access journal published by the National University of Food Technologies, Kyiv, Ukraine. The Journal publishes original research articles, short communications, review papers, news, and literature reviews covering all areas of food science, technology, engineering, nutrition, food chemistry, economics, and management.

Studies must be new, have a clear link to food science, and be of general interest to the international scientific community.

Topics covered by the journal include:

- Food engineering
- Food chemistry
- Food microbiology
- Food quality and safety
- Food processes
- Automation of food processes
- Food packaging
- Economics
- Food nanotechnologies
- Economics and management

Please note that the Journal does not consider:

1. Articles with medical claims (this topic is not covered in the Journal); articles in which the subject of the study is humans and animals.
2. Articles that do not have scientific value (solutions of typical practical and engineering problems).

Periodicity of the Journal

4 issues per year (March, June, September, and December).

Reviewing a Manuscript for Publication

The editor-in-chief checks the content of a newly received article to ensure it complies with the journal's profile, approves the design, style, and illustrative material of the article, may make suggestions for their improvement and makes a decision on sending it for review.

Articles submitted for publication in the Ukrainian Food Journal undergo double-blind peer review by at least two scientists appointed by the editorial board: one member of the editorial board and one external to the editorial board and/or publisher.

The full guide for authors can be found on our website:

<http://ufj.nuft.edu.ua>

International Editorial Board

Editor-in-Chief:

Olena Stabnikova, Dr., *National University of Food Technologies, Ukraine*

Members of Editorial Board:

Agota Giedrė Raišienė, PhD, *Lithuanian Institute of Agrarian Economics, Lithuania*

Báo Thy Vương, PhD, *Mekong University, Vietnam*

Cristina Luisa Miranda Silva, PhD, Assoc. Prof., *Portuguese Catholic University – College of Biotechnology, Portugal*

Cristina Popovici, PhD, Assoc. Prof., *Technical University of Moldova*

Dora Marinova, PhD, Prof., *Curtin University Sustainability Policy (CUSP) Institute, Curtin University, Australia*

Egon Schnitzler, PhD, Prof., *State University of Ponta Grossa, Ponta Grossa, Brazil*

Eirin Marie Skjøndal Bar, PhD, Assoc. Prof., *Norwegian University of Science and Technology, Trondheim, Norway*

Godwin D. Ndossi, PhD, Prof., *Hubert Kairuki Memorial University, Dar es Salaam, Tanzania*

Jasmina Lukinac, PhD, Assoc. Prof., *University of Osijek, Croatia*

Kirsten Brandt, PhD, *Newcastle University, United Kingdom*

Lelieveld Huub, PhD, *Global Harmonization Initiative Association, The Netherlands*

Mark Shamtsian, PhD, Assoc. Prof., *Black Sea Association of Food Science and Technology, Romania*

María S. Tapia, PhD, Prof., *Central University of Venezuela, Caracas, Venezuela; COR MEM of the Academy of Physical, Mathematical and Natural Sciences of Venezuela*

Moisés Burachik, PhD, *Institute of Agricultural Biotechnology of Rosario (INDEAR), Bioceres Group, Rosario, Argentina*

Noor Zafira Noor Hasnan, PhD, *Universiti Putra Malaysia, Selangor, Malaysia*

Octavio Paredes-López, PhD, Prof., *The Center for Research and Advanced Studies of the National Polytechnic Institute, Guanajuato, Mexico.*

Rana Mustafa, PhD, *Global Institute for Food Security, University of Saskatchewan, Canada*

Semih Otles, PhD, Prof., *Ege University, Turkey*

Sheila Kilonzi, PhD, *Karatina University, Kenya*

Sonia Amariei, PhD, Prof., *University "Ștefan cel Mare" of Suceava, Romania*

Stanka Damianova, PhD, Prof., *Ruse University "Angel Kanchev", branch Razgrad, Bulgaria*

Stefan Stefanov, PhD, Prof., *University of Food Technologies, Bulgaria*

Tetiana Pirog, PhD, Prof., *National University of Food Technologies, Ukraine*

Oleksandr Shevchenko, PhD, Prof., *National University for Food Technologies, Ukraine*

Viktor Stabnikov, PhD, Prof., *National University for Food Technologies, Ukraine*

Umezuruike Linus Opara, PhD, Prof., *Stellenbosch University, Cape Town, South Africa*

Yordanka Stefanova, PhD, Assist. Prof., *University of Plovdiv "Paisii Hilendarski", Bulgaria*

Yuliya Dzyazko, PhD, Prof., *Institute of General and Inorganic Chemistry of the National Academy of Sciences of Ukraine*

Yun-Hwa Peggy Hsieh, PhD, Prof. Emerita, *Florida State University, USA*

Yurii Bilan, PhD, Prof., *Tomas Bata University in Zlin, Czech Republic*

Managing Editor:

Oleksii Gubenia, PhD, Assoc. Prof., *National University of Food Technologies, Ukraine*

Contents

Food Technology	231
<i>Bruna Mainardes, Larissa Moreira Mikota, Camila Delinski Bet, Marina Tolentino Marinho, Radla Zabian Bassetto Bisinella, Stéphanie Schiavo Romko, Egon Schnitzler</i> Extraction and physical modification of Mango palmer kernel starch and its application in cookies.....	231
<i>Viktor Grek, Tetiana Pshenychna, Olena Onopriichuk, Olena Grek</i> Milk protein clots obtained by the addition of purple corn powder	247
<i>Dimitar Dimitrov, Tatyana Yoncheva</i> Volatile composition and aromatic descriptors of red wines from different regions of Bulgaria aged with oak chips.....	262
<i>Anastasiia Shevchenko, Eva Ivanišová, Eva Kováčiková, Lucia Benešová, Larysa Mykhonik</i> Effect of complex plant supplement on shelf life of wheat bread.....	274
<i>Oxana Radu, Eugenia Covaliov, Tatiana Capcanari</i> Technological properties and functional food potential of oilseed cakes.....	287
<i>Galyna Khomych, Tetiana Lebedenko, Galina Krusir</i> Use of chokeberry in the preparation of bakery products.....	303
Biotechnology, Microbiology	316
<i>Nataliia Borzova</i> Thermal stable α -galactosidase from <i>Penicillium restrictum</i> for biodegradation of galactooligosaccharides.....	316
<i>Viktor Stabnikov, Viktor Udymovych, Iryna Kovshar, Dmytro Stabnikov</i> Microbial producer of acid urease for its application in biocementation.....	331
Processes and Equipment	351
<i>Valentyn Petrenko, Viktor Ardashev, Dmytro Maksymenko, Oleksiy Pustovoit</i> Modeling of heat transfer processes by periodic perturbation of freely flowing liquid film flowing along vertical surface with large-amplitude waves.....	351

<i>Viktor Sidletsnyi, Oleksandr Kukhar</i> Change of crystallization process attributes in a vacuum pan of automation systems.....	366
Economics and Management	385
<i>Nataliya Skopenko, Iryna Fedulova, Tetiana Mostenska, Iryna Severyna, Larysa Kapinus</i> Risk assessment in target market selection by bread baking enterprises.....	385
Instructions for authors	406

Extraction and physical modification of Mango palmer kernel starch and its application in cookies

Bruna Mainardes, Larissa Moreira Mikota, Camila Delinski Bet, Marina Tolentino Marinho, Radla Zabian Bassetto Bisinella, Stéphanie Schiavo Romko, Egon Schnitzler

State University of Ponta Grossa – UEPG, Ponta Grossa, PR – Brazil

Abstract

Keywords:

Mango kernels
Starch
Ultrasound
Thermal
analysis

Introduction. The aim of this study was to extract, analyze and apply mango kernel starch (*Mangifera indica* L.) in cookies production.

Materials and methods. The starchy material was extracted using an aqueous medium, without chemical treatment, and cookies were produced with different amounts of modified mango seed starch. Determination of proteins, lipids, ash, and moisture was done according to AOAC standards. Thermogravimetry was performed to evaluate mass loss with heating, using TA-50 equipment. Thermal transitions and the gelatinization enthalpy of the starches were assessed using Differential Scanning Calorimetry. Scanning Electron Microscopy applied to observe the morphology of starch granules before and after modification.

Results and discussion The results of this study showed that the starch extracted from the seed kernel of Palmer mango exhibits distinct physico-chemical characteristics, with a higher content of carbohydrates and lipids compared to other starches, such as mango endocarp starch. Thermal analyses, including thermogravimetry and differential scanning calorimetry, indicated that the modified starch had greater thermal stability and higher gelatinization enthalpy, particularly in the 100% modified starch.

Scanning electron microscopy revealed differences in the morphology of the starch granules, with the modified starches showing significant changes compared to native starch, such as alterations in the shape and size of the granules. Colorimetric analysis showed that the modifications to the starch resulted in significant changes in color parameters, especially in luminosity (L^*), where the modified starches exhibited a lighter color than the native starch.

These results indicate that the modifications made to Palmer mango starch lead to improvements in thermal and morphological properties, making it a potentially useful material for industrial applications.

Conclusions. The modifications made to the starch from Palmer mango seed significantly improved its thermal and morphological properties, highlighting its potential for diverse industrial applications.

Article history:

Received
18.02.2024
Received in
revised form
11.05.2024
Accepted
2.07.2024

Corresponding author:

Egon Schnitzler
E-mail:
egons@uepg.br

DOI:

10.24263/2304-
974X-2024-13-2-
3

Introduction

Interest in new materials derived from renewable sources, with low market value and low environmental impact, has grown significantly (Stabnikova et al., 2021). Starch is one of the raw materials with high potential for application in various fields, such as the food industry (Demiate et al., 2011; O'Leary et al., 2010), the oil industry (Cescon et al., 2018; Jing et al., 2019), the textile industry, the cosmetics industry, and the pharmaceutical industry (Guo et al., 2018). The identification of alternative sources of starch, such as the kernel of the mango, can also help to obtain new properties or contribute to the replacement of conventional sources (Garcia et al., 2020).

The *Mangifera indica* L. plant, better known as mango, is native to the forests of South and Southeast Asia, specifically India. Approximately 40 to 60% of waste is generated during mango processing, of which 12 to 15% corresponds to the peels and 15 to 20% to the seeds. It is estimated that 60% of the seed mass consists of starch (Kringel et al., 2020). Thus, mango kernels can be considered a non-traditional source of starch. The starch extracted from mango kernels is a potential food ingredient, and the process of its utilization itself makes it possible to turn waste into a valuable food product (Chowhan et al., 2020; Naqash et al., 2017; Pappen et al., 2020; Sousa et al., 2021a).

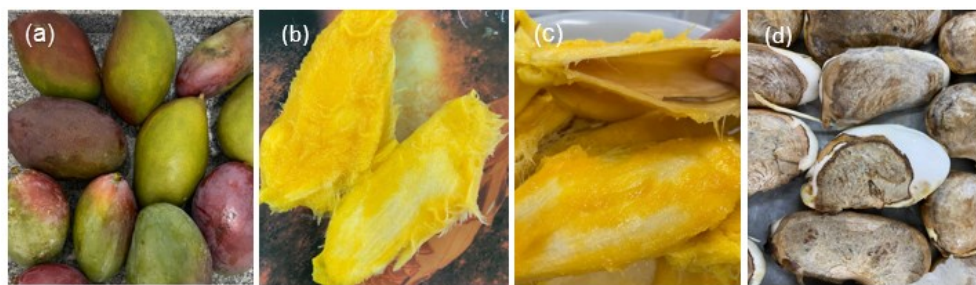


Figure 1. Morphology of the mango kernel:
a, whole mango, b and c, open core, and d, kernel

Given the ongoing challenge of developing gluten-free products, which remains a significant hurdle for the food industry (Naqash et al., 2017), there is a need for innovative solutions. Despite Brazil's substantial biscuit production, the availability of high-quality gluten-free options is limited due to difficulties in achieving sensory attributes comparable to conventional products (Pappen et al., 2020a).

The aim of this study was to extract, analyze and utilize starch from mango (*Mangifera indica* L.) kernels in cookies production.

Materials and methods

Materials

Mangoes of the Palmer variety were obtained from local markets in the region of Ponta Grossa, PR, in January 2023. The starchy material was extracted using an aqueous medium, without chemical treatment, using an adaptation of the methodology described by (Bet et al., 2018; Borsato et al., 2022).

Proximate analysis

Proximate analysis was performed following the official AOAC methodologies for proteins (920.87), lipids (968.20), ashes (923.03), and moisture (934.01). The carbohydrate content was calculated by difference.

Physical modification

The starch granules were modified using the Vibra Cell ultrasound equipment (SONICS), model USC 1400. The process followed the methodology outlined by Bisinella et al. (2022).

Thermogravimetry

The mass loss of each sample and the temperatures of each thermal event were obtained using the TGA-50 thermal analysis system (Shimadzu, Japan) with the aid of TA-60WS software, for which it was also possible to obtain DTG values, which are a mathematical resource for a more precise identification of the temperatures involved in the mass loss of the samples.

The sample mass ranged from 7–9 mg weighed in an open alumina crucible. The analysis conditions were: heating from 30 to 650 °C at a heating rate of 10 °C min⁻¹, under air flow of 100 mL min⁻¹. Derivative thermogravimetric (DTG) curves (first derivative of TG curves) were calculated. Before analysis, the instrument was preliminarily calibrated with standard weight and tested with standard calcium oxalate monohydrate (Bet et al., 2018; Borsato et al., 2022).

Differential Scanning Calorimetry

The DSC curves were obtained using a DSC-Q200 (TA-Instr., USA) thermal analysis system, with the following parameters: heating rate of 10 °C min⁻¹ under airflow of 50 mL min⁻¹, and samples weighing about 2.5 mg. A suspension was prepared at a 4:1 ratio (water: starch, w/w) and held for 60 minutes to equilibrate the moisture content. The aluminum crucibles were sealed, and after one hour, the curves were performed. The instrument was previously calibrated with indium (99.99% purity, T_p = 156.6°C, ΔH = 28.56 J g⁻¹) (Beninca et al., 2020; Bisinella et al., 2022).

Field Emission Gun (FEG)

The morphology and measurements of the starch granules were performed in a Vega 3 (Tescan, Czech Rep.) scanning electron microscope (SEM), under acceleration voltage of 25 kV and 1.500 x magnification. Before analysis, the samples were metallised with gold. The area of granules was calculated using Image J 1.47 for Windows software (Beninca et al., 2020).

Preparation of the biscuits

For the preparation of the biscuits, the dough was prepared using the following ingredients: corn starch, margarine, sugar, coconut milk, water, and mango kernel starch (Nunes et al., 2015). Table 1 shows the proportions of the raw materials used in the shortbread

formulations. It is clear that the main differences between the formulations are the percentage of corn starch, which was replaced by mango kernel starch, and the addition of pomace flour. The pomace flour corresponds to the fraction that remained in the sieve during the starch extraction, which was then dried in an oven with air circulation at 45 °C for 24 hours (Silva et al., 2016).

Table 1

Biscuit formulations

Ingredients	S0	S1	S2	S3	S4
Corn starch	25	12.5	12.5	12.5	12.5
Margarine	12.5	12.5	12.5	12.5	12.5
Sugar	12.5	12.5	12.5	12.5	12.5
Coconut milk	0.1	0.1	0.1	0.1	0.1
Water	12.5	12.5	12.5	12.5	12.5
Mango kernel starch	-	10	4.68	2.5	12.5
Bagasse flour	-	2.5	7.82	10	-

S0, Control cookie with corn starch;

Cookies with corn starch replaced by:

S1, 40% bagasse flour and 10% mango kernel starch;

S2, 18.72% bagasse flour and 31.28% mango kernel starch;

S3, 10% bagasse flour and 40% mango kernel starch;

S4, 50% mango kernel starch.

Colour parameters

The MiniScan (Hunter) reflectance spectrophotometer was used to determine the colour parameters. The equipment used was the portable colorimeter (Miniscan XE Plus, model 45/0-L, Hunter Associates Laboratory Inc., Reston, VA, USA) with CIE L*a*b* system.

Texture

Texture of cookies was measured with texturometer (TA.XT Plus Texture Analyser) by determining the hardness (peak breaking force) using a probe knife at a speed of 2 mm/s and distance of 20 mm through the cookies. Texture Exponent Lite software was used to evaluate the results.

Statistic

The results of the analyses were expressed as mean followed by standard deviation. Analysis of variance (Anova) and Tukey's test were used to compare the means between the samples with 95% confidence ($p < 0.05$).

Results and discussion

Proximate analysis

The results obtained for the proximate composition of native starch are presented in Table 2.

Table 2

Centesimal composition of mango kernel starch

Moisture	Ash	Lipids	Proteins	Carbohydrates
7.05±0.01	0.44±0.00	15.45±0.57	4.74±0.06	72.32±0.73

The value of carbohydrates and total fiber predominated in the proximal composition (72.32%), suggesting that the aqueous extraction allowed a good separation of the starchy fraction of the mango kernel. The starch had a high lipid content when compared to mango endocarp starch (Santos et al., 2015), which had 7.32%, and low levels of moisture (9.23%), ash (0.59%), and protein (5.30%).

Thermogravimetry

The TG/DTG curves (Figure 2) for native and modified starch allow an evaluation of the loss of mass and thermal stability of each sample during heating. Three stages of mass loss were observed for all samples, and they are associated with dehydration, decomposition, and oxidation, respectively. The derivative (DTG) was calculated to identify the temperature at which the maximum rate of loss occurs. When an inflection point in the TG curve is generated, these stages are replaced by peaks that delineate areas corresponding precisely to the changes in mass undergone by the sample.

Table 3 presents the TG/DTG results for native mango kernel starch and the 75% and 100% modified samples. Mass losses in the samples during thermal degradation occurred in three stages, as shown in Figure 3. The initial mass loss is attributed to the moisture content in the samples (Di-Medeiros et al., 2014; Ribeiro et al., 2014).

The second loss of mass, after a period of stability, corresponds to the decomposition of the main carbon chain. At this stage, there is a significant loss of mass, indicating the presence of a large number of compounds with similar thermal properties, a behavior characteristic of homopolysaccharides, to which starch belongs. In general, the second and third mass losses, which occur consecutively, are attributed to the decomposition and oxidation of organic matter to the formation of ash (Bet, 2021).

After ultrasound modification, a reduction in the thermal stability period of the starch was observed, especially when a higher vibration amplitude was applied. The reduction in stability may be associated with acoustic cavitation, which damages the structural order of the granules, facilitating the diffusion of water inside the chains and, consequently, the misalignment of hydrogen bonds (Bet, 2021).

The decomposition and oxidation of organic matter occur in consecutive stages during the second and third mass losses, as mentioned by Ribeiro et al. (2014). The lowest onset temperature of degradation was observed in the US100% starch, recording 244.65 °C, while the highest temperature was 249.55 °C for the native starch sample.

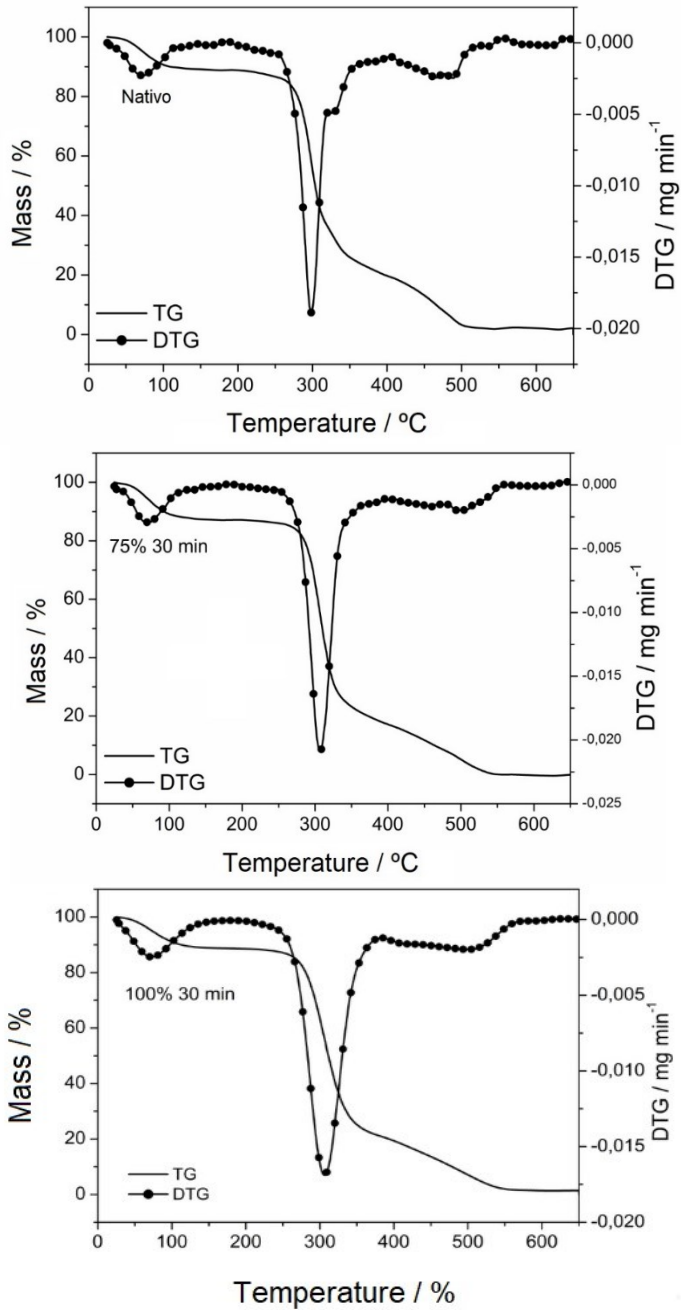


Figure 2. Thermogravimetry (TG) and Derivative Thermogravimetry (DTG) curves for the native starch, 75% modified starch, and 100% modified starch samples

Table 3

Results of TG/DTG for native and ultrasound-modified starch

Sample	Thermal event	1 ^a	Stability	2 ^a	3 ^a
	Ti–Tf °C	30.00– 131.59	131.59– 249.55	249.55– 376.24	376.24– 534.77
Native starch	T _p °C	71.95	–	298.34	488.59
	Δm %	10.67	–	67.73	20.66
	Ti–Tf °C	30–133.37	137.37– 248.85	248.85– 379.93	379.93– 576.56
Starch 75%	T _p °C	71.17	–	306.94	495.29
	Δm %	12.20	–	69.00	19.44
	Ti–Tf °C	30.00– 133.94	133.94– 244.63	244.63– 382.43	382.43– 567.01
Starch 100%	T _p °C	72.68	–	306.38	499.24
	Δm %	10.71	–	66.46	19.37

Δm = mass loss (%); Ti and Tf = initial and final temperatures (°C) for each stage of the thermal event; T_p = peak temperature (°C).

Differential Scanning Calorimetry

The differential scanning calorimetry (DSC) technique was used to study the gelatinization of starch, an endothermic process in which the ordered structure of the linear and branched starch chains passes into a disordered state, absorbing water and swelling the granules until they break. Consequently, this will lead to a change in enthalpy depending on the degree of disorder of the polymer chain. Table 4 shows the DSC results for native and modified starch at 75% and 100%, respectively.

These values were lower than those found in the literature for conventional starch sources such as corn starch (T_p: 73.2 °C) and higher than cassava starch (T_p: 69.0 °C), and were higher than the non-conventional amaranth starches (66.7–68.1 °C) mentioned by Bet et al. (2018).

When more intense ultrasound parameters are applied, damage to the starch granules is possible, which can result in changes in crystallinity. Ultrasound-induced cavitation facilitates the entry of water into the starch structure, thus accelerating the gelatinization process and reducing the enthalpy energy associated with this event.

In this study, with the modification of the starch there was a reduction in the gelatinization transition temperatures and a greater increase in the gelatinization enthalpy of the 100% modified starch, these data corroborate the study by Bisinella et al. (2022). Figure 3 shows the curves of the native and modified starches.

Table 4

Results of Differential Scanning Calorimetry for native and modified starches

Sample	T ₀	T _p	T _c	ΔH _{gel}
Native	69.22±0.08	72.96±0.08	78.36±0.33	4.65±0.01
Starch 75%	68.22±0.26	72.11±0.01	77.52±0.17	4.95±0.27
Starch 100%	67.19±0.52	71.88±0.11	77.87±0.15	8.62±0.26

T₀, Initial temperature;
 T_p, Peak temperature;
 T_c, Conclusion temperature;
 ΔH_{gel}, Enthalpy of gelatinization.

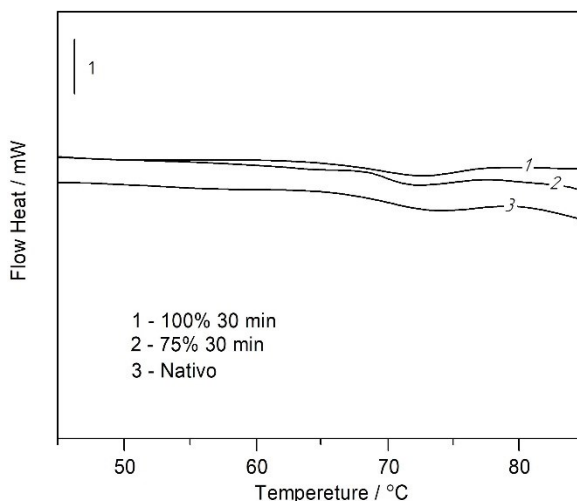


Figure 3. Differential Scanning Calorimetry curves for the native, 75%, and 100% modified starch samples

Morphology of starch granules

Using scanning electron microscopy, it was possible to check the morphology of the native and modified mango kernel starch granules (Figure 4). The starch showed elliptical granules and some spherical granules, which was expected, as observed in other studies (Espinosa-Solis et al., 2009; Santos, 2015).

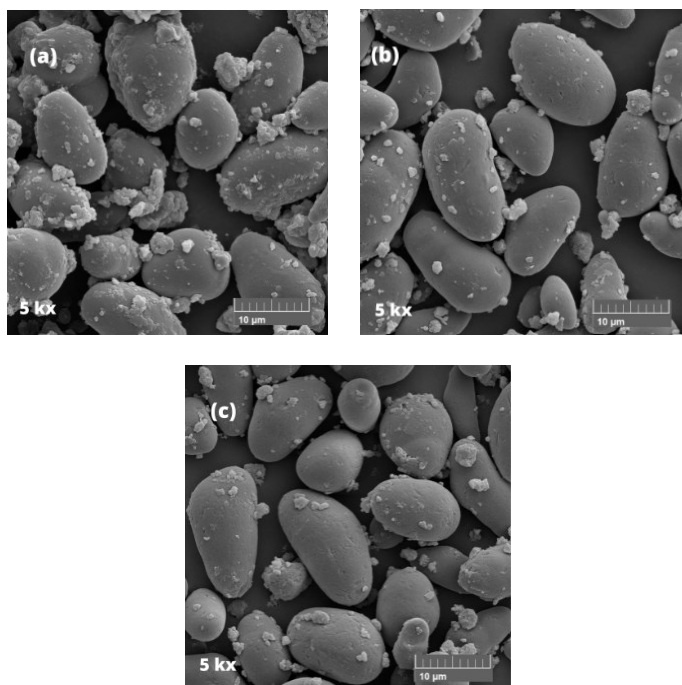


Figure 4. Microscopic images obtained by FEG for the samples: a, native starch; b, 75% modified starch; c, 100% modified starch.

Sandhu et al. (2004) reported that the diameter of mango starch is approximately 16 µm. Differences in starch morphology, hilum position and size can be attributed to different botanical origins, biosynthetic mechanisms of the amyloplast and plant physiology.

Colour parameters

The colorimetric parameters of native and modified starch are shown in Table 5.

Colorimetric analysis of starch

Table 5

Samples	L*	a*	b*
Native	61.73 ± 1.32 ^c	3.09 ± 0.12 ^a	19.54 ± 0.47 ^a
Modified starch 75%	73.71 ± 0.03 ^a	2.24 ± 0.03 ^c	16.64 ± 0.04 ^b
Modified starch 100%	69.59 ± 0.08 ^b	2.60 ± 0.04 ^b	17.06 ± 0.10 ^b
p	<0.001	<0.001	<0.001

Different letters in the same column represent significant differences according to Tukey's test (p<0.05).

The sample modified with a vibration amplitude of 75% showed greater luminosity. Compared to other studies, a^* values were higher than those of starch and cassava bagasse, whose values were in the range -0.23 to 3.25, and the b^* values ranged from 3.37 to 15.17 (Sandhu et al., 2004). With regard to b^* values, the modified mango kernel starches did not differ significantly from each other and the highest value was found for the native starch.

Texture profile

Results of texture analysis are presented in Table 6.

Table 6
Texture analysis of the biscuits

Samples	Hardness (kgf)
S1	51.95 ± 1.36 ^a
S2	32.14 ± 3.59 ^b
S3	7.01 ± 1.98 ^c
S4	8.56 ± 0.09 ^c
S0	6.73 ± 0.32 ^c
p	<0.001

Control biscuit (S0), biscuit (S1) with 30% substitution of bagasse flour and 20% mango starch, biscuit (S2) with 45% substitution of bagasse flour and 30% mango starch, biscuit (S3) with 20% substitution of bagasse flour and 30% mango starch, and biscuit (S4) with 50% substitution of mango starch, ABC_{letras} different letters in the same column represent significant differences according to Tukey's test ($p < 0.05$).

The highest hardness value was found in the sequilho-type biscuit formulation with a 30% substitution of bagasse flour and 20% mango starch (S1), followed by the biscuit formulation with a 45% substitution of bagasse flour and 30% mango starch (S2). The lowest values were observed when higher levels of mango starch were substituted in the biscuits (S3 and S4); however, no significant differences were found between these biscuits and the control biscuit (S0).

The hardness values obtained in the instrumental analysis ranged from 51.95 kgf to 6.73 kgf, with the lowest value for the control biscuit (S0). These values were higher compared to sour starch biscuits enriched with soluble and insoluble fibers, which ranged from 1.45 kgf to 3.90 kgf (Montenegro et al., 2008). When compared to whole biscuits made with residues from the extraction of pinhão starch, where the highest value found was 25.68 kgf and the lowest was 6.68 kgf, the results were slightly lower than the formulations (S2) and (S0) (Romko et al., 2019).

Since both sequilho-type biscuits and pinhão do not contain gluten, the starch present, along with their higher fiber content, contributes to water absorption, leading to a consequent reduction in hardness values (Romko et al., 2019).

Colour parameters of the biscuits

Colour parameters of the biscuits are shown in Table 7.

Table 7

Colorimetry analysis of the biscuits			
Formulations	L*	a*	b*
S1	52.56 ± 1.55 ^c	6.39 ± 0.02 ^b	25.26 ± 1.05 ^{ab}
S2	53.05 ± 1.07 ^c	7.28 ± 0.19 ^a	29.88 ± 0.45 ^a
S3	48.27 ± 0.55 ^d	6.03 ± 0.05 ^b	21.80 ± 0.04 ^{bc}
S4	56.56 ± 0.49 ^b	5.07 ± 0.07 ^c	23.59 ± 4.54 ^{bc}
S0	91.62 ± 0.05 ^a	0.05 ± 0.05 ^d	18.79 ± 0.41 ^c
p	<0.001	<0.001	<0.001

S0, Control biscuit;

S1, Biscuit with 30% substitution of bagasse flour and 20% mango starch;

S2, Biscuit with 45% substitution of bagasse flour and 30% mango starch;

S3, Biscuit with 20% substitution of bagasse flour and 30% mango starch;

S4, Biscuit with 50% substitution of mango starch.

The biscuits showed lower luminosity values compared to gluten-free "Biju" biscuits, which ranged from 67.99 to 72.85 (Ressutte et al., 2018), with the control biscuit (S0) having the highest luminosity. According to Esteller et al. (2005), lower L* luminosity values indicate less light reflectance, resulting in products with a darker coloration. All samples differed from each other, with the darkest coloration observed in the S3 formulation (Figure 5).

The S2 formulation exhibited the highest a* value (shift towards red), indicating a darker biscuit crust compared to gluten-free "Biju" biscuits, which ranged from 1.09 to 2.24 (Ressutte et al., 2018). In terms of the b* value, the S2 formulation was lower compared to biscuits made with pupunha flour, which ranged from 55.14 to 59.18 (Santos, 2022). The biscuit with 45% substitution of bagasse flour and 30% mango starch (S3) showed the highest b* value, indicating a stronger yellow hue.

In the samples subjected to baking, the breakdown of starch upon heating and swelling due to water exposure may have triggered the Maillard reaction, leading to a tendency for enzymatic browning and caramelization (Gama et al., 2010; Lohinova and Petrussha, 2023).

There is a noticeable color difference among the biscuits. The control biscuit (S0) exhibits a lighter color compared to the other biscuits (S1, S2, S3, S4), which are darker due to the addition of mango almond starch and bagasse flour. Additionally, darker granules can be observed in the biscuits (b, c, d), which contain the added mango almond bagasse flour.

In contrast, the S4 biscuit (e) shows no granules and has a lighter color compared to biscuits S1, S2, and S3 (b, c, d), as its formulation included 50% mango almond starch. Table 6 shows the results obtained from the centesimal analyses of the S0, S1, S2, S3 and S4 cookies.

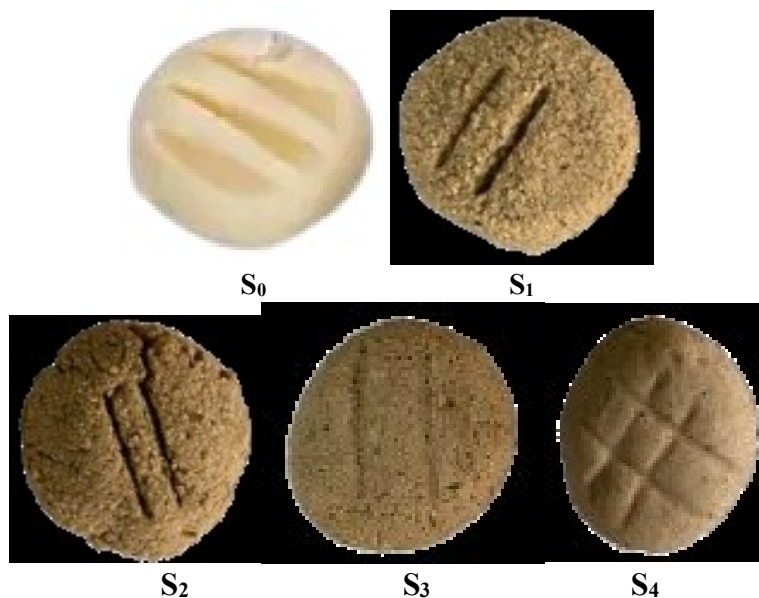


Figure 5. Baked sequilho-type biscuits:

S0, Control biscuit;

S1, biscuit with 30% substitution of bagasse flour and 20% mango starch;

S2, biscuit with 45% substitution of bagasse flour and 30% mango starch;

S3, biscuit with 20% substitution of bagasse flour and 30% mango starch;

S4, biscuit with 50% substitution of mango starch.

Physico-chemical characteristic of the cookies are shown in Table 8.

Table 8

Physico-chemical characteristic of the cookies

Cookies	Moisture	Proteins	Ash	Lipids	Carbohydrates
S0	3.78±0.02	0.39±0.08	0.06±0.03	7.95±1.06	87.81±1.16
S1	7.49±0.57	1.69±0.02	0.39±0.08	11.06±1.34	79.35±0.7
S2	7.16±0.66	2.57±0.30	0.48±0.01	15.27±0.64	74.82±0.02
S3	3.57±0.001	1.58±0.06	0.08±0.07	11.07±0.76	83.69±0.76
S4	6.66±2.27	1.58±0.007	0.09±0.01	11.63±0.07	79.95±2.29

Control cookie with corn starch (S0); and cookies with corn starch replaced by: (S1) 40% bagasse flour and 10% mango kernel starch; (S2) 18.72% bagasse flour and 31.28% mango kernel starch; (S3) 10% bagasse flour and 40% mango kernel starch; and (S4) 50% mango kernel starch.

It was observed that cookie S3 had the lowest percentage of moisture, while cookie S1 had the highest. After adding bagasse and mango kernel starch, there was an increase in protein, ash and lipid content.

When the cookies formulated in this study are compared to sequilla-type cookies formulated with amaranth, corn and rice flour (Pappen et al., 2020b), the cookies with mango kernel starch had a higher carbohydrate content in all formulations. In addition, they had lower lipid and protein content when compared to sequilla-type cookies with flour from the residual pequi pulp cake, which registered values between 14.72 and 18.54%; and from 5.37 to 9.18%, respectively (Sousa et al., 2021b).

The highest hardness (51.95 ± 1.36) kgf was found for cookie S1, with 40% bagasse flour and 20% mango kernel starch, a combination that increased the cookie's compressive strength. Cookie S2 (18.72% bagasse flour and 31.28% mango kernel starch) also showed high hardness (32.14 ± 3.59 kgf), although significantly lower than S1.

On the other hand, in formulations S3 and S4, the addition of mango kernel starch resulted in cookie hardness values (7.01 ± 1.98 kgf and 8.56 ± 0.09 kgf, respectively) with no significant difference compared to the control cookie containing corn starch (6.73 ± 0.32) kgf. This suggests that increasing the proportion of mango starch contributes to a softer texture in the cookies.

When compared with wholemeal cookies made with the residue from the extraction of pine nut starch, which showed hardness values of 6.68 kgf to 25.68 kgf it can be seen that the S2 and S0 formulations in this study are similar or slightly higher (Romko et al., 2019).

The absence of gluten in sequillos and pine nut cookies, together with the higher fiber content, influences water absorption and the reduction of hardness values (Ronko et al., 2020). This shows that the texture of cookies can be significantly adjusted by modifying the proportions of mango pomace flour and mango starch, offering variations that can meet the different texture preferences of consumers.

Conclusions

The starch from the Palmer mango seed (*Mangifera indica* L.) has excellent nutritional characteristics and is an important source of energy, being of great interest to the food industry. The modified starch exhibited morphology with elliptical and some spherical granules.

Through thermal analysis, it was observed that thermal stability allows application in baked bakery products. The development of "sequillos" type cookies using mango seed kernel starch proved to be feasible, showing a proximate composition that confirms its nutritional value as a source of protein, carbohydrates, and lipids, making it suitable for use in formulating new food products. It is worth noting that in formulations with a 50% substitution of mango starch, the cookies had a lighter color compared to those containing bagasse in their formulation.

The development of biscuits using mango seed starch proved to be viable, presenting a proximal composition that enhances its nutritional value as a source of proteins, carbohydrates and lipids, making it suitable for use in the formulation of new food products. It is worth mentioning that in the formulations with 50% replacement of mango starch, the cookies were lighter in color compared to those that contained pomace in their formulation and were softer. The effect of replacing corn starch with mango seed starch in the production of cookies seems very promising and could be the subject of new research and future studies, to add value to waste obtained during mango processing.

References

- Bet C.D. (2021), Extraction of starch from organic *Amaranthus caudatus* by ultrasonic irradiation and incorporation of fructooligosaccharides by ultrasound and freeze-drying, Thesis (Doctorate in Food Science and Technology) - State University of Ponta Grossa, Ponta Grossa.
- Bet C.D., Oliveira C.S. de, Colman T.A.D., Marinho M.T., Lacerda L.G., Ramos A.P., Schnitzler E. (2018), Organic amaranth starch: A study of its technological properties after heat-moisture treatment, *Food Chemistry*, 264, pp. 435–442, <https://doi.org/10.1016/j.foodchem.2018.05.026>
- Beninca C., Bisinella R.Z.B., Bet C.D., Oliveira C.S., Barboza R.A., Colman T.A.D., Demiate I.M., Schnitzler E. (2020), Effect of aqueous and ethanolic extracts from pinhão coats on the properties of corn and pinhão starches, *Journal of Thermal Analysis and Calorimetry*, 140, pp. 743–753, <https://doi.org/10.1007/s10973-019-08874-3>
- Bisinella R.Z.B., Beninca C., Bet C.D., de Oliveira C.S., Demiate I.M., Schnitzler E. (2022), Thermal, structural and morphological characterisation of organic rice starch after physical treatment, *Journal of Thermal Analysis and Calorimetry*, 1, pp. 1–10, <https://doi.org/10.1007/s10973-022-11367-x>
- Borsato M.P., Bet C.D., Bisinella R.Z.B., Lacerda L.G., Schnitzler E. (2022), Buckwheat starch (*Fagopyrum esculentum*): Aqueous extraction, modification by HMT and characterization, *Carpathian Journal of Food Science & Technology*, 14(2), pp. 147–154, <https://doi.org/10.34302/crpjfst/2022.14.2.12>
- Cescon S., Barbosa R., Barud H., Zanela T., Dalla Costa B., Fajardo A.R. (2018), Cationic starch derivatives as reactive shale inhibitors for water-based drilling fluids, *Journal of Applied Polymer Science*, 135(4), 45721, <https://doi.org/10.1002/app.45721>
- Chowhan A., Giri T.K. (2020), Polysaccharide as renewable responsive biopolymer for in situ gel in the delivery of drug through ocular route, *International Journal of Biological Macromolecules*, 150(Part A), pp. 559–572, <https://doi.org/10.1016/j.ijbiomac.2019.10.073>
- Demiate I.M., Kotovicz V. (2011), Cassava starch in the Brazilian food industry, *Food Science and Technology, Campinas*, 31(2), pp. 388–397, <https://doi.org/10.1590/S0101-20612011000200019>
- Di-Medeiros M.C.B., Pascoal A.M., Batista K.A., Bassinello P.Z., Lião L.M., Leles M.I.G., Fernandes K.F. (2014), Rheological and biochemical properties of *Solanum lycocarpum* starch, *Carbohydrate Polymers*, 104, pp. 66–72, <https://doi.org/10.1016/j.carbpol.2014.01.023>
- Espinosa-Solis V, Jane J.L., Bello-Perez L.A. (2009), Physicochemical characteristics of starches from unripe fruits of mango and banana, *Starch*, 61(5), pp. 291–299, <https://doi.org/10.1002/star.200800164>
- Esteller M.S., Lannes S.C.S. (2005), Parâmetros complementares para fixação de identidade e qualidade de produtos panificados, *Ciência e Tecnologia de Alimentos, Campinas*, 25(4), pp. 802–806.
- Jing L., Liu Y., Gao J., Xu M., Gou M., Jiang H., Li W. (2019), Effect of repeated freezing-thawing on structural, physicochemical and digestible properties of normal and waxy starch gels, *International Journal of Food Science & Technology*, 54, pp. 2668–2678, <https://doi.org/10.1111/ijfs.14144>
- Gama T.B., Masson M.A., Haracemiv S.M. C., Zanette F., Córdova K.R.V. (2010), A influência de tratamentos térmicos no teor de amido, colorimetria e microscopia de

- pinhão nativo (*Araucaria angustifolia*) e pinhão proveniente de polinização controlada, *Revista Brasileira de Tecnologia Agroindustrial*, 4(2), pp.161–178.
- Guo K., Lin L., Fan X., Zhang L., Wei C. (2018), Comparison of structural and functional properties of starches from five fruit kernels. *Food Chemistry*, 255, pp. 55–63, <https://doi.org/10.1016/j.foodchem.2018.02.066>
- Garcia M.A.V.T., Garcia C.F., Faraco A.A.G. (2020), Pharmaceutical and biomedical applications of native and modified starch: A review, *Stärke*, 72, 2000206, <https://doi.org/10.1002/star.202000206>
- Kringel D.H., Dias A.R.G., Zavareze E.D.R., Gandra E.A. (2020), Fruit wastes as promising sources of starch: Extraction, properties, and applications - A review, *Stärke*, 72(7–8), 2000157, <https://doi.org/10.1002/star.202000157>
- Lohinova A., Petrusha O. (2023), Maillard reaction in food technologies, *Ukrainian Journal of Food Science*, 11(2), pp. 81–109, <https://doi.org/10.24263/2310-1008-2023-11-2-4>
- Montenegro F.M., Gomes-Ruffi R.C., Vicente A.C., Collarez-Queiroz P.F., Steel J.C. (2008), Biscoitos de polvilho azedo enriquecidos com fibras solúveis e insolúveis, *Ciência e Tecnologia de Alimentos*, 28, pp.184–191.
- Naqash F., Gani A., Gani A., Masoodi F. A. (2017), Gluten-free baking: Combating the challenges - A review, *Trends in Food Science & Technology*, 66, pp. 98–107, <https://doi.org/10.1016/j.tifs.2017.06.003>
- Nunes J.S. (2015), Drying of tropical fruit residues to obtain flour and evaluation of the addition in sequilho-type biscuits, Federal University of Campina Grande, Campina Grande.
- O'Leary M., Hanson B., Smith C. (2010), Viscosity and non-Newtonian features of thickened fluids used for dysphagia therapy, *Journal of Food Science*, 75(6), pp. E330-E338, <https://doi.org/10.1111/j.1750-3841.2010.01708.x>
- Pappen D.R.H.P., Rigo D., Colet R., Fernandes I.A., Steffens J., Zeni J., Rigo E., Valduga E. (2020a), Preparation and characterization of biscuit type sequilho with amaranth flour, maize and rice, *Brazilian Journal of Development*, 6(9), pp. 72621–72636, <https://doi.org/10.34117/bjdv6n9-160>
- Pappen D.R.H.P., Rigo D., Colet R., Fernandes I.A., Steffens J., Zeni J., Rigo E., Valduga E. (2020b), Elaboração e caracterização de biscoito tipo sequilho com farinha de amaranto, milho e arroz, *Brazilian Journal of Development*, 6(9), pp. 72621–72636.
- Ressutte J.B., Manin L.P., Nakagawa A., Madrona G.S. (2018), Impacto da formulação de biscoitos sem glúten, do tipo "biju", elaborados com polvilho doce, açúcares e edulcorante (sucralose) nos atributos de cor e análise sensorial, 15-15 Maio, 2018, FAUPGS, Gramado, Brasília, https://www.schenautomacao.com.br/ssa/envio/files/98_arqnovo.pdf
- Ribeiro L.S., Cordoba L.P., Colman T.A.D., Oliveira C.S., Andrade M.M.P., Schnitzler E. (2014), Influence of some sugars on the thermal, rheological and morphological properties of "pinhão" starch, *Journal of Thermal Analysis and Calorimetry*, 117, pp. 935–942, <https://doi.org/10.1007/s10973-014-3758-9>
- Romko S.C., Beninca C., Bet C.D., Bisinella R.Z.B., Schnitzler E. (2019), Effect of addition of pinhão flour and bagasse generated after starch extraction on the formulation of cookie, *Ukrainian Food Journal*, 7(2), pp. 186–196, <https://doi.org/10.24263/2310-1008-2019-7-2-3>
- Ronko L.Z., Travalini A.P., Demiate I.M. (2020), Amido e bagaço de mandioca (*Manihot esculenta* C.): obtenção e caracterização de diferentes variedades, *Revista Brasileira*

- de *Tecnologia Agroindustrial*, 14(1), pp. 1–21, <https://doi.org/10.3895/rbta.v14n1.10466>
- Sandhu K.S., Singh N., Kaur M. (2004), Characteristics of the different corn types and their grain fractions: physicochemical, thermal, morphological and rheological properties of starches, *Journal of Food Engineering*, 64(1), pp. 119–127, <https://doi.org/10.1016/j.jfoodeng.2003.09.010>
- Santos K.O. (2015), Use of starch extracted from mango seeds (*Mangifera indica* L.) for application as a biomaterial, Monograph (Bachelor's degree in Industrial Chemistry) – Science and Technology Center, State University of Paraíba, Campina Grande.
- Santos K.T.L. (2022), Elaboração de biscoito sem glúten à base de farinha de pupunha (*Bactris gasipaes* Kunth), Monografia (Bacharelado em Engenharia de Alimentos), Departamento de Engenharia de Alimentos, Fundação Universidade Federal de Rondônia, Ariquemes.
- Silva G.C. (2016), Development of cookies enriched with mango seed flour: Incorporation of bioactive substances and use of agro-industrial waste, Fluminense Federal University, Niterói.
- Sousa C.D.T., Sousa M.R.S.S., Sousa Y.G.S., Leal M.K.V.S., Sousa E.O.S. (2021a), Production and quality of almond flours from typical fruits of the Cariri region, Ceará, *Brazilian Journal of Agrotechnology*, 11(2), pp. 34–38, <https://doi.org/10.35828/bja.2021.1134>
- Sousa E.O., Santos A.M.M., Duarte A.M.S., Silva M.T.G. (2021b), Uso da farinha da torta residual da polpa do pequi (*Caryocar coriaticum* Wittm) no desenvolvimento e caracterização de biscoito tipo sequilho, *Revista Brasileira de Engenharia de Biosistemas*, 15(4), pp. 632–643.
- Stabnikova O., Marinin A., Stabnikov V. (2021), Main trends in application of novel natural additives for food production, *Ukrainian Food Journal*, 10(3), pp. 524–551, <https://doi.org/10.24263/2304-974X-2021-10-3-8>

Cite:

UFJ Style

Mainardes B., Mikota L.M., Bet C.D., Marinho M.T., Bisinella R.Z.B., Romko S.S., Schnitzler E. (2024), Extraction and physical modification of Mango palmer kernel starch and its application in cookies, *Ukrainian Food Journal*, 13(2), pp. 231–246, <https://doi.org/10.24263/2304-974X-2024-13-2-3>

APA Style

Mainardes, B., Mikota, L.M., Bet, C.D., Marinho, M.T., Bisinella, R.Z.B., Romko, S.S., & Schnitzler, E. (2024). Extraction and physical modification of Mango palmer kernel starch and its application in cookies. *Ukrainian Food Journal*, 13(2), 231–246. <https://doi.org/10.24263/2304-974X-2024-13-2-3>

Milk protein clots obtained by the addition of purple corn powder

Viktor Grek, Tetiana Pshenychna, Olena Onopriichuk, Olena Grek

National University of Food Technologies, Kyiv, Ukraine

Abstract

Keywords:

Milk
Protein
Clots
Purple corn
Whey

Article history:

Received
01.12.2023
Received in revised
form 23.03.2024
Accepted 2.07.2024

Corresponding author:

Olena Onopriichuk
E-mail:
olena.onopriychuk@
gmail.com

DOI:

10.24263/2304-
974X-2024-13-2-4

Introduction. The aim of the present study was to determine the technological functions of purple corn powder on the qualitative and quantitative characteristics of milk protein clots from goat's milk.

Materials and methods. Milk protein clots were obtained by acid-rennet coagulation of proteins from goat's milk with the addition of purple corn powder. The dispersion of purple corn powder particles and the ability to swell were determined by microscopy and the weight method, active acidity – potentiometrically; content of moisture and moisture retention capacity by the thermogravimetric methods; color and turbidity by the colorimetric method.

Results and discussion. The dispersion of purple corn powder was determined, which was represented by particles up to 60 μm in size (70–75%). The parameters for the preparation of a grain additive for introduction into goat milk have been specified.

It was found that under the same conditions of the process of acid-rennet coagulation of milk proteins, the use of purple corn powder in the amount from 2% to 10% contributed to an increase in the yield of milk-protein clots by 3.5–17.9%, compared to the control, and the mass fraction of moisture, on the contrary, decreased from 73.4% to 67.2%. With an increase of the amount of grain additive, the active acidity of milk-protein clots decreased from 4.75 to 4.50 pH units. The highest values of moisture retention capacity were observed in samples with the addition of $8 \pm 2\%$ purple corn powder and were an average by 19–34% higher than for the control. Taking into account sensory limitations, the yield of milk protein clots and their quality properties, the optimal amount of purple corn powder was determined at the level from 6% to 8% of the mass of milk. The milk protein clots had a pronounced sour milk taste, with the aroma of the introduced additive, homogeneous to the extent of butter consistency and a purple color, uniform throughout the mass.

The colored whey obtained as a result of the production of milk protein clots had improved taste and color characteristics, the content of dry substances ranging from 6.1 to 7.3%, including protein 0.36–0.50%, turbidity and color according to optical density (1.57–1.75 and 1.02–1.19 conv. units, respectively).

Conclusions. The colored whey could be classified as a functional raw material, which has original taste and color characteristics and expands the use of colored whey drinks in technology. The use of colored products as a base for various dairy products will avoid using artificial food colors and flavors.

Introduction

The chemical composition and properties of goat's milk are close to cow's milk, but it differs favorably in a larger amount of protein – 3.6% (3.0% in cow's milk), including casein, 3.0% (2.7% in cow's milk), fat 4.3% (3.4% in cow's milk), and minerals, 0.85% (0.74% in cow's milk (Getaneh et al., 2016). Compared to cow's milk, the content of milk sugar is reduced to 4.5% (cow's milk has 4.8%) and is completely dissolved, while goat milk proteins show lower allergenicity than cow's milk (Antonenko et al., 2019; Benjamin-van Aalst et al., 2024).

According to the content of casein protein, which determines the syrupiness of milk, goat and cow's milk do not differ significantly; however, compared to cow's milk, goat's milk has a lower content of α -caseins and a higher content of β -caseins, which under certain conditions can complicate the formation milk-protein clots. The density of goat milk is about 1.033 g/ml, while for cow's milk this indicator varies between 1.024–1.037 g/ml (Stergiadis et al., 2019).

Goat milk contains the essential amino acids that enter the human body only with food: valine (0.242 g), isoleucine (0.209 g), lysine (0.291 g), leucine (0.315 g), methionine (0.082 g), threonine (0.164 g), tryptophan (0.045 g), phenylalanine (0.156 g). In terms of mineral content, goat milk has also advantages. Compared to cow's milk, goat's milk contains about 13% more calcium, 50% more copper and 33% more selenium (Singh et al., 2021), and the bioavailability of minerals in goat milk is higher than of minerals in cow milk (Turkmen, 2017).

Goat's milk has a higher biological value than cow's milk in terms of its vitamin composition. This is especially true for vitamin A, which is the most important difference in the content of vitamins in goat's milk and cow's milk (Turkmen, 2017). Goat's milk contained vitamin A by 47%, tiamin (vitamin B1) by 51%, riboflavin (vitamin B2) by 31%, vitamin C by 37% and niacin (vitamin B3) more by 3.4 times more than cow's milk (Park et al., 2007).

Goat's milk protein clots are absorbed by the human body faster than cow's ones, which is explained by its flake-like structure, compared to the dense characteristic of cow's milk protein clot, and will also be enriched with calcium, potassium, phosphorus, sodium, magnesium and antioxidants (Turkmen, 2017). Therefore, goat's milk is a promising raw material for milk protein products.

Craft products made in small batches, in-house, using unique high-quality raw materials, according to original individual recipes, are relevant. Goat farms are very common in European countries. The obtained milk is processed into cheese, butter, kefir, or yogurt. However, cheese is one of the main and best products of goat milk processing.

Different countries have their traditional types of cheese. For example, for France it is Brie and Camembert, for Italy it is Parmesan and Mozzarella, for the Netherlands it is Gouda and Edam. They have a characteristic taste of goat's milk and can be of different consistency from soft to hard. It is possible to use goat's milk in Camembert-type cheese technology (Gyorgy et al., 2021). The leading European countries in the production of goat cheese are France, Greece, and Spain (Hamad et al., 2012; Raynal-Ljutovac et al., 2011; Sant'Ana et al., 2013). In Ukraine, there is a tendency to produce cheese at craft cheese factories. Production centers and cheese factories can be found in almost all regions, but they are most concentrated in the west of Ukraine (Transcarpathian and Ivano-Frankivsk regions), where a unique product is produced from goat, cow, or sheep milk and their mixture (Abbas et al., 2014; Kochubei-Lytvynenko et al., 2019).

Goat's milk has a lower titrated acidity, a higher dispersion of fat globules and casein micelles. In addition, goat's milk differs favorably from cow's milk in the content of retinol,

thiamine and ascorbic acid, as well as in the content of allergenic α 1-casein and α -lactalbumin, which causes its increased biological value (Park et al., 2007; Turkmen, 2017).

Over the past few decades, the lifestyle of the population has changed significantly, and people's nutrition is characterized by high calorie content and a deficiency of vitamins, trace elements, plant fibers and other biologically active substances (Mendonca, 2023). A new trend in the manufacturing of dairy products to increase their biological value is incorporation of plant additives in them (Stabnikova et al., 2021). The addition of vegetable raw materials increases the nutritional and biological value, and expands the range of dairy products (Caleja et al., 2016; Hashim et al., 2009; Rabie et al., 2020).

Development and implementation of craft technologies of dairy and vegetable products allow reducing the costs of the main dairy raw materials. Grains, seeds and products of their processing are increasingly used in the recipes of dairy products. Thanks to this technological technique, a high level of balance of the dairy product in terms of amino acid composition is achieved, its digestibility increases and structural and mechanical properties are improved.

It is recommended to use wheat, rice, buckwheat, corn, and oats grain products in different forms (crushed grain, flour, malt) (Aparna et al., 2015; Grek et al., 2020a). The production technologies of fermented milk products using rice flour, corn flour, barley flour, oat flour, wheat germ, and wheat bran are well known. The introduction of these additives in the amounts from 5% to 10% significantly increases the nutritional value of cheese products (Romanchuk et al., 2016). The developed products meet the body's daily need for protein by 14-18%. The introduction of fillers increases the content of thiamine, riboflavin, and tocopherols. The use of corn flour and wheat bran somewhat slows down protein proteolysis.

Germinated wheat was added, 7%, in cheese (Denisova, 2015). As a filler that does not dictate the color and taste of the cereal supplement, it was recommended to add dried apricots or other chopped, brightly colored fruit and berry ingredients. The calorie content of the cheese product with cereal additives was changed slightly, while the product was enriched with dietary fibers, vitamins, and minerals.

Functional fermented milk products have been developed – curds and curd mass with cereal fillers and curd paste with crushed flakes (Ghanbari et al., 2017). Cereal grains that are introduced are obtained by the extrusion method and have a high moisture absorption capacity. In finished products, the content of fat, protein, carbohydrates increases by 15-17%, vitamins, macro- and microelements – by 5%.

The introduction of 3% dietary fibers from *Acacia senegal* var. *kerensis* contributed to an increase in the yield of soft cheese, an extension of the shelf life and an improvement of its quality characteristics (Kiiru et al., 2018). The use of fiber increases the nutritional value of the product and has a positive effect on the human digestive system (Kiiru et al., 2018).

Introduction of rice extrudate and apple fiber into the milk mixture before fermentation had a positive effect on the formation of the consistency of the finished product (Malyarenko, 2015). Oat flour added in a fermented product acted as a structure-builder of a dispersed system, increased the content of carbohydrates, proteins, and vitamins, and provided nutrients to lactic acid bacteria (Sukhova et al., 2019).

The combination of dairy and grain raw materials ensures the enrichment of nutritional value of products, reduction of caloric content and consumption of animal fats, sugars, cholesterol. However, when producing milk-protein products with grain components, it is necessary to take into account the chemical composition and functional properties of plant raw materials, the peculiarities of the technology of obtaining ingredients of plant origin and their compatibility at the sensory level with the milk base. Their use should not significantly complicate the technology of dairy products and provide sensory characteristics that are not inherent to finished products on a milk-protein basis.

Criteria for the selection of the above-mentioned ingredients for use in the technology of milk-protein products have been developed, which are presented in Figure 1.

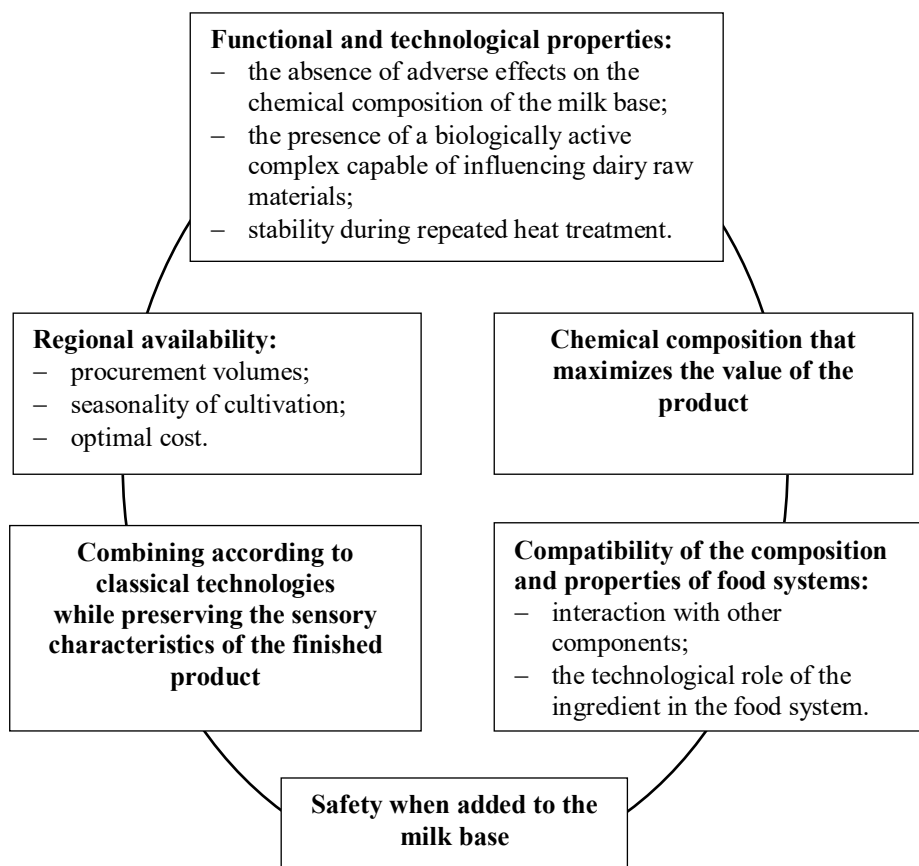


Figure 1. Criteria for selecting ingredients of plant origin

Some plants are considered as a possible source of ingredients to replace synthetic colors with natural ones, which meets consumer demands to minimize the use of synthetic additives in food products (Stabnikova et al., 2023). It can be elderberry juice or pomace (Cais-Sokolińska and Walkowiak-Tomczak, 2021; Delgado-Vargas et al., 2000; Domínguez et al., 2021), blackcurrant pasta (Grek et al., 2020b), or beetroot betalains (Güneşer, 2016). Purple corn can also be used to correct the color of dairy products.

Purple corn (*Zea mays* L.) is an annual plant of the cereal family, brightly purple in color due to the content of special anthocyanins, cyanidin-3-*O*-glucoside, the presence of which ensures the grain antioxidant properties. Purple corn flour contained, %, protein, 8.58; fat, 5.73; ash, 0.02, moisture 11.75; fiber, 2.91, and carbohydrates, 71.06 (Vilcacundo et al., 2020). Total phenolic content in purple corn flour was estimated as 140.7 mg gallic acid equivalent (GAE)/100 g dry matter (DW) (Mora-Rochin et al., 2010), and antioxidant activity determined using the 2,2-diphenyl-1-picrylhydrazyl (DPPH) method was 77000–84000 μ M Trolox equivalent (TE)/100 g (Trehanet et al., 2018). The content of total anthocyanins in purple corn dye powder with moisture content of 3.83% was 771 mg/100 g DM (Tacca et al., 2018). The content of minerals, mg/100 g, were as follows: potassium, 1200, calcium, 120, magnesium, 88, iron, 27, zinc, 2.7, copper, 0.3, manganese, 1, chromium,

63, molybdenum, 54. Calorie content in 100 g of purple corn is 283 (Ramos-Escudero et al., 2012).

The aim of the present research was to study the effect of purple corn powder addition on the qualitative and quantitative characteristics of milk protein clots from goat's milk.

Materials and methods

Materials

The object of the study was milk protein clots obtained by acid-rennet coagulation of goat milk proteins with the addition of purple corn powder.

Purple corn (RS. E4513813N – KBEOSA) ground to a powdery state was used for research.

To obtain samples of milk protein clots, pasteurization of goat milk was carried out at a temperature of $76\pm 2^\circ\text{C}$ with a holding time of 15-20 seconds.

Purple corn powder was mixed with goat's milk in a ratio of 3:1, brought to a temperature of 80°C and kept for 20 minutes to swell the proteins and obtain a uniform consistency. The resulting mixture was cooled to the fermentation temperature ($30\pm 2^\circ\text{C}$) and added to the total volume of milk, in amounts from 2% to 10% with a variation step of 2% and mixed for 3-5 minutes.

Then, the bacterial leaven *Vivo* for sour milk cheese, which contains the following strains of microorganisms, was added to the milk-cereal mixture prepared for fermentation: *Lactococcus lactis* subsp. *lactis*, *L. lactis* subsp. *cremoris*, *L. lactis* subsp. *lactis* biovar. *diacetylactis*, a calcium chloride solution at the amounts of 20-40 g of dry calcium chloride per 100 kg of milk and aqueous solution of the enzyme *Vivo* of plant origin chymosin at the amount of 1 g per 100 kg of milk. Fermentation of the mixture was carried out for 7-8 hours until the formation of a clot with a titrated acidity of $65\pm 2^\circ\text{T}$. The following technological operations were carried out to produce sour milk cheese from milk: processing (cutting, heating) of milk protein clot, whey separation and pressing of milk protein clot, cooling of $4\pm 2^\circ\text{C}$.

The control sample of the milk-protein clot was obtained according to the classical technology by fermenting pasteurized goat's milk using the acid-rennet method of protein coagulation with subsequent removal of serum.

Methods

Standard and well-known methods of research of technological and functional properties and quality indicators were used.

Determination of functional and technological properties of fine powder from purple corn

The dispersion of purple corn powder particles was determined by counting their sizes on a MICROMed XS-2610 microscope at a magnification of 150 times.

The ability to swell purple corn powder was determined by the weighing method, which consists in determining the change in the mass of the grain ingredient after immersing it in a solvent for a certain period. Quantitatively, this indicator is characterized by the degree

of swelling (K), which shows the relative increase in the mass of the system, mg/mg. The degree of swelling was calculated according to the formula:

$$K = \frac{m_1 - m_0}{m_0} = \frac{m_p}{m_0}$$

where m_0 , m_1 – mass of the system, respectively, before and after swelling, mg; m_p – mass of absorbed solvent, mg.

Quality indicators of milk-protein clots and whey

Sensory characteristics – appearance, color were controlled visually; taste and smell, consistency – sensoryally at the temperature of the milk-protein curd from 18°C to 20°C.

The yield of milk-protein clots (in g) was determined by the weighing method – the sample was weighed after self-pressing the clot for 30±2 minutes, which was obtained from 3000 ml of goat's milk.

The mass fraction of moisture retention capacity was measured by an accelerated method on a QUARTZ-21M-33 moisture meter by drying the sample to a constant mass and by a thermogravimetric method on a laboratory electronic scale-moisture meter of the ADS series manufactured by the company "AXIS" (Poland).

The active acidity of moisture retention capacity and stained serum was determined potentiometrically on a Sartorius PB-20 universal pH meter.

The moisture-retaining capacity of milk-protein clots was studied modification gravimetric method, based on the determination of the amount of water released from the product when lightly pressed and absorbed by the filter paper.

The content of dry matters in the coloured whey was found by the refractometric method according to the light refractive indices. First, check the correctness of the refractometer readings for distilled water at a temperature of 20±0.1 °C. With one or two water drops applied to the prism, the refractometer reading should be zero. The refractometer prism is wiped with a paper filter and one or two drops of a test whey sample are applied. On the right refractometer scale, the content of dry matters was found, which coincides with the distribution boundary of the dark and light fields.

Determination of chroma and turbidity of stained serum is based on measurement of optical density and comparison with relevant standards: colored solutions for chroma and turbidity suspensions (Grek et al., 2020b).

The study of the optical density of the filtered serum was carried out by the colorimetric method on a Helios Omega spectrophotometer (Thermo Scientific Spectronic, USA). The value of the optical density D_{gen} consists of D due to chroma due to coloring substances, and D_k due to turbidity due to the presence of proteins that scatter the light flux.

Results and discussion

Determination of functional and technological properties of purple corn powder

The quality of milk-protein products is significantly affected by the degree of dispersion of the additives introduced into their composition, since solid particles over 100 microns in size can be felt sensoryally and cause consistency defects. Considering the above, the dispersibility of purple corn powder, shown in Figure 2, was investigated.

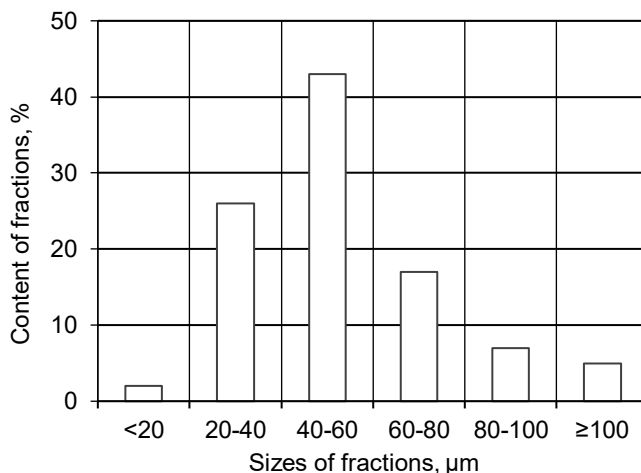


Figure 2. Dispersity of purple corn powder

According to the results of microstructural analysis, purple corn powder is characterized by high dispersion. The main fractions of its particles, mostly oval in shape, are in the range of 20–40 μm ($26 \pm 1.3\%$) and 40–60 μm ($43 \pm 2.1\%$), which dissolve in water at temperatures above 40 $^{\circ}\text{C}$ with the formation colloidal solutions, which in the future will not cause defects in the consistency of the product. Fractions larger than 100 μm do not exceed 10%.

For better distribution of purple corn powder in the structure of milk-protein clots, it is necessary to dissolve them beforehand. The relative increase in the mass of the system due to water absorption is characterized by the degree of swelling (K) and depends on the type of dispersion medium. Water and goat's milk were used as a liquid basis for swelling purple corn powder. The ability to swell purple corn powder at different temperatures is presented in Figure 3.

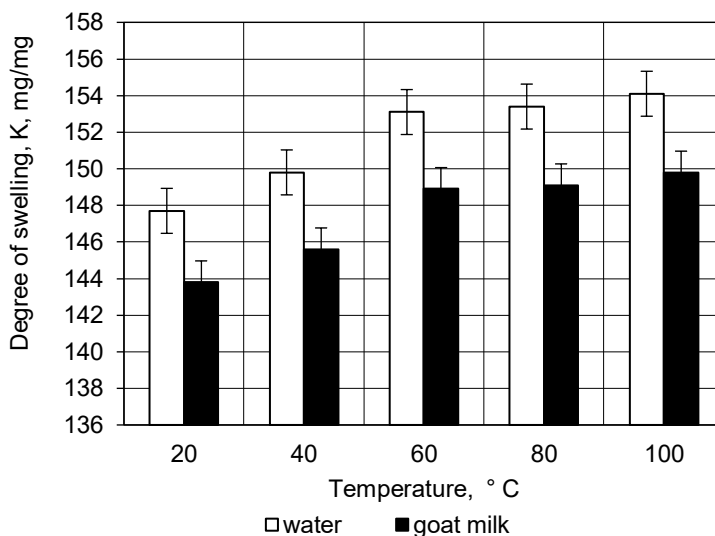


Figure 3. Swelling ability of purple corn powder

Swelling capacity is a technological characteristic of food systems and depends on the type of raw material, process temperature, degree of dispersion of components, type of solvent, etc. It was found that the degree of swelling of purple corn powder in water is 2.7-2.9% higher than in goat's milk. Pre-mixing purple corn powder with water before adding it to the normalized milk mixture reduces the nutritional value of the product. Replacing water with goat's milk prevents the occurrence of the above defect. The optimal dissolution temperature was determined at the level of 80 °C, which is the closest to the pasteurization regime and provides the necessary microbiological indicators.

The dependence of the swelling process of purple corn powder in goat's milk on the time and temperature of holding is shown in Figure 4.

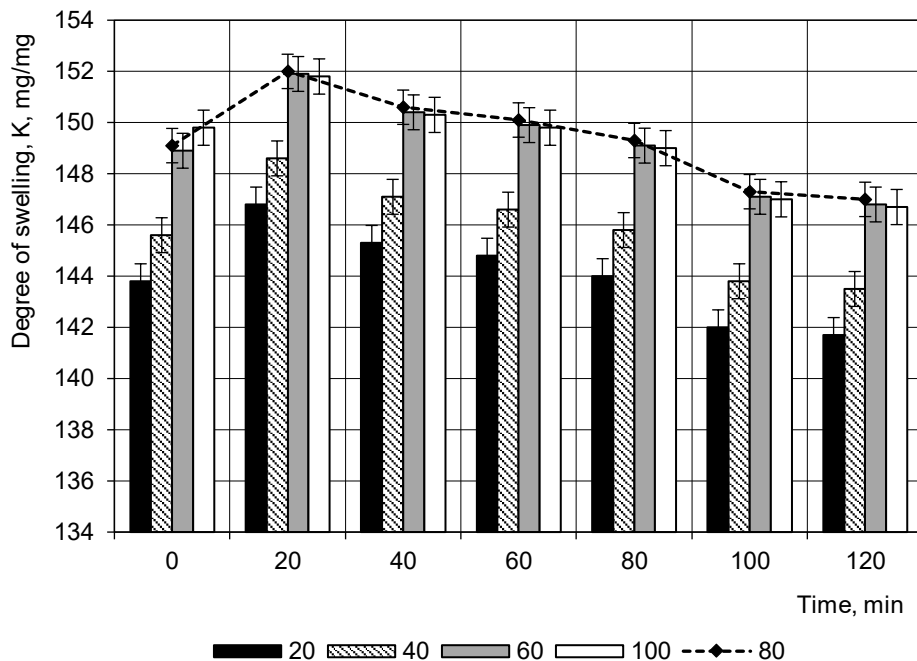


Figure 4. Dependence of the swelling process of purple corn powder in goat milk on the time and temperature of holding

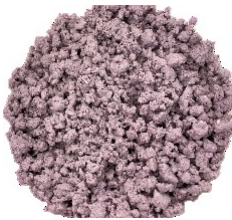
The most intensive swelling of purple corn powder occurs during the first 20 minutes at temperatures above 40 °C (Fig. 4). When interacting with goat's milk, the water-soluble substances of the grain additive absorb a significant amount of it and swell. The swelling process, caused by the interaction between the particles of the dispersed phase and the dispersion medium, slows down over time and is accompanied by the formation of a continuous spatial structure between the swollen particles of the ingredients. It was established that at a temperature of 80 °C and holding for 20 minutes, the value of the degree of swelling (K) is the highest and is 152 mg/mg, and the transition of dry substances into the solution is the lowest – at the level of 1.4%. With further interaction of purple corn powder with goat's milk, the swelling gradually decreases – on average by 1.03 times. Based on this, it can be assumed that the swelling and dissolution of purple corn powder occurs similar to these processes for polymers.

Determination of qualitative and quantitative indicators of milk protein clots and whey

The obtained milk protein clots and whey system is a polydisperse colloidal one, in which the dispersion medium is whey, and the dispersed phase is milk proteins and dry substances of the grain additive. The structure of milk protein clots is formed by the interaction between goat milk proteins and corn powder starch molecules. This process begins at the pasteurization stage of the mixture of goat milk and purple corn powder and ends during fermentation. The structure of milk protein clots characterizes the sensory properties. The resulting milk protein clots have a thixotropic coagulation-type structure with liquid interlayers between the particles. Liquid interlayers cause lower structural strength, but give milk-protein clots plasticity and elasticity (Grek et al., 2019).

The choice of the optimal amount of powder from purple corn was based on the preservation of normative sensory characteristics of milk-protein clots, which can be the basis for the production of various types of cheese. Table 1 shows the results of the sensory evaluation of milk-protein clots with purple corn powder.

Table 1
Sensory evaluation of milk-protein clots obtained with the addition of purple corn powder

Amount of purple corn powder, %	Sensory characteristics		
	Consistency and appearance	Taste and smell	Colour
2	Homogeneous, not viscous enough, too thin	Pure, sour-milk, unexpressed taste and aroma of purple corn powder	Barely noticeable light purple uniform over the entire mass
4			
6	Uniform, soft, moderately greasy	Pure sour milk with a light aroma of purple corn powder	Purple is uniform throughout the mass 
8			
10	Uniform, slightly brittle, floury	Pure sour milk with a pronounced taste and aroma of purple corn powder	Too pronounced saturated purple uniform throughout the mass

The best taste properties and consistency of milk protein clots were achieved with the addition of purple corn powder in the amounts of 6% and 8% to weight of milk. The samples had a pronounced sour milk taste with the aroma of the introduced additive, homogeneous to the extent of butter consistency and a purple color, uniform throughout the mass. The introduction of a filler in an amount greater than 8% causes negative changes in the sensory

properties of milk protein clots: a floury aftertaste and a fragile, floury consistency appear. The addition of purple corn powder in an amount of less than 6% did not have a noticeable positive effect on the structure of the product or on its sensory properties, and also did not significantly enrich the curd with biologically active nutrients – antioxidants, vitamins, dietary fibers, micro- and macroelements.

To confirm the obtained results of the sensory evaluation, further studies of the effect of different amounts of purple corn powder on the output of milk protein clots and the moisture content were conducted. The yield and content of moisture of milk protein clots depending on the amount of purple corn powder introduced are shown in Figure 5.

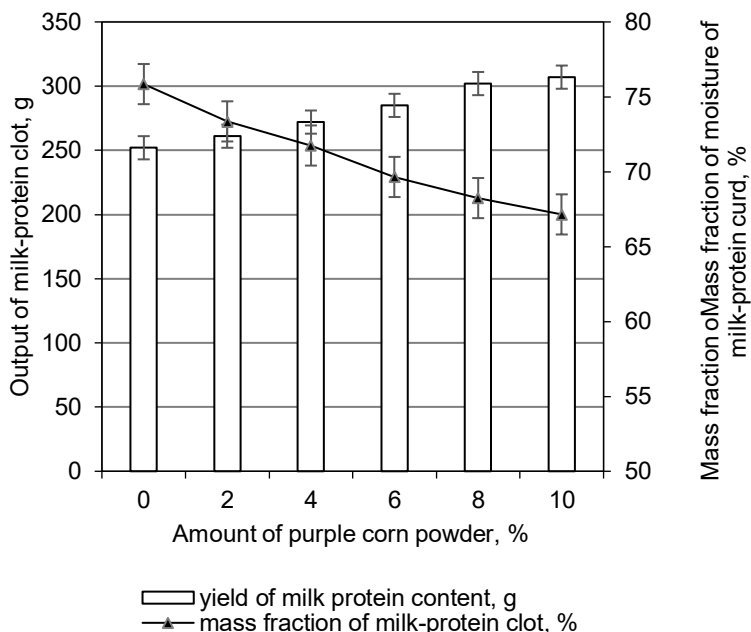


Figure 5. Yield and content of moisture in milk protein clots depending on the amount of purple corn powder

In general, the yield of milk protein clot is influenced by the type, composition and quality of milk, the amount of casein, pasteurization regimes, the type of coagulant and leavening agent, the density of the clot when cut, and technological parameters of production (Abd et al., 2011).

It was shown that under the same conditions of the acid-rennet coagulation process of milk proteins, the use of purple corn powder in an amount of 2% to 10% contributed to an increase in the yield of milk protein clots from 3 liters of goat milk by 9–55 g, and amounted to 3.45–17.91%, compared to the control. This allows reducing the consumption of dairy raw materials. (Fig. 5). The addition of more than 10% of purple corn powder did not have a significant effect on the yield increasing.

The content of moisture in milk-protein clots decreased from 73.36% to 67.15% when purple corn powder was added in amounts from 2 to 10%, respectively, and was 2.49–8.70% lower than in the control sample. Probably, the interaction of milk proteins with the

carbohydrates of the cereal supplement leads to the formation of additional complexes that differ in the presence of strong bonds between starch, fiber and whey proteins. The swelling of carbohydrates and, as a result, the reduction of the share of free moisture between the molecules of the milk protein clot leads to a stabilizing effect, due to the enveloping and strengthening of the protein framework. From a practical point of view, this is how you can justify the use of purple corn during acid-rennet coagulation of milk proteins to bind free moisture and prevent syneresis during curd storage.

At the next stage of research, the change in active acidity and moisture-retaining capacity of milk protein clots was studied depending on the amount of purple corn powder (Fig. 6).

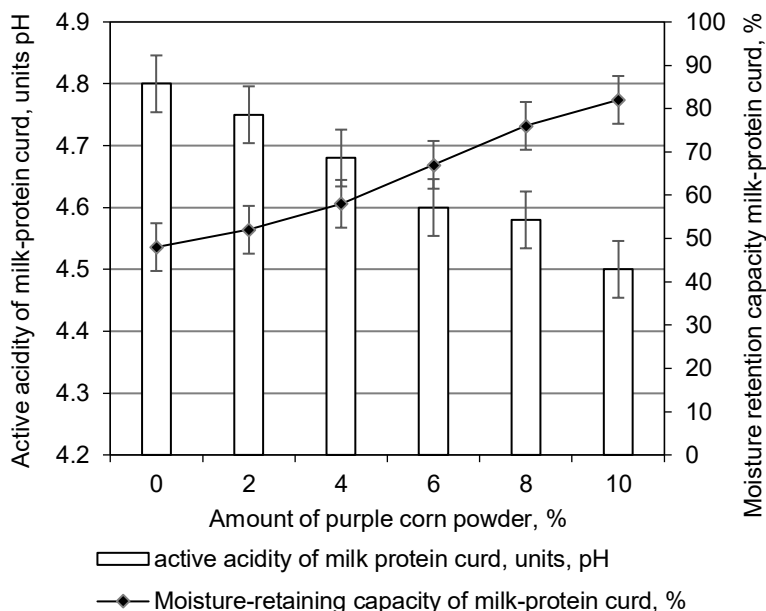


Figure 6. Active acidity and moisture-retaining capacity of milk-protein clots depending on the amount of purple corn powder

An increase in the content of purple corn powder during the production of milk protein clots, their active acidity decreased. pH, indicators of active acidity, ranged from 4.75 to 4.50 units, in samples of milk protein clots with a grain ingredient in the amount from 2% to 10%. The value of the active acidity of the experimental samples was by 0.05–0.30 pH units lower than in the control sample. When purple corn powder was added, the active acidity of the curd decreased, which indicates the effect of the grain additive on the microflora, in particular on the content of lactic acid bacteria.

From the obtained values of moisture-retaining capacity (Fig. 6) it can be seen that with an increase in the content of purple corn powder, this indicator changes for all milk protein clots, while the dynamics are different. This is due to the appropriate content of starch in corn powder, whose polysaccharides absorb water. When adding a grain additive 2% to 4%, the difference between the indicators of the moisture-holding capacity of the control and

experimental samples was less pronounced and consisted 4–10%. The highest values of retention capacity samples were observed in samples with the addition of 8±2% purple corn powder and were on average by 19–34% higher than for the control sample. In addition, the formation of a denser consistency than the control was characteristic of the above-mentioned samples of milk-protein clots.

During the production of protein clots, about 80% of the colored whey was obtained from the volume of milk raw materials. Serum samples had a natural purple color due to the high content of specific coloring substances in corn grains – bioflavonoids and anthocyanins, which are powerful antioxidants.

The qualitative characteristics and optical density reflected the turbidity and color of the dyed whey were determined and compared with the control, which are listed in Table 2.

Table 2
Qualitative characteristics and optical density of stained serum

Amount of powder from purple corn, %	Serum content		Active acidity, units pH	Optical density, D _k , cond. unit	Optical density after filtering, D, cond. unit
	dry substances, %	protein, %			
2	7.3±0.15	0.50±0.02	6.15±0.12	1.75±0.05	1.03±0.03
4	7.1±0.13	0.46±0.01	6.10±0.12	1.72±0.05	1.07±0.03
6	6.8±0.14	0.40±0.02	5.99±0.11	1.64±0.05	1.12±0.03
8	6.3±0.13	0.37±0.02	5.92±0.12	1.60±0.048	1.16±0.04
10	6.1±0.12	0.36±0.01	5.85±0.11	1.58±0.05	1.20±0.04
Control	7.5±0.12	0.52±0.02	6.19±0.12	–	–
Control*	–	–	–	1.63±0.05	1.15±0.03

* Colored whey drink "Actual" with watermelon-melon flavor produced by "Danon Dnipro" LLC

The content of dry substances of colored serum was at the level of 6.1–7.3%, including protein 0.36–0.50%. Compared with the control sample, the dyed serum had a lower content of dry matter and, accordingly, protein, which confirms the effectiveness of acid-serum coagulation of proteins. The active acidity of the dyed serum samples was within 5.85–6.15 units. The pH depended on the amount of purple corn powder added during the production of milk protein clots.

The optical density of serum samples when determining turbidity and color ranged from 1.57 to 1.75 and 1.02 to 1.19 μm. Almost all of these values have deviations from control up to 5%.

Coloured whey obtained as a result of the production of milk-protein clots with the addition of various amounts of grain additives can be used with or without additional processing (clarification, deacidification) as a base and recipe component for whey drinks of the type "pasteurized whey" or "pasteurized whey with sugar". This allows eliminating the use of artificial food colourings in their composition.

Conclusions

The possibility of effective use of purple corn powder in the production technology of milk protein clots by acid-rennet coagulation of goat milk proteins has been shown.

The dispersion of purple corn powder was determined, the main particle fractions of which were in the range from 20 to 40 microns ($26 \pm 1.3\%$) and from 40 to 60 microns ($43 \pm 2.1\%$). Parameters to prepare purple corn powder for addition to goat's milk are as follows: the swelling and dissolution temperature is $80\text{ }^\circ\text{C}$ and the holding time is 20 minutes.

It was found that when the amount of purple corn powder increased from 2 to 10%, the yield of milk protein clots increased from 3.45% to 17.91%, the content of moisture decreased from 73.36% to 67.15%, and their active acidity decreased from 4.75 to 4.50 pH units. The optimal amount of purple corn powder was 6% to 8% of the mass of goat's milk.

Milk protein clots can be used in the recipes of curd products with an adjustable content of moisture, active acidity, moisture-retaining ability and natural color.

The obtained colored whey could be classified as a functional raw material, which has original taste and color characteristics and expands the use of colored whey drinks in technology.

References

- Abbas H. M., Hassan F. A., Abd El-Gawad M. A., Enab A. K. (2014), Physicochemical characteristics of goat's milk, *Life Science Journal*, 11, pp. 307–317.
- Abd El-Gawad M. A. M., Ahmed N. S. (2011), Cheese yield as affected by some parameter, *Acta Scientiarum Polonorum, Technologia Alimentaria*, 10(2), pp. 131–153, https://www.food.actapol.net/volume10/issue2/1_2_2011.pdf
- Antonenko P. P., Chumak S. V., Chumak V. O. (2019), Physical and chemical composition of goat milk during smallholder production in the conditions of the natural and agricultural zone of the steppe of Ukraine, *Theoretical and Applied Veterinary Medicine*, 7(4), pp. 198–204, <https://doi.org/10.32819/2019.74035>
- Aparna S., Patel K., Patel S., Pinto S. (2015), Wheat and its application in dairy products, *Research & Reviews: Journal of Dairy Science and Technology*, 4(2), pp. 19–34.
- Benjamin-van Aalst O., Dupont C., van der Zee L., Garssen J., Knipping K. (2024), Goat milk allergy and a potential role for goat milk in cow's milk allergy, *Nutrients*, 16, 2402, <https://doi.org/10.3390/nu16152402>
- Caleja C., Ribeiro A., Barros L., Barreira J.C., Antonio A.L., Oliveira M.B.P., Barreiro M.F., Ferreira I.C. (2016), Cottage cheeses functionalized with fennel and chamomile extracts: Comparative performance between free and microencapsulated forms. *Food Chemistry*, 199(15), pp. 720–726, <https://doi.org/10.1016/j.foodchem.2015.12.085>
- Delgado-Vargas F., Jiménez A.R., Paredes-López O. (2000), Natural pigments: carotenoids, anthocyanins, and betalains — characteristics, biosynthesis, processing, and stability. *Critical Reviews in Food Science and Nutrition*, 40(3), 173–289, <https://doi.org/10.1080/10408690091189257>
- Denisova E.A. (2015), Cheese and cereal products, *Food and Processing Industry*, 2, pp. 12–13 (in Ukrainian).
- Domínguez R., Pateiro M., Munekata P.E.S., Santos López E.M., Rodríguez J.A., Barros L., Lorenzo J.M. (2021), Potential use of elderberry (*Sambucus nigra* L.) as natural colorant and antioxidant in the food industry. A review, *Foods*, 10(11), 2713, <https://doi.org/10.3390/foods10112713>
- Getaneh G., Mebrat A., Wubie A., Kendie H. (2016), Review on goat milk composition and its nutritive value, *Journal of Nutrition and Health Sciences*, 3(4), 401, <https://doi.org/10.15744/2393-9060.3.401>

- Ghanbari M., Mortazavian A.M., Ghasemi J.B., Mohammadi A., Hosseini H., Neyestani T.R. (2017), Formulation and development of a new prebiotic cereal-based dairy dessert: rheological, sensory and physical attributes, *Food Science and Technology Research*, 23(5), pp. 637-649, <https://doi.org/10.3136/fstr.23.637>
- Grek O., Tymchuk A., Tsygankov S., Onopriichuk, O., Savchenko O., Ochkolyas O. (2019), Methods for determining the characterization of mashes with fiber for semi-finished products on the milk-protein base, *EUREKA: Life Sciences*, 6, pp. 50–56, <https://doi.org/10.21303/2504-5695.2019.001046>
- Grek O., Ovsienko K., Tymchuk A., Onopriichuk O., Kumar A. (2020a), Influence of wheat food fiber on the structure formation process of wheycreamy cheeses, *Ukrainian Food Journal*, 9(2), pp. 332–343. <https://doi.org/10.24263/2304-974X-2020-9-2-6>.
- Grek O., Pshenychna T., Chubenko L., Onopriichuk O. (2020b), Polyphenol composition and technological characteristics of the coloured whey from various origin, *Ukrainian Food Journal*, 9(4), pp. 832–843, <https://doi.org/10.24263/2304-974X-2020-9-4-9>
- Güneşer O. (2016), Pigment and color stability of beetroot betalains in cow milk during thermal treatment, *Food Chemistry*, 196, 220–227, <https://doi.org/10.1016/j.foodchem.2015.09.033>
- Gyorgy E., Laslo E. (2021), Influence of milk used for cheese making on microbiological aspects of Camembert-type cheese. *Acta Universitatis Sapientiae Alimentaria*, 14, pp. 84–94, <https://doi.org/10.2478/ausal-2021-0005>
- Hamad M.N., Ismail M.M. (2012), Quality of soft cheese made with goat's milk as affected with the addition of certain essences, *Journal of Animal and Veterinary Advances*, 2(2), pp. 121–127, <https://doi.org/10.21608/jfds.2011.81945>
- Hashim I.B., Khalil A.H., Afifi H.S. (2009), Quality characteristics and consumer acceptance of yogurt fortified with date fiber, *Journal of Dairy Science*, 92(11), pp. 5403–5407, <https://doi.org/10.3168/jds.2009-2234>
- Kiiru S., Mahungu S., Omwamba M. (2018), Preparation and analysis of goat milk mozzarella cheese containing soluble fiber from *Acacia senegal* var. *kerensis*, *African Journal of Food Science*, 12(3), pp. 46–53, <https://doi.org/10.5897/AJFS2017.1652>
- Kochubei-Lytvynenko O., Korolchuk I., Yushchenko N., Kuzmyk U., Frolova N., Pasichny V., Mykoliv I. (2019), Perspective the use of goat milk in the production of soft milk cheeses, *Ukrainian Journal of Food Science*, 7(2), pp. 250-263, <https://doi.org/10.24263/2310-1008-2019-7-2-9>
- Malyarenko T.V. (2015), The effect of plant components on the consistency of fermented milk curds, *Scientific Bulletin "Askania-Nova"*, 8, pp. 68-78
- Mendonca V. (2023), Modern food habits and its impact on human health, *International Journal of Innovative Research in Engineering and Management*, 10 (4), pp. 182–185, <https://doi.org/10.55524/ijirem.2023.10.4.24>
- Mora-Rochin S., Gutiérrez-Uribe J.A., Serna-Saldivar S.O., Sánchez-Peña P., Reyes-Moreno C., Milán-Carrillo J. (2010), Phenolic content and antioxidant activity of tortillas produced from pigmented maize processed by conventional nixtamalization or extrusion cooking, *Journal of Cereal Science*, 52, pp. 502–508, <https://doi.org/10.1016/j.jcs.2010.08.010>
- Park Y., Juarez M., Ramos M., Haenlein G. (2007), Physico chemical characteristics of goat and sheep milk, *Small Ruminant Research*, 68(1–2), pp. 88-113, <https://doi.org/10.1016/j.smallrumres.2006.09.013>
- Rabie M.M., Faten Y.I., Youssif M.R.G., El-Ragal N.M.E. (2020), Effect of *Moringa oleifera* leaves and seeds powder supplementation on quality characteristics of cookies, *Journal of Food and Dairy Sciences*, 11(2), pp. 65–73, <https://doi.org/10.21608/jfds.2020.78888>
- Ramos-Escudero F., Muñoz A. M., Alvarado-Ortiz C., Alvarado A., Yáñez J.A. (2012), Purple corn (*Zea mays* L.) phenolic compounds profile and its assessment as an agent against oxidative stress in isolated mouse organs, *Journal of Medical Food*, 15(2), pp. 206-215, <https://doi.org/10.1089/jmf.2010.0342>
- Raynal-Ljutovac K., Le Pape M., Gaborit P., Barrucand P. (2011), French goat milk cheeses: An overview on their nutritional and sensorial characteristics and their impacts on consumers' acceptance, *Small Ruminant Research*, 101(1–3), pp. 64-72, <https://doi.org/10.1016/j.smallrumres.2011.09.026>

- Romanchuk I.O., Rudakova T.V., Moiseeva L.O., Gondar O.P. (2016), Rice flour as a stabilizer in fermented milk products, *Food Resources*, 7, pp. 46–52 (in Ukrainian)
- Ryzhkova T., Odarchenko A., Silchenko K., Danylenko S., Verbytskyi S., Heida I., Kalashnikova L., Dmytrenko A. (2023), Effect of herbal extracts upon enhancing the quality of low-fat cottage cheese, *Innovative Biosystems and Bioengineering*, 7(2), pp. 22–31, <https://doi.org/10.20535/ibb.2023.7.2.268976>
- Sant'Ana A. M. S., Bezerril F. F., Madruga M. S., Batista A. S. M., Magnani M., Souza E.L., Queiroga R.C.R.E. (2013), Nutritional and sensory characteristics of Minas fresh cheese made with goat milk, cow milk, or a mixture of both, *Journal of Dairy Science*, 96(12), pp. 7442–7453, <https://doi.org/10.3168/jds.2013-691>
- Singh S., Kaur G., Partap R., Preet G. (2021), Goat milk composition and nutritional value: A review, *The Pharma Innovation Journal*, 10(6), pp. 536–540.
- Stabnikova O., Marinin A., Stabnikov V. (2021), Main trends in application of novel natural additives for food production, *Ukrainian Food Journal*, 10(3), pp. 524–551, <https://doi.org/10.24263/2304-974X-2021-10-3-8>
- Stabnikova O., Stabnikov V., Paredes-López O. (2024), Fruits of wild-grown shrubs for health nutrition, *Plant Foods for Human Nutrition*, 79(1), pp. 20–37, <https://doi.org/10.1007/s11130-024-01144-3>
- Stergiadis S., Nørskov P., Purup S., Givens I., Lee M.R. (2019), Comparative nutrient profiling of retail goat and cow milk, *Nutrients*, 11, pp. 2–26, <https://doi.org/10.3390/nu11102282>
- Sukhova I.V., Romanova T.N., Korosteleva L.A., Baimishev R.H., Dolgosheva E.V. (2019), The effect of hydrated oatmeal on quality of the symbiotic fermented milk product, *BIO Web of Conferences*, 17, pp. 1–8, <https://doi.org/10.1051/bioconf/20201700052>
- Tacca L.E., Guzmán F.F., Yanamango E.G., Socantaype F.V. (2018), Evaluation of some functional properties of purple corn (*Zea mays* L.) dye, during its processing at pilot scale, *Innovation in Education and Inclusion : Proceedings of the 16th LACCEI International Multi-Conference for Engineering, Education and Technology*, July 18–20, 2018, Lima, Perú, <https://doi.org/10.18687/LACCEI2018.1.1.290>
- Trehan S., Singh N., Kaur A. (2018), Characteristics of white, yellow, purple corn accessions: Phenolic profile, textural, rheological properties and muffin making potential, *Journal of Food Science Technology*, 55, pp. 2334–2343, <https://doi.org/10.1007/s13197-018-3171-5>
- Turkmen, N. (2017). The nutritional value and health benefits of goat milk components. In: R.R. Watson, R.J. Collier, V.R. Preedy (Eds.), *Nutrients in Dairy and their Implications on Health and Disease*, pp. 441–449, <https://doi.org/10.1016/b978-0-12-809762-5.00035-8>
- Vilcacundo E., García A., Vilcacundo M., Morán R., Samaniego I., Carrillo W. (2020), Antioxidant purple corn protein concentrate from germinated andean purple corn seeds, *Agronomy*, 10(9), 1282, <https://doi.org/10.3390/agronomy10091282>

Cite:

UFJ Style

Grek V., Pshenychna T., Onopriichuk O., Grek O. (2024), Milk protein clots obtained by the addition of purple corn powder, *Ukrainian Food Journal*, 13(2), pp. 247–261, <https://doi.org/10.24263/2304-974X-2024-13-2-4>

APA Style

Grek, V., Pshenychna T., Onopriichuk, O., & Grek O. (2024). Milk protein clots obtained by the addition of purple corn powder. *Ukrainian Food Journal*, 13(2), 247–261. <https://doi.org/10.24263/2304-974X-2024-13-2-4>

Volatile composition and aromatic descriptors of red wines from different regions of Bulgaria aged with oak chips

Dimitar Dimitrov, Tatyana Yoncheva

Agricultural Academy, Institute of Viticulture and Enology, Pleven, Bulgaria

Abstract

Keywords:

Oak
Aroma
Red wines
Volatile
compounds
Bulgaria

Article history:

Received 14.01.2024
Received in revised
form 22.04.2024
Accepted 2.07.2024

Corresponding author:

Dimitar Dimitrov
E-mail:
dimitar_robertov@
abv.bg

DOI:10.24263/2304-
974X-2024-13-2-5

Introduction. The aim of the present study was to define the volatile composition and related aromatic descriptors in red wines from different regions of Bulgaria, aged with oak chips.

Materials and methods. Four red wines provided by the commercial network were analyzed. A different oak aging technology was applied. Gas chromatography-flame ionization detection was used to determine the volatile compounds. Organoleptic evaluation and descriptive analysis of the red wines were made.

Results and discussion. The highest total accumulation of volatile compounds in the analyzed commercial red wines obtained in contact with oak wood was found in Cabernet Franc wine. The most significant levels of total higher alcohols were also found in it. The ester fraction was quantitatively dominant in the Cabernet Sauvignon/Merlot wine, and the most terpenes were identified in the complex Carmenere/Cabernet Sauvignon/Cabernet Franc/Merlot blend. Main higher alcohols in red wines were 2-methyl-1-butanol, 3-methyl-1-butanol, 1-propanol and 1-butanol. The ester fraction was quantitatively dominated by ethyl acetate. The terpene fraction was represented by linalool, linalool oxide, and nerol. A major aldehyde was acetaldehyde, found at levels that positively affect the fruity aroma of the red wines. Methyl alcohol was found at levels significantly below the threshold of its normally permissible presence in red wines. Wines from the commercial network had different sensory characteristics in terms of color, aroma and taste, as well as characteristic aromatic descriptors, which was due to the different type and quantity of oak wood used, as well as the duration of contact.

Conclusions. All the studied wines showed a complex and varied volatile profile and different aromatic descriptors due to the varietal characteristics of the grapes used, the soil and climatic conditions of each specific harvest and region and the specific influence of the applied method of contact with oak wood.

Introduction

The aging of wines with oak wood is a technological practice widely used in winemaking nowadays. It initiates significant changes in the wine composition, which are expressed in the main several aspects: it complicates the aroma by accumulating new aromatic compounds in the wine; has a stabilizing effect on the wine color characteristics; has a positive effect on the clarification process (Mártinez-Gil et al., 2022). The contact with wood leads to a significant change of the wine volatile fraction through the accumulation of different compounds (specific to oak) that affect both the taste qualities of the wine and its aroma (Pérez-Juan and Luque de Castro, 2015). There are various studies concerning the application of oak wood in different forms and techniques. It is applied at various stages in the vinification process, as well as during storage and wine aging. González-Centeno et al. (2021) investigated the volatile composition and sensory profile of Merlot red wines in contact with oak wood applied in different forms during the fermentation and aging processes. It was found that the larger contact surface of the oak leads to the extraction and accumulation in the wine of high levels of specific aromatic compounds that intensify the aroma with two main descriptors – vanilla and spice. Cerdan et al. (2004) studied the accumulation of volatile compounds in two red wines (Cabernet Sauvignon and Merlot) during their aging in oak barrels for periods of 17 and 18 months, respectively. It was observed that Merlot wine extracted more specific compounds from the wood than Cabernet Sauvignon. Based on this, it was concluded that when aging red wines in oak barrels, it is not only the origin of the oak, its age and degree of roasting, but also the specific composition of the wine in contact that matters for the complexity of the wine's aroma. Perez-Prieto et al. (2002) found that when wines were aged in new and used American and French oak barrels, there was less accumulation of vanillin and lactones when the wine was in contact with a used barrel. Also, the volatile profile of wines aged in smaller barrels is significantly different from that of larger capacity barrels. Perez-Prieto et al. (2002) classified the detected concentration of *cis*-lactone in the wines as the most significant difference between the American and French oak used. Dimitriu et al. (2017) found that when Fetjaska Negra wines were aged for 1.5 and 3 months in oak barrels, the degree of wood roasting and contact time significantly influenced the aromatic and phenolic profile. Del Fresno et al. (2020) investigated the evolution in the volatile composition of wines aged for 8 months in oak barrels and found significant changes in the concentrations of volatile phenols, furans and phenolic aldehydes during the aging process. Herjavec et al. (2007) found an increase in furfural, 5-methylfurfural, guaiacol, eugenol and *cis*- and *trans*-lactones in Vugawa wines aged in oak barrels produced from *Quercus petraea* and *Quercus robur* wood. Lu et al. (2024) investigated the modification in the aroma of a dry wine aged in American, French and Slovakian oak barrels with different degrees of roasting and identified 30 oak-associated compounds, the amounts of which increased in the wine with increasing contact time, and the descriptors characterizing the wines were associated with prominent caramel, floral, fruity, smoky, roasted, and leather aromas.

The aim of the present study was to define the volatile composition and related aromatic descriptors in red wines from different regions of Bulgaria aged with oak chips.

Materials and methods

Researched wines /variety, harvest, region/ and contact with oak chips

The study was conducted in 2023. Four red wines provided by the commercial network were analyzed. A different oak aging technology was applied. The information about the examined wines is as follows:

Cabernet Franc red wine (town of Varna, region of Northern Bulgaria), harvest 2021. The wine was in contact with medium-roasted French oak chips, at a dose of 1 g/l. The duration of contact was 8 months.

Syrah red wine (town of Varna, region of Northern Bulgaria), harvest 2021. The wine was in contact with medium-roasted French oak chips, at a dose of 1 g/l. The duration of contact was 2–2.5 months.

Cabernet Sauvignon/Merlot red wine (town of Asenovgrad, Southern Bulgaria region), harvest 2019. The wine was in contact with American, highly roasted, medium-sized oak chips. The duration of contact was 3–4 months.

Red wine Carmenere (50%)/Cabernet Sauvignon (30%)/Cabernet Franc (20%)/Merlot (10%) (town of Harmanli, Southern Bulgaria region), harvest 2022. The wine was in contact with French oak chips, medium roasted, in a dose of 0.3 g/l. The duration of contact was 3 months.

Gas chromatographic analysis (GC-FID)

The content of the main volatile compounds was determined based on a stock standard solution prepared in accordance with IS 3752:2005 method. The method describes the preparation of a standard solution of one congener, but the preparation step was followed to prepare a solution of more compounds. The standard solution in the present study included the following compounds (purity > 99.0%): acetaldehyde, ethyl acetate, methanol, 2-propanol, isopropyl acetate, 1-propanol, 2-butanol, propyl acetate, 1-butanol, isobutyl acetate, ethyl butyrate, 2-butyl acetate, 2-methyl-1-butanol, 3-methyl-1-butanol, 4-methyl-2-pentanol, 1-pentanol, pentyl acetate, 1-hexanol, ethyl hexanoate, hexyl acetate, 1-heptanol, linalool oxide, dimethyl succinate, phenyl acetate, linalool, ethyl caprylate, 2-phenylethanol, α -terpineol, nerol, β -citronellol, geraniol, ethyl decanoate. The prepared standard solution containing all compounds was injected in an amount of 2 μ l into a gas chromatograph Varian 3900 (Varian Analytical Instruments, Walnut Creek, California, USA) with a capillary column VF max MS (30 m, 0.25 mm ID, DF= 0.25 μ m), equipped with flame ionization detector (FID). The carrier gas was helium. Hydrogen to support combustion was supplied to the chromatograph via a hydrogen bottle. The injection was manual, using a microsyringe. The gas chromatographic determination parameters were: injector temperature – 220°C, detector temperature – 250°C, initial oven temperature – 35°C/1 min retention, rise to 55°C with a step of 2°C/min for 11 min, rise to 230°C with a step of 15°C/min for 3 min. Total chromatography time – 25.67 min. After the retention times of the compounds in the standard solution were determined, the identification and quantification of the volatile compounds in the wines were conducted. The volatile composition was determined based on the injection of wine distillates. Samples were injected in an amount of 2 μ l into a gas chromatograph and identification and quantification of volatile compounds was performed.

Sensory profile and aroma descriptors

Nine members of the tasting commission in the Institute of Viticulture and Enology participated in the organoleptic analysis. The samples were evaluated on a 100-point scale, including the following indicators: color, aroma, taste and general impressions. When processing the results, the highest and lowest obtained marks were removed. To define the aromatic and taste wines characteristics, as a result of their contact with oak wood, the method of the main characteristics was used, through a descriptive analysis (Prodanova, 2008).

Results and discussion

The data on the detected volatile compounds in the analyzed red wines are presented in Table 1.

Total content of volatile compounds and individual higher alcohols

By the total accumulation of volatile compounds in red wines, Cabernet Franc dominated, 422.56 ± 70.93 mg/l. The Cabernet Sauvignon/Merlot and Syrah variants showed very close concentration of volatile compounds, and Carmenere/Cabernet Sauvignon/Cabernet Franc/Merlot accumulated the lowest levels of volatile compounds, 157.09 ± 20.89 mg/l, comparing it to the other three red wines.

This trend was preserved regarding the found total content of higher alcohols too, but the differences between the variants were smaller. The most significant total content of higher alcohols, 273.34 ± 30.17 mg/l, was found in Cabernet Franc.

The main representatives of the higher alcohols fraction identified in all red wines were 2-methyl-1-butanol, 3-methyl-1-butanol, 1-propanol and 1-butanol. The highest amount of these four main higher alcohols was characterized by 3-methyl-1-butanol. In Cabernet Franc wine, it was found in the highest concentration, 120.27 ± 13.89 mg/l, followed by Cabernet Sauvignon/Merlot with an almost twice lower concentration, 69.98 ± 8.83 mg/l. The other two variants showed similar levels in the quantitative presence of this higher alcohol. Martinez-Gil et al. (2022) studied the changes occurring in red wines during the aging process in oak barrels for 12 months at different levels of oxygen transmission. It was found that 3-methyl-1-butanol was the higher alcohol present in the highest concentration. Its variation in the studied variants ranged from 234.50 ± 2.61 mg/l to 292.10 ± 4.07 mg/l. The concentrations found in the present study were lower. Slightly lower concentrations of 3-methyl-1-butanol, ranged from 36.77 ± 0.53 mg/l to 42.25 ± 2.25 mg/l, were found by Slaghenaufi et al. (2021) in a study of the volatile composition of single-varietal red wines from San Pietro in Cariano, Italy.

The second /by concentration/ higher alcohol identified in all analyzed red wines was 1-butanol. It was present in the highest amount in Carmenere/Cabernet Sauvignon/Cabernet Franc/Merlot, 50.33 ± 10.03 mg/l. Its concentrations in Cabernet Sauvignon/Merlot and Cabernet Franc wines were very close, and the lowest amount of this higher alcohol, 31.41 ± 9.56 mg/l, was identified in Shiraz. The amount of this component normally varies in wines from 1.00 to 64.00 mg/l (Chobanova, 2012). Slaghenaufi et al. (2021) found a variation of 1-butanol from 82.16 ± 2.28 mg/l to 155.50 ± 2.65 mg/l in seven red wines from the San Pietro in Cariano region, Italy. Kim et al. (2018) investigating the aromatic compounds in 11 red wines from introduced varieties grown in the Republic of Korea found the presence of 1-butanol in only two of the studied wines – Chancellor and Marchel, and in very low concentrations, respectively 99.10 µg/l and 13.59 µg/l.

Table 1
Volatile compounds in commercial red wines obtained by contact with oak wood

Identified compounds, mg/l	Red wines			
	Cabernet Sauvignon/Merlot	Cabernet Franc	Carmenere/Cabernet Sauvignon/Cabernet Franc/Merlot	Shiraz
Acetaldehyde	27.77±0.00	52.27±7.47	8.92±0.00	57.65±4.26
Methanol	3.13±0.39	7.37±3.79	12.28±5.10	6.55±0.41
2-methyl-1-butanol	15.34±1.02	25.03±5.98	11.17±1.77	7.05±2.78
3-methyl-1-butanol	69.98±8.83	120.27±13.89	44.84±1.24	42.29±12.82
4-methyl-1-pentanol	nd	1.60±0.00	0.95±0.19	nd
1-propanol	0.70±0.23	7.60±1.42	1.58±0.22	5.91±0.49
1-pentanol	nd	nd	nd	0.65±0.23
1-butanol	49.57±15.63	46.48±5.48	50.33±10.03	31.41±9.56
2-butanol	6.50±3.90	41.99±2.62	2.50±0.00	nd
1-hexanol	nd	30.37±0.78	nd	nd
2-phenylethanol	nd	nd	nd	48.67±7.01
Total higher and aromatic alcohols	142.09±29.61	273.34±30.17	111.37±13.45	135.98±32.89
Ethyl acetate	53.91±4.69	18.90±8.52	22.60±2.26	34.31±4.90
Pentyl acetate	40.26±6.71	nd	nd	nd
Propyl acetate	nd	nd	nd	1.51±0.00
Isopropyl acetate	nd	2.78±0.46	nd	nd
Isobutyl acetate	nd	nd	nd	nd
Phenyl acetate	29.18±1.36	nd	nd	nd
Ethyl hexanoate	nd	nd	nd	20.52±1.02
Ethyl butyrate	nd	2.32±1.35	1.02±0.00	1.66±0.55
Ethyl decanoate	nd	64.88±19.08	nd	9.26±0.93
Total esters	123.35±12.76	88.88±29.41	23.62±2.26	67.26±7.40
Linalool oxide	nd	0.23±0.05	nd	nd
Linalool	0.23±0.06	0.47±0.04	0.90±0.08	nd
Nerol	nd	nd	nd	0.12±0.01
Geraniol	nd	nd	nd	nd
Total terpenes	0.23±0.06	0.70±0.09	0.90±0.08	0.12±0.01
Total content	296.57±42.82	422.56±70.93	157.09±20.89	267.56±44.97

Note: Cabernet Sauvignon/Merlot, harvest 2019, Asenovgrad, Southern Bulgaria; Cabernet Franc, harvest 2021, Varna, Northern Bulgaria; Carmenere/Cabernet Sauvignon/Cabernet Franc/Merlot, harvest 2022, Harmanli, Southern Bulgaria; Shiraz, harvest 2021, Varna, Northern Bulgaria.

*nd – not detected

2-methyl-1-butanol ranked third by the concentration presence in the analyzed wines. It was found in the highest amount, 25.03±5.98 mg/l, in Cabernet Franc. Its concentration was the lowest, 7.05±2.78 mg/l, in Shiraz. Dimitriu et al. (2019) investigated the effect of different types of oak chips (American and French) applied at different doses (3 and 5 g/l) and different contact times with the chips (1.5 to 3 months) with Fetjaska Negra wine

(Romania) on its aromatic composition. The determined content of 2-methyl-1-butanol varied between the variants from 531.00 ± 7.00 mg/l to 571.00 ± 1.00 mg/l. The content of 2-methyl-1-butanol in the present study was lower. Martinez-Gil et al. (2022) when studying changes in the composition of red wines in oak barrels at different oxygen transmission found a variation in the content of 2-methyl-1-butanol between the variants from 58.55 ± 1.20 mg/l to 74.05 ± 1.27 mg/l.

1-propanol was also identified in the four red wines studied. The highest concentration, 7.60 ± 1.42 mg/l, was found in Cabernet Franc wine, followed by Shiraz, 5.91 ± 0.49 mg/l. In the other two wines, its contents were lower, and in the Cabernet Sauvignon/Merlot variant, this higher alcohol was found in the lowest amount, 0.70 ± 0.23 mg/l. Different studies of red wines in contact with oak wood found a variation of this higher alcohol from 26.85 ± 2.20 mg/l to 34.58 ± 0.52 mg/l and from 36.00 ± 0.20 mg/l to 40.00 ± 1.00 mg/l, levels which were higher than those found in the present study (Dimitriu et al., 2019; Martinez-Giletal., 2022). In Spanish red wines of traditional varieties, it was found to vary from 19.48 ± 0.71 mg/l to 30.18 ± 6.94 mg/l (Cortés-Diéguez et al., 2015). The data obtained in the present study on the presence of 1-propanol in the analyzed red wines correlated with the results of Zhang et al. (2012), who investigated young red Merlot wines from different regions of China and determined 1-propanol content from 4.152 mg/l to 9.723 mg/l.

1-pentanol and 1-hexanol were found in two of the examined wines – Shiraz and Cabernet Franc, respectively in concentrations of 0.65 ± 0.23 mg/l and 30.37 ± 0.78 mg/l. At low and close to established concentrations, 1-pentanol was identified in Cabernet Sauvignon and Cabernet Gernischt red wines from a region in China, at concentrations of 0.1767 mg/l and 0.1468 mg/l, respectively (Jiang and Zhang, 2010). The same authors found 1-hexanol in the two studied red wines at concentrations of 4.01 mg/l and 2.54 mg/l, respectively – levels that were significantly lower than those found in the present study. 1-hexanol imparts a grassy aroma and was also found in another study on the volatile composition of red wines from China in amounts from 0.80 to 3.70 mg/l (Zhang et al., 2012). The levels of this alcohol found in the present study were higher.

2-butanol was identified in three of the red wines studied. This component was not identified only in Shiraz wine. Its highest levels, 41.99 ± 2.62 mg/l, were found in Cabernet Franc. The lowest amounts, 2.50 ± 0.00 mg/l, were found in Carmenere/Cabernet Sauvignon/Cabernet Franc/Merlot.

2-phenylethanol was identified only in Shiraz wine in the amount of 48.67 ± 7.01 mg/l. It is an aromatic alcohol characterized by a rose aroma. 2-phenylethanol was found in concentrations from 19.80 ± 1.11 mg/l to 26.67 ± 1.67 mg/l in single-varietal red wines from Italy (Slaghenaufi et al., 2021). According to Chobanova (2012), phenylethanol can be found in wine in very wide concentration ranges - from 10.00 to 150.00 mg/l. The data obtained in the present study correlated with this range.

Total content of esters and individual representatives

Regarding the total esters accumulation, their amount, 123.35 ± 12.76 mg/l, was highest in Cabernet Sauvignon/Merlot red wine. Cabernet Franc also showed high esters levels, 88.88 ± 29.41 mg/l, and the lowest concentration of esters, 23.62 ± 2.26 mg/l, was found in Carmenere/Cabernet Sauvignon/Cabernet Franc/Merlot. Manolache et al. (2018) studied red wines from four varieties from Romania and found a variation in the total ester content from 11.16 ± 0.03 mg/l to 41.16 ± 0.54 mg/l, which was consistent with that found in Carmenere/Cabernet Sauvignon/Cabernet Franc/Merlot in the present study. The remaining varieties of red wines studied showed a higher total content of esters.

The main ester was ethyl acetate. It was present in the highest amount, 53.91 ± 4.69 mg/l, in Cabernet Sauvignon/Merlot wine. In the other variants, it changed from 18.90 ± 8.52 mg/l (Cabernet Franc) to 34.31 ± 4.90 mg/l (Shiraz). The data obtained for this ester correlated with those established by Dimitriu et al. (2019), who investigated the influence of oak chips and arcs with different roasting degrees on the aromatic composition of red wines from the Fetjaska Negra variety grown in Romania. The period of contact with the wood was 1.5 to 3 months. In the experimental variants, they found a variation in ethyl acetate content from 28.0 ± 1.0 mg/l to 34.0 ± 1.0 mg/l, which was actually not significant between the control and experimental variants. The data on the concentration presence of this ester in the present study also correlated with that established by Martinez-Gil et al. (2022). They investigated the evolution in aromas of red wines aged in oak barrels for periods of 3, 6, 9 and 12 months at different oxygen transmission and found a variation in ethyl acetate content from 47.12 ± 0.11 mg/l to 85.75 ± 1.50 mg/l, with the lowest level in the control variant (0 months). All concentrations of ethyl acetate found in the present study were in a range having a positive effect on the aroma of the studied wines – with the appearance of fruity nuances.

Ethyl butyrate was detected in three of the red wines tested. It was missing only in the Cabernet Sauvignon/Merlot variant. Its difference between the three experimental variants was not large, and it varied between them from 1.02 ± 0.00 mg/l (Carmener/Cabernet Sauvignon/Cabernet Franc/Merlot) to 2.32 ± 1.35 mg/l (Cabernet Franc). In the study of Dimitriu et al. (2019) this ester was found in lower amounts ranging from 0.250 ± 0.006 to 0.532 ± 0.037 mg/l. Lower levels were found also by Česnik et al. (2015) in a study of 82 wines from the Kras region, Slovenia, from three harvests (2011-2013). The ethyl butyrate in them varied from 0.08 ± 0.014 mg/l to 0.11 ± 0.052 mg/l.

Other established esters were pentyl acetate, which was identified only in Cabernet Sauvignon/Merlot variant at a concentration of 40.26 ± 6.71 mg/l; propyl acetate identified only in Shiraz variant with amount of 1.51 ± 0.00 mg/l; isopropyl acetate – found in Cabernet Franc in an amount of 2.78 ± 0.46 mg/l; phenyl acetate – present in Cabernet Sauvignon/Merlot in the amount of 29.18 ± 1.36 mg/l; and ethyl decanoate, which was found in two of the examined wines – Cabernet Franc and Shiraz in amounts of 64.88 ± 19.08 mg/l and 9.26 ± 0.93 mg/l, respectively.

Total content of terpenes and individual representatives

The highest total terpene content, 0.90 ± 0.08 mg/l, in the studied red wines was found in the Carmenere/Cabernet Sauvignon/Cabernet Franc/Merlot variant. Cabernet Franc also showed high levels, 0.70 ± 0.09 mg/l. The levels of total terpenes identified were low, 0.23 ± 0.06 mg/l, in Cabernet Sauvignon/Merlot, and Shiraz showed the lowest, 0.12 ± 0.01 mg/l, total terpene content. Monoterpenes are responsible for the so-called muscat aroma and accordingly in muscat varieties they are contained in an amount on average up to about 6.0 mg/l, in non-muscat aromatic varieties their concentration varies from 1.0 to 4.0 mg/l, and in neutral varieties their amount are lower than 1.0 mg/l (Mateo and Jimenez, 2000). Data for total monoterpene content found in the present study were in agreement with the above ranges and characterize the wines from the investigated varieties as neutral.

The linalool was the terpene identified in three of the wines studied. It was absent only in Shiraz wine. The highest linalool amount, 0.90 ± 0.08 mg/l, was identified in Carmenere/Cabernet Sauvignon/Cabernet Franc/Merlot. In Cabernet Franc it was present in a concentration of 0.47 ± 0.04 mg/l, and its lowest levels were identified in Cabernet Sauvignon/Merlot, 0.23 ± 0.06 mg/l. Gonzalez et al. (2022) identified linalool content in red wines aged in pine barrels ranging from 0.01 ± 0.00001 mg/l to 0.16 ± 0.005 mg/l. The results

in the present study regarding the amount of this terpene were higher. Linalool gives a characteristic jasmine aroma (Chobanova, 2012).

The linalool oxide is obtained by oxidation of linalool. It was found only in Cabernet Franc at a concentration of 0.23 ± 0.05 mg/l, and nerol was present only in Shiraz at an amount of 0.12 ± 0.01 mg/l. Nerol is contained in wines in concentrations from 0.014 to 0.45 mg/l (Chobanova, 2012). The data obtained in the present study correlated with this range.

Acetaldehyde and methanol concentrations in the analyzed wines

Acetaldehyde was found in the highest amount, 57.65 ± 4.26 mg/l, in Shiraz wine. Its concentration was slightly lower, 52.27 ± 7.47 mg/l, in Cabernet Franc, and the lowest levels, 8.92 ± 0.00 mg/l, were found in Carmenere/Cabernet Sauvignon/Cabernet Franc/Merlot. Martinez-Gil et al. (2022) found a variation in acetaldehyde concentration during storage of red wines in oak barrels over a period of 12 months, from 10.00 ± 0.82 mg/l to 36.25 ± 9.74 mg/l. The content of acetaldehyde in white and red wines averaged between 20.00 to 40.00 mg/l, respectively, with minimum and maximum levels ranging from 1.00 mg/l to 232.00 mg/l (Morneau, 2006). The data in the present study were in agreement with those stated by the cited authors.

Methanol is a normal component of wine volatiles. In red wines, it is allowed in a concentration of up to 300.00 mg/l (Chobanova, 2012). In the analyzed red wines, it was found in low amounts, below the maximum permissible threshold. It varied between the four red wines studied from 3.13 ± 0.39 mg/l (Cabernet Sauvignon/Merlot) to 12.28 ± 5.10 mg/l (Carmenere/Cabernet Sauvignon/Cabernet Franc/Merlot).

Wines sensory evaluation

The sensory profile and established aroma descriptors of the four wines are presented in Figures 1–3.

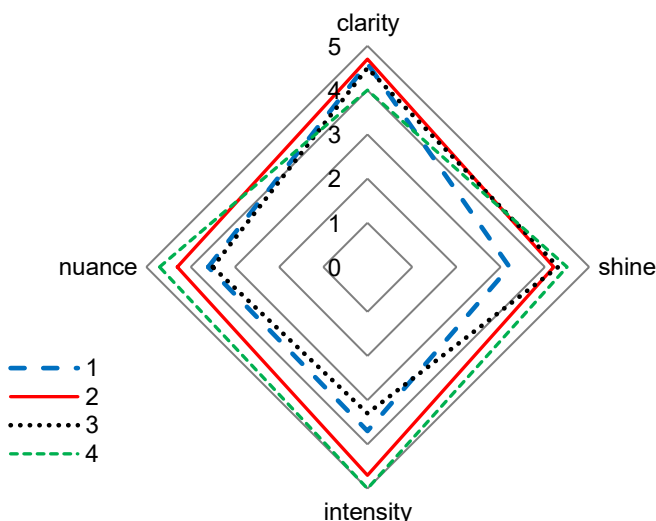


Figure 1. Colour evaluation:

- 1 – Cabernet Sauvignon/ Merlot, harvest 2019, Asenovgrad;
- 2 – Shiraz, harvest 2021, Varna;
- 3 – Cabernet Franc, harvest 2021, Varna;
- 4 – Carmenère/Cabernet Sauvignon/Cabernet Franc/Merlot, harvest 2022, Harmanli

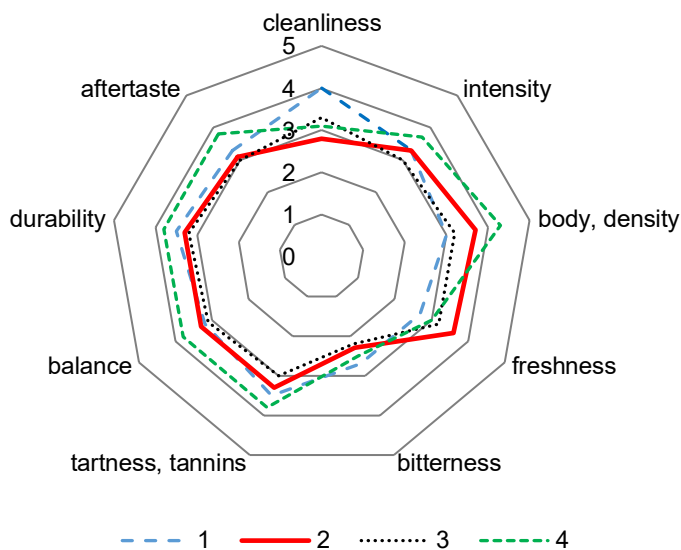


Figure 2. Flavor evaluation

- 1 – Cabernet Sauvignon/ Merlot, harvest 2019, Asenovgrad;
- 2 – Shiraz, harvest 2021, Varna;
- 3 – Cabernet Franc, harvest 2021, Varna;
- 4 – Carmenère/Cabernet Sauvignon/Cabernet Franc/Merlot, harvest 2022, Harmanli

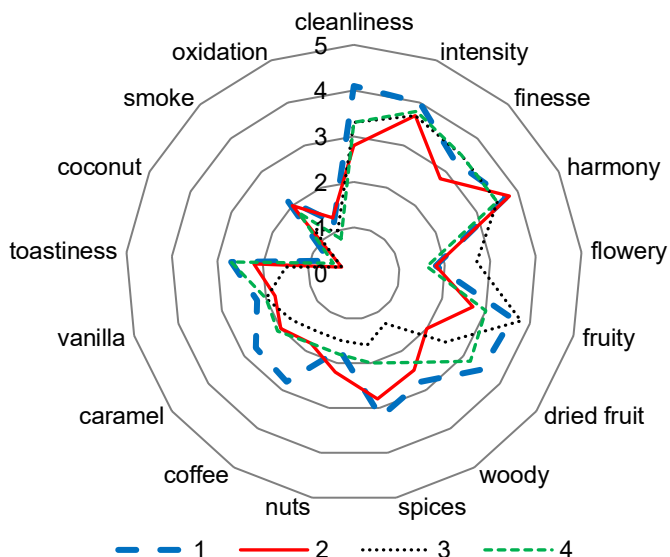


Figure 3. Aromatic descriptors evaluation

- 1 – Cabernet Sauvignon/ Merlot, harvest 2019, Asenovgrad;
- 2 – Shiraz, harvest 2021, Varna;
- 3 – Cabernet Franc, harvest 2021, Varna;
- 4 – Carmenère/Cabernet Sauvignon/Cabernet Franc/Merlot, harvest 2022, Harmanli

In connection with aroma, all samples have good intensity, finesse and harmony. Different but characteristic aroma descriptors were identified. In Cabernet Franc, harvest 2021, floral and fruity notes were more intense, despite 8 months of contact with oak chips. The 2019 Cabernet Sauvignon/Merlot wine exhibited more prominent aromas of dried fruit, spice, coffee, caramel, toastiness and smokiness. The aroma of spices also stands out in the Shiraz sample, harvest 2021, and of toast bread – in all samples. In connection with taste the blend Carmenere/Cabernet Sauvignon/Cabernet Franc/Merlot, harvest 2022, showed the best characteristics in terms of the specified descriptive indicators. This sample had the best intensity, density, tartness, balance, persistence and aftertaste. Cabernet Sauvignon/Merlot, harvest 2019, and Cabernet Franc, harvest 2021 had the best purity of taste. In terms of bitterness, tartness, balance, persistence and aftertaste, Cabernet Sauvignon/Merlot, Shiraz and Cabernet Franc had similar characteristics.

Conclusions

The highest total accumulation of volatile compounds in the analyzed commercial red wines obtained in contact with oak wood was found in Cabernet Franc wine. The most significant levels of total higher alcohols were also found in it. The ester fraction was quantitatively dominant in the Cabernet Sauvignon/Merlot wine, and the most terpenes were identified in the complex Carmenere/Cabernet Sauvignon/Cabernet Franc/Merlot blend.

Main higher alcohols in red wines were 2-methyl-1-butanol, 3-methyl-1-butanol, 1-propanol and 1-butanol. The ester fraction was quantitatively dominated by ethyl acetate. The terpene fraction was represented by linalool, linalool oxide and nerol.

A major aldehyde was acetaldehyde, found at levels that positively affect the fruity aroma of the red wines.

Methyl alcohol was found at levels significantly below the threshold of its normally permissible presence in red wines.

Wines from the commercial network had different organoleptic characteristics in terms of color, aroma and taste, as well as characteristic aromatic descriptors, which was due to the different type and quantity of oak wood used, as well as the duration of contact. All the studied wines showed a complex and varied volatile profile, due to the varietal characteristics of the grapes used, the soil and climatic conditions of each specific harvest and region and the specific influence of the applied method of contact with oak wood.

References

- Cerdan T., Goñi D., Azpilicueta C. (2004), Accumulation of volatile compounds during ageing of two red wines with different composition, *Journal of Food Engineering*, 65, pp. 349–356, <https://doi.org/10.1016/j.jfoodeng.2004.01.032>
- Česnik H., Bavčar D., Lisjak K. (2015), Volatile profile of wine Teran PTP, *Acta Agriculturae Slovenica*, 105(1), pp. 5–14, <https://doi.org/10.14720/aas.2015.105.1.01>
- Chobanova D. (2012), *Enology. Part I: Composition of wine*, Academic Press of University of Food Technologies, Plovdiv, Bulgaria, pp. 264. (BG)
- Cortés-Diégués S., Rodríguez-Solana R., Dominguez J., Diaz E. (2015), Impact odorants and sensory profile of young red wines from four Galician (NW of Spain) traditional

- cultivars, *Journal of the Institute of Brewing*, 121, pp. 628–635, <https://doi.org/10.1002/jib.252>
- Del Fresno J.M., Morata A., Loira I., Escott C., Suárez-Lepe J.A. (2020), Evolution of the phenolic fraction and aromatic profile of red wines aged in oak barrels, *ASC Omega*, 5(13), pp. 7235–7243, <https://doi.org/10.1021/acsomega.9b03854>
- Dimitriu G., López de Lerma N., Zamfir C., Cotea V., Peinado F. (2017), Volatile and phenolic composition of red wines subjected to ageing in oak cask of different toast degree during two periods of time, *LWT – Food Science and Technology*, 86, pp. 643–651, <https://doi.org/10.1016/j.lwt.2017.08.057>
- Dimitriu G., Teodosiu C., Gabur I., Cotea V., Peinado R., Lerma N. (2019), Evolution of aroma compounds in the process of wine aging with oak chips, *Foods*, 8(12), pp. 662, <https://doi.org/10.3390/foods8120662>
- Gonzalez P., Dans E., Ballester J. (2022), Volatile composition of light red wines aged in Canary pine barrels from La Palma (Canary Islands, Spain), *Oeno One*, 56(4), pp. 29–40, <https://doi.org/10.20870/oeno-one.2022.56.4.5486>
- González-Centeno M.R., Teissedre P.L. Chira K. (2021), Impact of oak wood ageing modalities on the (non)-volatile composition and sensory attributes of red wines, *OENO One*, 55(2), pp. 285–299, <https://doi.org/10.20870/oeno-one.2021.55.2.4673>
- Herjavec S., Jeromel A., Orlic S., Kozina B. (2007), Changes in volatile composition and sensory properties of Vugava wines aged in Croatia oak barrels, *Journal of Central European Agriculture*, 8 (2), pp. 195–204.
- Jiang B., Zhang Z. (2010), Volatile compounds of young wines from Cabernet Sauvignon, Cabernet Gernischt and Chardonnay varieties grown in the Loess Plateau Region in China, *Molecules*, 15(12), pp. 9184–9196, <https://doi.org/10.3390/molecules15129184>
- Kim H., Hur Y., Jung S., Im D., Ho K., Su C., Kim S. (2018), Characteristics of aroma compounds of 11 red wines from international grape cultivars grown in Korea, *Korean Journal of Food Preservation*, 25(5), pp. 491–500, <https://doi.org/10.11002/kjfp.2018.25.5.491>
- Lu H., Cheng B., Lan Y., Duan C., He F. (2024), Modifications in aroma characteristics of ‘Merlot’ dry red wines aged in American, French and Slovakian oak barrels with different toasting degrees, *Food Science and Human Wellness*, 13(1), pp. 381–391, <https://doi.org/10.26599/fshw.2022.9250032>
- Manolache M., Pop T., Babes A., Farcas I., Munaciu M., Călugăr A., Gal E. (2018), Volatile composition of some red wines from Romania assessed by GC-MS, *Studia UBB Chemia*, LXIII, pp. 125–142, <https://doi.org/10.24193/subbchem.2018.2.12>
- Martinez-Gil A., Alamo-Sanza M., Barrio-Galán R., Nevares I. (2022), Alternative woods in oenology: Volatile compounds characterization of woods with respect to traditional oak and effect on aroma in wine, a review, *Applied Sciences*, 12(4), 2101, <https://doi.org/10.3390/app12042101>
- Martinez-Gil A., Alamo-Sanza M., Nevares I. (2022), Evolution of red wine in oak barrels with different oxygen transmission rates. Phenolic compounds and colour, *LWT – Food Science and Technology*, 158, 113133, <https://doi.org/10.1016/j.lwt.2022.113133>

- Mateo J., Jimenez M. (2000), Monoterpenes in grape juice and wine, *Journal of Chromatography A*, 881(1–2), pp. 557–567, [https://doi.org/10.1016/s0021-9673\(99\)01342-4](https://doi.org/10.1016/s0021-9673(99)01342-4)
- Morneau A. (2006), Acetaldehyde in wines and its metabolism by lactic acid bacteria, Thesis for the Degree of Master of Science, University of Guelph, Canada.
- Pérez-Juan P., Luque de Castro M. (2015), Use of oak wood to enrich wine with volatile compounds, In: V. Preedy (Ed.), *Processing and impact on active components in food*, Academic Press, pp. 471–481, <https://doi.org/10.1016/b978-0-12-404699-3.00057-3>
- Pérez-Prieto L.J., López-Roca J.M., Martínez-Cutillas A., Minguez F., Gomez-Plaza E. (2002), Maturing wines in oak barrels. Effect of origin, volume and age of the barrel on the wine volatile composition, *Journal of Agricultural and Food Chemistry*, 50(11), pp. 3272–3276, <https://doi.org/10.1021/jf011505r>
- Prodanova N. (2008), *Tasting or how to get to know the wine*, Sofia, Gourmet, pp. 105–118, ISBN: 9789542917205.
- Slaghenaufi D., Peruch E., De Cosmi M., Nouvelet L. Ugliano M. (2021), Volatile and phenolic composition of monovarietal red wines of Valpolicella appellations, *Oeno One*, 55(1), pp. 279–294, <https://doi.org/10.20870/oeno-one.2021.55.1.3865>
- Zhang L., Tao Y., Wen Y., Wang H. (2012), Aroma evaluation of young Chinese Merlot wines with denomination of origin, *South African Journal of Enology and Viticulture*, 34(1), pp. 46–53, <https://doi.org/10.21548/34-1-1080>

Cite:

UFJ Style

Dimitrov D., Yoncheva T. (2024), Volatile composition and aromatic descriptors of red wines from different regions of Bulgaria aged with oak chips, *Ukrainian Food Journal*, 13(2), pp. 262–273, <https://doi.org/10.24263/2304-974X-2024-13-2-5>

APA Style

Dimitrov, D., & Yoncheva, T. (2024). Volatile composition and aromatic descriptors of red wines from different regions of Bulgaria aged with oak chips. *Ukrainian Food Journal*, 13(2), 262–273. <https://doi.org/10.24263/2304-974X-2024-13-2-5>

Effect of complex plant supplement on shelf life of wheat bread

Anastasiia Shevchenko¹, Eva Ivanišová^{2,3}, Eva Kováčiková⁴,
Lucia Benešová⁴, Larysa Mykhonik¹

1 – National University of Food Technologies, Kyiv, Ukraine

2 – Institute of Food Sciences, Faculty of Biotechnology and Food Sciences, Slovak University of Agriculture, Slovak Republic

3 – Food Incubator, AgroBioTech Research Centre, Slovak University of Agriculture, Slovak Republic

4 – AgroBioTech Research Centre, Slovak University of Agriculture, Slovak Republic

Abstract

Keywords:

Wheat bread
Shelf life
Rice
By-products
Antioxidant activity
Firmness

Introduction. The purpose of the work was to determine the effect of the complex plant supplement on the preservation of freshness of bread.

Materials and methods. Complex plant supplement consisted of sunflower lecithin, rice flour, rice protein concentrate and dry lamium leaves which were added to recipe of wheat bread. Brittleness, firmness, water activity, amount of water absorbed by the crumb, deformation of the bread crumb, content of total polyphenols, phenolic acids, and flavonoids, as well as antioxidant activity and oxidative stability of bread were studied.

Results and discussion. It was proved that the crumb of wheat bread added with a complex plant supplement was less susceptible to deformation during 48 hours of storage and faster regained form. The brittleness of the developed product decreased compared to the control due to change in hydrophilic properties – water absorption capacity of the crumb. Studies of the hydrophilic properties of bread crumb showed that the developed bread had a higher water absorption capacity and lost its hydrophilic properties more slowly. The water activity index of bread with additives was lower compared to the control. After 48 hours of storage, the increase in the firmness of bread with added complex plant supplement was lower compared to the control, which indicates the ability to preserve the textural properties of bread. Determination of moisture bond forms in the crumb of bread showed that after 48 hours of storage the free moisture in the control bread was removed at a lower temperature – 92°C, while for the developed sample – at 105°C. It means that more energy is needed to remove free moisture from the developed bread. It was proved that the addition of rice flour, rice protein concentrate, sunflower lecithin and dry lamium leaves had a stable antioxidant effect in relation to the processes of free radical oxidation of lipids. An increase in the content of phenolic compounds, phenolic acids and flavonoids was found in breads after baking, and their decrease in the developed products during the storage process was more rapid, compared to the control.

Conclusions. Therefore, the introduction of the complex plant supplement – rice flour, rice protein concentrate, sunflower lecithin and dry lamium leaves extended the shelf life of wheat bread and increased its antioxidant activity.

Article history:

Received
14.02.2023
Received in revised
form 18.05.2024
Accepted 2.07.2024

Corresponding author:

Anastasiia
Shevchenko
E-mail:
nastyusha8@ukr.net

DOI:

10.24263/2304-
974X-2024-13-2-6

Introduction

Bread belongs to products with a short shelf life. The term of its freshness depends on many factors, one of which is the properties of the raw materials included in its composition.

Despite the general tendency to increase number of products with a high content of dietary fiber in the human diet, there are people who suffer from inflammatory bowel diseases and they are not recommended to use these functional ingredients (Forbes et al., 2017; Zallot et al., 2013). In this aspect, rice-processing products attract attention, in particular rice flour, which contains 5 – 6 times less amount of dietary fibers than wheat flour (Kaur et al., 2022).

An increase in firmness of the crumb of wheat bread with an increase in the dosage of rice flour (to substitute 0-50% wheat flour) was observed. It was explained by different structure and smaller size of rice starch granules (0 – 400 μm) compared to wheat starch as well as greater susceptibility of rice flour starch to amylolysis (Rathore and Pandey, 2023). Similar results were obtained in other studies (Khoshgozaran-Abras et al., 2014). It was found that replacement 5 – 10% wheat flour with rice flour led to increase of firmness of the crumb by 8.3 – 11.8%.

The effect of replacing 30% of wheat flour with rice flour from three different varieties of rice on the preservation of freshness of bread was determined. It was found that replacing 30% wheat flour with waxy rice flour reduced the firmness of bread over three days due to higher amylose content in its starch compared to wheat flour (Purna et al., 2011). Addition of other types of rice flour increased firmness compared to bread from wheat flour. Aoki et al. (2012) established similar dependencies.

Bread has a soft, porous texture that can be deformed. The control bread crumb almost restored the structure after deformation and bread with rice flour with lower amylose content had a lower recovery and a stickier texture. Blending rice flour with wheat flour reinforced resistance to deformation because of an increase in crumb extensibility (Sasaki et al., 2014).

When rice flour was added to wheat flour, there was a redistribution of moisture bond forms in bread, the amount of weak-bounded moisture increased, so the structure became more compact, which caused decrease in the amount of energy needed to remove moisture, and therefore, staleness (Chen et al., 2022).

Rice by-products are mostly used in the technology of gluten-free rice bread. In addition, bread mostly has a low biological value and requires correction of the protein component in order to increase the content and applicability of protein by the body. Rice and wheat flour have different fractional composition of proteins and starch (Shevchenko and Litvynchuk, 2022), which affects the structural and mechanical indicators of bread, water absorption capacity of the crumb, crumbliness, and therefore the preservation of freshness by bread.

The mixture of rice flour and starch was replaced by 5 and 10% of rice protein, and the indicators that characterize the staleness of bread were determined. A decrease in crust moisture by 10.6-14.1% (Pico et al., 2019) and water activity by 9.6% (García-Segovia et al., 2020) was found in bread in case of replacing 5 and 10% mixture of rice flour and starch with rice protein.

The preservation of freshness in bread is also depends on the content of raw materials with antioxidant properties due to their ability to reduce free radical oxidation of lipids (Wang et al., 2023), in particular due to the introduction of raw materials with a powerful antioxidant complex into the bread recipe. Antioxidant activity and concentration of total soluble phenolic compounds was evaluated in rice grains with light brown, red and black pericarp colors. Concentrations of total soluble phenolic compounds were 7 to 15 times higher in the

grains with red and black pericarp colors compared to grains with a light brown pericarp color (Walter et al., 2013).

Taking into account the need for development of recipes for bakery products with high biological and nutritional value, as well as extending the shelf life of products, the aim of the present study was to determine the effect of complex plant supplement – rice flour, rice protein concentrate, sunflower lecithin and dry lamium leaves on the freshness of bread.

Materials and methods

Materials

Bread was prepared from main components – premium wheat flour, 1.5% of salt - and 3% of pressed baker's yeast. Complex plant supplement consisted of 3% sunflower lecithin, 5% rice flour instead of wheat flour, 4% rice protein concentrate to the weight of flour and 1% dry lamium leaves to the weight of flour, which was added to recipe of wheat bread. Sunflower lecithin is used as emulsifier and source of phospholipids. Rice protein concentrate with 74.2% of protein was extracted from rice bran by enzymatic method (Shevchenko et al., 2023). Bread without sunflower lecithin, rice flour, rice protein concentrate and dry lamium leaves was the control. Bread was obtained using preparing dispersed phase and dough on its base.

Methods

Brittleness of bread

Two pieces of 5 g of bread crumb were put into conical flask and mixed for 5 minutes. Then the mass of the whit formed by rubbing two pieces of bread was weighed. Brittleness was calculated as relation of weight of the whit to the initial weight of the bread pieces. Analyzis was done after 4, 24 and 48 hours after baking.

Amount of water absorbed by the crumb of bread

Crumb, 3 g, was crushed and weighed. The crumb was put onto a sieve and 17 ml of distilled water was slowly added to them from a pipette over 5 minutes. The soaked crumb was collected and weighed.

Deformation of the bread crumb

The total deformation of the bread crumb was studied after 4, 24 and 48 hours after baking using automatic penetrometer AP-4/2 (Germany). For measurement, a piece of bread crumb was put on the plate and a body with a certain mass for a certain time immerse into the crumb. The data was in expressed in penetrometric units (Zlateva and Chochkov, 2019).

Water activity of bread

Water activity of bread crumb was determined on a water analyzer at a temperature of 20 °C in the measurement range of 0 – 1 a_w (0 – 100%). A piece of bread crumb was placed in a container and a measuring chamber. A water activity probe was located on its top. The

measurement cycle lasts 3–5 minutes, after which the water activity and temperature values for each probe were shown on the display (Kochubei-Lytvynenko et al., 2018).

Bread firmness

Bread firmness was determined using TA.XT Plus Texture Analyser (Stable Micro Systems, Surrey, UK). The loaves of bread were cut into equal slices of 20 mm thick. For slices of this thickness, one slice was used for each test sample, and the end crust slices of the loaf were discarded. The measurement was performed in 3 replicates for each sample. Firmness is defined as the force (in grams) required to compress the product by a pre-set distance (i.e. force taken at 25% compression of 25 mm). A 25% compression of a 25 mm thick sample = 6.25mm compression distance at which point the compression force value (CFV) is taken (Wongsagonsup et al., 2015).

Moisture bond forms in the crumb of bread

Moisture bond forms in the crumb of bread during its storage was determined by the thermogravimetric method on a Q-1500 derivatograph. The sample and the standard are loaded into the working volume and heated at a constant rate. The temperature, the difference between the temperatures of the sample and the standard reference temperature, sample mass change, the difference in masses of the reference and working samples were measured. 1 g of the standard sample and a test sample was loaded in two crucibles. They are heated in the temperature range of 20–250 °C and at a rate of 1.25 °C/min. The recording device captures the graphs (Pivovarov et al., 2018).

Total polyphenol content in bread

Total phenolic content was determined spectrophotometrically using Folin-Ciocalteu procedure in a microplate method according to (Xiong et al., 2020) with slight modifications. In a 96 well-plate, 50 µL of distilled water were added, followed by 25 µL of the sample or standard (in triplicate), and 25 µL of Folin-Ciocalteu reagent. After 6 min, 100 µL of 7.5% sodium carbonate solution were added to all wells. The plate was then left in the dark for 90 min at room temperature and then read using a UV–Vis plate reader (Glomax Multi+, Promega Corp., Madison, USA) at 765 nm. The UV–vis measurements were calibrated against gallic acid curve (0 – 500 mg/L; $R_2=0.9989$), and the results were presented as gallic acid equivalent (GAE) in mg per g of dry weight.

Total phenolic acid content in bread

Total phenolic acid content was determined using method of Jain et al. (2017). A 0.5 ml of sample extract was mixed with 0.5 ml of 0.5 M hydrochloric acid, 0.5 ml Arnova reagent (10% NaNO_2 + 10% Na_2MoO_4), 0.5 ml of 1 M sodium hydroxide (w/v) and 0.5 ml of water. Absorbance at 490 nm was measured using the spectrophotometer Jenway (6405 UV/Vis, England). Caffeic acid (1 – 200 mg/L, $R_2 = 0.999$) was used as a standard and the results were expressed in mg/g caffeic acid equivalents.

Total flavonoid content in bread

Total flavonoid content was determined using the modified method of Willett, (2002).

The sample (0.5 ml) was mixed with 0.1 ml of 10% (w/v) ethanolic solution of aluminium chloride, 0.1 ml of 1 M potassium acetate and 4.3 ml of distilled water. After 30 min in darkness the absorbance at 415 nm was measured using the spectrophotometer Jenway (6405 UV/Vis, England). Quercetin (0.5-20 mg/L; R²=0.989) was used as the standard and the results were expressed in mg/g quercetin equivalents.

Antioxidant activity of bread

Antioxidant activity was determined spectrophotometrically using DPPH assay described by Brand-Williams et al., (1995) adapted to microplate protocol. Briefly, to prepare the 2,2-diphenyl-1-picrylhydrazyl (DPPH) reagent, 25 mg was dissolved in 100 mL of 96% ethanol and adjusted to an absorbance of 0.7. Into a 96 well-plate, 25 μ L of the sample, blank (DPPH) or standard (in triplicate) were added, followed by 180 μ L of DPPH solution. The plate was then left in the dark for 10 min at RT, while simultaneously shaking at 500 rpm, and read using a UV-Vis plate reader (Glomax Multi+, Promega Corp., Madison, USA) at 515 nm. Determination of AA was calculated as a percentage of DPPH inhibition according to the formula (1):

$$\text{DPPH inhibition (\%)} = [(\text{AbsBlank} - \text{AbsSample}) / \text{AbsBlank}] \times 100 \quad (1)$$

Subsequently, the ability to scavenge DPPH radical was expressed as Trolox equivalent antioxidant capacity (TEAC) in mg per g of dry weight (DW), calculated using a Trolox standard curve (0 – 100 mg/L; R²=0.9982).

Oxidative stability of bread

The oxidative stability was determined in 892 Rancimat apparatus from Metrohm (Switzerland) according to ISO 6886:1997 utilizing a sample of 0.5 \pm 0.01 g. All samples were studied in temperature 120 $^{\circ}$ C, under a constant airflow (20 L/h). The induction times were printed automatically by apparatus software with the accuracy of 0.005.

Statistical analysis

The data represents the mean of a minimum three replicates \pm standard deviation (S.D.). Graphical presentation of experimental data was performed using program Microsoft Excel 2010.

Results and discussions

The influence of recipe components (mixture of 3% sunflower lecithin by weight of flour, 5% rice flour instead of wheat flour, 4% rice protein concentrate to the weight of flour and 1% of dry lamium leaves to the weight of flour) on the shelf life of bread was determined by indicators of crumb deformation, crumbliness, water absorption, water activity and redistribution of moisture in the crumb.

Studies of crumb deformation using a penetrometer during 48 h of storage showed (Table 1) that the total deformation of the samples with additives was lower than in the control.

Table 1
Indicators of deformation of the crumb of the products according to the penetrometer

Indicator	Control bread	Experimental bread
General deformation of the pulp, units of device		
after 4 hours	47±1	58±2
after 24 hours	32±1	48±1
after 48 hours	24±2	34±1
Degree of preservation of freshness relative to initial freshness, %		
after 24 hours	68±1	83±3
after 48 hours	51±2	58±1

Results are given as M ± SD (mean ± standard deviation) for triplicate trials.

It was proved that the crumb of the developed bread was less susceptible to deformation by 23.4% after 4 hours of storage, by 50.0% and 41.6% after 24 and 48 hours, respectively, and faster regained form. This is explained by the higher water absorbing and moisture-retaining capacity of the rice flour (Shevchenko and Litvynchuk, 2022a), rice protein concentrate and dry lamium leaves.

Changes in the physico-mechanical properties of crumb, which affect aging, were determined by indicators of brittleness and water absorption capacity (Table 2).

Table 2
Brittleness and water absorption capacity of bread

Indicator	Control bread	Experimental bread
Brittleness of bread, % to mass of crumb		
after 4 hours	2.4±0.1	1.5±0.1
after 24 hours	9.2±0.2	7.1±0.3
after 48 hours	11.8±0.1	9.9±0.1
Water absorption capacity of the crumb of products, % dry matter		
after 4 hours	456±2	498±2
after 24 hours	416±1	439±2
after 48 hours	336±2	388±2

Results given as M ± SD (mean ± standard deviation) of triplicate trials.

It was found that the brittleness of the experimental bread decreased by 22.8% after 24 hours and by 16.1% after 48 hours, compared to the control. This is explained by a smaller loss of hydrophilic properties of bread crumb, which led to a delay in the aggregation of amylose and amylopectin of flour starch (Scott and Awika, 2023).

Determination of the hydrophilic properties of bread crumb showed that the water absorption capacity of experimental bread was higher after 24 hours by 5.5% and by 15.5% after 48 hours compared to the control sample. At the same time, the developed bread lost its hydrophilic properties more slowly. This is explained by the higher water absorption and water retention capacity of the added complex plant supplement, so bread had a higher moisture content, which helps to delay the staleness.

Staleness significantly determined by the state of moisture in bread, which is affected by the activity of water (De Luca et al., 2021). It was established (Figure 1) that bread belong to products with intermediate water activity because the value of the indicator lies within the

limits 0,9 – 0,6, the water activity index of the developed product was lower compared to the control by 2.0%. This may be due to a lower indicator of water activity of raw materials included in the recipe. This is positive considering the fact that products with high values of this indicator undergo microbiological spoilage more intensively (Tapia et al., 2008). From the point of view of preservation of freshness, it is important to analyze the change in water activity values in bread during storage. After 48 hours, the value of water activity for the control did not change, but for the developed product it increased slightly by 0.6%. However, the value was lower by 1.4% than for the control bread after 48 h, which is a positive factor considering the lower microbiological activity in this product.

The freshness of bread was also determined by changes in its firmness after 48 hours of storage. The firmness of bread after baking and after 48 h of storage was found (Figure 2).



Figure 1.
Activity of water of bakery products during storage

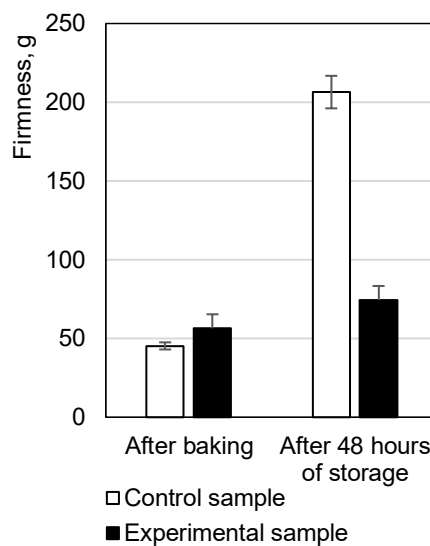


Figure 2.
Firmness of bakery products

It was established that complex plant supplement increased the firmness of bread after baking, which is associated with the difference in the fractional composition and properties of proteins and starch of rice and wheat flour (Shevchenko and Litvynchuk, 2022b). However, after 48 h, the increase of the firmness of bread with complex plant additive was lower compared to the control, which demonstrates the ability of this additive to contribute to the preservation of the textural properties of bread during storage.

The effect of addition of complex plant supplement on the duration of freshness of products can be estimated by the change in the amount of free and bound moisture during storage and the energy consumption of the dehydration process using the thermogravimetric method (Matejtschuk, 2016). The research was carried out on a derivatograph (Figure 3, 4).

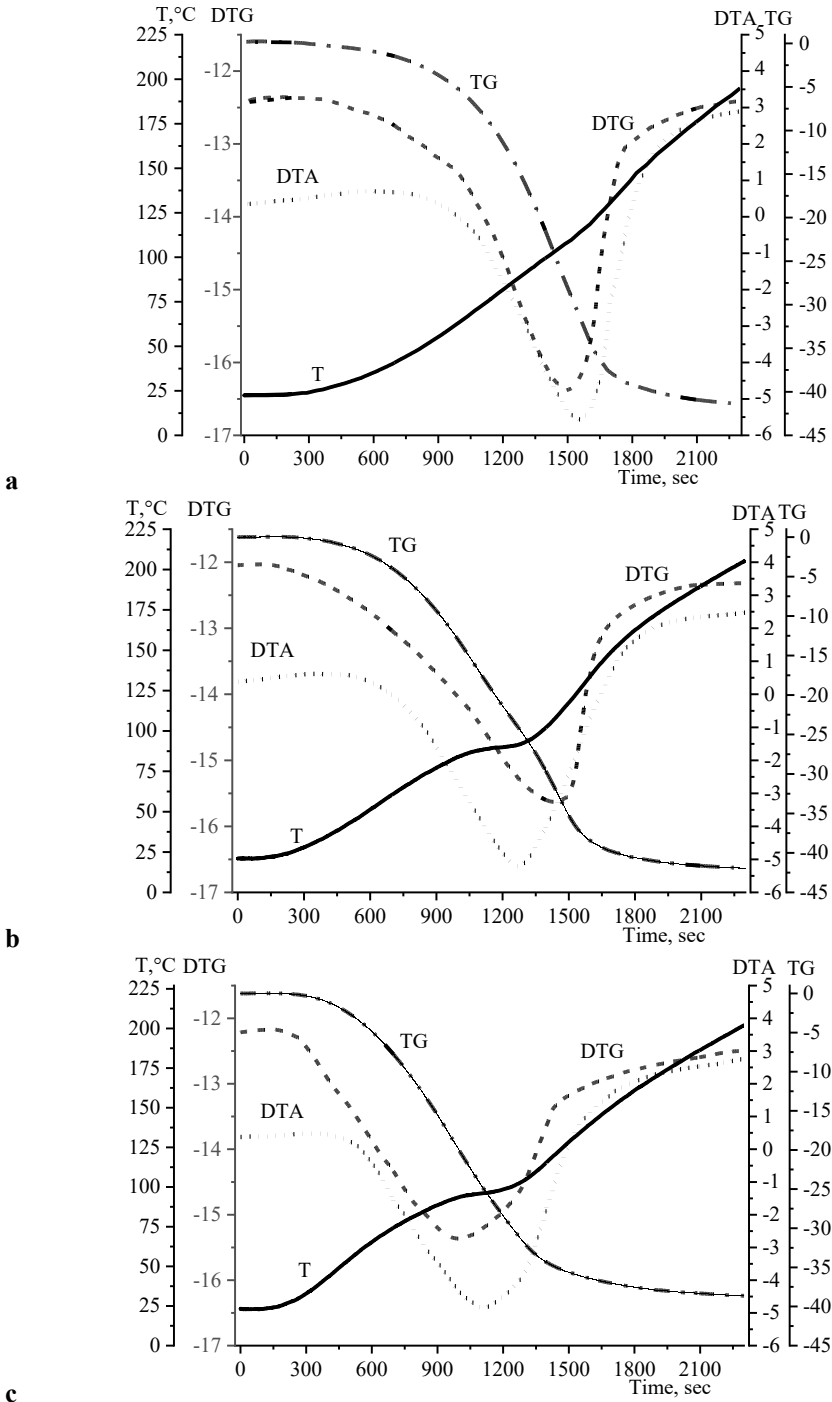


Figure 3. Derivatograms of control bread crumb thermolysis:
a, b, c – control after 4, 24, 48 hours of storage

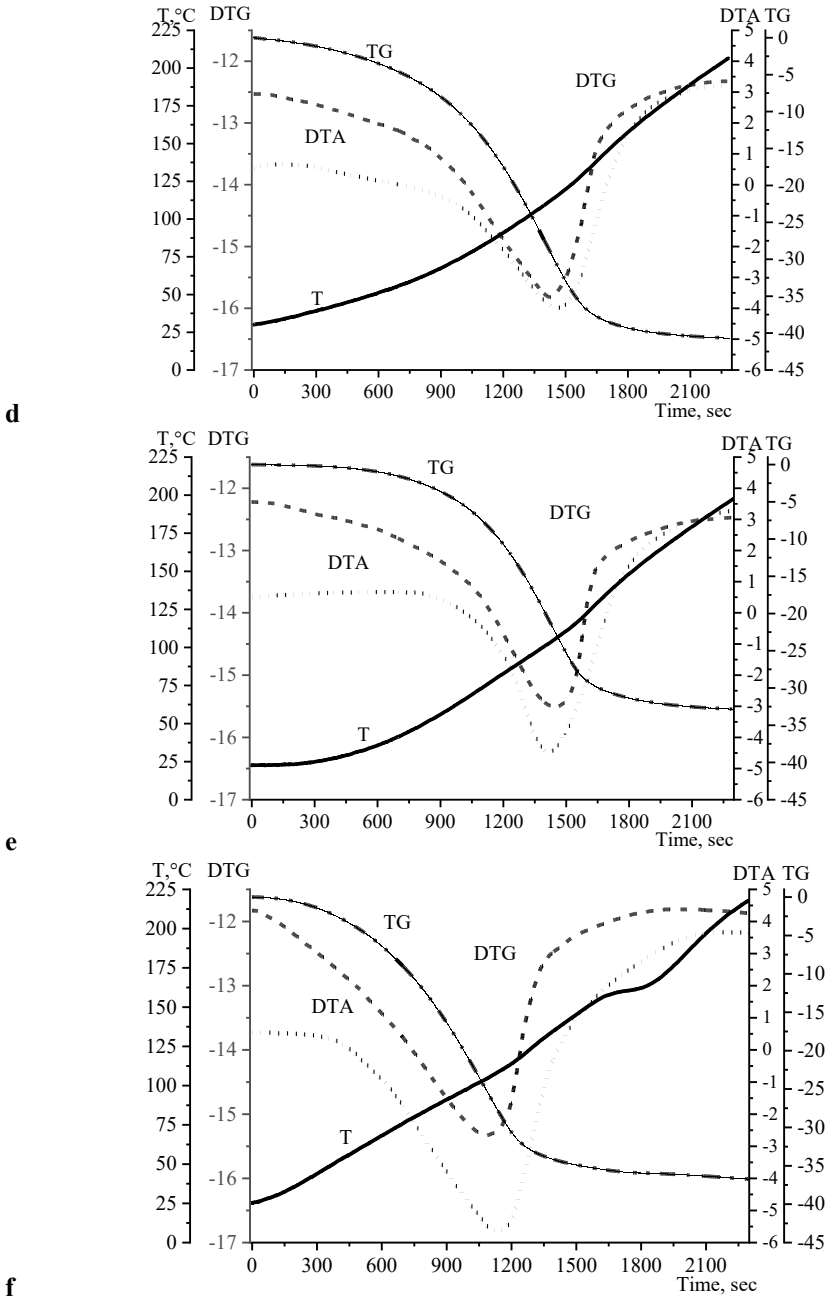


Figure 4. Derivatograms of experimental bread crumb thermolysis:
d, e, f – experimental sample after 4, 24, 48 hours of storage

Curves were built: DTG curve, which indicates the processes of decreasing the weight of the samples, DTA curve is a curve of temperature difference between the sample material and the reference material versus temperature and time, TG curve shows the change in sample weight as a function of temperature or time under controlled gas atmosphere, T curve shows temperature change.

In both samples, one endoeffect was recorded on the DTG curves. In the bread samples after 4 and 24 hours of storage, the final stage of free moisture removal occurred at the same temperature - 115°C. After 48 h of storage, the trend changed and the free moisture of the control was removed at a lower temperature - 92°C, while for the developed sample at 105°C. This is explained by the need for more energy to remove free moisture from the developed bread, which will contribute to longer preservation of moisture inside the product and a lower degree of its evaporation. In the control sample a more rapid loss of moisture was observed, and in the developed product, the slowing down of moisture loss occurred due to its binding by proteins under the influence of temperature. This indicates that the energy supplied to the samples was spent largely on the course of destructive processes in the control than in the developed sample.

Added complex plant supplement, especially dry lamium leaves, have a high content of compounds with antioxidant properties. Therefore, it is advisable to investigate their content in the developed products.

Table 5

Antioxidant compounds in bakery products

Indicator	Control sample		Experimental sample	
	After baking	After 48 hours of storage	After baking	After 48 hours of storage
Total polyphenol content, mg GAE/g	2.15±0.02	1.69±0.02	3.09±0.03	2.49±0.03
Total phenolic acid content, mg CAE/g	0.19±0.01	0.04±0.01	1.62±0.04	1.34±0.04
Total flavonoid content, mg QE/g	2.15±0.03	0.27±0.03	3.06±0.03	2.01±0.03
Antioxidant activity, (mg TEAC /g)	0.32±0.01	0.07±0.01	0.55±0.03	0.13±0.03
Oxidative stability, induction time (hours)	35±0.25	32±0.25	7.8±0.28	6.5±0.28

Results given as M ± SD (mean ± standard deviation) of triplicate trials.

It was proved that the addition of rice flour, sunflower lecithin, rice protein concentrate and dry lamium leaves to the recipe showed a stable antioxidant effect in relation to the processes of free radical oxidation of lipids. An increase in the content of phenolic compounds, phenolic acids and flavonoids was found in bread samples after baking compared to the control bread because of their higher content in added complex plant supplement. At the same time, their decrease in the developed products during the storage process was more rapid, compared to the control. A decrease in the content of phenolic

compounds correlates with an increase in antioxidant activity in the developed bakery product.

Therefore, the added complex plant supplement due to their higher hydrophilic and antioxidant properties are able to extend the shelf life of bread and save its freshness longer. This is a promising way to obtain bread with good consumer properties.

Conclusions

1. The crumb of bread with added rice flour, sunflower lecithin, rice protein concentrate and dry lamium leaves was less susceptible to deformation by 23.4% after 4 hours of storage, by 50.0% and 41.6% after 24 and 48 hours, respectively, and faster regained form.
2. The brittleness of the developed bread with added rice flour, sunflower lecithin, rice protein concentrate and dry lamium leaves decreased by 22.8% after 24 hours and 16.1% after 48 hours, compared to the control bread because the loss of moisture of the crumb was less.
3. Bread with additional components had a higher water absorption capacity during storage by 5.5% after 24 hours and by 15.5% after 48 hours compared to the control and lost its hydrophilic properties more slowly.
4. Water activity index of the developed product was lower compared to the control by 2.0%.
5. Added components increased the firmness of bread after baking, but after 48 hours, the increase in the firmness was smaller compared to the control, which indicates the ability of this complex plant supplement to contribute to the preservation of the textural properties of bread.
6. Determination of moisture bond forms in the crumb of bread showed that after 48 hours of storage the free moisture in the control bread was removed at a lower temperature – 92°C, while for the developed sample – at 105°C. In the control, a more rapid loss of moisture was observed.
7. The addition of the proposed recipe components in the complex showed a stable antioxidant effect in relation to the processes of free radical oxidation of lipids.

Acknowledgement. Authors would like to thank the Operational Program Integrated Infrastructure: Demand-driven research for sustainable and innovative food, Drive4SIFood 313011V336, co-funded by the European Regional Development Fund for administrative and technical support.

References

- Aoki N., Umamoto T., Hamada S., Suzuki K., Suzuki Y. (2012), The amylose content and amylopectin structure affect the shape and hardness of rice bread, *Journal of Applied Glycoscience*, 59, pp. 75–78, https://doi.org/10.5458/jag.jag.jag-2011_013
- Brand-Williams W., Cuvelier M.E., Berset C. (1995), Use of a free radical method to evaluate antioxidant activity, *LWT - Food Science and Technology*, 28(1), pp. 25–30, [https://doi.org/10.1016/S0023-6438\(95\)80008-5](https://doi.org/10.1016/S0023-6438(95)80008-5)

- Chen F., Ji Y., Yang C., He Y., Liu L., Zhang G., Tang X. (2022), Study on modification mechanism of rice protein network based on sodium pyrosulfite combined with Tgase, <https://doi.org/10.21203/rs.3.rs-2395840/v1>
- De Luca L., Aiello A., Pizzolongo F., Blaiotta G., Aponte M., Romano R. (2021), Volatile organic compounds in breads prepared with different sourdoughs, *Applied Sciences*, 11(3), 1330, <https://doi.org/10.3390/app11031330>
- García-Segovia P., Igual M., Martínez-Monzó J. (2020), Physicochemical properties and consumer acceptance of bread enriched with alternative proteins, *Foods*, 9(7), 933, <https://doi.org/10.3390/foods9070933>
- Purna S.K., Miller R.A., Seib P.A., Graybosch R.A., Shi Y.C. (2011), Volume, texture, and molecular mechanism behind the collapse of bread made with different levels of hard waxy wheat flours, *Journal of Cereal Science*, 54, pp. 37–43, <https://doi.org/10.1016/j.jcs.2011.02.008>
- Forbes A., Escher J., Hébuterne X., Kłęk S., Krznaric Z., Schneider S., Bischoff C. (2017), Clinical nutrition in inflammatory bowel disease, *Clinical Nutrition*, 36(2), pp. 321–347, <https://doi.org/10.1016/j.clnu.2019.11.002>
- ISO 6886:1997. Animal and vegetable fats and oils-determination of oxidation stability (accelerated oxidation test). International Organization for Standardization, Geneva, Switzerland.
- Jain R., Rao B., Tare A.B. (2017), Comparative analysis of the spectrophotometry based total phenolic acid estimation methods, *Journal of Analytical Chemistry*, 72, pp. 972–976, <https://doi.org/10.1134/S106193481709009X>
- Kaur S., Kumar K., Singh L., Sharanagat V.S., Nema P.K., Mishra V., Bhushan B. (2022). Gluten-free grains: importance, processing and its effect on quality of gluten-free products, *Critical Reviews in Food Science and Nutrition*, pp. 1–28, <https://doi.org/10.1080/10408398.2022.2119933>
- Khoshgozaran-Abras S., Azizi M.H., Bagheripoor-Fallah N., Khodamoradi A. (2014), Effect of brown rice flour fortification on the quality of wheat-based dough and flat bread, *Journal of Food Science and Technology*, 51(10), pp. 2821–2826, <https://doi.org/10.1007/s13197-012-0716-x>
- Kochubei-Lytvynenko O., Yatsenko, O. Yushchenko N., Kuzmyk U. (2018), Astabilizing system for butter pastes based on the dry concentrates of milk protein, *Eastern-European Journal of Enterprise Technologies*, 5(11(95)), pp. 30–36, <https://doi.org/10.15587/1729-4061.2018.143105>
- Matejtschuk P., Duru C., Malik K., Ezeajughi E., Gray E., Raut S., Mawas F. (2016), Use of thermogravimetric analysis for moisture determination in difficult lyophilized biological samples, *American Journal of Analytical Chemistry*, 7(3), pp. 260–265, <https://doi.org/10.4236/ajac.2016.73023>
- Pivovarov A., Mykolenko S., Hez' Y., Shcherbakov S. (2018), Plasma-chemically activated water influence on staling and safety of sprouted bread. *Technology and Food Safety*, 12(2), pp. 100–107, <https://doi.org/10.15673/fst.v12i2.940>
- Rathore S., Pandey A.K. (2023), Optimization study of the effect of rice and wheat flour blend ratio and water content on bread texture and sensory quality, *Journal of the Institution of Engineers (India): Series A*, 104, pp. 195–206.
- Sasaki T., Kohyama K., Miyashita K., Okunishi T. (2014), Effects of rice flour blends on bread texture and staling, *Cereal Chemistry*, 91(2), pp. 146–151, <https://doi.org/10.1094/CCHEM-08-13-0150-R>
- Pico J., Reguilón M. P., Bernal J., Gómez M. (2019), Effect of rice, pea, egg white and whey proteins on crust quality of rice flour-corn starch based gluten-free breads, *Journal of Cereal Science*, 86, pp. 92–101, <https://doi.org/10.1016/j.jcs.2019.01.014>
- Scott G., Awika J. M. (2023), Effect of protein–starch interactions on starch retrogradation and implications for food product quality, *Comprehensive Reviews in Food Science and Food Safety*, 22, pp. 2081–2111, <https://doi.org/10.1111/1541-4337.13141>
- Shevchenko A., Litvynchuk S. (2022), Influence of rice flour on conformational changes in the dough during production of wheat bread, *Ukrainian Journal of Food Science*, 10(1), pp. 5–15, <https://doi.org/10.24263/2310-1008-2022-10-1-3>

- Shevchenko A., Litvynchuk S. (2022a), Functional properties of rice flour and its effect on conformational changes in the structure of wheat dough and bread, *Scientific Works of the National University of Food Technologies*, 28(6), pp. 150–159, <https://doi.org/10.24263/2225-2924-2022-28-6-16>
- Shevchenko A., Litvynchuk S. (2022b), Influence of rice flour on conformational changes in the dough during production of wheat bread, *Ukrainian Journal of Food Science*, 10(1), pp. 5–15, <https://doi.org/10.24263/2310-1008-2022-10-1-3>
- Shevchenko A., Litvynchuk S., Koval O. (2023), The influence of rice protein concentrate on the technological process of wheat bread production, *EUREKA: Life Sciences*, 4, pp. 22–29, <https://doi.org/10.21303/2504-5695.2023.003031>
- Tapia M.S., Alzamora S.M., Chirifé J. (2008), Effects of water activity (aw) on microbial stability: as a hurdle in food preservation, In: G.V. Barbosa-Cánovas, A.J. Fontana, S.J. Schmidt, T.P. Labuza (Eds.), *Water Activity in Foods: Fundamentals and Applications*, 239–271, <https://doi.org/10.1002/9780470376454.ch10>
- Walter M., Marchesan E., Massoni P.F.S., Picolli da Silva L., Sartori G.M.S., Ferreira R.B. (2013), Antioxidant properties of rice grains with light brown, red and black pericarp colors and the effect of processing, *Food Research International*, 50(2), pp. 698–703, <https://doi.org/10.1016/j.foodres.2011.09.002>
- Wang D., Xiao H., Lyu X., Chen H., Wei F. (2023), Lipid oxidation in food science and nutritional health: A comprehensive review, *Oil Crop Science*, 8(1), pp. 35–44, <https://doi.org/10.1016/j.ocsci.2023.02.002>
- Willet W.C. (2002), Balancing lifestyle and genomic research for disease prevention, *Science*, 292, pp. 695–698, <https://doi.org/10.1126/science.1071055>
- Wongsagonsup R., Kittisuban P., Yaowalak A., Suphantharika M. (2015), Physical and sensory qualities of composite wheat-pumpkin flour bread with addition of hydrocolloids, *International Food Research Journal*, 22(2), pp. 745–752.
- Xiong Y., Ng K., Zhang P., Warner R., Shen S., Tang H.Y., Liang Z., Fang Z. (2020), In vitro α -glucosidase and α -amylase inhibitory activities of free and bound phenolic extracts from the bran and kernel fractions of five sorghum grain genotypes, *Foods*, 9, <https://doi.org/10.3390/foods9091301>
- Zallot C., Quilliot D., Chevaux J.B., Peyrin-Biroulet C., Guéant-Rodriguez R.M., Freling E., Collet-Fenetrier B., Williet N., Ziegler O., Bigard M.A., Guéant J.L., Peyrin-Biroulet L. (2013), Dietary beliefs and behavior among inflammatory bowel disease patients, *Inflammatory Bowel Disease*, 19(1), pp. 66–72, <https://doi.org/10.1002/ibd.22965>
- Zlateva D., Chochkov R. (2019), Effect of *Spirulina platensis* on the crumb firming of wheat bread during storage, *Ukrainian Food Journal*, 8(4), pp. 851–860, <https://doi.org/10.24263/2304-974X-2019-8-4-15>

Cite:

UFJ Style

Shevchenko A., Ivanišová E., Kováčiková E., Benešová L., Mykhonik L. (2024), Effect of complex plant supplement on shelf life of wheat bread, *Ukrainian Food Journal*, 13(2), pp. 274–286, <https://doi.org/10.24263/2304-974X-2024-13-2-6>

APA Style

Shevchenko, A., Ivanišová, E., Kováčiková, E., Benešová, L., & Mykhonik, L. (2024). Effect of complex plant supplement on shelf life of wheat bread. *Ukrainian Food Journal*, 13(2), 274–286. <https://doi.org/10.24263/2304-974X-2024-13-2-6>

Technological properties and functional food potential of oilseed cakes

Oxana Radu, Eugenia Covaliov, Tatiana Capcanari

Technical University of Moldova, Chisinau, Republic of Moldova

Abstract

Keywords:

Oilseed cake
Flour
Dough
Sunflower
Flaxseed
Pumpkin
Walnut

Introduction. The study aims to optimize processing methods, including grinding and sifting, to produce high-quality oilseed cakes flour suitable for various food applications. The focus is on the water absorption capacity necessary for flour products, leveraging by-products from the oil and fat industry.

Materials and methods. Oilseed cake samples from sunflower, linseed, pumpkin, walnut, and almond seeds were analyzed for particle size, sedimentation value, and moisture content. The Roseboom, Gibbs, and Stokes triangular method was used to formulate dough samples with oilseed cake flour, wheat flour, and water, developing five recipes to assess the technological properties of flour products.

Results and discussion. The study of the properties of analyzed oilseed cakes and their flours, focusing on bakery flour production was performed. Pressing at temperatures reaching 50–60°C produced varied cake forms, with flaxseed (0.5–2.0 mm thick, 10–15 cm long) and almond cakes (1.0–3.0 mm thick, 1–5 cm long) being suitable for fine flour due to their size. Sunflower seeds produced the highest oil yield at 62%, compared to almonds at 47%. Almonds had the lowest water loss at 8.2±0.3%, suggesting the need for specific storage and processing conditions for the resulting cake to prevent biological spoilage.

Flaxseed and walnut cakes were homogeneous, needing minimal sifting, whereas sunflower and pumpkin oilseed cakes required mandatory sifting due to peel fragments. Almond and walnut cakes had large particle sizes (0.2–3.2 mm), affecting flour texture and requiring individual processing. Concerning sedimentation value, except for pumpkin flour, all samples show high values (≥ 40 ml), which requires the regulation of the amount of water in the production of flour products.

Conclusion. To obtain flour from oilseed cake, the optimal dough composition was determined. The formulation includes 40% water, with a recommended ratio of 1:1 between oilseed cake flour and wheat flour.

Article history:

Received
22.12.2023
Received in
revised form
10.03.2024
Accepted
2.07.2024

Corresponding author:

Tatiana Capcanari
E-mail:
tatiana.capcanari@
toap.utm.md

DOI:

10.24263/2304-
974X-2024-13-2-7

Introduction

Oilseed cakes and meals, by-products of the oil and fat industry, are gaining attention due to their rich nutritional compositions and potential functional food applications (Arrutia et al., 2020; Karnika et al., 2022). Oilseed cakes, produced through mechanical pressing of seeds, typically contain 8–15% fat. In contrast, oilseed meals, obtained via solvent extraction, have a much lower fat content, less than 1% (Capcanari et al., 2024). Despite these differences, both forms are good sources of dietary fibre, essential fatty acids, and vegetable proteins, making them valuable for food innovation and health promotion (Usman et al., 2023; Wanasundara, 2011).

Historically, oilseed cakes were mainly used as animal feed due to their coarse texture and high fibre content (Glencross et al., 2007). However, advancements in food technology and growing consumer interest in plant-based ingredients have revitalized their potential for human consumption (Amoah et al., 2020; Oseyko et al., 2020; Stabnikova et al., 2023). This shift is driven by a global trend towards sustainable food systems and the reduction of food waste, creating a need to optimize the use of oilseed cakes (Nevara et al., 2023; Sharma et al., 2016; Sunil et al., 2016; Tsykhanovska et al., 2023).

In bakery applications, oilseed cakes offer several technological benefits. They enhance the protein profile of baked goods and improve texture and nutritional density due to their high protein and fibre content (Behera et al., 2013). The incorporation of oilseed cakes can affect the dough's gluten network, influencing the elasticity and texture of the final product (Tarek-Tilistyák et al., 2014). Their moisture-retention properties help maintain freshness and extend shelf life (Łopusiewicz et al., 2023). Additionally, some oilseed cakes have antioxidant properties that contribute to product stability and reduce spoilage (Capcanari et al., 2023). They can also impart unique flavours and aromas, enriching the sensory profile of bakery items. However, the effects on gluten formation and dough characteristics can vary with the seed source, necessitating careful formulation (De Lamo & Gómez, 2018). The potential benefits of oilseed cakes in enhancing nutritional profiles and extending shelf life make them a promising ingredient for functional food development, with ongoing research revealing new applications in the bakery industry.

The objective of this study is to refine the processing methods for oilseed cakes to enhance their application in food production. By focusing on optimizing grinding and sifting techniques, the study aims to produce oilseed cake flours with desirable properties, such as uniform particle size and appropriate water absorption capacity, to meet the needs of the food industry, especially in the creation of pastry products (Abedini et al., 2022). These innovations are expected to support the development of new food products enriched with unsaturated fatty acids, high-quality vegetable proteins, and fibres, contributing to both health benefits and sustainable food production.

Materials and methods

Oilseed cakes

By-products from the oil and fat industry were sourced to assess their quality. Especially, oilseed cakes derived from sunflower seeds (*Helianthus annuus*), flaxseeds (*Linum usitatissimum*), pumpkin seeds (*Cucurbita pepo*), walnuts (*Juglans regia*), and almonds (*Prunus amygdalus*) were collected, 2 kg, from different parts of the receiving

hopper to account for potential variability within batches and stored in vacuum sealed bags at 4 ± 2 °C.

Determination of oilseed cake particle sizes

To determine the particle size of oilseed cake samples, a Motic Digital Microscope (B1 Advanced Series, China) was utilized. For this analysis, 0.1 g of the test sample was placed on a glass slide next to a calibration scale. The sample was then positioned under the microscope. Photographs of the samples were captured using additional imaging devices for further analysis (Drakos et al., 2018).

Determination of moisture content in oilseed cakes

Moisture content in flour and oilseed cakes was determined using a gravimetric method. Samples weighing 5.0 ± 0.1 g were dried in a preheated oven at 102 ± 2 °C for 4 hours. Post-drying, samples were cooled in a desiccator to room temperature and reweighed. The moisture content (W , %) was calculated by the equation (1):

$$W(\%) = \frac{\text{Initial Weight} - \text{Dry weight}}{\text{Initial weight}} \times 100 \quad (1)$$

This method accurately measures the moisture content by evaluating the mass loss upon drying (Bradley, 2010; Nielsen, 2010).

Preparation of oilseed cake flour

The collected samples of oilseed cakes were homogenized by mixing to ensure consistency. Then each sample was ground into fine flour using a laboratory mill (IKA Tube Mill Control, Germany). The milling process was standardized to achieve a uniform particle size distribution, typically in the range of 200–250 microns.

Determination of sedimentation value for oilseed cake flour

The sedimentation value was determined using the micromethod by Pumpyansky, which requires the preparation of a working solution 18 hours before analysis. A 2% acetic acid solution was prepared by mixing 20 ml of glacial acetic acid (98% pure) with 200 ml of distilled water and diluting it to 1 litre. The working solution consisted of one part of ethanol mixed with four parts of the acetic acid solution, aiding in the distinct precipitation of flour samples. A 0.5 g flour sample was suspended in 10 ml of the working solution, shaken for homogeneity, and the sediment volume was recorded after 5 minutes. The sedimentation value was calculated by multiplying the sediment volume by 10, classifying flour as strong (>50 ml), valuable (30–40 ml), or weak (<30 ml) (Kibkalo, 2022; Zhygunov et al., 2018).

Analytical method for dough preparation

The equilateral triangle method of Rozeboom, Gibbs, and Stokes was employed for dough sample preparation. This technique involves the systematic blending of ingredients (premium quality wheat flour, drinkable water, and different types of oilseed cakes) to create

a matrix of potential combinations, allowing for the comprehensive analysis of their physical and chemical properties. Initially, each by-product sample – sunflower seed cake, linseed cake, pumpkin seed cake, walnut cake, and almond cake was finely ground and sieved to ensure uniformity in particle size. Afterward, the oilseed cake samples were mixed in various proportions with wheat flour and water, maintaining equal intervals, to form an equilateral triangle matrix. This approach facilitated the study of interactions between different components and their collective effects on the quality parameters being measured. Each mixture was thoroughly homogenized before further analytical procedures, ensuring consistent moisture levels and sample integrity. This method allows the optimization of ingredient combinations, ultimately enhancing the quality and functionality of the resulting mixtures (Radu, 2020). All the dough samples were baked, and quantitative and qualitative analyses were performed.

Determination of water absorption capacity of baked dough samples

The water absorption capacity of baked dough samples was assessed by measuring the mass increase after submersion in 20 °C water using stainless steel mesh with 2 mm holes. The procedure involves weighing the dry sample on the mesh submerging it in water for 2–4 minutes depending on the product removing and draining excess water, wiping the exterior and reweighing. The water absorption percentage is calculated as presented in equation (2).

$$X (\%) = \frac{m - m_1}{m_1} \times 100 \quad (2)$$

where m = the mass of the mesh with the wet product;
 m_1 = the mass of the dry product (Schopf and Scherf, 2021).

Determination of baking loss

Baking loss, also known as weight loss, refers to the difference in weight between the raw and baked final product. This loss occurs due to water evaporation from the product during the baking process (Covaliov et al., 2023).

To measure baking loss in bakery products, the raw product is first weighed to record its initial weight before baking. After baking, the finished product is allowed to cool to room temperature and then weighed again to record its final weight. The difference between the initial and final weights represents the baking loss.

Typically, baking loss is expressed as a percentage relative to the initial weight of the raw product. This measurement is crucial in the baking industry to assess the efficiency of the baking process and ensure consistent quality of the finished products (Milde et al., 2012).

Statistical analysis

All experiments were performed in triplicate. The results were presented as mean \pm standard deviation (SD). All calculations were performed with XLstat (2020 version) software.

Results and discussion

Analysis of the technological process used for oilseed cake obtaining

The production process for vegetable oils begins with storing raw materials in a controlled environment ($\leq +5^{\circ}\text{C}$, 70% humidity) to prevent contamination (Nerín et al., 2016). No chemical treatments are applied to maintain organic quality. Seeds are sorted by type and expiration, and stored in suitable bags to minimize oxidation. Weighed seeds are dried and purified with warm air, hulled, and ground for easier oil extraction. The ground seeds are fed into a hopper, where a screw conveyor regulates flow to the press, extracting oil and expelling the cake through a controlled process (Mwaurah et al., 2020).

The pressing was conducted at ambient temperature, but the pressure caused the temperature to rise to $50\text{--}60^{\circ}\text{C}$. The form of obtained oilseed cakes varied, depending on the type of the used raw material:

- Flaxseed cake: thin slabs, 0.5–2.0 mm thick, 10–15 cm long;
- Sunflower seed cake: thick slabs, 3.0–5.0 mm thick, 1–4 cm long;
- Pumpkin seed cake: slabs sometimes tubular, 1.0–2.0 mm thick, 10–14 cm long;
- Almond cake: slabs, 1.0–3.0 mm thick, 1–5 cm long;
- Walnut cake: slabs, 2.0–4.0 mm thick, 3–7 cm long.

With regards to the physical characteristics of various oilseed cakes, flaxseed and almond cakes have an advantage in storage and processing into flour for bakery products. The thin slabs of flaxseed cakes, about 0.5–2.0 mm thick and 10–15 cm in length, make them easier to grind into fine flour, suitable for products that need a smooth texture. Almond cakes, with their slab size of 1.0–3.0 mm thick and 1–5 cm long, are of a manageable size for the production of homogeneous flour. Sunflower seed cakes have thick slabs of 3.0–5.0 mm thick and 1–4 cm long, so there could be non-homogeneous grinding, although the greater oil content may be to its advantage if it is processed correctly. The cakes may be of a size that could cause difficulties with milling, such as pumpkin seed cakes in the form of tubular slabs, 1.0–2.0 mm thick and 10–14 cm long. Walnut cakes will end up with a more intensive grinding process because the slabs are thick and large, 2.0–4.0 mm thick, and 3–7 cm long, which may raise the cost. Therefore, flaxseed and almond cakes will ensure more efficient and effective flour production for bakery applications.

During the technological processing of seeds for oil extraction, drying at temperatures of $40\text{--}60^{\circ}\text{C}$ is applied to reduce the moisture content to approximately 6–8% (Mujumdar and Law, 2010). This step is crucial for achieving high-quality oil, maximizing yield, and preventing further degradation of the raw material (Rakita et al., 2023). Given this fact, the study evaluated the oil yield, seed water loss before pressing, and the amount of by-products generated based on the type of seed used (Figure 1). These parameters are essential for optimizing the efficiency of the oil extraction process and ensuring the quality of the final product (Hafids, 2018).

Based on the provided data (Figure 1), the analysis of oilseed cakes yield and seed water loss reveals notable differences among seeds. Sunflower seeds had the highest oil yield at $62.1\pm 0.8\%$, making them the most efficient for oil extraction. Walnuts showed the lowest oil yield at $43.3\pm 0.6\%$, indicating less efficiency in oil production. Almonds had a low water loss at $8.2\pm 0.3\%$, suggesting the need for specific storage and processing conditions for the resulting cake to prevent biological spoilage.

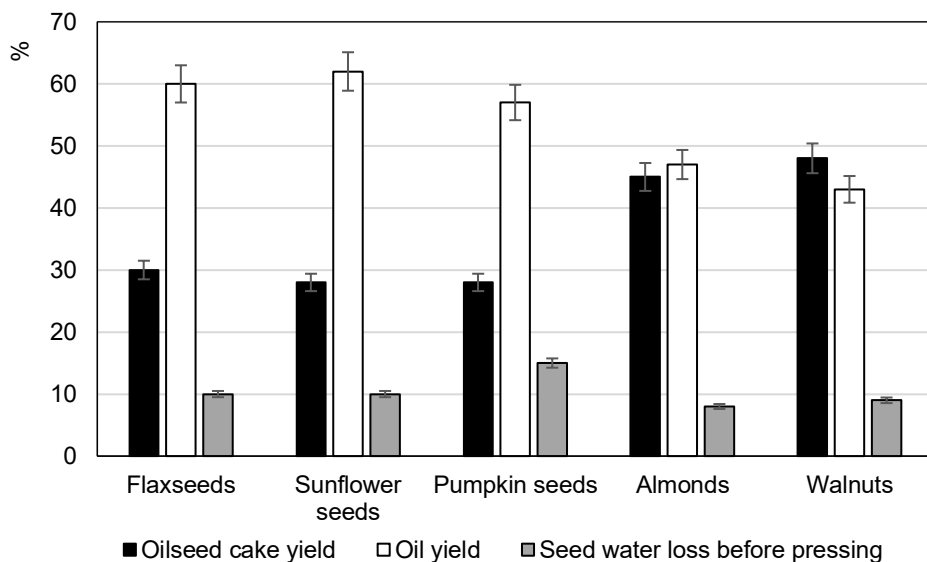


Figure 1. Yield of oilseed cakes obtained under industrial conditions, %

The small-sized oil pressing equipment used to obtain the studied samples had a processing capacity of 400 kg of seeds within 12 hours, or approximately 33 kg per hour. This type of equipment, although less advanced, tends to produce oilseed cake that is richer in biologically active substances such as proteins, vitamins, minerals, lipids, and dietary fibres (Siregar et al., 2015). The higher content of these nutrients in the oilseed cake makes it more valuable for the food industry compared to those produced by more advanced equipment, which might extract more oil but leave behind less nutritious oilseed cakes (Terpinc et al., 2012).

Characteristics of flour production from industrial oilseed cakes


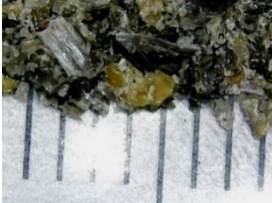








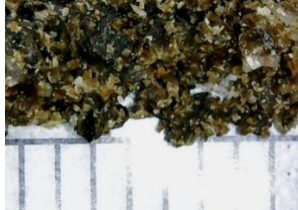




To ensure high-quality flour, a critical step involves cleaning and sorting the oilseed cake to remove impurities and unwanted residues (Wysocka et al., 2024). This process involves eliminating foreign particles, hulls, and other contaminants, ensuring a clean and high-quality cake suitable for further processing (Cappelli and Cini, 2021).

Recent studies have shown the importance of thorough cleaning and sorting in the preparation of oilseed cakes for flour production (Ortega-Rivas, 2012). Proper cleaning techniques not only enhance the nutritional quality of the final product, but also improve its safety and marketability (Mashanova et al., 2024).

The cleaned cake is subjected to grinding to produce the desired flour using specialized equipment like flour mills or grinders (Kaushal and Kumar, 2022). This grinding process reduces the cake to fine particles, resulting in a consistent flour suitable for various recipes and food products (Catterall and Cauvain, 2007).

For flour derived from sunflower and pumpkin oilseed cakes, sieving is essential due to their pressing in the peel. This step removes any remaining peels or impurities, ensuring a fine, homogeneous final product. Similarly, sieving is a crucial step for almond cake, as these nuts are processed with their skin, which can impart bitterness to the flour. Sieving was performed using specialized screens to eliminate larger particles and produce high-quality flour.

Table 1
Characteristics of particle size in different types of oilseed cakes

Oilseed cakes	Oilseed cakes images	Particle sizes	Flour images	Flour characteristics
Flaxseed cake		 1.0–2.0 mm		Homogeneous without solid impurities, sifting is optional
Sunflower seed cake		 0.2–1.0 mm		The amount of peel is very high, it requires sifting
Pumpkin seed cake		 0.4–2.2 mm		Pieces of seed peel of undesirable size are present, sifting is necessary
Almond cake		 0.2–2.5 mm		Solid pieces of peel are present, mandatory sifting is required
Walnut cake		 0.8–3.2 mm		Homogeneous without solid impurities, screening is optional

To determine the optimal method for producing flour from industrial cakes, particle size analysis was conducted. The digital microscope examination assessed the external appearance, contour shape, and surface characteristics of the particles, ensuring a thorough understanding of the grinding process and its outcomes.

The larger particle size of the oilseed cakes results in higher fat retention within the oilseed cakes, which can pose challenges in achieving a uniform flour texture (Souza, 2017). As shown in Table 1, the particle sizes of almond and walnut cakes are notably large, ranging from 0.2 to 3.2 mm, while other characteristics remain similar. These variables necessitate customized processing methods, such as grinding and sifting, to produce high-quality flour suitable for various food applications.

Consequently, oilseed cakes from almonds and walnuts exhibit substantial fat content that can impact both the nutritional profile and technological properties of baked products. Simultaneously, addressing particle size issues is critical to ensuring consistency and quality in the final flour product.

It should also be noted that oil from sunflower and pumpkin seeds is obtained by pressing the whole seeds without prior removal of the peels. This indicates that additional, thorough sieving or other processing steps are necessary to produce high-quality flour. The presence of peels in the final flour product from these seeds can further affect its texture and consistency.

Sedimentation value of flours from industrial oilseed cakes

The sedimentation value (SV) is a critical factor influencing the functionality of oilseed cake flours, particularly in the formulation of flour products, where moisture (W) management is essential (Cauvain, 2016).

The flour strength was evaluated by determining the sedimentation value (Figure 2), which measures the protein's capacity to swell in weak acid solutions. Except for pumpkin seed cake, all flour samples fall into the valuable or strong category based on sedimentation value (≥ 40 ml) (Kibkalo, 2022; Zhygunov et al., 2018). This suggests a need for minor adjustments in the water quantity when preparing flour semi-finished products.

While most oilseed cake flours exhibit a high sedimentation value (Figure 2), which is advantageous for texture and moisture retention in baked products, this characteristic also requires careful adjustment of water content during product development (Hay et al., 2023; Tafese Awulachew, 2020). Notably, pumpkin seed flour deviates from this trend, highlighting the need for specific processing adaptations to optimize its use in functional food products.

The technological properties of industrial oilseed cake flours were analyzed through baking tests using 50 g dough samples, formulated according to the Roseboom, Gibbs, and Stokes triangular method (Figure 3). Given the high strength of the oilseed cake flour (Figure 2), it was proposed to add water in amounts ranging from 30% to 50%. Wheat flour was used for comparative purposes.

Based on the obtained diagram (Figure 3), five recipes were developed for dough formulation using oilseed cake flour, water, and wheat flour: sample 1 – 30% oilseed cake, 30% wheat flour, 40% water; sample 2 – 40% oilseed cake, 10% wheat flour, 50% water; sample 3 – 20% oilseed cake, 50% wheat flour, 30% water; sample 4 – 10% oilseed cake, 40% wheat flour, 50% water; sample 5 – 50% oilseed cake, 20% wheat flour, 30% water.

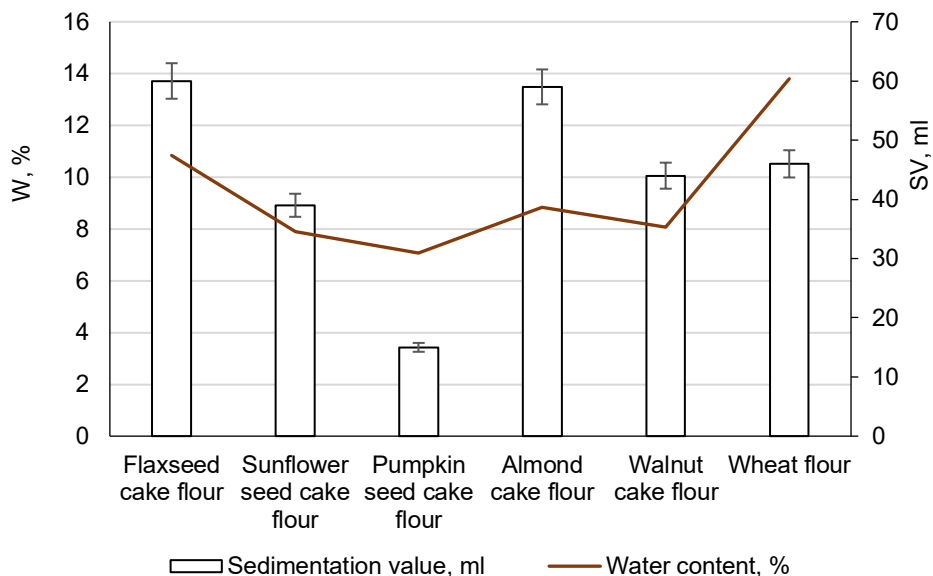


Figure 2. Sedimentation value (ml) and water content (%) of different types of oilseed cake flour

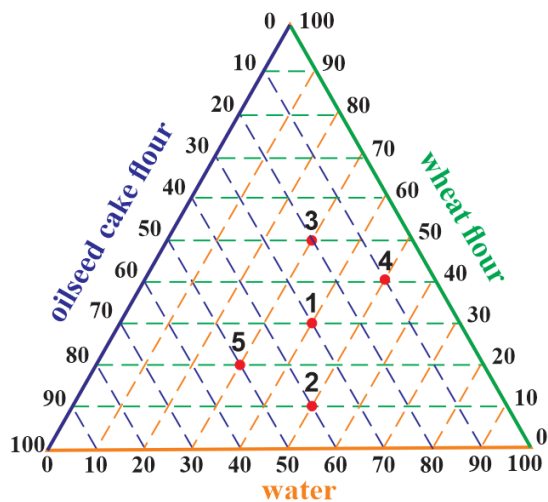


Figure 3. Dough composition formulation using oilseed cake flour, water, and wheat flour

The obtained semi-preparations were baked for 20 minutes at a temperature of 180°C. The sensory characteristics of flour products with industrial oilseed cakes are shown in Table 2.

Table 2

Sensory characteristics of flour products with industrial oilseed cakes

Flour product samples	Flour products with oilseed cakes				
	Flaxseed cake	Sunflower seed cake	Pumpkin seed cake	Almond cake	Walnut cake
Sample 1 (30% oilseed cake, 30% wheat flour, 40% water)	A subtle flax flavour, light brown colour, and a uniform texture with a well-shaped, crack-free surface.	A pleasant sunflower seed flavour, a light grey colour, and a uniform texture.	A pleasant smell, mild pumpkin taste, light green-yellow colour, and a uniform texture with a thick crust.	A noticeable almond smell, pleasant almond taste, brown colour, and a uniform texture with a crack-free surface.	A faint nutty smell, mild nut taste, brown colour, and a uniform texture with no cracks.
Sample 2 (40% oilseed cake, 10% wheat flour, 50% water)	A strong flax flavour, brown colour, and a hard, crumbly texture with a well-shaped surface and small cracks.	A strong sunflower seed smell and taste, dark grey colour, and a soft, uniform texture with a well-shaped, crack-free surface and some peel.	A pronounced pumpkin smell and taste, green-yellow colour, and a soft, uniform texture with many small cracks, and some peel.	A pronounced almond smell, a bitter almond taste, a dark brown colour, and a hard, uniform texture with small pieces of skin and no cracks.	A faint nutty smell, slightly bitter nut taste, dark brown colour, and a soft, uniform texture with no cracks.
Sample 3 (20% oilseed cake, 50% wheat flour, 30% water)	A neutral smell, flax and wheat flour taste, light brown colour, and a hard, uniform, crumbly texture with small cracks.	A sunflower seed smell and taste, light grey colour, and a hard, uniform, floury texture with a crack-free surface.	A neutral smell, mild pumpkin taste, light green-yellow colour, and a uniform texture with a well-shaped, crack-free surface.	A faint almond smell and taste, a light brown colour, and a hard, uniform texture and no cracks.	A faint nutty smell, mild nut taste, light brown colour, and a hard, uniform texture with no cracks.
Sample 4 (10% oilseed cake, 40% wheat flour, 50% water)	A mild flax flavour, light brown colour, and a soft, uniform, elastic texture with a well-shaped, crack-free surface.	A light sunflower seed smell and taste, light grey colour, a soft, uniform, elastic texture and no cracks.	A neutral smell, mild pumpkin taste, light green-yellow colour, and a soft, uniform, elastic texture with a crack-free surface.	A light almond smell and taste, a light brown colour, a soft, uniform texture and no cracks.	A neutral smell, mild nut taste, light brown colour, and a soft, uniform texture with no cracks.
Sample 5 (50% oilseed cake, 20% wheat flour, 30% water)	A strong flax smell and taste, dark brown colour, and a hard, crumbly texture with a dense, uniform surface and large cracks. Inedible.	A strong sunflower seed smell and taste, dark grey colour, and a soft, uniform texture with a well-shaped, crack-free surface and a large amount of peel.	A pronounced pumpkin taste, neutral smell, light green-yellow colour, and a hard, uniform texture with a well-shaped surface and many cracks. Inedible.	A faint almond smell, a strong bitter almond taste, a dark brown colour, and a hard, uniform texture with small pieces of skin and no cracks. Inedible.	A faint nutty smell, pronounced slightly bitter nut taste, dark brown colour, and a hard, uniform texture with no cracks.

The substitution of wheat flour with various cake flours (flaxseed, sunflower, pumpkin, almond, and walnut) significantly influences the resulting dough's baking properties and sensory attributes (Table 2). For instance, the composition with 30% wheat flour, 40% water, and 30% flaxseed cake flour maintained a uniform surface without cracks, showing a strong flaxseed aroma and flavour, and a firm homogeneous texture. Higher proportions of flaxseed cake flour led to minor cracks and a pronounced linseed flavour, affecting overall palatability. Similarly, the sunflower cake flour samples exhibited a strong sunflower seed aroma and flavour, with a dark grey colour and firm texture. The sunflower samples with 40% oilseed cake flour and 50% water showed no cracks but had a dense, homogeneous structure.

Pumpkin seed cake flour resulted in a pleasant appearance with a green-yellow colour and homogeneous structure (Table 2). Samples with higher pumpkin oilseed cake flour content demonstrated a pronounced pumpkin flavour and a soft, elastic texture, making them more appealing in terms of sensory characteristics. Almond cake flour, on the other hand, showed a significant impact on the dough's colour and taste. Higher almond oilseed cake content led to a strong almond aroma and bitter taste, with a firm texture and the presence of small skin pieces, which might not be desirable for all consumers. Walnut oilseed cake flour exhibited unique properties, including a mild nutty flavour and firm homogeneous texture. Samples with 30% wheat flour, 40% water, and 30% walnut oilseed cake showed a dark brown colour and slight bitterness, maintaining a good form and homogeneous surface without cracks.

The effect of three variables (oilseed flour, water, and wheat flour content) on baking loss and water absorption capacity was investigated (Figure 4).

According to the data in Figure 4, among the different flours, flaxseed cake and walnut cake showed the most significant variations in baking loss, with walnut cake reaching as high as $33.9 \pm 0.4\%$ and flaxseed cake at $17.7 \pm 0.6\%$. These high baking losses suggest an impact on the structural integrity of the final product. In terms of water absorption capacity, flaxseed cake exhibited the highest value at $15.3 \pm 0.2\%$, indicating its potential to retain more moisture during baking. On the other hand, sunflower and pumpkin oilseed cake flours demonstrated moderate to high water absorption, with sunflower reaching $5.9 \pm 0.2\%$ and pumpkin $10.0 \pm 0.3\%$. These variations highlight the importance of adjusting formulations based on the specific flour type used to optimize both the texture and moisture content of the final baked goods.

Thus, it was established that to obtain flour items, the composition of the dough from oilseed cake flour must include 40% water, and the recommended ratio between oilseed cake and wheat flour is 1:1.

The substitution of wheat flour with different oilseed cake flours affects not only the baking loss and water absorption capacity but also the sensory attributes of the final product. These variations can be leveraged to produce flour products with diverse flavours and textures, catering to different consumer preferences and dietary needs. Further research into optimizing these blends could enhance the functional and sensory qualities of the resulting baked goods.

In addition to health benefits, integrating vegetable fibres and proteins into food products offers significant economic and ecological advantages. The vegetable protein market is expanding, and diversifying the product range with items based on oilseed cakes from flaxseed, sunflower, pumpkin, almonds, and walnuts can help meet growing consumer demand. This diversification not only enhances food options but also contributes to sustainable agricultural practices by utilizing the by-products of oil extraction, thus promoting a circular economy.

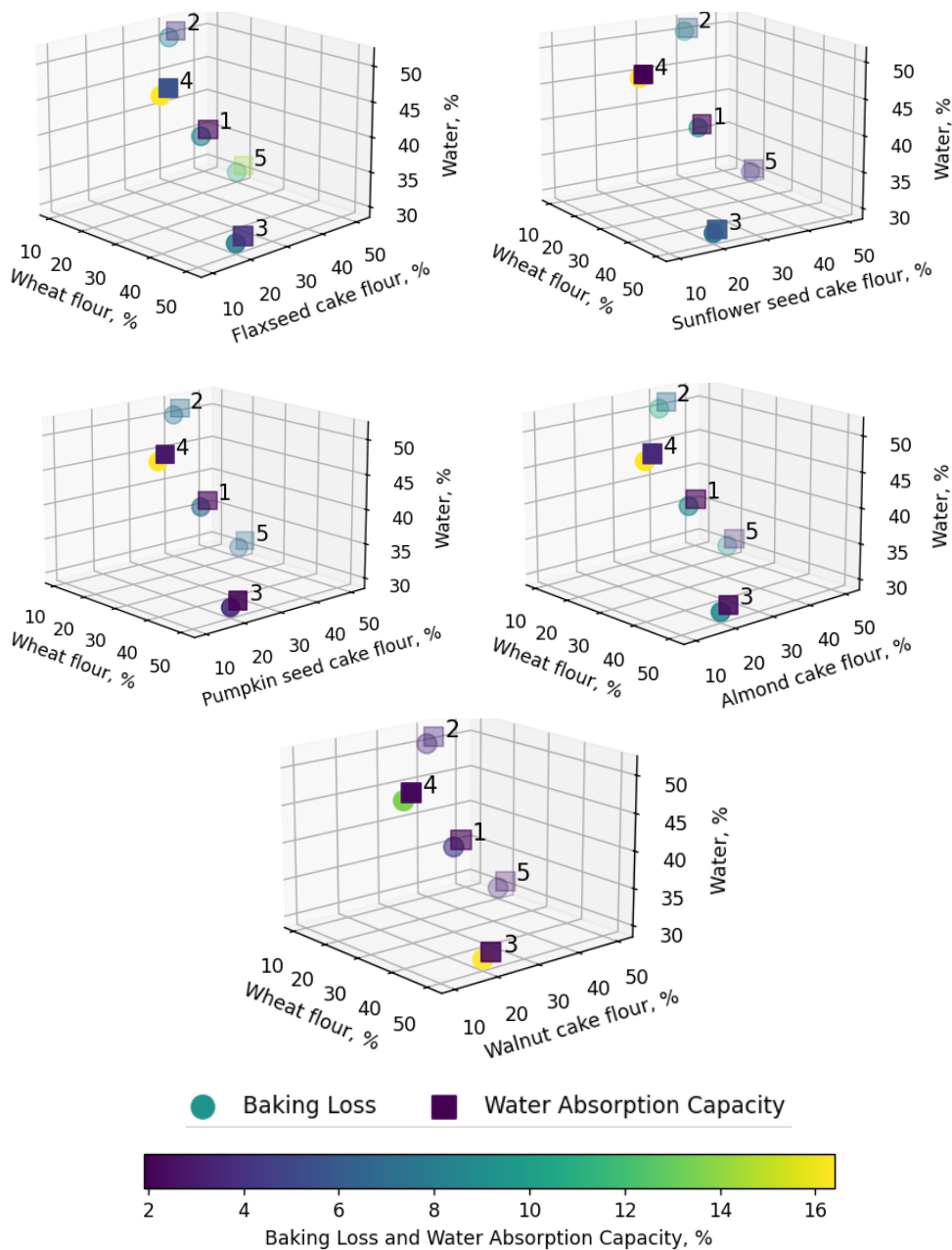


Figure 4. Effect of different dough compositions on baking losses and water absorption capacity of final flour products:

- 1 – 30% oilseed cake, 30% wheat flour, 40% water;
- 2 – 40% oilseed cake, 10% wheat flour, 50% water;
- 3 – 20% oilseed cake, 50% wheat flour, 30% water;
- 4 – 10% oilseed cake, 40% wheat flour, 50% water;
- 5 – 50% oilseed cake, 20% wheat flour, 30% water.

Conclusions

1. Flaxseed and almond cakes are advantageous for flour production due to their thinner, more manageable slab sizes, facilitating smoother grinding. In contrast, sunflower, pumpkin, and walnut cakes may present challenges due to their thicker or larger slabs, potentially affecting grinding efficiency and cost. Meanwhile, sunflower seeds offer the highest oil yield and quality oilseed cakes. Almonds present challenges due to the low water loss before pressing.
2. The industrial method of oil obtaining plays a decisive role in determining oilseed cakes' physicochemical and technological properties. Large particle sizes in almond and walnut oilseed cakes require specialized processing to ensure uniform flour texture. In addition, the presence of peels in flours from sunflower and pumpkin oilseed cakes requires extra sieving to obtain high-quality flour, impacting texture and consistency.
3. Most flours from oilseed cake exhibit a high sedimentation value, beneficial for texture and moisture retention in baked goods. However, flour from pumpkin oilseed cake requires specific processing adaptations due to its lower sedimentation value. Proper water adjustments are necessary during product development to optimize these flours' use in functional food products.
4. To obtain flour products from oilseed cake, the optimal dough composition was determined. The formulation includes 40% water, with a recommended ratio of 1:1 between oilseed cake flour and wheat flour.

Acknowledgment. The research was supported by Institutional Project, subprogram 020405 “Optimizing food processing technologies in the context of the circular bioeconomy and climate change”, Bio-OpTehPAS, being implemented at the Technical University of Moldova.

References

- Abedini A., Alizadeh A.M., Mahdavi A., Golzan S.A., Salimi M., Tajdar-Oranj B., Hosseini H. (2022), Oilseed cakes in the food industry; A review on applications, challenges, and future perspectives, *Current Nutrition & Food Science*, 18(4), pp. 345–362, <https://doi.org/10.2174/1573401317666211209150147>
- Amoah I., Taarji N., Johnson P.N.T., Barrett J., Cairncross C., Rush, E. (2020), Plant-based food by-products: Prospects for valorisation in functional bread development, *Sustainability*, 12(18), 7785, <https://doi.org/10.3390/su12187785>
- Arrutia F., Binner E., Williams P., Waldron K.W. (2020), Oilseeds beyond oil: Press cakes and meals supplying global protein requirements, *Trends in Food Science & Technology*, 100, pp.88–102, <https://doi.org/10.1016/j.tifs.2020.03.044>
- Behera S., Indumathi K., Mahadevamma S., Sudha M.L. (2013), Oil cakes – a by-product of agriculture industry as a fortificant in bakery products, *International Journal of Food Sciences and Nutrition*, 64(7), pp. 806–814, <https://doi.org/10.3109/09637486.2013.801405>

- Bradley R.L. (2010), Moisture and total solids analysis, *Food Analysis*, pp. 85–104, https://doi.org/10.1007/978-1-4419-1478-1_6
- Capcanari T., Covaliov E., Negoita C. (2024), Hemp (*Cannabis sativa L.*) seeds nutritional aspects and food production perspectives: A review, *Food Systems*, 7(1), pp. 52–58, <https://doi.org/10.21323/2618-9771-2024-7-1-52-58>
- Capcanari T., Covaliov E., Negoita C., Siminiuc R., Chirsanova A., Reșitca V., Țurcanu D. (2023), Hemp seed cake flour as a source of proteins, minerals and polyphenols and its impact on the nutritional, sensorial and technological quality of bread, *Foods*, 12(23), 4327, <https://doi.org/10.3390/foods12234327>
- Cappelli A., Cini E. (2021), Challenges and opportunities in wheat flour, pasta, bread, and bakery product production chains: A systematic review of innovations and improvement strategies to increase sustainability, productivity, and product quality, *Sustainability*, 13(5), 2608, <https://doi.org/10.3390/su13052608>
- Catterall P., Cauvain S.P. (2007), Flour milling, *Technology of Breadmaking*, pp. 333–369, https://doi.org/10.1007/0-387-38565-7_12
- Cauvain S.P. (2016), Bread and other bakery products, In: P. Subramaniam (Ed.), *The stability and shelf life of food*, pp. 431–459, <https://doi.org/10.1016/B978-0-08-100435-7.00015-0>
- Covaliov E., Capcanari T., Reșitca V., Chirsanova A. (2023), Quality evaluation of sponge cake with milk thistle (*Silybum marianum L.*) seed powder addition. *Ukrainian Food Journal*, 12(1), pp. 7–20, <https://doi.org/10.24263/2304-974X-2023-12-1-3>
- De Lamo B., Gómez M. (2018), Bread Enrichment with oilseeds. A review, *Foods*, 7(11), 191, <https://doi.org/10.3390/foods7110191>
- Drakos A., Pelava E., Evageliou V. (2018), Properties of flour films as affected by the flour's source and particle size. *Food Research International*, 107, pp. 551–558, <https://doi.org/10.1016/j.foodres.2018.03.005>
- Glencross B.D., Booth M., Allan G.L. (2007), A feed is only as good as its ingredients? A review of ingredient evaluation strategies for aquaculture feeds, *Aquaculture Nutrition*, 13(1), pp. 17–34, <https://doi.org/10.1111/j.1365-2095.2007.00450.x>
- Hafids S. (2018), Optimization of drying temperature in the production process of tea seed oil, *Indonesian Food Science & Technology Journal*, 2(1), pp. 9–12, <https://doi.org/10.22437/iftst.v2i1.6296>
- Hay F.R., Rezaei S., Wolkis D., McGill C. (2023), Determination and control of seed moisture, *Seed Science and Technology*, 51(2), pp. 267–285, <https://doi.org/10.15258/sst.2023.51.2.11>
- Karnika, Verma J., Rani S., Deepankar, Kumar S. (2022), Nutrition evaluation of oilseed meals, *Journal of Agriculture Research and Technology*, Special (01), pp. 45–56, <https://doi.org/10.56228/JART.2022.SP109>
- Kaushal P., Kumar, N. (2022), Processing of cereals, In: H.K. Sharma, N. Kumar (Eds.), *Agro-Processing and Food Engineering*, pp. 415–454, https://doi.org/10.1007/978-981-16-7289-7_10
- Kibkalo I. (2022), Effectiveness of and perspectives for the sedimentation analysis method in grain quality evaluation in various cereal crops for breeding purposes, *Plants*, 11(13), 1640, <https://doi.org/10.3390/plants11131640>
- Łopusiewicz Ł., Kowalczewski P.Ł., Baranowska H.M., Masewicz Ł., Amarowicz R., Krupa-Kozak U. (2023), Effect of Flaxseed oil cake extract on the microbial quality, texture and shelf life of gluten-free bread, *Foods*, 12(3), 595, <https://doi.org/10.3390/foods12030595>
- Mashanova N., Satayeva Z., Smagulova M., Kundyzbayeva N., Karimova G. (2024), Nutritional and structural evaluation of gluten-free flour mixtures incorporating various oilseed cakes, *Processes*, 12(8), 1616, <https://doi.org/10.3390/pr12081616>

- Milde L.B., Ramallo L.A., Puppo M.C. (2012), Gluten-free bread based on tapioca starch: Texture and sensory studies, *Food and Bioprocess Technology*, 5(3), pp. 888–896, <https://doi.org/10.1007/s11947-010-0381-x>
- Mujumdar A.S., Law C.L. (2010), Drying technology: Trends and applications in postharvest processing, *Food and Bioprocess Technology*, 3(6), pp. 843–852, <https://doi.org/10.1007/s11947-010-0353-1>
- Mwaurah P. W., Kumar S., Kumar N., Attkan A. K., Panghal A., Singh V. K., Garg M. K. (2020), Novel oil extraction technologies: Process conditions, quality parameters, and optimization, *Comprehensive Reviews in Food Science and Food Safety*, 19(1), pp. 3–20, available at: <https://doi.org/10.1111/1541-4337.12507>
- Nerín C., Aznar M., Carrizo D. (2016), Food contamination during food process, *Trends in Food Science & Technology*, 48, pp. 63–68, <https://doi.org/10.1016/j.tifs.2015.12.004>
- Nevara G.A., Giwa Ibrahim S., Syed Muhammad S.K., Zawawi N., Mustapha N.A., Karim R. (2023), Oilseed meals into foods: An approach for the valorization of oilseed by-products, *Critical Reviews in Food Science and Nutrition*, 63(23), pp. 6330–6343, <https://doi.org/10.1080/10408398.2022.2031092>
- Nielsen S. S. (2010), Determination of moisture content, *Food Analysis Laboratory Manual*, pp. 17–27, https://doi.org/10.1007/978-1-4419-1463-7_3
- Ortega-Rivas E. (2012), Common preliminary operations: Cleaning, sorting, grading, *Food Engineering Series*, pp.11–25, https://doi.org/10.1007/978-1-4614-2038-5_2
- Oseyko M., Romanovska T., Shevchyk V. (2020), Justification of the amino acid composition of sunflower proteins for dietary and functional products. *Ukrainian Food Journal*, 9(2), pp. 394–403, <https://doi.org/10.24263/2304-974X-2020-9-2-11>
- Radu O. (2020), *Compoziții alimentare pe baza uleiului de nucă (Juglans regia L.) rezistente la degradări oxidative*, PhD theses, http://www.cnaa.md/files/theses/2020/56546/oxana_radu_thesis.pdf
- Rakita S., Kokić B., Manoni M., Mazzoleni S., Lin P., Luciano A., Ottoboni M., Cheli F., Pinotti L. (2023), Cold-pressed oilseed cakes as alternative and sustainable feed ingredients: A review, *Foods*, 12(3), 432, <https://doi.org/10.3390/foods12030432>
- Schopf M., Scherf K.A. (2021), Water absorption capacity determines the functionality of vital gluten related to specific bread volume, *Foods*, 10(2), 228, <https://doi.org/10.3390/foods10020228>
- Sharma S.K., Bansal S., Mangal M., Dixit A.K., Gupta R. K., Mangal A.K. (2016), Utilization of food processing by-products as dietary, functional, and novel fiber: A review, *Critical Reviews in Food Science and Nutrition*, 56(10), pp. 1647–1661, <https://doi.org/10.1080/10408398.2013.794327>
- Siregar A.N., Ghani J.A., Haron C.H.C., Rizal M., Yaakob Z., Kamarudin S.K. (2015), Comparison of oil press for jatropha oil: A review, *Research in Agricultural Engineering*, 61(1), pp. 1–13, <https://doi.org/10.17221/22/2013-RAE>
- Souza T.M. (2017), *Rheological properties for quality control of wheat and dry cake mixes*, PhD theses, <https://hdl.handle.net/11244/54575>
- Stabnikova O., Shevchenko A., Stabnikov V., Paredes-López O. (2023), Utilization of plant processing wastes for enrichment of bakery and confectionery products, *Ukrainian Food Journal*, 12(2), 299–308, <https://doi.org/10.24263/2304-974X-2023-12-2-11>
- Sunil L., Prakruthi A., Prasanth K.P., Gopala K.A. (2016), Development of health foods from oilseed cakes, *Journal of Food Processing & Technology*, 7(11), 631, <https://doi.org/10.4172/2157-7110.1000631>
- Tafese Awulachew M. (2020), Understanding basics of wheat grain and flour quality, *Journal of Health and Environmental Research*, 6(1), 10, <https://doi.org/10.11648/j.jher.20200601.12>

- Tarek-Tilistyák J., Agócs J., Lukács M., Dobró-Tóth M., Juhász-Román M., Dinya Z., Jekő J., Máthé E. (2014), Novel breads fortified through oilseed and nut cakes, *Acta Alimentaria*, 43(3), pp. 444–451, <https://doi.org/10.1556/AAlim.43.2014.3.11>
- Terpinc P., Čeh B., Ulrih N.P., Abramovič H. (2012), Studies of the correlation between antioxidant properties and the total phenolic content of different oil cake extracts, *Industrial Crops and Products*, 39, pp. 210–217, <https://doi.org/10.1016/j.indcrop.2012.02.023>
- Tsykhanovska I., Yevlash V., Tovma L., Adamczyk G., Alexandrov A., Lazarieva T., Blahyi O. (2023). Flour from sunflower seed kernels in the production of flour confectionery, In O. Stabnikova, O. Shevchenko, V. Stabnikov, O. Paredes-López (Eds.), *Bioconversion of waste to value-added products*, pp. 129-167, CRC Press, Boca Raton, London, New York, <https://doi.org/10.1201/9781003329671-5>
- Usman I., Saif H., Imran A., Afzaal M., Saeed F., Azam I., Afzal A., Ateeq H., Islam F., Shah Y.A., Shah M.A. (2023), Innovative applications and therapeutic potential of oilseeds and their by-products: An eco-friendly and sustainable approach. *Food Science & Nutrition*, 11(6), pp. 2599–2609, <https://doi.org/10.1002/fsn3.3322>
- Wanasundara J.P.D. (2011), Proteins of *Brassicaceae* Oilseeds and their potential as a plant protein source, *Critical Reviews in Food Science and Nutrition*, 51(7), pp. 635–677, <https://doi.org/10.1080/10408391003749942>
- Wysocka K., Cacak-Pietrzak G., Feledyn-Szewczyk B., Studnicki M. (2024), The baking quality of wheat flour (*Triticum aestivum* L.) Obtained from wheat grains cultivated in various farming systems (organic vs. integrated vs. conventional), *Applied Sciences*, 14(5), 1886, <https://doi.org/10.3390/app14051886>
- Zhygunov D., Kovalova V., Kovalov M., Donets A. (2018), Development of technological solutions for flour production with specified quality parameters, *Food Science and Technology*, 12(3), <https://doi.org/10.15673/fst.v12i3.1043>

Cite:

UFJ Style

Radu O., Covaliov E., Capcanari T. (2024), Technological properties and functional food potential of oilseed cakes, *Ukrainian Food Journal*, 13(2), pp. 287–302, <https://doi.org/10.24263/2304-974X-2024-13-2-7>

APA Style

Radu, O., Covaliov, E., & Capcanari, T. (2024). Technological properties and functional food potential of oilseed cakes. *Ukrainian Food Journal*, 13(2), 287–302. <https://doi.org/10.24263/2304-974X-2024-13-2-7>

Use of chokeberry in the preparation of bakery products

Galyna Khomych¹, Tetiana Lebedenko², Galina Krusir³

1 – Poltava University of Economics and Trade, Poltava, Ukraine

2 – Odesa National Technological University, Odesa, Ukraine

3 – Institute of Eco-Entrepreneurship, School of Life Sciences, University of Applied Sciences and Arts Northwestern Switzerland, Muttenz, Switzerland

Abstract

Keywords:

Bakery
Wheat bread
Chokeberry
Phytoadditives
Quality
Freshness
Storage
Stability

Article history:

Received
27.12.2023
Received in revised
form 11.05.2024
Accepted
2.07.2024

Corresponding author:

Tetiana Lebedenko
E-mail:
tatyanaledenko27
@gmail.com

DOI:

10.24263/2304-
974X-2024-13-2-8

Introduction. The purpose of the study was to determine the quality indicators of chokeberry fruits and their by-products, to select the most promising ones for improving the sensory and physicochemical properties of bakery products and their stability during storage.

Materials and methods. Chokeberry fruit, puree, and juice were used for their inclusion to the recipe of bakery products. The titrated and active acidity, content of dry substances, pectin, L-ascorbic acid, colorants, phenolic substances, organic acids, sugars and biological activity were determined in phyto-raw materials.

Results and discussion. The valuable chemical compounds, g/100 g fresh weight (FW): phenolic substances (0.9), organic acids (2.3), sorbitol (7.19), glucose (3.67), fructose (3.22), fiber (2.3), ash (0.85), and, mg/100 g FW: ascorbic acid (37) and high biological activity were found in the chokeberry by-products. It was found the presence of citric acid – 0.04 g/100 g, malic acid – 1.20 g/100 g, succinic acid – 1.05 g/100 g of fresh fruits. Malic acid dominated among organic acids – 52.0% of the total content, succinic acid – 45.9%. Colorants predominated among phenolic substances consisted 70.5%. The content of anthocyanins was 95.9% of total the flavonoids.

When preparing bread from wheat flour of the 1st grade, chokeberry puree was added in the amount of 3, 6, 9, and 12% to the weight of flour, intensification of dough fermentation was found. The addition of puree in the amount of 3 to 9% to the mass of flour had a positive effect on the specific volume, porosity and acidity of the products. The color of the crust and crumb of the bread changed, and an uncharacteristic color and taste of the finished product appeared. The volume of bread increased by 2.6%, porosity by 3.7%, and the structural and mechanical properties of the pulp improved. Loss of freshness of bread enriched with 9.0% chokeberry puree after 72 hours of storage was 22.7%, and the total deformation of the crumb decreased by 49.4% compared to the control. Chokeberry puree was effective in preventing the development of potato disease of bread within 120 hours of storage.

Conclusions. The studies of the quality characteristics of chokeberry by-products showed their valuable chemical composition and high biological activity. Addition of chokeberry puree to bread increased its specific volume, porosity, and sensory characteristics.

Introduction

Considering the need to ensure food security, sustainable development in the world and improve the nutritional value of food products, herbal raw materials are widely used in the food industry (Ivanov et al., 2021; Stabnikova et al., 2021).

Chokeberry fruits are rich in valuable compounds in its composition. Ripe fruits contain 74.1–81.0% water, 6.5–10.6% sugars, 0.3–0.6% pectin substances, 0.1–0.2% nitrogen substances, 0.7–1.8% organic acids. The total amount of mineral substances varied from 1.85 to 2.97% dry matter (DM). The iodine content in it is 0.005–0.01 mg/100 g of ripe fruits, while only red currants and persimmons contain the same amount of iodine – 0.0021–0.0021 mg/100 g (Bakhshaliyeva et al., 2023), although feijoa fruits contain more of it – 0.008–0.009 mg/100 g (Ferrara and Montesano, 2001). However, the most valuable component in the composition of chokeberry is bioflavonoids – catechins, flavonols, and anthocyanins (Sidor and Gramza-Michałowska, 2019). Chokeberry and their by-products have antioxidant properties, which makes them a valuable additive to different food products (Aksoy, 2023).

Chokeberry fruits are characterized by a tart and bitter taste. That is why they are rarely consumed in fresh form. They are processed for the production of juices, jams, beverages, preserves, wines, liqueurs, and infusions, jellies, and for obtaining food extracts and colorants (Kitryte et al., 2017).

Nowadays, chokeberry fruits in form of dry powder or extracts are used in preparation of functional food products, such as yogurt (Cuşmenco and Bulgaru, 2020; Ryzhkova et al., 2023), kefir (Du and Myracle, 2018), confectionary (Ghendov-Mosanu et al., 2022; Sady and Sielicka-Różyńska, 2019), and bakery (Koshak and Pokrashinskaya, 2020).

The technology of cookies with chokeberry additives was developed. Addition of 5% chokeberry powder and 5% chokeberry extract to the mass of wheat flour showed that the protein content increased by $1.3 \pm 0.1\%$ in cookies compared to the control sample without chokeberry, phenolic compounds – by 0.04–0.21%. The determination of the peroxide index of lipids in cookies showed its decrease by 38.75–42.5% because of the effect of chokeberry phenolic substances on reduction free fatty acids and volatile carbonyl compounds (aldehydes and ketones) formation, which will contribute to slowing down the oxidation of fats during storage (Sady and Sielicka-Różyńska, 2019).

The effect of chokeberry powder on the quality of pasta made from flour with different gluten content (2.5 – 25%) was investigated. It was established that when using flour of normal quality with 25% gluten content, the addition of chokeberry powder in the amount of 5% to the weight of flour had a positive effect on the mechanical strength of pasta products, increasing it by 20% compared to the control sample without chokeberry powder. When using flour with 18% gluten content, pasta was obtained with a strength of 0.66 N and the amount of dry substances that passed into the cooking water was less than 7.9%. It means that chokeberry can be used as a pasta improver (Koshak and Pokrashinskaya, 2020).

During the processing of chokeberry fruits, pomace is obtained which is waste. Pomace has greater antioxidant activity than juice or powder (Mayer-Miebach et al., 2012). Lyophilized chokeberry pomace was added to wheat bread in the amount 1, 2, 3, 4, 5, and 6% to the weight of flour. The addition of pomace increased the water absorption of the flour, but caused a decrease in stability and loosening of the dough, leading to an increase in softening. The volume of bread decreased, and the hardness of the crumb increased. Bread enriched with pomace had higher content of minerals, dietary fibers, phenolic compounds and a higher antioxidant activity compared to the control bread. Sensory evaluation showed that the rational dosage of lyophilized chokeberry pomace was no more than 3%. Then dietary fiber content increased by 80.9%, ash content – by 2.6%, fat content – by 26.5%, and

total phenolic content – by 272%. Protein content reduced by 1.2% and the carbohydrate content – by 4% compared to the control sample (Cacak-Pietrzak et al., 2023).

Considering the valuable components of chokeberry and the mass consumption of baked goods, it is important to consider the possibility of using chokeberry to improve the quality and nutritional value of bakery products.

The aim of the present study was to determine the effect of chokeberry puree on sensory and physicochemical properties of bread from wheat flour, and its stability during storage.

Materials and methods

Materials

Chokeberry fruit (variety ‘Vseslava’, Ukraine), puree and juice were used for research. Dough samples were prepared according to the recipe, % by mass of flour: wheat flour – 100.0%, pressed baker's yeast – 3.0%, salt – 1.5%. Black chokeberry puree was added to the experimental samples in the amount of 3.0%, 6.0%, 9.0%, and 12.0% to the mass of flour. The dough with 44.0% moisture was kneaded in a steamless method. The fermentation period lasted for 60 – 90 minutes. The dough was kneaded in a two-speed Kenwood KVC 5100T kneading machine (China). The dough pieces were left in a thermostat at a temperature of $38\pm 2^{\circ}\text{C}$ and a relative humidity of $78\pm 2\%$ until ready. The products were baked in a Sveba-Dahlen cabinet oven (Italy) at a temperature of $200\text{--}220^{\circ}\text{C}$ with humidification of the baking chamber for 30 minutes.

Methods

Phenolic compounds content in chokeberry by-products

The content of phenolic compounds was determined by the method of high-performance liquid chromatography on an Agilent Technologies chromatograph (model 1100). A chromatographic column 2.1×150 mm filled with an octadecylsilyl sorbent with granule size of $3.5\ \mu\text{m}$, "ZORBAX" SB-C18, was used for the analysis.

The detection parameters were set: wavelength – 313 nm (for phenolic acids and their derivatives), 350 nm (for glycosides of flavones), 371 nm (for flavones), 525 nm (for anthocyanins); for a fluorescent detector extinction was 280 nm, emission – 320 nm for catechin and epicatechin; measurement scale – 1.0; scan duration – 2 sec. Parameters of spectrum capture – each peak 190 – 600 nm.

Identification of phenolic compounds was carried out by retention time of standards and spectral characteristics (compared to literature data of high-performance liquid chromatography of berries and juices) (de Araujo et al., 2014).

Amount of sugars and organic acids in chokeberry by-products

To analyze the content of sugars and organic acids in chokeberry processed products, 5 g of pulp was placed in a 10 ml measuring tube and brought up to the mark with water. After 30 min of exposure in an ultrasonic bath, the solution was filtered through a Teflon membrane filter with a pore size of $0.45\ \mu\text{m}$ into a vial for analysis.

A carbohydrate chromatographic column 7.8×300 mm "Supelcogel-C610H" was used to analyze the content of organic acids and sugars by the method of high-performance liquid chromatography.

To carry out the analysis, the following chromatography mode was set: mobile phase supply rate 0.5 ml/min, eluent aqueous 0.1% H₃PO₄ solution, the working pressure of the eluent was 33-36 kPa, the temperature of the column thermostat was 30 °C, sample volume – 5 µl.

Spectrophotometric detection parameters were set as follows: wavelength 210 nm, gap width 8 nm, scanning time 0.5 – 1.0 s.

Identification of organic acids and sugars was carried out according to the retention time of the corresponding standards (Rodrigues et al., 2021).

Biological activity in chokeberry by-products

For determination of biological activity in chokeberry fruit (Patent of Ukraine G01N33/00/ The method of determining the biological activity of objects of natural origin), fruits were ground in the presence of quartz sand and a phosphate buffer solution at pH 6.8-7.4. Then, it was transferred with a buffer solution into a volumetric flask at a dilution of 1:(50-200), infused with a buffer solution for 8-12 minutes and filtered. The prepared extract was diluted in distilled water in a ratio of 1:(10-100) and added to a mixture of buffer and potassium ferrocyanide, a solution of NAD×H₂ was introduced, and the biological activity was calculated by the ratio of the change in the oxidation rate NAD×H₂/NAD in the control and test samples, taking into account the dilution. The oxidation rate was determined by measuring the optical density of the solutions of the test and control samples at a wavelength of 325 nm and a thickness of the absorbing layer of 10 mm (at t=120 s) according to the formula (1):

$$BA = \frac{(A_0^s - A_{120}^s) \cdot V \cdot K}{(A_0^c - A_{120}^c) \cdot m} \quad (1)$$

where BA – biological activity, units of activity; A_0^s – initial optical density of the test sample; A_{120}^s – initial optical density of the test sample after 120 s; A_0^c – initial optical density of the control sample; A_{120}^c – initial optical density of the control sample after 120 s; V – capacity of the measuring flask, ml; K – the degree of dilution of the extract in distilled water, m – weight of raw material, g.

The indicator of biological activity in chokeberry juice was determined by the method of controlling the electron transport activity of juice in the system of reduced nicotinamide adenine dinucleotide (NAD · H₂) – potassium ferrocyanide in a phosphate buffer (pH=7.5) (Ivanisová et al., 2015). During the interaction of reduced nicotinamide adenine dinucleotide with potassium ferrocyanide in a phosphate buffer, the transfer of electrons was catalyzed by the phenolic compounds of juice, that possess electron transport properties, in particular, the transfer rate depends on their nature and concentration. The value of biological activity was calculated from the ratio of the oxidation rate of NAD · H₂/NAD in the control sample and the test sample, taking into account the dilution, and the oxidation rate was determined by measuring the relative density of the analyzed solutions at a wavelength of 325 nm and a thickness of the absorbing layer of the cuvette of 10 mm according to the formula (2):

$$BA = \frac{\Delta A_s}{\Delta A_c} K \quad (2)$$

where BA – biological activity, units of activity, ΔA_s – value of the optical density of the test sample, ΔA_c – value of the optical density of the control, K – the dilution factor.

Gas-forming capacity of flour

The gas-forming capacity of flour was determined using the AG-1 device by the amount of released carbon dioxide (ml) at a temperature of 30 °C during 5 hours of fermentation of the dough from 100 g of the studied flour, 60 ml of water and 10 g of pressed yeast (Shevchenko et al., 2023a).

Amount and quality of gluten in flour

The amount of wet gluten in flour was measured as the ratio of the mass of washed raw gluten to the mass of flour, expressed as a percentage.

Gluten deformation index was measured using the principle of the residual deformation of the gluten sample after the effects of the tare load during the 30 sec (Shevchenko et al., 2023b).

Sensory evaluation of bread

Bread quality was assessed by sensory parameters – appearance, surface condition, crust color, porosity structure, taste, smell (Galenko et al., 2024). The scoring of bread was carried out with the involvement of 20 tasters by the 5-point scale of individual indicators (Sammalisto et al., 2021).

Moisture of bread crumb

Moisture of bread crumb was determined by drying the weight in a SESH-3M drying cabinet (Ukraine) at a temperature of 130°C for 40 min (Hetman et al., 2021).

Acidity of bread crumb

Acidity of bread crumb was determined by titrating the extract prepared from bread crumb with sodium hydroxide solution or potassium in the presence of a phenolphthalein indicator (Hetman et al., 2021).

Porosity of bread crumb

The porosity of bread crumb was determined as the volume of pores in a certain volume of crumb, expressed as a percentage of the total volume.

Specific volume of bread

The volume of bread was determined on special device - a volume meter (capacity with small grain), which works on the principle of squeezing out grain with bread. The volume of extruded grain (ml), measured using a cylinder, corresponds to the volume of bread (Shevchenko et al., 2022). The specific volume of bread was determined by dividing the volume of bread by its mass and was expressed to the nearest 1 ml/100 g (Zhu et al., 2016).

Dimensional stability of bread

The dimensional stability of bread was determined by measuring the height and diameter of bread (mm) and was evaluated by their ratio (Shevchenko et al., 2022).

Deformation of bread crumb

Deformation of bread crumb is measured as the amount of immersion (penetration) of an equipment of a certain shape and size under the influence of a certain load for a certain time. To characterize the structural and mechanical properties of pulp, its relative plasticity and elasticity were determined (Bilyk et al., 2022; Wongsagonsup et al., 2015).

Mold and Potato disease of bread

Bread crumb is put to the plate containing a growth medium (agar) and then analyzing the plate under a microscope for colonies of mold (viable or cultured sample analysis) (Garcia and Copetti, 2019). Potato disease of bread was determined after baking and storage during 2 days by observation the process of growth of molds (Uazhanova, 2014).

Statistical analysis

The data represents the mean of a minimum three replicates \pm standard deviation (S.D.).

Results and discussions

Chokeberry fruits were analyzed at the stage of consumer ripeness. According to the sensory evaluation, chokeberry fruits had intensive black color, a pleasant astringent taste and a weak aroma.

Physico-chemical indicators of raw materials are important for determining their potential influence on the quality characteristics of products, to the recipe of which they will be added. It was determined that the chemical composition of chokeberry fruits contain up to 80.0% water, they have a sufficiently high titrated acidity (Table 1).

Table 1
Physico-chemical characteristics of chokeberry fruit

Indicators	Content	Indicators	Content
Dry matter, g/100 g FW	20.5 \pm 0.1	Citric acid, g/100 g FW	0.04
Titrated acidity, grades	1.38 \pm 0.12	Malic acid, g/100gFW	1.20
Pectin, g/100 g FW	0.3 \pm 0.1	Succinic acid, g/100 g FW	1.05
Protopectin, g/100 g FW	0.6 \pm 0.1	L-ascorbic acid, mg/100 g FW	37.50 \pm 0.75
Fiber, g/100 g FW	2.3 \pm 0.2	Colorants*, mg/100 g FW	718.86 \pm 5.14
Ash, g/100 g FW	0.85 \pm 0.03	Phenolic compounds, mg/100 g FW	1020 \pm 15.81

Note: * – conversion to cyanidin

Among the organic compounds carbohydrates predominated. Polysaccharides consisted mainly of pectin substances and fiber. The content of pectin substances was 0.9%. Determination of the composition of organic acids of chokeberry fruits indicated the presence of citric acid – 0.04 g/100 g of raw material, malic acid – 1.20 g/100 g, succinic acid – 1.05 g/100 g. Malic acid dominated among organic acids and consisted 52.0% of the total content, followed by succinic acid, 45.9%. The presence of these acids is valuable in view of their properties. It is known that malic acid has anti-inflammatory, anti-edematous, and laxative effects (Chen et al., 2024), and succinic acid has the ability of a reducing and radical-accepting agent responsible for antioxidant protection (Chien et al., 2008).

The largest amount of soluble solids in chokeberry fruits were sugars. It was found that they are represented by hexoses – glucose – 3.67 g/100 g of raw material and fructose – 3.22 g/100 g of raw material. Chokeberry fruits contains sorbitol – 7.19 g/100 g of raw material, which consisted 51% of the total sugar content. The presence of sorbitol indicates the therapeutic and preventive properties of chokeberry fruits (Banjari et al., 2017). The high content of phenolic substances was determined in chokeberry fruits (Table 1), and colorants predominated among phenolic substances, their content was 70.5% of their total content.

Flavonoids were also present in chokeberry fruits (Zheng and Wang, 2003). Fractional composition of phenolic compounds in chokeberry fruits is shown in Table 2.

Table 2

Composition of phenolic compounds in chokeberry fruits

Compounds	Oxycinnamic acids and their derivatives	Flavones and their derivatives	Anthocyanins	Total amount of flavonoids
Content, mg/100 g	180.97	29.32	689.55	718.87

It was determined that anthocyanins predominated among the flavonoids of chokeberry fruits. In chokeberry fruits anthocyanins were represented by glycosidamicianidin with carbohydrates – glucose, galactose, arabinose and xylose. The amount of anthocyanins among the flavonoids was 95.9%. The composition of anthocyanins was dominated by cyanidin-3-O-galactoside – 442.43 mg/100 g (64.2% of the total content of anthocyanins), cyanidin-3-O-arabinoside – 185.36 mg/100 g (26.9%) and almost equal proportions of cyanidin-3-O-glucoside (31.72 mg/100 g) and cyanidin-3-O-xyloside (30.03 mg/100 g). Among the flavonoids there were representatives of flavones, their amount was 4.1% of the total content of flavonoids, and they were represented by quercetin-3-O-glucoside (20.95 mg/100 g) and quercetin-3-O-galactoside (8.37 mg/100 g).

The highest content of phenolic substances and, in particular, colorants was found in the peel of the fruit, their content was 2050 mg/100 g and 1500 mg/100 g, respectively.

The food industry often uses by-products of chokeberry processing – juice and puree, so the quality indicators were determined specifically in them (Table 3).

The obtained results show that the content of pectin, colorants and pectin substances in puree was higher than in juice obtained by pressing from crushed chokeberry fruits. During such preliminary processing of raw materials, the yield of juice was only 50% of the mass of raw materials, and the yield of puree was 76%. The extracts obtained after extracting juice contained 810 mg/100 g of colorants and 1050 mg/100 g of phenolic substances in their composition, which also confirms the fact that a significant part of them removes as waste, which can also be used for further processing with obtaining low-grade puree, extracts or powders.

Table 3

Physico-chemical characteristics of chokeberry by-products

Indicators	Chokeberry juice	Chokeberry puree
Dry matter, g/100 g FW	15.20±0.62	16.80±0.73
Titrated acidity, degrees	1.34±0.17	1.31±0.07
Pectin, g/100 g FW	0.45±0.05	0.88±0.08
L-ascorbic acid, mg/100 g FW	18.21±1.12	14.20±0.98
Colorants, mg/100 g FW	224.80±9.80	340.80±9.93
Phenolic compounds, mg/100 g FW	368.20±15.50	530.50±15.80
pH, units	3.46±0.05	3.50±0.05

The presence of phenolic substances in chokeberry fruits and by-products, in particular, anthocyanins cause their high biological activity and antioxidant properties (Figure 1).

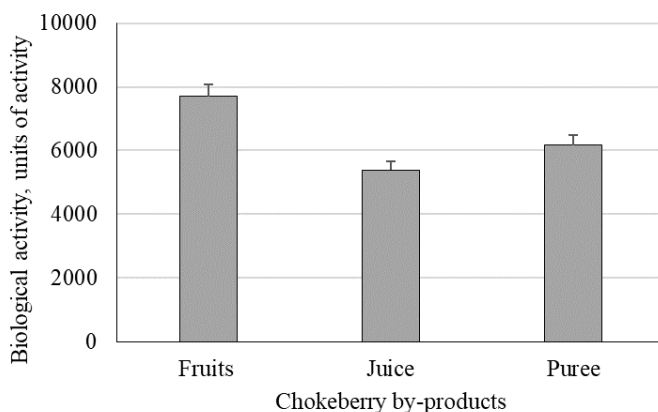


Figure 1. Biological activity of chokeberry fruits and by-products

The results of studies of biological activity during the production of juices and purees showed their decrease compared to fruits. However, in puree samples, the indicator of biological activity was higher by 14% in comparison with juice.

Thirty-five volatile compounds were determined in chokeberry juice, 34 of which were identified. Aromatic compounds included alcohols, acids, aldehydes, ketones, lactones, ethers, and heterocyclic compounds. The dominant group of acids was benzoic acid (15 mg/l), which indicated the presence of a natural antioxidant in chokeberry.

Thus, a more rational was using chokeberry puree to enrich food products. When producing bread of high quality when adding chokeberry by-products the properties of flour as the main raw material are extremely important.

The flour was characterized by average baking properties: flour moisture – 14%, wet gluten content – 29.2%, gluten deformation index – 85 device units, extensibility – 17.5 cm, gas generating capacity – 1500 ml/100 g. Fermentation was more intensive in all experimental samples. The best effect was in the dough with the content of puree in the amount of 9.0% by mass of flour (Figure 2).

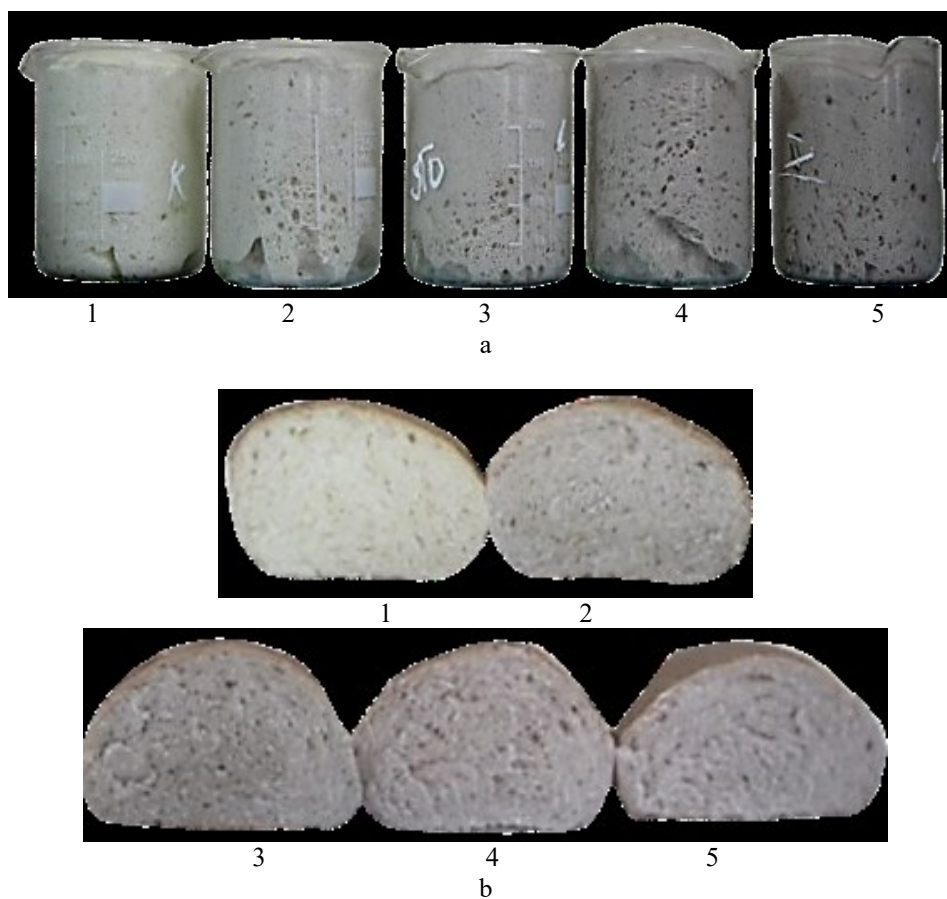


Figure 2. Dough (a) and bread (b) with different amount of chokeberry puree:
1 – control; 2 – 3%; 3 – 6.0%; 4 – 9.0%; 5 – 12.0%

The addition of chokeberry puree caused a change in color, giving a pleasant purple color, intensity of which increased with increasing dosage (Figure 3).

The addition of puree in the amount of 3 to 9% to the mass of flour had a positive effect on the specific volume, porosity and acidity of the products, a tendency to strengthen the structure of the dough and increased the dimensional stability of bread (Table 4).

Addition of 12% chokeberry puree decreased specific volume by 1.02%.

In the case of adding puree to the dough, the general, plastic and elastic deformation of the pulp improved in all samples. However, the best result was obtained with a puree content of 9% by weight of flour. Thus, the loss of freshness of bread enriched with 9.0% puree after 72 hours amounted to 22.7% compared to the control bread, the total deformation of the crumb during this period decreased by 49.4%.

Evaluation of the microbiological stability of samples of bread wrapped in polyethylene film during 120 hours of storage showed that the addition of chokeberry puree was effective in preventing the development of potato disease and mold.

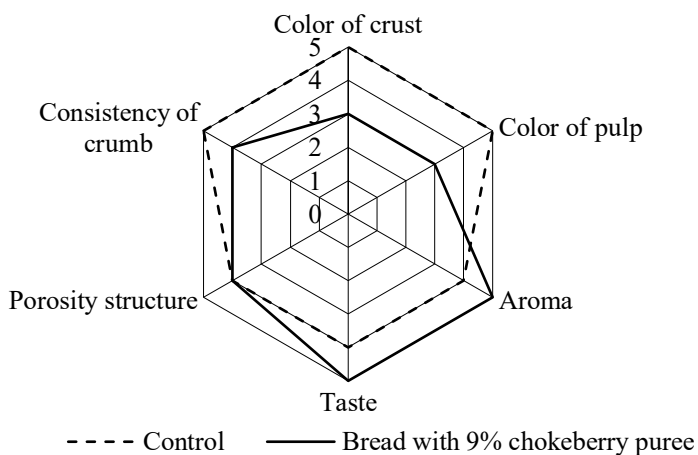


Figure 3. Evaluation of sensory indicators of wheat bread with 9% of chokeberry puree

Table 4
Physico-chemical and microbiological indicators of the quality of wheat bread with chokeberry puree

Indicators	Control	Additive dosage, % by mass of flour			
		3	6	9	12
Moisture content, %	42.8	43.2	43.0	42.8	43.6
Specific volume, ml/g	2.93	2.92	3.13	3.19	2.90
Form stability, H/D	0.59	0.65	0.63	0.61	0.57
Porosity, %	69.8	70.1	71.6	72.4	69.7
Acidity, degrees	2.2	2.6	2.9	3.2	3.5
Deformation of the crumb, units of penetrometer					
after 4 hours	79	82	84	88	800
after 72 hours	40	58	65	68	65
Mold	after 96 hours	not detected			
Potato disease of bread	after 48 hours	not detected			

Therefore, the conducted studies of the quality indicators of chokeberry by-products and the quality indicators of bread with this raw material testified to the improvement of the specific volume, porosity of bread and the possibility of increasing its the antioxidant activity. However, some aspects require further research. There are substantiation of the methods of storage of chokeberry by-products, preparation for production, quality standardization, which will ensure the formation of the necessary functional and technological properties while preserving the valuable biologically active substances, physiological and preventive effects.

Conclusions

1. The valuable chemical composition and high biological activity of chokeberry fruits were found, which was ensured by the high content of pectin, phenolic substances, organic acids, sorbitol, ascorbic acid.
2. The obtained results show that the content of pectin and colorants in puree was higher than in juice obtained by pressing from crushed chokeberry fruits. During such preliminary processing of raw materials, the yield of juice was only 50% of the mass of raw materials, and the yield of puree was 76%. The extracts contained 810 mg/100 g of colorants and 1050 mg/100 g of phenolic substances in their composition, which also confirms the fact that a significant part of them removes as waste, which can also be used for further processing with obtaining low-grade puree, extracts or powders.
3. For use in the preparation of bread from wheat flour of the first grade, the use of chokeberry in the form of puree was proposed.
4. The influence of chokeberry puree in dosages of 3, 6, and 9% to the weight of flour had a positive effect on the specific volume, porosity and acidity of the products, a tendency to strengthen the structure of the dough and increased the dimensional stability of bread. Addition of 12% chokeberry puree decreased specific volume by 1.02%.
5. In the case of adding puree to the dough, the general, plastic and elastic deformation of the pulp improved in all samples. However, the best result was obtained with a puree content of 9% by weight of flour. Thus, the loss of freshness of bread enriched with 9.0% puree after 72 hours amounted to 22.7%, compared to the control bread, the total deformation of the crumb during this period decreased by 49.4%.

References

- Aksoy A. S. (2023), A review of the nutritional profile, chemical composition and potential health benefits of *Aronia melanocarpa* (Chokeberry) berries and products, *Turkish Journal of Agriculture - Food Science and Technology*, 11(10), pp. 2027–2043.
- Bakhshaliyeva N., Aliyeva K., Mammadov J., Hummatov A. (2023), The content of microelements in fruits of the oriental persimmon (*Diospyros kaki*) and its dietary role in remedying micronutrient deficiency in the region, *Regulatory Mechanisms in Biosystems*, 3, pp. 444–450, <https://doi.org/10.15421/10.15421/022365>
- Banjari I., Misir A., Šavikin K., Jokić S., Molnar M., De Zoysa H. K. S., Waisundara V. Y. (2017), Antidiabetic effects of *Aronia melanocarpa* and its other therapeutic properties. *Frontiers in Nutrition*, 4, 53, <https://doi.org/10.3389/fnut.2017.00053>
- Bilyk O., Burchenko L., Bondarenko Yu., Vasheka O., Rak V. (2022), Application of a multi-component bakery improver in the technology of wheat bread enriched with the mixture of sprouted grains, *Ukrainian Journal of Food Science*, 10(2), pp. 136–148, <https://doi.org/10.24263/2310-1008-2022-10-2-4>
- Cacak-Pietrzak G., Dziki D., Gawlik-Dziki U., Parol-Nadłonek N., Kalisz S., Krajewska A., Stępniewska S. (2023), Wheat bread enriched with black chokeberry (*Aronia melanocarpa* L.) pomace: physicochemical properties and sensory evaluation, *Applied Sciences*, 13, 6936, <https://doi.org/10.3390/app13126936>
- Chen M., Zhao Y., Li S., Chang Z., Liu H., Zhang D., Wang S., Zhang X., Wang J. (2024), Maternal malic acid may ameliorate oxidative stress and inflammation in sows through modulating gut microbiota and host metabolic profiles during late pregnancy, *Antioxidants*, 13, 253, <https://doi.org/10.3390/antiox13020253>

- Chien S. C., Chen M. L., Kuo H. T., Tsai Y. C., Lin B. F., Kuo Y. H. (2008), Anti-inflammatory activities of new succinic and maleic derivatives from the fruiting body of *Antrodia camphorate*, *Journal of Agricultural and Food Chemistry*, 56(16), pp. 7017–22, <https://doi.org/10.1021/jf801171x>
- Cuşmenco T., Bulgaru, V. (2020), Quality characteristics and antioxidant activity of goat milk yogurt with fruits, *Ukrainian Food Journal*, 9(1), pp. 86–98, <https://doi.org/10.24263/2304-974X-2020-9-1-8>
- de Araújo K. M., de Lima A., Silva J. do N., Rodrigues L. L., Amorim A. G., Quelemes P. V., Dos Santos R. C., Rocha J. A., de Andrades É. O., Leite J. R., Mancini-Filho J., da Trindade R. A. (2014), Identification of phenolic compounds and evaluation of antioxidant and antimicrobial properties of *Euphorbia Tirucalli* L., 17(3(1)), pp. 159–175. <https://doi.org/10.3390/antiox3010159>
- Du X., Myracle A.D. (2018), Development and evaluation of kefir products made with aronia or elderberry juice: Sensory and phytochemical characteristics, *International Food Research Journal*, 25(4), pp. 1373–1383, Available at: [http://ifrj.upm.edu.my/25%20\(04\)%202018/\(7\).pdf](http://ifrj.upm.edu.my/25%20(04)%202018/(7).pdf)
- Ghendov-Mosanu A., Ungureanu-Iuga M., Mironeasa S., Sturza R. (2022), Aronia extracts in the production of confectionery masses, *Applied Sciences*, 12(15), 7664, <https://doi.org/10.3390/app12157664>
- Ryzhkova T., Odarchenko A., Silchenko K., Danylenko S., Verbytskyi S., Heida I., Kalashnikova L., Dmytrenko A. (2023), Effect of herbal extracts upon enhancing the quality of low-fat cottage cheese, *Innovative Biosystems and Bioengineering*, 7(2), pp. 22–31, <https://doi.org/10.20535/ibb.2023.7.2.268976>
- Ferrara L., Montesano D. (2001), Nutritional characteristics of feijoa sellowiana fruit: the iodine content, *Rivista di Scienza dell'Alimentazione*, 30(4), pp. 353–356.
- Galenko O., Shevchenko A., Ceccanti C., Mignani C., Litvynchuk S. (2024), Transformative shifts in dough and bread structure with pumpkin seed protein concentrate enrichment, *European Food Research and Technology*, 250, pp. 1177–1188, <https://doi.org/10.1007/s00217-023-04454-z>
- Garcia M.V., Copetti M. (2019), Alternative methods for mold spoilage control in bread and bakery products, *International Food Research Journal*, 26(3), pp. 737–749.
- Hetman I., Mykhonik L., Kuzmin O., Shevchenko A. (2021), Influence of spontaneous fermentation leavens from cereal flour on the indicators of the technological process of making wheat bread, *Ukrainian Food Journal*, 10(3), pp. 492–506, <https://doi.org/10.24263/2304-974X-2021-10-3-6>
- Ivanisová E., Francáková H., Ritschlová P., Dráb S., Solgajová M., Tokár M. (2015), Biological activity of apple juice enriched by herbal extracts, *The Journal of Microbiology, Biotechnology and Food Sciences*, 4, pp. 69–73, <https://doi.org/10.15414/jmbfs.2015.4.special3.69-73>
- Ivanov V., Shevchenko O., Marynin A., Stabnikov V., Gubenia O., Stabnikova O., Shevchenko A., Gavva O., Saliuk A. (2021), Trends and expected benefits of the breaking edge food technologies in 2021–2030, *Ukrainian Food Journal*, 10(1), pp. 7–36, <https://doi.org/10.24263/2304-974X-2021-10-1-3>
- Kitryte V., Kraujaliene V., Sulniute V., Pukalskas A., Rimantas Venskutonis P. (2017), Chokeberry pomace valorization into food ingredients by enzyme-assisted extraction: Process optimization and product characterization, *Food and Bioprocess Processing*, 105, pp. 36–50, <https://doi.org/10.1016/j.fbp.2017.06.001>
- Koshak Z., Pokrashinskaya A. (2020), Black chokeberry powder as an improver for pasta, *Food Science and Technology*, 14(1), pp. 125–133, <https://doi.org/10.15673/fst.v14i1.16>
- Mayer-Miebach E., Adamiuk M., Behsnilian D. (2012), Stability of chokeberry bioactive polyphenols during juice processing and stabilization of a polyphenol-rich material from the by-product, *Agriculture*, 2, pp. 244–258, <https://doi.org/10.3390/agriculture2030244>
- Rodrigues D. P., Daltro M., Lima V. A., Barreto-Rodrigues M., Pereira E. A. (2021), Simultaneous determination of organic acids and sugars in fruit juices by High performance liquid chromatography: characterization and differentiation of commercial juices by principal component analysis, *Ciência Rural*, 51(3), <https://doi.org/10.1590/0103-8478cr20200629>

- Sady S., Sielicka-Różyńska M. (2019), Quality assessment of experimental cookies enriched with freeze-dried black chokeberry, *Acta Scientiarum Polonorum, Technologia Alimentaria*, 18(4), pp. 463–471, <https://doi.org/10.17306/J.AFS.2019.0686>
- Sammalisto S., Laitinen M., Sontag-Strohm, T. (2021), Baking quality assessment of twenty whole grain oat cultivar samples, *Foods*, 10(10), 2461, <https://doi.org/10.3390/foods10102461>
- Shevchenko A., Drobot V., Galenko O. (2022), Use of pumpkin seed flour in preparation of bakery products, *Ukrainian Food Journal*, 11(1), pp. 90–101, <https://doi.org/10.24263/2304-974X-2022-11-1-10>
- Shevchenko A., Litvynchuk S., Koval, O. (2023a) The influence of rice protein concentrate on the technological process of wheat bread production, *EUREKA: Life Sciences*, 4, pp. 22–29, <https://doi.org/10.21303/2504-5695.2023.003031>
- Shevchenko A., Fursik O., Drobot V., Shevchenko O. (2023b), The use of wastes from the flour mills and vegetable processing for the enrichment of food products, In O. Stabnikova, O. Shevchenko, V. Stabnikov, and O. Paredes-López (Eds.), *Bioconversion of Wastes to Value-added Products*, CRC Press, Boca Raton, London, Available at: <https://doi.org/10.1201/9781003329671>
- Sidor A., Gramza-Michałowska A. (2019), Black chokeberry *Aronia melanocarpa* L. a qualitative composition, phenolic profile and antioxidant potential, *Molecules*, 24(20), 3710, <https://doi.org/10.3390/molecules24203710>
- Stabnikova O., Marinin A., Stabnikov V. (2021), Main trends in application of novel natural additives for food production, *Ukrainian Food Journal*, 10(3), 524–551, <https://doi.org/10.24263/2304-974X-2021-10-3-8>
- Uazhanova R.U. (2014), The research of the microbiological stability during storage of bread affected by potato disease, *World Applied Sciences Journal*, 30(10), pp. 1394–1396, <https://doi.org/10.5829/idosi.wasj.2014.30.10.14180>
- Wongsagonsup R., Kittisuban P., Yaowalak A., Supphantharika M. (2015), Physical and sensory qualities of composite wheat-pumpkin flour bread with addition of hydrocolloids, *International Food Research Journal*, 22(2), pp. 745–752.
- Zheng W., Wang S. Y. (2003), Oxygen radical absorbing capacity of phenolics in blueberries, cranberries, chokeberries, and lingonberries, *Journal of Agricultural and Food Chemistry*, 51(2), pp. 502–509, <https://doi.org/10.1021/jf020728u>
- Zhu F., Sakulnak R., Wang S. (2016), Effect of black tea on antioxidant, textural, and sensory properties of Chinese steamed bread, *Food Chemistry*, 194, pp. 1217–1223, <https://doi.org/10.1016/j.foodchem.2015.08.110>

Cite:

UFJ Style

Khomych G., Lebedenko T., Krusir G. (2024), Use of chokeberry in the preparation of bakery products, *Ukrainian Food Journal*, 13(2), 303–315, <https://doi.org/10.24263/2304-974X-2024-13-2-8>

APA Style

Khomych, G., Lebedenko, T., & Krusir, G. (2024). Use of chokeberry in the preparation of bakery products. *Ukrainian Food Journal*, 13(2), 303–315. <https://doi.org/10.24263/2304-974X-2024-13-2-8>

Thermal stable α -galactosidase from *Penicillium restrictum* for biodegradation of galactooligosaccharides

Nataliia Borzova

D.K. Zabolotny Institute of Microbiology and Virology, National Academy of Sciences of Ukraine, Kyiv

Abstract

Keywords:

A-galactosidase
Penicillium restrictum
Stability
Specificity
Galacto-oligosaccharides

Article history:

Received 4.01.2024
Received in revised form 23.04.2024
Accepted 2.07.2024

Corresponding author:

Nataliia Borzova
E-mail:
nvb.imv@gmail.com

DOI: 10.24263/2304-974X-2024-13-2-9

Introduction. Studying the functional properties of practically important enzymes, in particular α -galactosidases, is a necessary step towards obtaining stable preparations with high selectivity of action to be used in the food industry for biodegradation and modification of raw materials.

Materials and methods. Gel filtration and ion exchange chromatography on TSK-gels were used to purify the microbial α -galactosidase. To determine the activity and specificity of the enzymatic action, *p*-nitrophenyl- α -D-galactopyranoside, raffinose, stachyose, and galactomannan were used as substrates.

Results and discussion. α -Galactosidase with a specific activity of 49.1 IU/mg was isolated from the culture liquid of *Penicillium restrictum* and purified to a homogeneous state. The molecular weight of the enzyme was 17 kDa according to the data of gel filtration on Sepharose 6B. The optimum pH for the enzyme action was 4.0, and the thermal optimum was 60 °C. Enzyme showed high stability in the temperature ranged from 40 to 60 °C. The half-life of α -galactosidase from *Penicillium restrictum* at 70°C increased in 2-fold in the presence of 20–40% glycerol and 2.3-fold in the presence of 4 M sorbitol. K_m for the hydrolysis of *p*-nitrophenyl- α -galactopyranoside, raffinose, stachyose, and galactomannan were 0.9 mM, 2.2 mM, 2.4 mM, and 3.8 mM, respectively. It was shown that the rate and efficiency of hydrolysis of galactose-containing natural substrates by *Penicillium restrictum* α -galactosidase decreased with increasing their molecular weight. The enzyme was completely inhibited in the presence of 10^{-3} M Ag^+ , Hg^{2+} , Ca^{2+} , and Cd^{2+} . α -Galactosidase from *Penicillium restrictum* was resistant to action of proteinase K, pronase E, and trypsin.

Conclusions. The high thermal stability and efficiency of α -galactosidase from *Penicillium restrictum* for the modification of galactooligosaccharides suggests its broad-range applicability for food and animal feed processing.

Introduction

Currently, industry for the production of food and feed increasingly involves biotechnological processes. Among them, enzymatic treatment is a convenient and effective way for obtaining food products of improved quality (Meszaros et al., 2021). Compared to inorganic catalysts, enzymes have such valuable properties as high specificity of action, selectivity for certain substrates, exceptional efficiency under conditions of moderate temperatures, normal pressure and neutral pH values, as well as environmental friendliness and safety (Bilal and Iqbal, 2020).

Commercial enzymes are produced by microorganisms, mainly by bacteria or fungi. The diversity of microorganisms and their adaptation systems, which ensure the existence of microbes in extreme conditions, allow us to find enzyme producers with the most diverse properties among them (Anisha et al., 2009; Huang et al., 2018; Lee et al., 2012). In addition, modern methods of genetic and molecular engineering make it possible to successfully modify them to improve technological properties (Boukid et al., 2023; Cao et al., 2009).

Today the market of microbial enzymes is extremely wide and a significant share of it is occupied by glycosidases, which are characterized by the ability to cleave the glycosidic bond in oligo-, polysaccharides and glycoconjugates (Singh et al., 2016; Yi et al., 2021). Most of such enzymes are used in technologies for processing plant raw materials of various compositions (Choi et al., 2015).

Microbial α -galactosidases (EC 3.2.1.22) are enzymes that play an important role in the cleavage of alpha-galactosidic bonds in carbohydrates, such as raffinose, melibiose, stachyose, galactomannans and galacto-glucomannans, which are present in food products and are important components of the diet of the general population (Ivanov et al., 2021). Enzyme α -galactosidase can be used in food industry to hydrolyze galactooligosaccharides in soy-based food production (soybean milk, soy protein, and others) and to treat sugar beet molasses promoting sugar crystallization process (Alvarez-Cao et al., 2019; Bhatia et al., 2020). Cleavage of alpha-galactosidic bonds in the difficult-to-digest galactooligosaccharides of the raffinose family helps maintain gut health, ensure efficient digestion, and reduce discomfort associated with soy milk and flour consumption. This enzyme is often used as a food additive to improve digestion in combination with amylolytic and lipolytic enzymes (“Beano Ultra”, “Doctor's Best Digestive Enzymes”, “Vitacost Gas Enzyme Alpha-galactosidase”).

Wide ranges of microorganisms are involved in the industrial production of α -galactosidase: *Aspergillus niger*, *Bacillus subtilis*, *Trichoderma reesei*, *Saccharomyces cerevisiae*, *Mortierella vinacea*, and others (Katrolia et al., 2014). However, the search for new producers of α -galactosidases, which have special functional properties and substrate specificity, remains an urgent task. Enzymes that exhibit activity in a wide range of pH and temperature values attract the special attention of researchers, as these indicators are an important characteristic of biocatalyst stability.

Earlier, in the culture fluid of the soil micromycete *Penicillium restrictum*, high levels of α -galactosidase activity was detected. The purpose of the present study was to isolate and characterize α -galactosidase from *P. restrictum*, to evaluate its substrate specificity and efficiency to hydrolyse various galactooligosaccharides.

Materials and methods

Strain, medium, and growth conditions

The object of the study was α -galactosidase from *Penicillium restrictum* Gilman & Abbott, a strain registered in the Depository of the D.K. Zabolotny Institute of Microbiology and Virology of National Academy of the Sciences of Ukraine under the number of IMV F-100139. Cultivation of *P. restrictum* to obtain the enzyme was carried out in a liquid medium of the following composition, g/l: KH_2PO_4 – 1.6; $\text{MgSO}_4 \times 7\text{H}_2\text{O}$ – 0.75; CaCl_2 – 0.3; $(\text{NH}_4)_2\text{SO}_4$ – 0.8; yeast autolysate – 0.15, soy flour – 10, pH 6.0 in Erlenmeyer flasks at a temperature of 25 °C under shaking of 220 rpm for 5 days.

Purification of α -galactosidase from *P. restrictum*

Isolation of the enzyme was carried out by fractionation with ammonium sulfate: dry salt was added to the supernatant of the culture liquid up to 90 percent saturation under pH control. The mixture was kept for 24 h at 4 °C and centrifuged at $2.5 \times g$ for 30 min. The precipitate was collected, dissolved in three times the volume of 3 M ammonium sulfate, and 0.01 M sodium azide was added for preservation. The methods of ion exchange and gel permeation chromatography were used to purify the enzyme. The sediment obtained as a result of fractionation with ammonium sulfate was centrifuged, dissolved in 1.5 volumes of the appropriate buffer, pH 6.0 – 7.5. The samples were subjected to gel filtration on a column (1.8×50 cm) with neutral TSK gel — Toyopearl HW-55 (Toson, Japan), equilibrated with 0.01 M phosphate buffer, pH 6.0. Elution was carried out at a rate of 20 ml/h. Ion exchange chromatography was performed on a column (2.5×40 cm) with Toyopearl DEAE-650 (M) (Toson, Japan), equilibrated with 0.01 M Tris-HCl buffer pH 7.5. The sample (about 100 mg of protein) was applied to the column, elution was carried out with the same buffer in a linear NaCl gradient (0-1 M, 200 ml each) at a rate of 30 ml/h. Fractions showing enzymatic activity were collected, combined and concentrated under vacuum approximately 5 times.

Rechromatography was performed on a column (1.3×52 cm) with Sepharose 6B, equilibrated with 0.01 M phosphate buffer, pH 6.0. Elution was carried out with the same buffer with 0.1 M NaCl at a rate of 60 ml/h. 1 ml of sample (20 mg of protein) was applied to the column. Protein content was recorded on a DeNovix DS-11 spectrophotometer/fluorimeter, fractions containing enzymatic activity were collected, combined and concentrated (10 times) by evaporation under vacuum.

Molecular weight determination

Determining of the enzymes molecular weight (MW) in the native system was performed by the gel-filtration on the column (1.3×50 cm) with Sepharose 6B. Elution was done by the 0.01 M phosphate buffer (pH 5.0) with 0.1 M NaCl. Standard curve for MW calculations was plotted using high-molecular protein-markers (Pharmacia, Sweden): ribonuclease (13.7 kDa), proteinase K (25 kDa), ovalbumin (43 kDa) and bovine serum albumin (67 kDa). The calibration curve was plotted using the gel-phase distribution coefficient (K_{av}) versus logarithm of the molecular weight (Log Mw).

$$K_{av} = (V_e - V_o)/(V_c - V_o),$$

where V_e is elution volume, V_o is column void volume, V_c is geometric column volume.

Enzyme activity assays

α -Galactosidase activity was determined using as a substrate *p*-nitrophenyl- α -D-galactopyranoside (*p*-NPGal) (“Sigma-Aldrich”, USA). To determine activity 0.1 ml of the enzyme solution was mixed with 0.2 ml 0.1 M phosphate-citrate buffer (PCB) pH 5.0 and 0.1 ml 0.01 M substrate solution in PCB. Reaction mixture was incubated for 10 min at 40 °C. The reaction was stopped by adding 2 ml of 1 M sodium bicarbonate. The amount of released nitrophenol as a result of hydrolysis was determined colorimetrically by the absorption at 400 nm. One international unit of enzyme activity (IU) was defined as the amount of enzyme that releases 1 μ mol of *p*-nitrophenol per min at 40 °C in 0.1 M PCB, pH 5.0.

Determination of the rate of splitting of raffinose, stachyose and guar galactomannan was carried out in the supernatant of *P. restrictum* by estimating the amount of galactose formed because of the hydrolysis of the corresponding substrate. The amount of galactose was determined by the dinitrosalicylic method (Miller, 1959). The reaction mixture containing 0.25 ml of culture liquid and 0.25 ml of substrate (1% galactomannan or 50 mM solutions of raffinose and stachyose in 0.1 M PCB pH 5.2 was incubated for 30 min at 40 °C, then 0.25 ml of dinitrosalicylic reagent was added and boiled for 10 min. The color intensity was estimated spectrophotometrically at 500 nm. Galactose was used as a standard.

The content of total protein in the supernatant of the culture liquid was determined by the Lowry method (Lowry et al., 1951). The calibration curve was constructed using bovine serum albumin as a standard.

Characteristics of enzyme

The optimum pH for the activities of α -galactosidase was determined by incubating the enzyme preparation with *p*-NPGal in 0.1 M citrate, PCB and 0.01 M Tris-HCl buffers at the pH range from 2 to 9. Activities were measured at 24 h using the standard protocol. The optimum temperature of α -galactosidase was determined by incubating the assay mixture for 10 min at temperature ranging from 5 to 80 °C. Thermal stability was measured by preincubation of the enzymes at the optimum pH at different temperatures (30, 40, 50, 60, 65, 70 and 75 °C) with the exposition time of 180 min.

Thermal inactivation of α -galactosidase was studied at 55–75 °C, pH 4.0–6.0 (0.1 M PCB). The enzyme samples (5 IU/ml) were kept at given temperature for 15–180 min; the aliquots in 0.1 ml were collected in definite intervals (15 min) for measurement of residual activity. Enzyme treatment with glycerol and sorbitol was carried out as follows: to 5–40 % glycerol or 0.1–5.0 M sorbitol in 0.1 M PCB was added enzyme solution (5 IU/ml) and the mixture was incubated at room temperature for 60 min. Thermal inactivation was carried out as described above.

Kinetic experiments were carried out at 37 °C at the pH 5.0. The maximum reaction rate (V_{max}) and Michaelis constant (K_m) were determined according to Lineweaver-Burk from curves defining dependence of the enzyme reaction rate on the substrate (from 0.1 to 10 mg/ml). Inhibition studies were performed using D-galactose at concentrations ranging from 1 to 10 mM.

The efficiency of hydrolysis was evaluated by the ratio of V_{max} to K_m .

The half-life period (in min) was calculated from the first-order inactivation rate constants, which were obtained from linear regression in logarithmic coordinates by equation:

$$t_{1/2} = \ln 2/k,$$

where k is the rate constant and $\ln 2$ is the natural log of 2 = 0.693.

To determine the resistance of galactosidase to the action of proteolytic enzymes, commercial and laboratory protease preparations were used: proteinase K, pronase E (*Streptomyces griseus*), trypsin (“Merk”, Germany), and a laboratory sample of protease from *Bacillus sp.* The reaction mixture contained equal amounts of galactosidase and protease (≈ 1 mg). Enzyme solutions in 0.1 M PCB pH 5.0 were mixed and kept under stirring for 1–24 hours. Glycosidase activity was measured as described above. Thermal inactivation of enzyme in the presence of proteases was performed according to the thermal inactivation method.

Effect of various reagents on the enzyme activities

The effects of various chemical reagents and cations (L-cysteine, β -Mercaptoethanol, Glutathione, Dithiothreitol (DTT), *p*-Chlormercuribenzoate (*p*-CMB), Diethyl pyrocarbonate (DEPC), N-ethylmaleimide, 1-(3-dimethylaminopropyl)-3-ethylcarbodiimide methiodide (EDC methiodide), Succinic anhydride, Hydrogen peroxide, Guanidine chloride, Potassium ferricyanide, Sodium azide, *o*-Phenanthroline, NH_4^+ , K^+ , Na^+ , Li^+ , Ag^+ , Hg^{2+} , Cd^{2+} , Ca^{2+} , Co^{2+} , Mg^{2+} , Ni^{2+}) on enzyme activity were investigated by their incorporation at a concentration of 0.01 M in standard assay. Reactions were carried out for 60 min at 40 °C and pH 5.0 (0.1 M PCB) in the presence or absence of the compounds examined.

All experiments were performed in 3–5 repetitions. The analysis of the obtained results was carried out by their statistical processing using the Student’s *t*-test. The results presented graphically were obtained using the Microsoft Excel 2007 program. Values at *P* 0.05 were considered reliable.

Results and discussions

Purification and characterization of α -galactosidase from *P. restrictum*

α -Galactosidase with a specific activity of 49.1 IU/mg of protein was obtained from the culture fluid of *P. restrictum* as a result of precipitation with ammonium sulfate and 3-step purification on TSK gels and Sepharose 6B (Table 1).

Table 1

Steps for purification of α -galactosidase from *P. restrictum*

Steps	Total protein, mg	Total activity, IU	Specific activity, IU/mg	Yield, %	Fold purification
Culture liquid supernatant (0.5 l)	450	3000	6.7	100	1.0
90 % ammonium sulfate	390	2700	6.9	86	1.1
TSK-gel Toyopearl HW-55	120	2123	17.7	26	2.6
Toyopearl DEAE-650M	52	1444	27.8	12	4.1
Sepharose 6B	20	1045	49.1	4.4	7.3

According to gel filtration, the MW of α -galactosidase was 17 kDa (Figure 1).

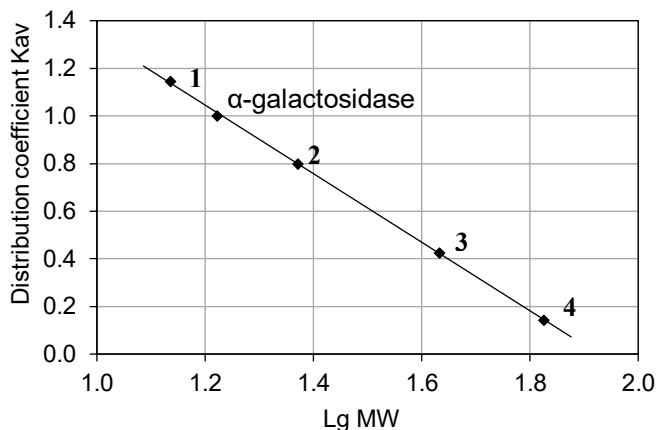


Figure 1. Molecular weight (MV) determination of *P. restrictum* α -galactosidase in the native system.

Molecular markers:

ribonuclease (13.7 kDa) (1), proteinase K (25 kDa) (2), chicken ovalbumin (43 kDa) (3), bovine serum albumin (67 kDa)(4), α -galactosidase – purified enzyme.

A similar low molecular weight α -galactosidase (18 kDa) from *Aspergillus awamori* was also described (Vidya et al., 2020). However, molecular weight in the range from 100 to 400 kDa are more typical for fungal α -galactosidases: 210 kDa in *Rhizopus* sp. (Cao et al., 2009), 118 kDa in *A. awamori* (El-Gindy et al., 2008), 106 kDa in *A. foetidus* (Liu et al., 2012), 99 and 430 kDa in *A. niger* (Borzova and Varbanets, 2007; Othman et al., 2023).

The enzyme had optimum activity at 60 °C and pH 4.0. In the pH range of 4.0-6.0, the half-life period of α -galactosidase of *P. restrictum* at 60 °C was 180-210 min, and at 65 °C – 20 min (Figure 2).

The thermal stability of the enzyme is higher than that of the previously described α -galactosidases of the micromycetes *Penicillium canescens* and *A. oryzae* (Borzova and Varbanets, 2010; Wang et al., 2020). In addition, *P. restrictum* α -galactosidase retained 100 % activity at pH 4.0-5.0 in the temperature range of 20-50 °C during 4 hours of incubation and during storage at 4 °C. Other researchers (Anisha et al., 2009; Farzadi et al., 2011; Yakimova et al., 2017) showed that the pH value of the optimum for the action of α -L-rhamnosidase of fungal and bacterial producers varies in a wide range from 2.0 to 11.0. However, unlike bacterial enzymes that operate in a region close to neutral or alkaline, fungal α -galactosidase is more active at slightly acidic values.

The resistance of the enzyme to proteolysis was also investigated. The activity of α -galactosidase of *P. restrictum* was evaluated after treatment with protease of *S. griseus*, proteinase K, protease of *Bacillus* sp. and trypsin. It was shown that *P. restrictum* α -galactosidase retained more than 90 % of its activity after 24 hours of incubation with proteases. High resistance to the action of proteolytic enzymes is also noted for other α -galactosidases, in particular, α -galactosidase of *A. oryzae* (Wang et al., 2020), tetrameric α -galactosidase from *Gibberella* sp. and α -galactosidase of *Rhizopus* sp. from the GH36 family (Cao et al., 2009). The enzyme from *Pleurotus djamor* also showed resistance to acid protease and varying degrees of tolerance to other proteases:

trypsin > collagenase type I > α -chymotrypsin-neutral protease > proteinase K

(Hu et al., 2017).

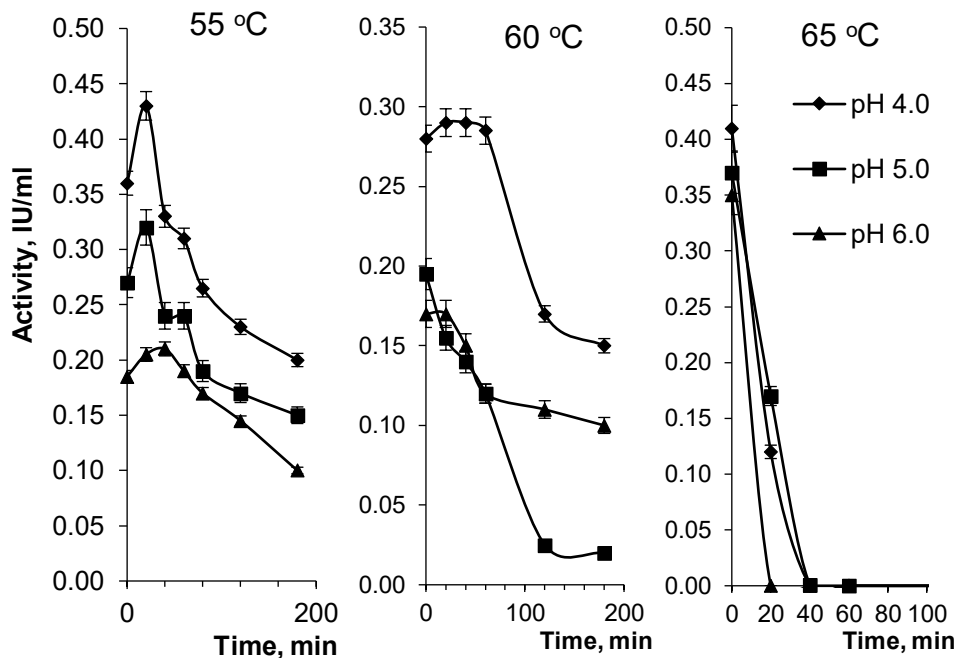


Figure 2. Thermal stability of α -galactosidase *P. restrictum* at different temperature and pH.
The mean values and standard errors are shown (n=5)

Therefore, α -galactosidase of *P. restrictum* may be an interesting object of research in terms of its activity and stability, especially in the context of use in industrial processes.

Kinetic parameters of α -galactosidase from *P. restrictum*

Currently, there is data in the literature that synthetic *p*-nitrophenyl substrates inhibit many of the studied α -galactosidases at high concentrations (Bhatia et al., 2020; Katrolia et al., 2014). The curve of dependence of *P. restrictum* α -galactosidase activity on time had the usual form, where there is a gradual increase in the activity of the enzyme, but after a certain period of time the reaction rate becomes constant. The rate of *p*-NPG hydrolysis by *P. restrictum* α -galactosidase plateaued at substrate concentrations of 4–5 mg/ml or 1.5 mM at different pH (Figure 3). Inhibition of the reaction was observed at substrate concentrations > 10 mg/ml.

α -Galactosidase of *P. restrictum* cleaved α -1,6-linked galactose from oligo- and polygalactosides at a high rate. It was shown that the rate and efficiency of hydrolysis of galactose-containing natural substrates by *P. restrictum* α -galactosidase decreased with increasing their molecular weight (Table 2). In addition, the speed of splitting galactose from the main chain of oligosaccharides (raffinose and stachyose) was significantly higher than when splitting the galactosidic bond of mannan side chains.

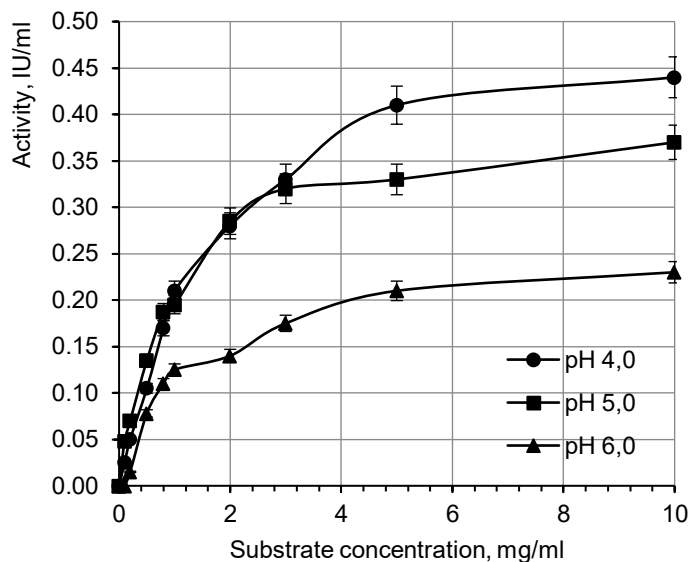


Figure 3. Dependence of α -galactosidase reaction rate on substrate concentration at different pH (0.1 M PCB, 37 °C).

The mean values and standard errors are shown (n=3)

Table 2

Kinetic parameters of α -galactosidase *P. restrictum*

Substrate	Type of bond	K_m , mM	V_{max} , $\mu\text{mol}/\text{min}/\text{mg}$	V_{max}/K_m
<i>p</i> -NPGal	α -1	0.9 ± 0.05	90.1 ± 2.5	100.1 ± 4.1
Raffinose	α -1,6	2.2 ± 0.08	134.6 ± 3.8	61.3 ± 1.7
Stachyose	α -1,6	2.4 ± 0.08	116.5 ± 4.5	48.1 ± 2.2
Galactomannan	α -1,6	3.8 ± 0.11	27.5 ± 1.4	7.1 ± 0.2

The high rate of hydrolysis of oligosaccharides indicates the suitability of this enzyme for use as a dietary supplement to improve digestion when using various products, especially legumes, and to improve the quality of products containing soy milk or flour (Boukid et al., 2023; Hu et al., 2017). The capacity of the enzyme to degrade the polysaccharide galactomannan of guar is also a valuable property for its use in the food industry. Enzymatic hydrolysis of guar galactomannan improves its ability to gel, which makes it possible to reduce the cost of production processes of ice cream and frozen desserts, sauces, cream cheeses, in comparison with the use of carob gum (Katrolia et al., 2012). In addition, the glycosidic modification of galactomannans, which are present in a large number of tree biomass, can provide bioprocessing plants with a sufficient number of raw materials for the production of ethanol (Choi et al., 2015).

Effects of metal ions and reagents

Nowadays, wide ranges of specific reagents, which modify the side chains of amino acids in protein molecules with varying efficiency, are known. Most of them are used to identify functionally active groups of proteins and study their structure, but often this approach helps to obtain more stable and active forms of enzymes.

It was shown that the activity of α -galactosidase of *P. restrictum* is completely inhibited in the presence of cations Ag^+ , Cd^{2+} , Ca^{2+} , Hg^{2+} (Figure 4).

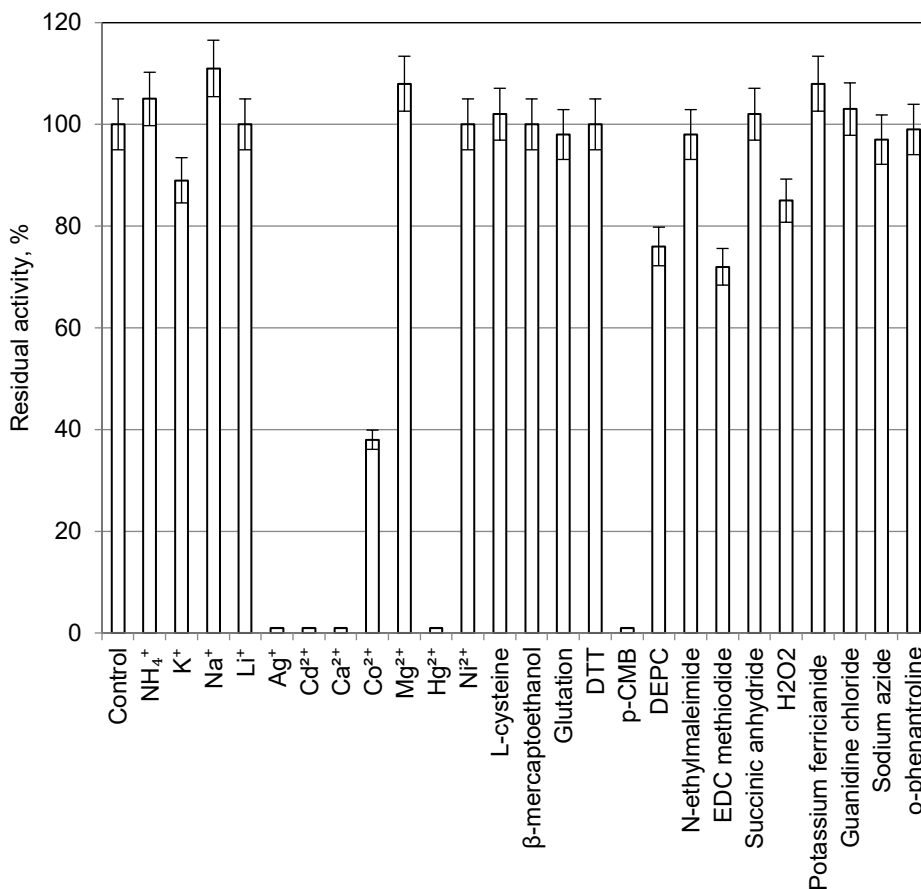


Figure 4. The influence of various chemical reagents on the activity of α -galactosidase. Concentration of additives 0.01M, pH 5.0, 37 °C, time exposition 60 min. The mean values and standard errors are shown (n=5)

In addition, the reversible nature of activity inhibition in the presence of Hg^{2+} and Ag^+ was established, which is characteristic of most of the described glycosidases. Inactivation by Hg^{2+} ions was noted in enzymes from *P. djamor* (Hu et al., 2017), *A. niger* (Othman et al., 2023), *Pseudobalsamia microspora* (Yang et al., 2015). Inhibition of enzyme activity in the presence of carboxyl modifying reagent EDC methiodide and DEPC was noted, which indicates the important role of carboxyl groups of dicarboxylic acids and the imidazole group

of histidine for the activity of α -galactosidase of *P. restrictum*. Today it is known that α -galactosidases from the GH4, GH27, GH36, and GH57 families can use glutamic or aspartic acids as a catalytic nucleophile (Chen et al., 2020; Okuyama et al., 2009) and $\text{NH}^+(\text{His})$ acts as an electrophile in sweet almond α -galactosidase (Dey and Pridham, 1972).

Sulfhydryl groups of cysteine residues often play an important role in the manifestation of the functional activity of many proteins. Under conditions close to physiological, they are effective nucleophilic agents with high reactivity. Their modification can be carried out with the help of iodoacetamide, aminoethylation with ethyleneimine, reaction with *p*-CMB, oxidation of H_2O_2 to derivatives of cysteine acid, oxidation under mild conditions with the formation of inter- and intramolecular disulfide bonds under the action of ferricyanide, condensation with N-ethylmaleimide according to pH 7.0.

Modification of the SH-groups of the studied α -galactosidase p-CHMB led to a complete loss of its activity, and hydrogen peroxide inhibited the *P. restrictum* enzyme by 13 %. At the same time, ferricyanide and N-ethylmaleimide had almost no effect on the activity of α -galactosidase of *P. restrictum*. Thus, a wide variability of effects among modifiers of SH groups within the studied enzyme molecule was noted, which may be a consequence of different availability of sulfhydryl groups for these reagents. The enzyme was insensitive to the influence of chelating agents (o-phenanthroline) and reagents of thiosulfide exchange. Stability in the presence of the denaturing agent guanidine chloride may indicate the monomeric structure of the studied glycosidase molecule.

Therefore, the obtained data suggest that functionally active and reactive groups in the studied glycosidase are the carboxyl groups of dicarboxylic amino acids, the imidazole group of histidine, and the sulfhydryl groups of cysteine. By modifying these groups, it is possible to influence the conformational stability of the *P. restrictum* enzyme and develop a strategy for obtaining a thermostable enzyme preparation based on it.

Thermal stabilization of α -galactosidase from *P. restrictum*

Increasing the stability of industrially important proteins, which allows effective use of biocatalysts for a long time with minimal loss of their activity, is definitely a priority task of modern applied enzymology. The lack of data on all essential aspects of the mechanism of protein denaturation does not allow us to offer universal ways of their stabilization today and requires an individual approach to solving these problems in accordance with the structural and functional features of the protein (Lopina, 2017).

It is known that enzymes can be inactivated by the aggregation mechanism. In this case, one of the ways to stabilize the protein is to increase the viscosity of the solution, which allows reducing the frequency of collisions between enzyme molecules and slowing down inactivation.

Studies of the effect of high concentrations of glycerol and sorbitol on the thermostabilization of the enzyme showed that glycerol at a concentration of 25–40% had no protective effect on the α -galactosidase of *P. restrictum*. The use of sorbitol solutions in concentrations of 1.6 and 2.5 M at a temperature of 65 °C (pH 4.0–5.0) made it possible to increase the half-life of *P. restrictum* α -galactosidase to 60–180 min (Figure 5). In the presence of 5 M sorbitol, 50–70% of the enzyme activity was preserved for 120–180 min at 65 and 70 °C (Figure 6).

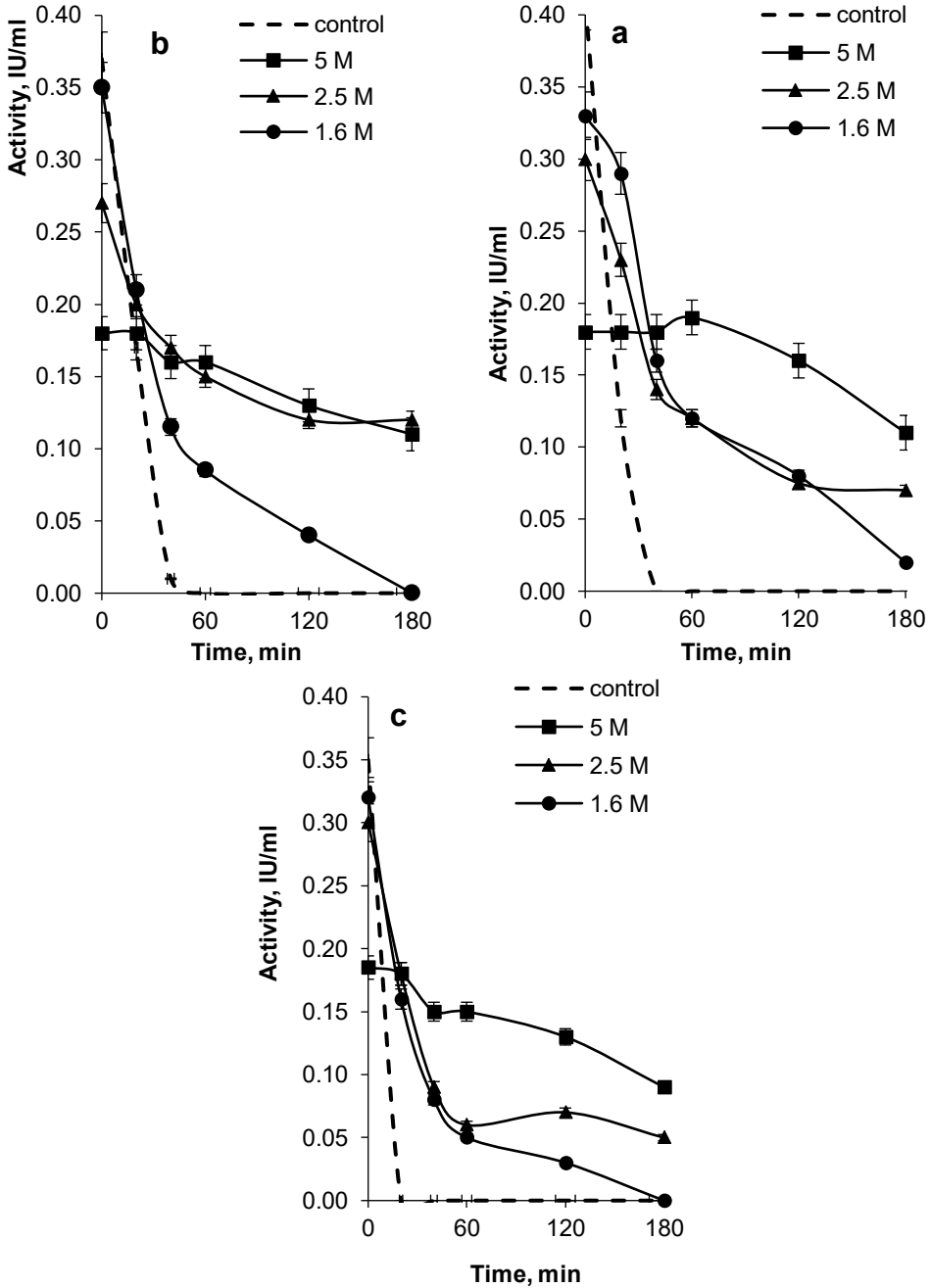


Figure 5. Thermoinactivation of *P. restrictum* α -galactosidase at 65 °C in the presence of different concentrations of sorbitol: a, pH 4.0; b, pH 5.0; c, pH 6.0.

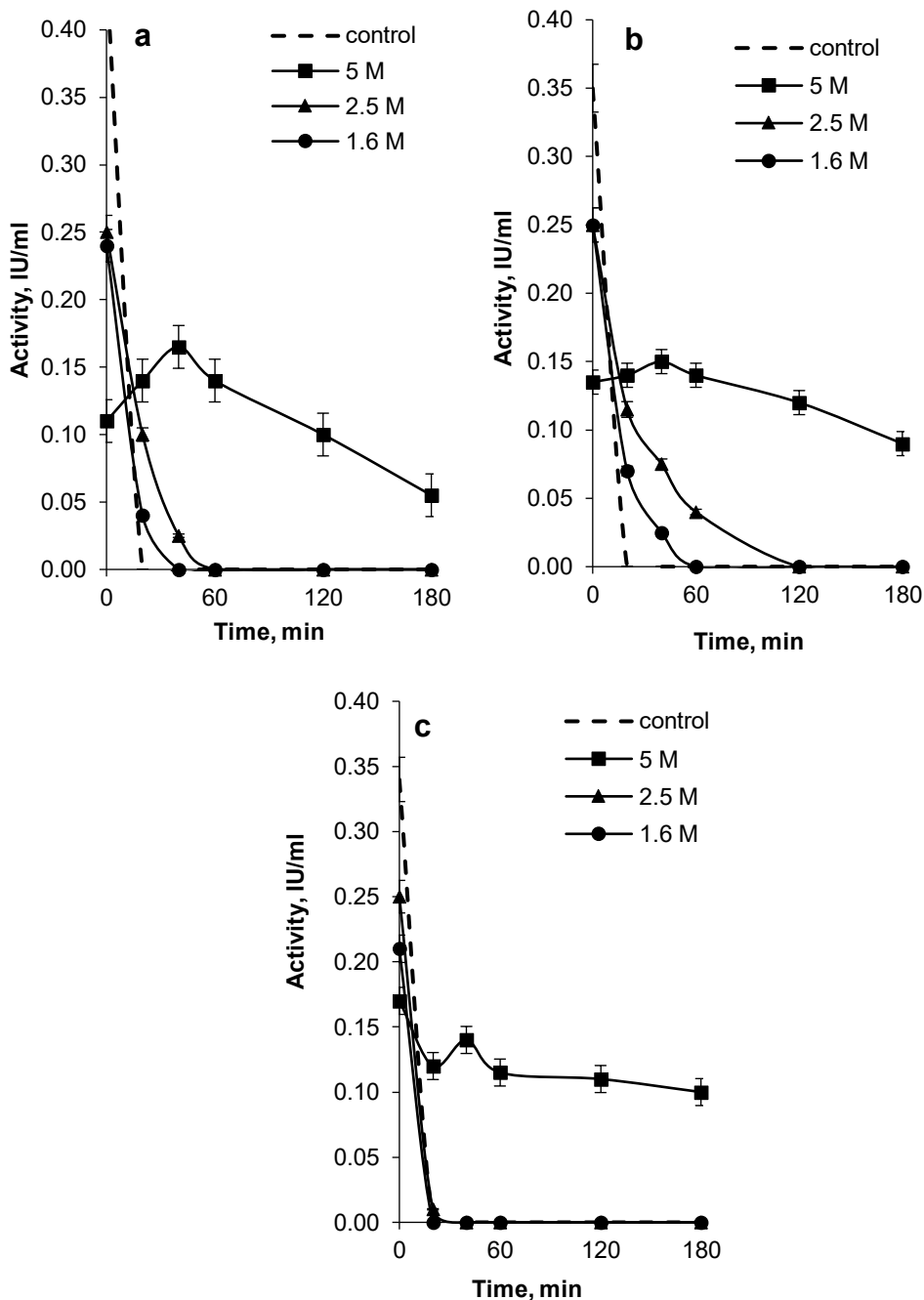


Figure 6. Thermostability of *P. restrictum* α -galactosidase at 70 °C in the presence of different concentrations of sorbitol: a, pH 4.0; b, pH 5.0; c, pH 6.0.

Conclusions

1. The results of the study of the functional and thermal stability of the practically important microbial α -galactosidase, which was isolated from the culture fluid of the micromycete *P. restrictum*, are presented. The enzyme showed high activity and stability in the pH range from 4.0 to 6.0 and at temperatures from 40 to 60 °C. It was established that the use of high concentrations of sorbitol allows for a significant increase in the half-life of the enzyme under conditions of thermal denaturation at 70–75 °C.
2. The functional properties and specificity of action on α -1,6-linked galactosyl residues in the main and side chains of galactoglycosides indicate the potential of *P. restrictum* α -galactosidase for use in industrial processes where rapid and efficient conversion of carbohydrate substrates is required. The use of α -galactosidase for the biodegradation of galactooligosaccharides of the raffinose family (raffinose and stachyose) allows for to improvement of the quality of soy products, which are the basis of dietary nutrition of various segments of the population. As a result of processing soy milk with α -galactosidase, difficult-to-digest oligosaccharides are transformed into simple sugars — galactose, glucose, sucrose, or fructose, which increases its nutritional value and allows the consumer to be spared from negative effects, including flatulence, diarrhea and other inefficient food digestion. In addition, the use of α -galactosidase in combination with other glycosidases for the modification of fruit pectins makes it possible to obtain functional drinks and purees with a high content of prebiotic oligosaccharides. With the help of α -galactosidase also can to improve the gelling ability of guar galactomannan. This will make it possible to replace more expensive raw materials in the food industry, such as locust bean gum, with more affordable.
3. Thus, the obtained active enzyme preparation is of considerable value not only for understanding and supplementing the theoretical aspects of protein chemistry and engineering but also can compete with imported enzyme compositions and significantly expand the use of enzymatic biotransformation in technological processes of the food industry.

References

- Alvarez-Cao M.E., Cerdán M.E., Gonzalez-Siso M.I., Becerra M. (2019), Bioconversion of beet molasses to alpha-galactosidase and ethanol, *Frontiers in Microbiology*, 10, 405, <https://doi.org/10.3389/fmicb.2019.00405>
- Anisha G.S., John R.P., Prema P. (2009), Biochemical and hydrolytic properties of multiple thermostable α -galactosidases from *Streptomyces griseoalbus*: obvious existence of a novel galactose tolerant enzyme, *Process Biochemistry*, 44(3), pp. 327–333, <https://doi.org/10.1016/j.procbio.2008.11.009>
- Bhatia S., Singh A., Batra N., Singh J. (2020), Microbial production and biotechnological applications of α -galactosidase, *International Journal of Biological Macromolecules*, 150, pp. 1294–1313, <https://doi.org/10.1016/j.ijbiomac.2019.10.140>
- Bilal M., Iqbal H.M.N. (2020), State-of-the-art strategies and applied perspectives of enzyme biocatalysis in food sector – current status and future trends, *Critical Reviews in Food Science and Nutrition*, 60(12), pp. 2052–2066, <https://doi.org/10.1080/10408398.2019.1627284>
- Borzova N.V., Varbanets L.D. (2007), α -Galactosidase of *Aspergillus niger*: purification and properties, *Studia Biologica*, 1(1), pp. 53–64.
- Borzova N.V., Varbanets L.D. (2010), Термоінактивација α -галактозидазы *Penicillium canescens*, *Ukrainskii Biokhimičeskii Zhurnal*, 82(3), pp. 24–30.

- Boukid F., Ganeshan S., Wang Y., Tülbek M.Ç., Nickerson M.T. (2023), Bioengineered enzymes and precision fermentation in the food industry, *International Journal of Molecular Sciences*, 24(12), 10156, <https://doi.org/10.3390/ijms241210156>
- Cao Y., Wang Y., Luo H., Shi P., Meng K., Zhou Z., Zhang Z., Yao B. (2009), Molecular cloning and expression of a novel protease-resistant GH-36 alpha-galactosidase from *Rhizopus* sp. F78 ACCC 30795, *Journal of Microbiology and Biotechnology*, 19(11), pp. 1295–1300, <https://doi.org/10.4014/jmb.0904.4003>
- Chen S.C., Wu S.P., Chang Y.Y., Hwang T.S., Lee T.H., Hsu C.H. (2020), Crystal structure of α -galactosidase from *Thermus thermophilus*: insight into hexamer assembly and substrate specificity, *Journal of Agricultural and Food Chemistry*, 68(22), pp. 6161–6169, <https://doi.org/10.1021/acs.jafc.0c00871>
- Choi J.M., Han S.S., Kim H.S. (2015), Industrial applications of enzyme biocatalysis: Current status and future aspects, *Biotechnology Advances*, 33(7), pp. 1443–1454, <https://doi.org/10.1016/j.biotechadv.2015.02.014>
- Dey P.M., Pridham J.B. (1972), Biochemistry of α -galactosidases. *Advances in Enzymology and Related Areas of Molecular Biology*, 36, pp. 91–130, <https://doi.org/10.1002/9780470122815.ch3>
- El-Gindy A.A., Ali U.F., Ibrahim Z.M., Isaac G.S. (2008), A cost-effective medium for enhanced production of extracellular α -galactosidase in solid substrate cultures of *Aspergillus awamori* and *A. carbonarius*, *Australian Journal of Basic and Applied Sciences*, 2(4), pp. 880–899.
- Farzadi M., Khatami S., Mousavi M., Amirmozafari N. (2011), Purification and characterization of α -galactosidase from *Lactobacillus acidophilus*, *African Journal of Biotechnology*, 10(10), pp. 1873–1879, <https://doi.org/10.1873-1879>. 10.5897/AJB10.357
- Hu Y., Tian G., Zhao L., Wang H., Ng T.B. (2017), A protease-resistant α -galactosidase from *Pleurotus djamor* with broad pH stability and good hydrolytic activity toward raffinose family oligosaccharides, *International Journal of Biological Macromolecules*, 94(Pt A), pp. 122–130, <https://doi.org/10.1016/j.ijbiomac.2016.10.005>
- Huang Y., Zhang H., Ben P., Duan Y., Lu M., Li Z., Cui Z. (2018), Characterization of a novel GH36 α -galactosidase from *Bacillus megaterium* and its application in degradation of raffinose family oligosaccharides, *International Journal of Biological Macromolecules*, 108, pp. 98–104, <https://doi.org/10.1016/j.ijbiomac.2017.11.154>
- Ivanov V., Shevchenko O., Marynin A., Stabnikov V., Gubenia O., Stabnikova O., Shevchenko A., Gavva O., Saliuk A. (2021), Trends and expected benefits of the breaking edge food technologies in 2021–2030, *Ukrainian Food Journal*, 10(1), pp. 7–36, <https://doi.org/10.24263/2304-974X-2021-10-1-3>
- Katrolia P., Rajashekhara E., Yan Q., Jiang Z. (2014), Biotechnological potential of microbial α -galactosidases, *Critical Reviews in Biotechnology*, 34(3), pp. 307–317, <https://doi.org/10.3109/07388551.2013.794124>
- Lee J., Park I., Cho J. (2012), Production and partial characterization of α -galactosidase activity from an Antarctic bacterial isolate, *Bacillus* sp. LX-1, *African Journal of Biotechnology*, 11(60), pp. 12396–12405, <https://doi.org/10.5897/AJB12.1219>
- Liu C.Q., He G.Q. (2012), Multiple α -galactosidases from *Aspergillus foetidus* ZU-G1: purification, characterization and application in soybean milk hydrolysis, *European Food Research and Technology* 234(5), pp. 743–751. <https://doi.org/10.1007/s00217-012-1679-x>
- Lopina O.D. (2017), Enzyme inhibitors and activators. In: Senturk M. (Ed.), *Enzyme Inhibitors and Activators*. InTech. Available at: <http://dx.doi.org/10.5772/67248>
- Lowry O.H., Rosebrough N.J., Farr A.L., Randall R.J. (1951), Protein measurement with folinphenol reagent, *Journal of Biological Chemistry*, 193, pp. 265–275.
- Meszaros Z., Nekvasilova P., Bojarová P., Křen V., Slamova K. (2021), Advanced glycosidases as ingenious biosynthetic instruments, *Biotechnology Advances*, 49, 107733, <https://doi.org/10.1016/j.biotechadv.2021>
- Miller G.L. (1959), Use of dinitrosalicylic acid reagent for determination of reducing sugars, *Analytical Chemistry*, 31(3), pp. 426–428, <https://doi.org/10.1021/ac60147a030>
- Okuyama M., Matsunaga K., Watanabe K.I., Yamashita K., Tagami T., Kikuchi A., Ma M., Klahan P., Mori H., Yao M., Kimura A. (2017), Efficient synthesis of α -galactosyl

- oligosaccharides using a mutant *Bacteroides thetaiotaomicron* retaining α -galactosidase (BtGH97b), *The FEBS Journal*, 284(5), pp. 766–783, <https://doi.org/10.1111/febs.14018>
- Othman A.M., Elshafei A.M., Elsayed M.A., Ibrahim G.E., Hassan M.M., Mehanna N.S. (2023), Biochemical characterization and insights into the potency of the acidic *Aspergillus niger* NRC114 purified α -galactosidase in removing raffinose family oligosaccharides from soymilk yogurt, *BMC Biotechnology*, 23(1), 3, <https://doi.org/10.1186/s12896-023-00773-x>
- Singh R., Kumar M., Mittal A., Mehta P.K. (2016), Microbial enzymes: industrial progress in 21st century, *3 Biotech*, 6(2), 174, <https://doi.org/10.1007/s13205-016-0485-8>
- Vidya C.H., Gnanesh Kumar B.S., Chinmayee C.V., Singh S.A. (2020), Purification, characterization and specificity of a new GH family 35 galactosidase from *Aspergillus awamori*, *International Journal of Biological Macromolecules*, 156, pp. 885–895, <https://doi.org/10.1016/j.ijbiomac.2020.04.013>
- Wang J., Yang X., Yang Y., Liu Y., Piao X., Cao Y. (2020), Characterization of a protease-resistant α -galactosidase from *Aspergillus oryzae* YZ1 and its application in hydrolysis of raffinose family oligosaccharides from soymilk, *International Journal of Biological Macromolecules*, 158, pp. 708–720, <https://doi.org/10.1016/j.ijbiomac.2020.04.256>
- Yakimova B., Tchobanov B., Stoineva I. (2017), Alpha-galactosidase and invertase from *Penicillium chrysogenum* sp.23. Purification, characteristics and hydrolysis of raffinose, *Bulgarian Chemical Communications*, 49(2), pp. 101–106
- Yang D., Tian G., Du F., Zhao Y., Zhao L., Wang H., Ng T.B. (2015), A fungal alpha-galactosidase from *Pseudobalsamia microspora* capable of degrading raffinose family oligosaccharides, *Applied Biochemistry and Biotechnology*, 176(8), pp. 2157–2169, <https://doi.org/10.1007/s12010-015-1705-0>
- Yi D., Bayer T., Badenhorst C.P.S., Wu S., Doerr M., Höhne M., Bornscheuer U.T. (2021), Recent trends in biocatalysis, *Chemical Society Reviews*, 50(14), pp. 8003–8049, <https://doi.org/10.1039/d0cs01575j>

Cite:

UFJ Style

Borzova N. (2024), Thermal stable α -galactosidase from *Penicillium restrictum* for biodegradation of galactooligosaccharides, *Ukrainian Food Journal*, 13(2), pp. 316–330, <https://doi.org/10.24263/2304-974X-2024-13-2-9>

APA Style

Borzova, N. (2024). Thermal stable α -galactosidase from *Penicillium restrictum* for biodegradation of galactooligosaccharides. *Ukrainian Food Journal*, 13(2), 316–330. <https://doi.org/10.24263/2304-974X-2024-13-2-9>

Microbial producer of acid urease for its application in biocementation

Viktor Stabnikov¹, Viktor Udymovych¹,
Iryna Kovshar¹, Dmytro Stabnikov^{1,2}

1 – National University of Food Technologies, Kyiv, Ukraine

2 – University of Wrocław, Wrocław, Poland

Abstract

Keywords:

Biocementation
Acid urease
Cell inactivation
Bone meal
Permeability

Article history:

Received
15.12.2023
Received in
revised form
17.02.2024
Accepted
2.07.2024

Corresponding author:

Viktor Stabnikov
E-mail:
vstabnikov1
@gmail.com

DOI:

10.24263/2304-
974X-2024-13-2-
10

Introduction. A popular biocementation method, microbially initiated precipitation of calcium carbonate, is accompanied by the release of ammonia and ammonium ions into the environment. The aim of the present study was selection of a producer of acid urease for its application in biocementation based on the calcium phosphate formation.

Materials and methods. Isolation, selection, identification, and characteristics of bacterial producer of acid-tolerant urease were conducted. Sequencing the 16S rRNA gene of isolate was done for its identification. Bone meal served as a source of calcium for biocementation using inactivated cells of bacterial producer of acid-tolerant urease. Assessment of sand biocementation was provided by the change of its water permeability.

Results and discussion. Selection of a bacterial strain that synthesized acid urease was carried out among bacteria isolated from acidic soil. The strain with the highest urease activity was identified by rRNA gene amplification and sequencing as *Staphylococcus saprophyticus* AU1. The physiological properties of the strain were studied. The maximum growth rate of strain AU1 was 0.15 h⁻¹, the maximum accumulation of biomass was 6.9 g/l of dry biomass, and the maximum urease activity was 8.1 mM hydrolyzed urea/min. The highest urease activity of *Staphylococcus saprophyticus* AU1 was found in the pH range from 4.5 to 5.5, and it gradually decreased with pH increasing. To ensure environmental biosafety, the use of inactivated bacterial cells that retain urease activity has been proposed. To receive completely inactive cells, they were treated with 0.5% sodium dodecyl sulfate solution for 90 minutes. Biocementation of sand was conducted using inactivated cells of *S. saprophyticus* AU1 and acid hydrolysate of bone meal, which has calcium in the form of phosphorus-containing compounds. The water permeability of biocemented sand was 2·10⁻⁵ m/s, which makes it possible to use biocementation of this type to strengthen the soil to reduce its liquefaction, for example after an earthquake, or to control dust erosion for prevention of atmospheric pollution.

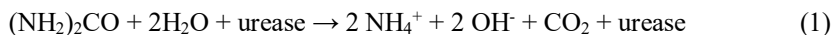
Conclusions. The main advantage of the proposed method for biocementation is the diminishing of urea consumption up to 75% and, thereby, reduction of emissions of ammonium and ammonia into the environment. In addition, the problem of bone waste disposal is solved and the cost of materials for biocementation is reduced.

Introduction

Traditional cement is widely used in construction and for grouting due to its relatively low cost and high strength. Cement production is growing worldwide at 0.8–1.2% per year, and its consumption is expected to increase to 3.7–4.4 billion tons in 2050 (Benhelal et al., 2013). The disadvantage of cement is the high viscosity of the suspension, which limits its use. In addition, cement production requires large amounts of electricity (approximately 2.6% of global energy consumption) and is accompanied by the release of 0.73 – 0.99 tons of CO₂ per ton of cement produced, which accounts for 8.0 – 8.6% of global anthropogenic carbon dioxide emissions (Aprianti, 2017; Miller et al., 2018; Nie et al., 2022). CO₂ emissions from cement production are expected to increase by up to 260% between 1990 and 2050 (Cuzman et al., 2015) and global emissions will be 2.34 billion tons of CO₂ in 2050 (Mishra et al., 2022).

It is known that the release of greenhouse gases into the atmosphere causes global warming, while climate change is recognized as one of the world's most important environmental problems. The increasing trend of carbon dioxide emissions worldwide and in leading countries is directly related to the production of cement, which is considered the second most consumed material in the world after water (Avramenko et al., 2022; Imbabi et al., 2012).

In recent years, active research has been conducted in the world to obtain an alternative material – biocement, based on the use of bacteria producing urease, which in the presence of urea and calcium ions form insoluble calcite crystals that adhere to a solid surface. The main advantage of biocement over conventional cement is the low viscosity of the biocement solution, which allows it to penetrate into small pores and microchannels of the soil and microcracks in rocks and concrete. Due to the activity of bacteria producing urease, urea hydrolysis occurs, which leads to an increase in pH and the release of carbonate ions:



Carbon dioxide in water turns into carbonate ion and in the presence of calcium ions and high pH forms insoluble calcium carbonate (Stocks-Fischer et al., 1999):



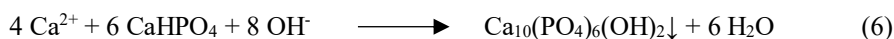
Thus, biocement is a mixture of at least three components: (1) an inorganic component that forms calcium carbonate, (2) a component that changes the pH and initiates the precipitation of calcium carbonate, and (3) the urease enzyme or living microbial cells with urease activity, or non-living microbial cells but retaining enzymatic activity and catalyzing a change in pH to values at which precipitation of calcium carbonate occurs. The inorganic component is soluble calcium salts that are converted into an insoluble substance. The component that changes the pH and supplies CO₂ for carbonation is urea, which is hydrolyzed by the catalytic action of microbial cells with urease activity or enzyme urease.

Several hundred scientific articles are published annually on the topic of biocementation, which indicates a growing interest in this direction of biotechnology development (Chu et al., 2012; Ivanov et al., 2019a; Omoregie et al., 2020). One of the reasons preventing the large-scale application of this biotechnology is the release of toxic

ammonia gas into the atmosphere during the biocementation process and the possible release of ammonium ions into groundwater and surface water (Gowthaman et al., 2020; Ivanov et al., 2019a).

When carrying out traditional microbially initiated biocementation, the pH of the environment, in which biocementation occurs, reaches values of 8.5 – 9.5 due to the release of ammonium ions and toxic ammonia. It is known that 99% of the released nitrogen will be in the form of ammonium ions NH_4^+ at a pH value of 7.3, but if the pH value exceeds 7.5, there is a sharp change towards the formation of NH_3 gas (Gowthaman et al., 2021). To prevent soil contamination with ammonium ions, several methods have been proposed that provide additional treatment for their removal, in particular the addition of zeolite (Keykha et al., 2019), the retention of ammonium ions near the cathode during electrobiocementation of soil (Keykha and Asadi, 2017), precipitation of ammonium ions in the form of struvite (Mohsenzadeh et al., 2021; Yu et al., 2020), washing the biocemented sand column to remove water-soluble ammonium (Lee et al., 2019), and adsorption of the removed ammonium with sulfuric acid (Ivanov and Stabnikov, 2017). But the problem of ammonia emissions remains unresolved. A promising highly environmentally friendly alternative for reducing the release of toxic ammonia into the environment may be biocementation based on calcium phosphate formation (Ivanov et al., 2019a). Calcium phosphate, similar to calcium carbonate, is a promising structural material with sufficient strength characteristics. The use of calcium phosphate compounds for soil improvement has significant advantages such as (a) calcium phosphates are non-toxic and environmentally friendly materials. They are known to be major constituents of bones and vertebral teeth, including most human hard tissues (Toshima et al., 2014), what does it prove their safety in soil application; (b) the solubility of phosphorus-containing calcium compounds depends on the pH of the environment, therefore, at an acidic pH in the soil, they can be in an insoluble state (Ivanov et al., 2019a; Kawasaki and Akiyama, 2013); (c) calcium phosphate formed in the soil can serve as phosphorus fertilizer for crop plants (Akiyama and Kawasaki, 2012). Biogrouting of soil can be carried out based on the precipitation of calcium phosphate compounds to form insoluble and strong hydroxyapatite crystals (Akiyama and Kawasaki, 2012; Yu and Jiang, 2018) from inorganic (Dilrukshi et al., 2015; 2016) or organic phosphates (Roeselers and van Loosdrecht, 2010). So, calcium phosphate is considered to be a promising structural material with fairly high strength properties.

The production of calcium phosphate can occur according to equation:



Precipitation by this method can occur due to enzymatic hydrolysis of urea, which increases the pH from 4.4 to 7.0. An economic advantage of the hydroxyapatite application is the possibility of using bone meal, obtained from cattle bones and partially used as a component of feed or fertilizer. However, about half of the bones remaining after meat processing are usually burned in cement kilns.

Urease (urea amidohydrolase, EC 3.5.1.5) is an enzyme that catalyzes the hydrolysis of urea into ammonia and carbon dioxide and is widely distributed in the natural world, including plants, animals, and microorganisms. Ureases used in biocementation processes currently have optimal reaction pH values in the range from neutral to alkaline, and are not only labile and prone to deactivation in an acidic environment, but also do not even catalyze the reaction of urea hydrolysis, especially if the ambient temperature is higher than 25°C.

More often, biocement is produced by precipitation of calcium carbonate at an alkaline pH value. However, the use of acid urease may be beneficial under certain environmental

conditions where the initial pH is low, for example when using calcium bicarbonate as a calcium source or when producing calcium phosphate.

The aim of the present study was to select a microbial producer of acid urease for biocementation using calcium phosphate.

Materials and methods

Urease-producing bacterial strain and its cultivation

Urease-producing bacterium (UPB) strain *Bacillus* sp. VUK5 (Stabnikov et al., 2013a; 2014) was used in this study. Strain of *Bacillus* sp. VUK5 is an alkaliphilic, halotolerant, aerobic, and spore-forming Gram-positive rod. The strain was grown on a nutrient medium with the following composition: Tryptic Soy Broth (Difco Laboratories, Detroit, Michigan, USA); urea, 20 g; NaCl, 100 g; NiCl₂·6H₂O, 24 mg; phenol red, 10 mg; distilled water 1 l (TSB medium). The indicator phenol red was added to the medium to detect the development of urease-producing bacteria: its color is yellow at pH 6.8, but gradually changes to red if the pH rises to 8.2 and becomes bright pink (purple) at pH higher than 8.2. All components of the medium, except urea, were sterilized at 121°C for 15 minutes. A concentrated urea solution, 100 g/l, was sterilized by filtration through a 0.22 µm nitrocellulose filter to prevent urea decomposition during heat sterilization and 20 ml/l was added to sterile media (TSB). 2 ml of a concentrated solution of trace elements was added to a sterile TSB medium. The concentrated solution of trace elements had the following composition: ZnSO₄·7H₂O, 0.1 g; MnSO₄·H₂O, 0.085 g; H₃BO₃, 0.06 g; CoCl₂·6H₂O, 0.02 g; CuCl₂, 0.004 g; Na₂MoO₄·2H₂O, 0.04 g; FeCl₂, 0.3 g; deionized water to 1 l. pH was adjusted to 2.0 by 1N HCl (Stabnikov et al., 2013a).

Selection of a bacterial strain that synthesizes acid-tolerant urease

Acidic soil taken under pine trees, into which urea was previously added, serves as an inoculum to obtain an enrichment culture of bacteria producing acid urease. 10 g of soil was added to 30 ml of 1.5% NaCl solution, mixed thoroughly and allowed to settle. The liquid fraction served as the starting material for obtaining an enrichment culture. Enrichment cultures were grown on a TSB nutrient medium with initial pH 5.8. An indicator bromocresol purple was added to the medium to show the pH change: at pH 5.4 to 6.8 the medium has yellow-green color, and when urea hydrolysis occurs and the pH increases, the color changes to purple, indicating that pH > 6.8. Enrichment culture, in which the color changed faster and was more intense, was used for the selection of pure cultures producing acidic urease.

Characteristics of a pure culture of acid urease-producing bacteria and its identification

The morphology of bacterial cells was observed using a Zeiss EV050 scanning electron microscope, UK. Gram staining was performed using a Gram stain kit.

The nearly full-length 16S rRNA gene was amplified by polymerase chain reaction (PCR) with forward primer 27F and reverse primer Universal 1492R (Lane, 1991). Purified PCR products were sequenced using an ABI PRISM 3730xlDNA sequencer and a ready-made ABI PRISM BigDye Terminator Cycle Sequencing reaction kit. Primers 27F, 530F, 926F, 519R, 907R and 1492R were used to sequence both strands of the 16S rRNA gene:

27F (5'-AGAGTTTGATCMTGGCTCAG-3'); 530F (5'-GTGCCAGCMGCCGCGG-3'); 926F (5'-AAA CTY AAA KGA ATT GAC GG-3'); 519R (5'-GWATTACCGCGGCKGCTG-3'); 907R (5'-CCG TCH ATT CMT TTR AGT TT-3'); 1492R (5'-ACGGYTACCTTGTTACGACTT-3'). The resulting PCR products were purified and sequenced using an ABI PRISM3730xl DNA capillary analyzer (Applied Biosystems, Foster City, CA, USA) and a BigDye Terminator Cycle Sequencing ready-reaction kit (Applied Biosystems). The forward and reverse sequences obtained on the ABI 3730 XL analyzer for AU1 were aligned using BioEdit version 7.1.9. The sequences were finally assembled to obtain the full-length sequence, and the full-length sequence was compared to other sequences available in the NCBI Genbank database using BLAST (<http://blast.ncbi.nlm.nih.gov>).

Microscopic analysis

Gram staining was performed using a standard set of dyes. Scanning electron microscopy (SEM) was performed using a Zeiss EV050, UK. Samples were fixed in 2% glutaraldehyde for 2 hours, washed three times with 0.1 M cacodylate buffer for 20 minutes, and stepwise dehydrated in 50, 70, 85, and 95% (v/v) ethanol solutions for 10 minutes, dried in a Polavon E3100 vacuum dryer, Quorum Technologies, UK, and then sputter coated with Au-Pt using an Emitech SC7620, Quorum Technologies, UK.

Estimation the concentration of bacterial cells by plating on solid nutrient media

The number of colony-forming units (CFU) in the experiment with inactivation of *Staphylococcus saprophyticus* AU1 cells by treatment with dodecyl sulfate was determined by seeding 0.1 ml of a suspension of bacterial cells from its ten-fold sterile dilutions on a Petri dish, which were filled with agar. The number of CFUs was counted after incubation of Petri dishes at 30°C for 2 days.

Determination of bacterial biomass concentration

Bacterial biomass concentration was determined using a calibration graph based on optical density. Optical density measurements were carried out using a photoelectrocolorimeter at 590 nm and the biomass concentration was determined using a calibration graph. The content of absolutely dry biomass (ADB) of bacteria was determined by the standard method after filtering and drying the sample at a temperature of 105°C to constant weight.

Determination of physiological characteristics of acid urease producer

The specific growth rate was determined using the equation:

$$\mu = (\ln X_1 - \ln X_0) / (t_1 - t_0), \quad (7)$$

where X_1 and X_0 are biomass concentrations at time t_1 and t_0 , respectively.

pH determination

pH was measured on a pH meter Eutech instruments pH 2700. A pH meter with a measurement range from -2 to 20 pH having 0.002 pH accuracy.

Determination of urease activity

Urease activity was determined using a TDS-3 portable conductometer: the amount of released ammonium was determined according to the calibration graph by changing the electrical conductivity of the solution, $\mu\text{S}/\text{cm}$, due to hydrolysis of urea under the action of the urease enzyme (Stabnikov et al., 2022). The molar concentration of NH_4^+ (Y) correlated linearly ($R^2 = 0.999$) with the change in the electrical conductivity of the solution (ΔX) in $\mu\text{S}/\text{cm}$ over 5 minutes. Urease activity (UA) was defined as the amount of ammonium formed in 1M urea solution per minute.

Materials for biocementation

Sand. River sand was sifted through a metal sieve with a pore opening diameter of 0.5 mm (Fig. 1a).

Bone meal (Manufacturer: ODO "Lisichansk Gelatin Plant") with a wet content of 5%, protein 6.8%, lipids 1.8%, calcium 29.3%, phosphorus 13.4% (Fig. 1b).



Figure 1. Sifted sand (a) and bone meal (b).

Analysis of particle size distribution of sand and bone meal

Particle size distribution and average size were measured using a Bettersizer S3 Plus particle size analyzer (Bettersize Instruments, Dandong, China). For each sample, 3 measurements were taken to determine the average particle size. The maximum sizes of 10% (D10), 50% (D50) and 90% (D90) of all particles were determined.

Bone meal dissolution was carried out according to (Gowthaman et al., 2021). Bone flour, 50 g, was added under stirring to 200 ml of distilled water, and 60 ml of hydrochloric acid, 2 M HCl (5 ml per minute) was gradually added. The hydrolysis process lasted 80 minutes. The remaining bone meal was filtered off and the resulting solution was used in further studies.

Determination of water permeability of biocemented sand

To determine the water permeability of the treated sand samples, 0.1–0.2 l of tap water was supplied by gravity from 1 l of a container with water at a practically constant hydraulic pressure of 0.5 m of water. This measurement was close to ASTM D2434-68 (2006)

"Standard Test Method for Permeability of Granular Soils". The hydraulic permeability of sand, P , in a sand core was calculated according to equation:

$$P = V/(t \cdot A), \text{ m/s}, \quad (8)$$

where V is the volume of water, which was used to determine the water permeability of a sand column, m^3 ; t is the time for which water passes through the sand, s ; A is the cross-sectional area of the column, m^2 .

Biocementation of sand using inactivated *Staphylococcus saprophyticus* AU1 cells with urease activity

Sifted river sand was added to columns with a volume of 50 ml (height 7 cm, diameter 3 cm) in an amount of 60 g and was carefully compacted. The prepared columns were mounted on laboratory stands (Fig. 2).



Figure 2. Sand columns for biocementation.

A suspension of inactivated bacterial cells, 20 ml, was slowly supplied into the column, the effluent outlet from the column was closed and kept for 2 hours for cell adsorption. The culture liquid was separated from the column by gravity, the sand in the column was washed with 20 ml of distilled water, and biocementation was carried out by feeding 20 ml of biocementation solution for 24 hours (one bioprocessing cycle).

Acid hydrolysate of bone meal, which has calcium in the form of a phosphorus-containing compound, was used as a source of dissolved calcium in the biocementing solution. To reduce the water permeability of sand, the biocementation cycle was repeated 8 times. As a control, a column into which a calcium solution was supplied, but without urea was used.

Statistical analysis

The experiments were carried out in triplicates. Statistical processing of the experimental results was carried out using special programs for personal computers. Data are presented as mean \pm standard deviation.

Results and discussion

Isolation and identification of a strain producing acid urease

A tenfold dilution of enrichment culture with a sterile 1.5% NaCl solution was distributed onto solidified liquid medium TBS in Petri dishes and incubated at 30°C for 2 days. Single colonies, the color of the medium near changed from yellow-green to purple, were isolated into pure cultures and tested for urease activity when grown on a liquid medium under aerobic conditions in a batch cultivation mode in flasks on a shaker at room temperature for 4 days (Fig. 3).

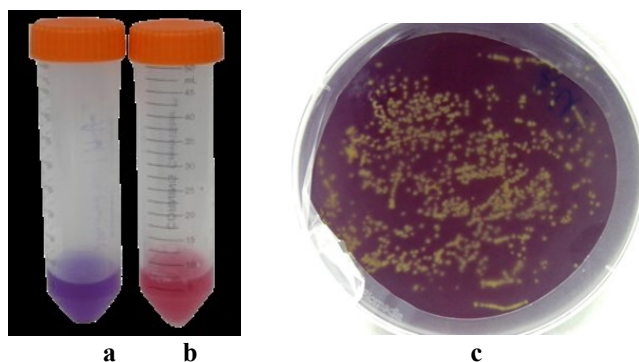


Figure 3. Growth of an acid urease producer in a liquid medium (a, left tube) and on solid medium in the presence of the bromocresol purple indicator (c); growth of *Bacillus* sp. VUK5 in a liquid medium with phenol red is shown (b).

Urease activity of strains isolated from an enrichment culture is shown in Figure 4.

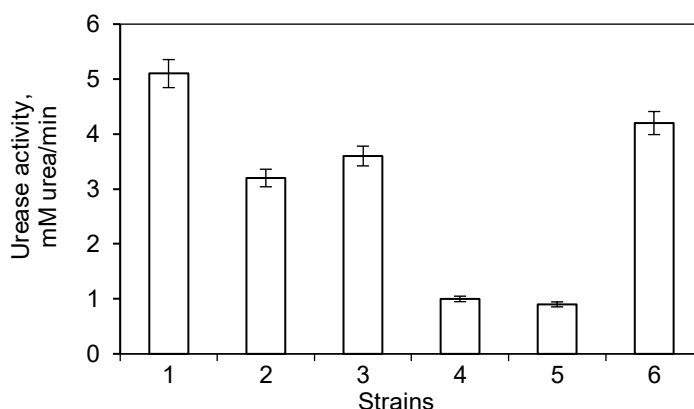


Figure 4. Urease activity of isolated strains producing acidic urease.

Strain AU1 with higher urease activity was selected for further studies. The strain was identified by rRNA gene amplification and sequencing. Partial nucleotide sequences were combined to obtain the complete nucleotide sequence of the 16S rRNA gene. Strain AU1 was nonsporeforming Gram-positive spherical cells. Determination of the nearest neighbor phylogenetic sequences of the 16S rRNA gene of strain AU1 using the BLAST search program against known species in the National Center for Biotechnology Information database revealed that it is a member of the genus *Staphylococcus*: related strains are *Staphylococcus saprophyticus* ZK-3(100% identity); *Staphylococcus* sp. WW60 (100% identical), and *Staphylococcus saprophyticus* T86 (100% identity). Complete nucleotide sequence of the 16S rRNA gene of strain AU1 is as follows:

```
GCTCAGGATGAACGCTGGCGGCTGCTAATACATGCAAGTCGAGCGAACAGATAAGGAGCTTGCT
CCTTTGACGTTAGCGGGACGGGTGAGTAACACGTGGGTAACCTACCTATAAGACTGGGATAACTT
CGGGAAACCGGAGCTAATACCGGATACATTTGGAACCGCATGGTCTAAAGTGAAAGATGGTTTTG
CTATCACTATAGATGGACCCGCGCCGTATTAGCTAGTTGGTAAGGTAACGGCTTACCAAGGCGACG
ATACGTAGCCGACCTGAGAGGGTGATCGGCCACACTGGAAGTGAACACGGTCCAGACTCCACGG
GAGGCAGCAGTAGGGAATCTTCCGCAATGGGCGAAAGCCTGACGGAGCAACGCCGCGTGAGTGATG
AAGGGTTTCGGCTCGTAAAACCTGTATTAGGGAAGAACAAACGTGTAAGTAACTGTGCACGCTT
GACGGTACCTAATCAGAAAGCCACGGCTAACTACGTGCCAGCAGCCGCGGTAATACGTAGGTGGCA
AGCGTTATCCGAAATTATTGGGCGTAAAGCCGCGGTAGGCGGTTCTTAAAGTCTGATGTGAAAGCC
ACGGCTCAACCGTGGAGGGTCATTGGAAACTGGGAAACTTGAGTGCAGAAGAGGAAAGTGAATTC
CATGTGTAGCGGTGAAATGCGCAGAGATATGGAGGAACACCAGTGGCGAAGGCGACTTTCTGGTCT
GTAACGTACGCTGATGTGCGAAAGCGTGGGGATCAAAACAGGATTAGATACCCTGGTAGTCCACGCC
GTAAACGATGAGTGCTAAGTGTAGGGGGTTCCGCCCTTAGTGCTGCAGCAACGCATTAAGCACT
CCGCTGGGGAGTACGACCCGCAAGGTTGAAACTCAAAGGAATTGACGGGGACCCGCAACAAGCGGTG
GAGCATGTGGTTAATTGCAAGCAACGCGAAAACCTTACCAAATCTTGACATCCTTTGAAAACCTTA
GAGATAGAGCCTTCCCCTTCGGGGGACAAAGTGACAGGTGGTGCATGGTTGTCGTCAGCTCGTGTCG
TGAGATGTTGGGTTAAGTCCCGCAACGAGCGCAACCCCTAAGCTTAGTGGCCATCATTAAAGTTGGG
ACTAGGTTGACTGCCGTTGACAAACCGGAGGAAGGTGGGGATGACGTCAAATCATCATGCCCTTAT
GATTTGGGCTACACACGTGCTACAATGGACAATACAAAGGGCAGCTAAACCGCGAGGTCATGCAAAA
TCCCATAAAGTTGTTCTCAGTTCCGATTGTAGTCTGCAACGACTACATGAAGCTGGAATCGCTAGTA
ATCGTAGATCAGCATGCTACGGTGAATACGTTCCCGGGTCTGTACACACCGCCCGTACACCACGA
GAGTTTGTAACACCCGCGTGGAGTAACCATTTATGGAGCTAGCCGTCGAAGGTGGGACAAA
TGATTGGGGTGAATCTAA.
```

The marine bacterium *Staphylococcus saprophyticus*, a producer of alkaliphilic protease with a wide range of temperature activity (10-80 °C) was identical (99%) to *Staphylococcus saprophyticus* ZK3 and *Staphylococcus* sp. WW60 (99%) (Uttatree and Charoenpanich, 2018). *Staphylococcus* sp. WW60 is an endophytic bacterium with strong activity against *Candida* yeasts (Das et al., 2019). A scanning electron microscope (SEM) image of strain AU1 cells is shown (Fig. 5).

Characteristics of the isolated strain of urease-producing bacteria *Staphylococcus saprophyticus* AU1

The isolated strain *Staphylococcus saprophyticus* AU1 was cultivated and its urease activity was compared with the known strain *Bacillus* sp. UK5 (Stabnikov, 2013a). Strains UK5 and AU1 were grown on the appropriate nutrient media described in section Materials and methods. The initial pH value of the medium for the UK5 strain was 7.2 and 5.8 for the AU1. Cultivation was carried out under aeration conditions under shaking 150 rpm for 3 days. The growth curves and changes in urease activity during the cultivation of these two strains are shown in Figure 6.

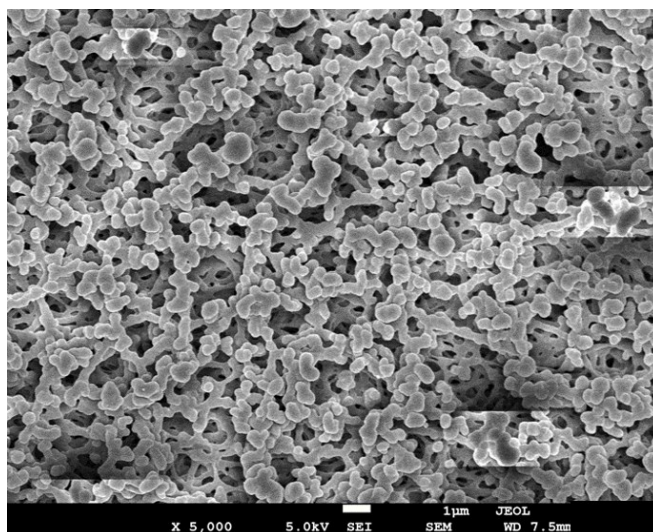


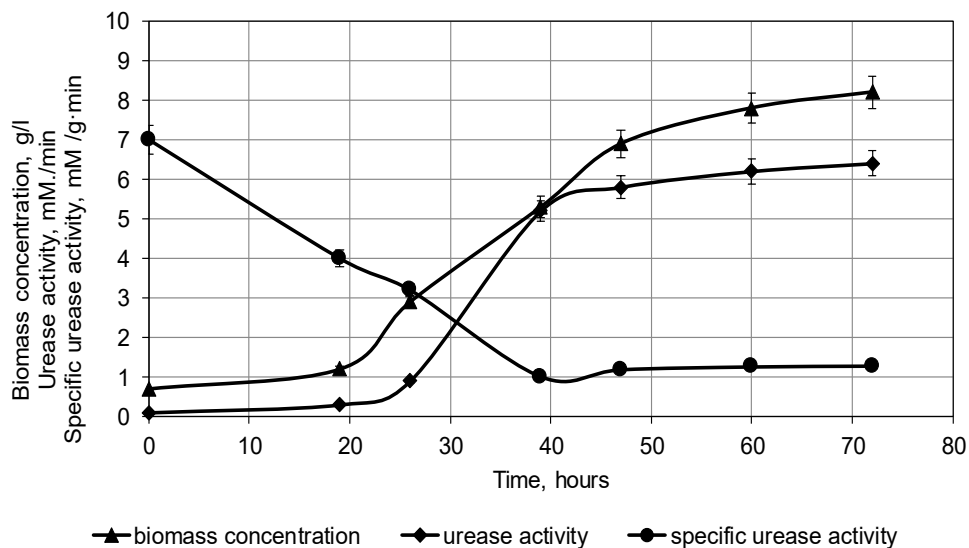
Figure 5. SEM images of cells of the strain of acid-tolerant urease producing bacteria *Staphylococcus saprophyticus* AU1.

When periodically cultivated under aeration conditions, strain UK5 showed a maximum growth rate of 0.11 h^{-1} , a maximum biomass accumulation of 8.2 g/l of dry biomass after 3 days of cultivation, and the maximum urease activity $6.4 \text{ mM hydrolyzed urea/min}$ (Fig. 6a), while the maximum growth rate of strain AU1 was 0.15 h^{-1} , the maximum biomass accumulation was 6.9 g/l dry biomass, and the maximum urease activity was $8.1 \text{ mM hydrolyzed urea/min}$ (Fig. 6b). Thus, the acid-tolerant strain AU1 had a maximum biomass accumulation by 19% lower, a maximum growth rate by 36.3% higher, and a maximum urease activity of the culture liquid by 26.5% higher than the same indicators for the UK5 strain.

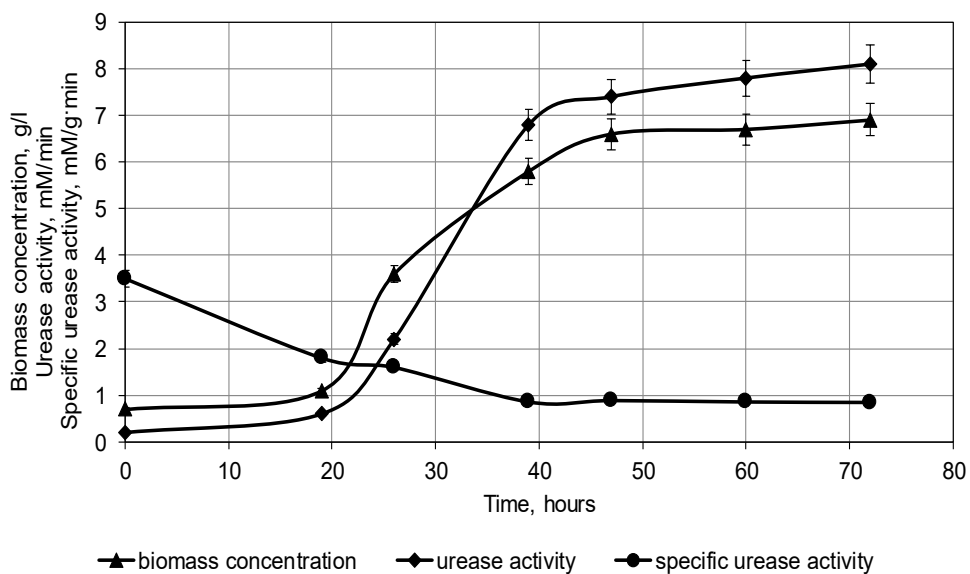
The urease activity values obtained for the acid-tolerant strain AU1 are also close to the urease activity of other strains used for biocementation, for example, *Sporosarcina pasteurii* ATCC 11859, $13.3 \text{ mM hydrolyzed urea/min}$ (Whiffin, 2004), and a strain of *Bacillus* sp., isolated from the soil in Australia, $3 \text{ mM hydrolyzed urea/min}$ (Al-Thawadi and Cord-Ruwisch, 2012). The same urease activities were used in the biocementation of sand using pure urease enzyme: urease activity ranged from 2.5 mM/min to 10.5 mM/min (Almajed et al., 2019) and 5.9 mM/xB (Jiang et al., 2016).

Changes in urease activity of *Staphylococcus saprophyticus* AU1 cells depending on the pH of the environment

The dependence of the activity of acid urease of *Staphylococcus saprophyticus* AU1 on the pH of the medium was determined in the range from 4.0 to 8.0 (Fig. 7).



a



b

Figure 6. Change in biomass concentration, g dry biomass/l (▲), urease activity, mM/min (■) and specific urease activity (●) during batch cultivation of *Bacillus sp.* UK5 (a) and *Staphylococcus saprophyticus* AU1 (b).

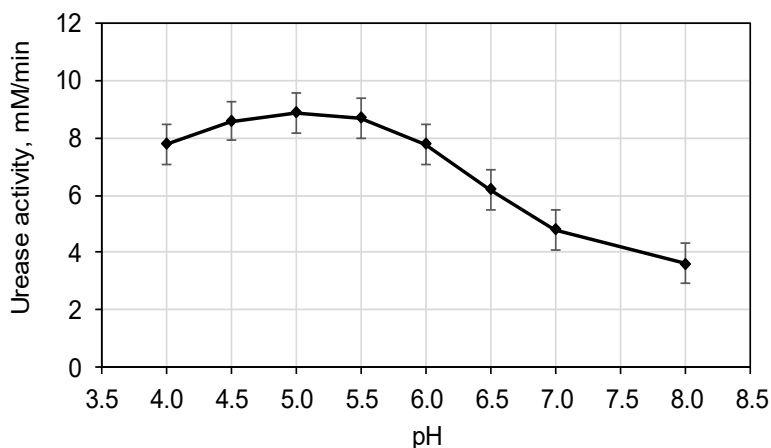


Figure 7. Urease activity of *Staphylococcus saprophyticus* AU1 depending on the pH of the medium.

The highest urease activity was observed in the pH range from 4.5 to 5.5, gradually decreasing with pH increasing. The optimal pH value for the action of acidic ureases, according to the literature, was 4.5 for urease, the producer of which was the strain *Enterobacter* sp. R-SYB082 (Yang et al., 2010); 4.2 for urease produced by the strain *Arthrobacter mobilis* SAM 0752 (Miyagawa et al., 1999). Commercially available Nagapshin urease, produced by Nagase Chemtex Corporation (Kyoto, Japan) and used in (Gowthaman et al., 2021), was active in the pH range from 4.0 to 8.0 with an optimum for action at pH 5.0.

Changes in urease activity during inactivation of *Staphylococcus saprophyticus* AU1 cells

The use of inactivated bacterial cells for biocementation has been proposed to maintain environmental biosafety. As has been shown in the work (Stabnikov et al., 2016), inactivated bacterial cells of *Yaniella* sp. VS8, which retained urease activity, can be used for bioclogging of soil. The use of pure urease enzyme in large-scale biocementation is expensive. In addition, the use of bacterial cells has advantages such as the creation of calcium carbonate crystallization centers in the processed materials due to the adhesion of cells on their surface. When comparing the effectiveness of such methods for inactivating cells of bacteria *Yaniella* sp., based on rupture of the cell membrane, such as treating a cell suspension with ultrasound; incubation for 1 hour in ethanol solutions and incubation in sodium dodecyl sulfate solution with a final concentration of 0.5% (w/v), it was shown that (1) sonication (750 watts; 20 megahertz; amplitude 50%) for 30 s, 60 s, and 300 s did not inactivate cells; (2) incubation of bacterial cells in 25% (v/v), 50% (v/v), and 70% (v/v) ethanol solutions significantly reduced the concentration of living cells from $5.2 \cdot 10^8$ CFU/ml to $4.9 \cdot 10^2$ CFU/ml, while (3) treatment with a 0.5% dodecyl sulfate solution for 120 minutes ensured complete inactivation of cells, while maintaining urease activity.

The inactivating effect of dodecyl sulfate was confirmed by scanning electron microscopy, which showed the destruction of treated bacterial cells of urease-producing

bacteria. Based on these data, it was proposed to use sodium dodecyl sulfate to inactivate *Staphylococcus saprophyticus* AU1 cells; its inhibitory effect on bacteria is based on the dissolution of the cell membrane (Hansen et al., 2011). The cell suspension with pH 5.0 was added with calculated amount of sodium dodecyl sulfate and kept at a room temperature. Data on keeping a bacterial suspension of *Staphylococcus saprophyticus* in a 0.5% sodium dodecyl sulfate are given in Table 1.

Table 1
Effect of treatment time of *Staphylococcus saprophyticus* AU1 cells in 0.5% sodium dodecyl sulfate on their urease activity and survival

Time of incubation, min	Urease activity, mM hydrolyzed urea/min during incubation in a solution of 1M urea, min *		CFU/ml**
	5	30	
0	7.7	4.8	$1.2 \cdot 10^8$
10	4.2	7.7	$2.9 \cdot 10^2$
30	3.8	6.9	$0.7 \cdot 10^1$
60	3.4	5.9	6.0
90	3.3	5.7	0

* the measurement accuracy was less than 10%.

** the measurement accuracy was less than 20%.

Incubation of bacterial suspension of *Staphylococcus saprophyticus* AU1 in a 0.5% sodium dodecyl sulfate significantly reduced the concentration of living cells, and exposure for 40 minutes allowed their complete inactivation. Urease activity decreased, but remained quite high – the percentage of losses during processing for 40 minutes was 26% of the original (Table 1). Complete inactivation of cells of *Yaniella* sp.VS8, when treated with 0.5% sodium dodecyl sulfate solution, was observed after 120 minutes of exposure (Stabnikov et al., 2016).

According to the results, urease activity of the treated cells increased with the time of incubation in a 1M urea solution, which indicates the constitutive nature of urease synthesis in *Staphylococcus saprophyticus*, which becomes more accessible when the cell ruptures. This is also evidenced by data on changes in urease activity during incubation in a 1 M urea solution (Table 2).

Table 2
Urease activity (UA) for different times of incubation of bacterial cells in 1 M urea solution

Cells of <i>S. saprophyticus</i> AU1	UA*, mM hydrolyzed urea/min during contact with 1M urea solution, min					
	5	30	60	90	120	150
Live untreated	7.7	4.8	3.9	3.6	3.0	2.1
Inactivated after incubation in 0.5% sodium dodecyl sulfate solution for 90 minutes	3.3	5.7	6.9	5.7	3.9	2.3

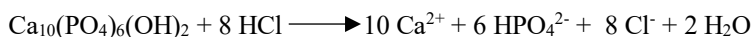
* The measurement accuracy was less than 10%.

Thus, the most suitable method for inactivating bacterial cells while maintaining their urease activity is incubation of a bacterial suspension in a 0.5% sodium dodecyl sulfate for 90 minutes, which will ensure biosafety when using *Staphylococcus saprophyticus* AU1 cells for biocementation.

Staphylococcus saprophyticus AU1 bacteria were grown under sterile conditions in a liquid medium prepared from Tryptic Soy Broth under the shaking at 200 rpm at room temperature. Cells were inactivated by adding 0.5% (w/v) dodecyl sulfate and holding for 90 min. The treated cells were separated by centrifugation at 5000 rpm for 10 minutes, resuspended in 2% (w/v) NaCl solution and used for biocementation of sieved river sand.

Preparing a bone meal solution

Bone meal was used as a source of calcium. As shown in Gowthaman et al. (2021) calcium and phosphorus are present in bone meal as hydroxyapatite $\text{Ca}_{10}(\text{PO}_4)_6(\text{OH})_2$. Hydrochloric acid dissolution of bone meal (bone hydroxyapatite) was carried out according to the equation:



pH and calcium concentration were measured during dissolution Ca^{2+} (Fig. 8).

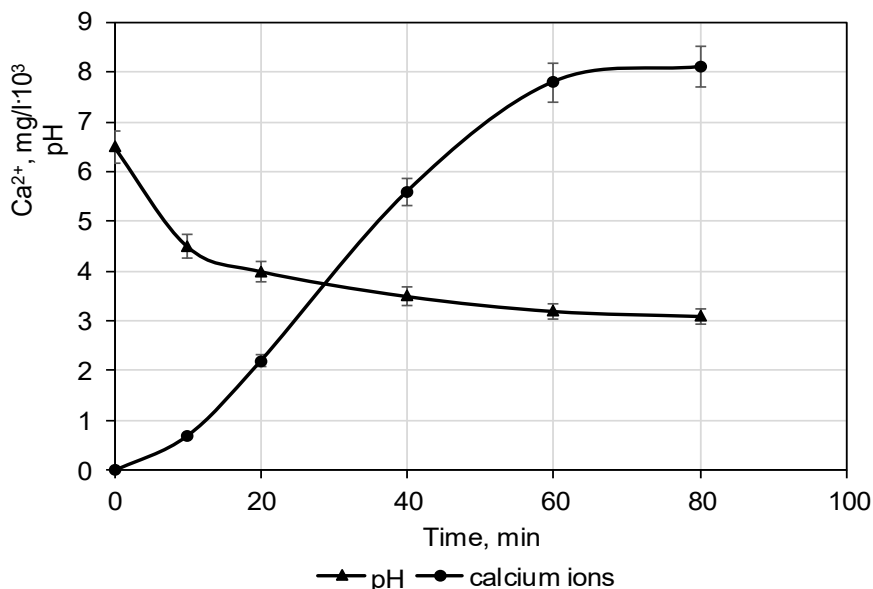


Figure 8. Changes in pH and calcium concentration when bone meal is dissolved in hydrochloric acid.

The final pH value after 80 min of bone meal dissolution was 3.5, and the concentration of calcium ions was 7800 mg/l. The remaining bone meal was filtered off and the resulting solution was used in further studies. The indicators of the filtered solution of Ukrainian bone meal hydrolysate were similar to those obtained in the study of Japanese researchers: 8800 mg/l of calcium ions and a pH value of 3.4 (Gowthaman et al., 2021).

Biocementation of sand using hydrolyzed bone meal as a source of calcium

The possibility of using bone meal as a source of calcium for biocementation was tested using inactivated cells of an acid-tolerant urease producer. Bone meal is one of the excellent and inexpensive sources of calcium and inorganic phosphate and can be used as a cementing material instead of calcium chloride. To use bone meal as a component for the formation of biocement, it was pre-dissolved in dilute hydrochloric acid. Bone meal dissolved in acid along with urea and a source of acidic urease was introduced into sand for biocementation. The components for biocementation were: (a) bone meal hydrolysate, (b) a suspension of inactivated cells of acid urease bacterial producer, and (c) urea. Sand was biocemented at the ratio of calcium and urea ion concentrations according to Table 3.

Table 3

Variants for sand biocementation

Sample	Concentration of Ca ²⁺ , g/l	Concentration of urea, g/l	Mole ratio
1	7.8	1.8	0.25
2	7.8	3.9	0.50
3	7.8	5.7	0.75

For biocementation, sifted river sand was used. Particle size distribution and average size were measured using a Bettersizer S3 Plus particle size analyzer (Bettersize Instruments, Dandong, China) (Fig. 9).

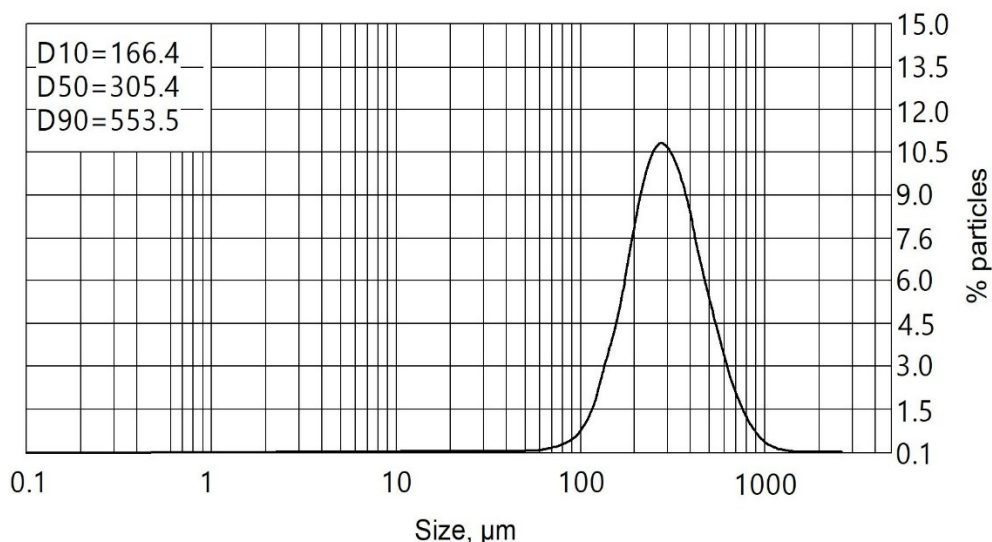


Figure 9. Size distribution of sifted sand particles.

Thus, the main sand fractions had particles ranging from 200 to 300 μm (30.31%) and 300.0 to 400 μm (23.74%). $D_{10}=166.4 \mu\text{m}$; $D_{50}=305.4 \mu\text{m}$; $D_{90}=553.5 \mu\text{m}$, that is, 10% of the sand had particles less than 166.4 μm , 50% less than 330 μm and 90% less than 1600 μm .

Sand according to particle size is classified as fine – particle size from 75 to 425 μm ; medium – particle size from 425 to 20500 μm , and coarse - particle size from 2000 to 4750 μm . That is, the sand that was used for biocementation in the present research was fine. For comparison, biocementation studies typically use: ASTM (American Society for Testing and Testing Materials) graded sand with an average particle size of 400 μm ; standard sand with rounded particles (Societe Nouvelle du Littoral, France Ser) with an average particle size of 420 μm ; standard Ottawa sand with an average size of 300 μm with particle size varying from 150 to 1180 μm .

Sand, 60 g, was placed in a column with a volume of 50 ml and an internal diameter of 30 mm. Suspension of inactivated bacterial cells (20 ml) was slowly supplied into the column. The sand with inactivated cells was kept for 2 hours for cell adsorption, and then the suspension was drained by gravity. The sand was washed with 20 ml of water. After gravity removal of water, 20 ml of biocementing solution was supplied into the column according to Table 3. Incubation was carried out for 24 hours, and the remaining solution was removed by gravity.

To increase the strength of the treated sand, a biocementing solution was injected into each column 8 times. The control was a sample in which a calcium solution was supplied, but without urea. The results of calcium accumulation showed that in the control calcium was not retained in the sand, but was washed out. Thus, only in the presence of urea with an increase in pH due to its enzymatic hydrolysis, dissolved calcium is converted into an insoluble calcium-phosphorus-containing compound, which fills the pores of the sand and holds it together. Thus, a small amount of calcium during biocementation of this type will be precipitated in the form of calcium carbonate, and the bulk will be precipitated as a calcium-phosphorus-containing compound that allows reducing the amount of urea used for biocementation, and, as a result, significantly diminishing the release of ammonium and ammonia into the environment. The change in permeability of sand is shown in Figure 10.

Sand biocemented by the proposed method does not have the same strength as with conventional biocementation due to the formation of calcium carbonate, and its water permeability has decreased only to $2 \cdot 10^{-5}$ m/s, when with biocementation it usually consists about $1 \cdot 10^{-6}$ m/s. It is not practical to carry out a larger number of bio-treatments, but the data obtained allow the use of bio-cementation of this type to strengthen the soil to reduce its erosion, for example after an earthquake, or to combat dust erosion to reduce atmospheric pollution (Stabnikov et al., 2013b). The main advantage of this method is the possibility of a significant reduction (by 75%) emissions of ammonium and ammonia into the environment.

Thus, compared with the conventional biocementation method based on microbially initiated calcium carbonate precipitation, the use of bone meal hydrolysate as a source of calcium when using acid-tolerant urease offers significant environmental and economic advantages, namely: (a) reduction in the release of ammonium and toxic ammonia into the environment; (b) reduction in material costs, and (c) solution of bone waste disposal problem.

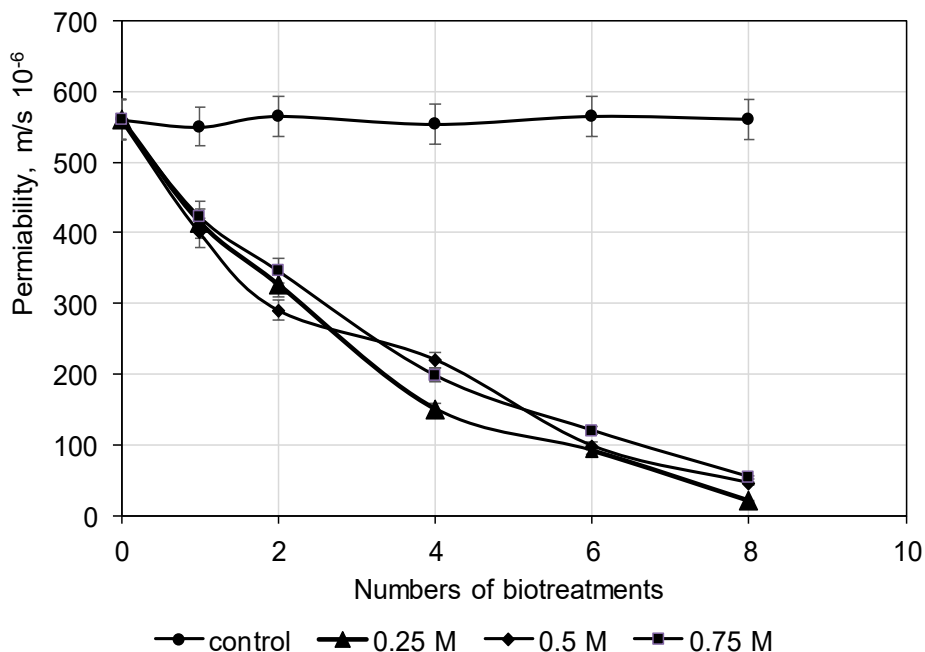


Figure 10. Changes in the water permeability of sand during biocementation using bone meal hydrolysate and a reduced amount of urea (0.25 M, 0.5 M, and 0.75 M), the hydrolysis of which occurred under the action of inactivated cells of acid urease producer.

Conclusions

1. Selection of a bacterial strain that synthesized acid urease was carried out among bacteria isolated from acidic soil. The strain with the highest urease activity was identified by rRNA gene amplification and sequencing as *Staphylococcus saprophyticus* AU1.
2. The physiological properties of the strain were studied: the maximum growth rate of strain AU1 was 0.15 h^{-1} , the maximum accumulation of biomass was 6.9 g/l of dry biomass, and the maximum urease activity was 8.1 mM hydrolyzed urea/min. The highest urease activity of the *Staphylococcus saprophyticus* AU1 strain was observed at the pH range from 4.5 to 5.5, gradually decreasing with increasing pH.
3. To ensure environmental biosafety, the use of inactivated bacterial cells that retain urease activity has been proposed for biocementation. Complete inactivation of cells was observed when cells were treated with 0.5% sodium dodecyl sulfate solution for 90 minutes.
4. Application of bone meal containing calcium in the form of hydroxyapatite allows reducing the amount of urea during the biocementation process. The water permeability of sand biocemented using hydrolyzed bone meal and acid-tolerant urease, was $2 \cdot 10^{-5} \text{ m/s}$, which makes it possible to use biocementation of this type to strengthen the soil to reduce its liquefaction, for example after an earthquake, or to control dust erosion for reduction of atmospheric pollution.

5. The main advantage of this method is the ability to significantly reduce by 75% urea consumption and, thereby, reduce emissions of ammonium and ammonia into the environment. In addition, the problem of bone waste disposal is solved and the cost of materials for biocementation is reduced.

References

- Almajed A., Tirkolaei H.K., Kavazanjian E., Hamdan N. (2019), Enzyme induced biocemented sand with high strength at low carbonate content, *Scientific Reports*, 9, 1135, <https://doi.org/10.1038/s41598-018-38361-1>
- Al-Thawadi S., Cord-Ruwisch R. (2012), Calcium carbonate crystals formation by ureolytic bacteria isolated from Australian soil and sludge, *Journal of Advanced Scientific Education and Research*, 2(1), pp. 12–26.
- Akiyama M., Kawasaki S. (2012), Novel grout material comprised of calcium phosphate compounds: in vitro evaluation of crystal precipitation and strength reinforcement, *Engineering Geology*, 125, pp. 119–128, <https://doi.org/10.1016/j.enggeo.2011.11.011>
- Aprianti E. (2017), A huge number of artificial waste material can be supplementary cementitious material (SCM) for concrete production—a review, Part II, *Journal of Cleaner Production*, 142, pp. 4178–4194, <https://doi.org/10.1016/j.jclepro.2015.12.115>
- Avramenko M., Nakashima K., Kawasaki S. (2022), State-of-the-art review on engineering uses of calcium phosphate compounds: An eco-friendly approach for soil improvement, *Materials*, 15, 6878, <https://doi.org/10.3390/ma15196878>
- Benhelal E., Zahedi G., Shamsaei E., Bahadori A. (2013), Global strategies and potentials to curb CO₂ emissions in cement industry, *Journal of Cleaner Production*, 51, pp. 142–161, <https://doi.org/10.1016/j.jclepro.2012.10.049>
- Chu J., Ivanov V., Stabnikov V., He J., Li B., Naemi M. (2012), Biocement: Green building- and energy-saving material, *Advanced Materials Research*, 347–353, pp. 4051–4054, <https://doi.org/10.4028/www.scientific.net/AMR.347-353.4051>
- Cuzman O.A., Richter K., Wittig L., Tiano P. (2015), Alternative nutrient sources for biotechnological use of *Sporosarcina pasteurii*, *World Journal of Microbiology and Biotechnology*, 31, pp. 897–906, <https://doi.org/10.1007/s11274-015-1844-z>
- Das G., Park S., Choi J., Baek K.H. (2019), Anticandidal potential of endophytic bacteria isolated from *Dryopteris uniformis* (Makino), *Jundishapur Journal of Microbiology*, 12(1), e69878. <https://doi.org/10.5812/jjm.69878>
- Dilrukshi R.A.N., Watanabe J., Kawasaki S. (2015), Sand cementation test using plant-derived urease and calcium phosphate compound, *Materials Transactions*, 56(9), pp. 1565–1572, <https://doi.org/10.2320/matertrans.M-M2015818>
- Dilrukshi R.A.N., Watanabe J., Kawasaki S. (2016), Strengthening of sand cemented with calcium phosphate compounds using plant-derived urease, *International Journal of GEOMATE*, 11(3), 2, pp. 2461–2467, <https://geomatejournal.com/geomate/article/view/2740/2321>
- Gowthaman S., Yamamoto M., Nakashima K., Ivanov V., Kawasaki S. (2021), Calcium phosphate biocement using bone meal and acid urease: An eco-friendly approach for soil improvement, *Journal of Cleaner Production*, 128782, <https://doi.org/10.1016/j.jclepro.2021.128782>
- Hansen J.S., Vararattanavech A., Plasencia I., Greisen P.Jr., Bomholt J., Torres J., Emnéus J., Hélix-Nielsen C. (2011), Interaction between sodium dodecyl sulfate and membrane reconstituted aquaporins: A comparative study of spinach SoPIP2;1 and *E. coli* AqpZ, *Biochimica et Biophysica Acta*, 1808(10), pp. 2600–2607, <https://doi.org/10.1016/j.bbamem.2011.05.021>

- Imbabi M.S., Carrigan C., McKenna S. (2012), Trends and developments in green cement and concrete technology, *International Journal of Sustainable Built Environment*, 1, pp. 194–216, <https://doi.org/10.1016/j.ijbsbe.2013.05.001>
- Ivanov V., Stabnikov V. (2017), *Construction biotechnology: Biogeochemistry, microbiology and biotechnology of construction materials and processes*, Green Energy and Technology, Springer, <https://doi.org/10.1007/978-981-10-1445-1>
- Ivanov V., Stabnikov V., Kawasaki S. (2019a), Ecofriendly calcium phosphate and calcium bicarbonate biogrouts, *Journal of Cleaner Production*, 218, pp. 328–334, <https://doi.org/10.1016/j.jclepro.2019.01.315>
- Ivanov V., Stabnikov V., Stabnikova O., Kawasaki S. (2019b), Environmental safety and biosafety in construction biotechnology, *World Journal of Microbiology and Biotechnology*, 35, 26, <https://doi.org/10.1007/s11274-019-5862-9>
- Jiang N.J., Yoshioka H., Yamamoto K., Soga K. (2016), Ureolytic activities of a urease-producing bacterium and purified urease enzyme in the anoxic condition: Implication for seafloor sand production control by microbially induced carbonate precipitation (MICP), *Ecological Engineering*, 90, pp. 96–104, <https://doi.org/10.1016/j.ecoleng.2016.01.073>
- Kawasaki S., Akiyama M. (2013), Effect of addition of phosphate powder on unconfined compressive strength of sand cemented with calcium phosphate compound, *Materials Transactions*, 54(11), pp. 2079–2084, <https://doi.org/10.2320/matertrans.M-M2013827>
- Keykha H., Asadi A. (2017), Solar powered electro-bio-stabilization of soil with ammonium pollution prevention system, *Advances in Civil Engineering Materials*, 6, pp. 360–371, <https://doi.org/10.1520/ACEM20170001>
- Keykha H., Mohamadzadeh H., Asadi A., Kawasaki S. (2019), Ammonium-free carbonate-producing bacteria as an ecofriendly soil biostabilizer, *Geotechnical Testing Journal*, 42(1), pp. 19–29, <https://doi.org/10.1520/GTJ20170353>
- Lane D.J. (1991), 16S/23S rRNA Sequencing. In Stackebrandt E., Goodfellow M. (Eds.), *Nucleic acid techniques in bacterial systematics*, John Wiley and Sons, Chichester, pp. 115–175.
- Lee C., Lee H., Kim O.B. (2018), Biocement fabrication and design application for a sustainable urban area, *Sustainability*, 10(11), 4079, <https://doi.org/10.3390/su10114079>
- Miyagawa K., Sumida M., Nakao M., Harada M., Yamamoto H., Kusumi T., Yoshizawa K., Amachi T., Nakayama T. (1999), Purification, characterization, and application of an acid urease from *Arthrobacter mobilis*, *Journal of Biotechnology*, 68(2-3), pp. 227–236, [https://doi.org/10.1016/s0168-1656\(98\)00210-7](https://doi.org/10.1016/s0168-1656(98)00210-7)
- Miller S.A., Horvath A., Monteiro P.J. (2018), Impacts of booming concrete production on water resources worldwide, *Nature Sustainability*, 1, 69, <https://doi.org/10.1038/s41893-017-0009-5>
- Mishra U.C., Sarsaiya S., Gupta A. (2022), A systematic review on the impact of cement industries on the natural environment, *Environmental Science and Pollution Research*, 29, pp. 18440–18451, <https://doi.org/10.1007/s11356-022-18672-7>
- Nie S., Zhou J., Yang F., Lan M., Li J., Zhang Z., Sanjayan J.G. (2022), Analysis of theoretical carbon dioxide emissions from cement production: Methodology and application, *Journal of Cleaner Production*, 334, 130270, <https://doi.org/10.1016/j.jclepro.2021.130270>
- Omeregic A.I., Ginjom R.H., Nissom P.M. (2018), Microbially induced carbonate precipitation via ureolysis process: A mini-review, *Transactions on Science and Technology*, 5, pp. 245–256, <http://tost.unise.org/pdfs/vol5/no4/5x4x245-256.pdf>
- Roeselers G., van Loosdrecht M.C.M. (2010), Microbial phytase-induced calcium-phosphate precipitation – a potential soil stabilization method, *Folia Microbiologica*, 55, pp. 621–624, <https://doi.org/10.1007/s12223-010-0099-1>
- Stabnikov V., Chu J., Ivanov V., Li Y. (2013a), Halotolerant, alkaliphilic urease-producing bacteria from different climate zones and their application for biocementation of sand,

- World Journal of Microbiology and Biotechnology*, 29(8), pp. 1453–1460, <https://doi.org/10.1007/s11274-013-1309-1311>
- Stabnikov V., Chu J., Myo A.N., Ivanov V. (2013b), Immobilization of sand dust and associated pollutants using bioaggregation, *Water, Air, & Soil Pollution*, 224(9), pp. 1631–1700, <https://doi.org/10.1007/s11270-013-1631-0>
- Stabnikov V., Ivanov V., Chu J. (2016), Sealing of sand using spraying and percolating biogroups for the construction of model aquaculture pond in arid desert, *International Aquatic Research*, 8(3), pp. 207–216, <https://doi.org/10.1007/s40071-016-0136-z>
- Stabnikov V., Stabnikov D., Udymovych V. (2022), Increase the ecological safety of the soil biogrouting using plant urease, *Ukrainian Food Journal*, 11(2), pp. 302 – 314, <https://doi.org/10.24263/2304-974X-2022-11-2-10>
- Stocks-Fischer S., Galinat J.K., Bang S.S. (1999), Microbiological precipitation of CaCO₃, *Soil Biology and Biochemistry*, 31(11), pp. 1563–1571, [https://doi.org/10.1016/S0038-0717\(99\)00082-6](https://doi.org/10.1016/S0038-0717(99)00082-6)
- Toshima T., Hamai R., Tafu M., Takemura Y., Fujita S., Chohji T., Tanda S., Li S., Qin G.W. (2014), Morphology control of brushite prepared by aqueous solution synthesis, *Journal of Asian Ceramic Societies*, 2, pp. 52–56, <https://doi.org/10.1016/j.jascer.2014.01.004>
- Whiffin, V.S. (2004). Microbial CaCO₃ precipitation for the production of biocement, PhD thesis, School of Biological Sciences and Biotechnology, Murdoch University, Perth.
- Uttatree S., Charoenpanich J. (2018), Purification and characterization of a harsh conditions-resistant protease from a new strain of *Staphylococcus saprophyticus*, *Agriculture and Natural Resources*, 52(1), pp. 16-23, <https://doi.org/10.1016/j.anres.2018.05.001>
- Yang L., Wang S., Tian Y. (2010), Purification, properties, and application of a novel acid urease from *Enterobacter* sp., *Applied Biochemistry and Biotechnology*, 160(2), pp. 303–313, <https://doi.org/10.1007/s12010-008-8159-6>
- Yu X., Jiang J. (2018), Mineralization and cementing properties of biocarbonate cement, bio-phosphate cement, and bio-carbonate/phosphate cement: A review, *Environmental Science and Pollution Research*, 25, pp. 21483–21497, <https://doi.org/10.1007/s11356-018-2143-7>

Cite:

UFJ Style

Stabnikov V., Udymovych V., Kovshar I., Stabnikov D. (2024), Microbial producer of acid urease for its application in biocementation, *Ukrainian Food Journal*, 13(2), pp. 331–350, <https://doi.org/10.24263/2304-974X-2024-13-2-10>

APA Style

Stabnikov, V., Udymovych, V., Kovshar, I., & Stabnikov, D. (2024). Microbial producer of acid urease for its application in biocementation. *Ukrainian Food Journal*, 13(2), 331–350. <https://doi.org/10.24263/2304-974X-2024-13-2-10>

Modeling of heat transfer processes by periodic perturbation of freely flowing liquid film flowing along vertical surface with large-amplitude waves

Valentyn Petrenko, Viktor Ardashev,
Dmytro Maksymenko, Oleksiy Pustovoi

National University of Food Technologies, Kyiv, Ukraine

Abstract

Keywords:

Evaporation
Heat transfer
Film
Waves
Turbulence

Article history:

Received
19.11.2023
Received in
revised form
22.02.2024
Accepted
2.07.2024

Corresponding author:

Valentyn
Petrenko
E-mail:
Petrenkovp@
ukr.net

DOI:

10.24263/2304-
974X-2024-13-2-
11

Introduction. The aim of the study was the theoretical and experimental determination of the influence of periodic disturbances of the liquid film surface on the intensity of heat transfer during evaporation.

Materials and methods. The theoretical results were obtained based on mathematical modeling of heat transfer processes in flowing liquid films with disturbance of its surface by large waves. Physical modeling was performed on an experimental stand, on which heat exchange processes in the film were reproduced in a 9-m-long pipe with a diameter of 30 mm, which was heated by dry saturated steam. The heat flow was measured at the discrete-local level.

Results and discussion. The model of heat exchange in a liquid film flowing down a vertical surface is presented, which is cyclically mixed either due to the passage of low-frequency waves of large amplitude, or due to a system of mechanical obstacles in the way of the film movement. The analytical expression for the temperature field in the turbulent film is obtained by the approximate solution of the convective heat conduction equation with the boundary conditions under which vapor formation occurs on the free surface of the film. An analytical expression for the heat transfer coefficient is presented, which includes, as parameters, the distance between the heat transfer intensifiers and the maximum value of the turbulence function, which is proportional to the height of the mechanical turbulators. For film currents flowing in long, smooth heat exchange channels, the role of the parameters is played by the distance between the crests of large waves and their amplitude. The practical implementation of the obtained results of the mathematical modeling of heat transfer in the processes of cyclic disturbance and restoration of the hydrodynamic structure of flowing films is demonstrated by generalization on its basis of the data of experimental studies of heat exchange in a flowing film of water in a pipe with a diameter of 30 mm and a height of 9 m in the range of changes in the mass density of irrigation 0.16–0.72 kg/m sec with.

Conclusions. A mathematical model of heat exchange in a liquid film flowing down a vertical surface disturbed either by low-frequency waves of large amplitude or by a system of ring intensifiers of heat exchange has been developed.

Introduction

Thanks to the action of gravity, the movement of liquid flowing down the vertical surface of the film occurs in the absence of stagnant zones, and heat and mass exchange processes, due to the small thickness of the films, proceed rapidly in small volumes and are characterized by high intensity. These factors become especially important during the concentration of viscous thermolabile food solutions under rarefaction, where the hydrostatic temperature depression, which is absent in film evaporators, increases rapidly. At the same time, during the movement of highly concentrated thick films of solutions, the intensification of heat exchange processes becomes relevant.

Intensification of heat exchange can be implemented with the help of various types of mechanical turbulating inserts, or the implementation of forced low-frequency pulsations of the fluid flow. When using long evaporation channels, low-frequency deformed waves of high amplitude develop, which make the main contribution to the process of heat exchange intensification in films. The processes of heat transfer intensification by large waves are given much attention by researchers (Choudhury et al., 2023; Gourdon et al., 2015; Kostoglou et al., 2010; Malamatairis et al., 2008; Mascarenhas et al., 2013; Ruyer-Quil et al., 2005).

The amplitude of large waves is 2–3 times greater than the average thickness of the film. In addition, the speed of large waves is 1.5–2.5 times higher than the average speed of the film. As a result of the braking effect of the heat exchange surface, large waves are deformed and further destroyed, changing the nature of the wave movement to the movement of a wedge-shaped thickening in the form of a shaft, the front part of which undergoes rotational movement, forming a central vortex. Under these conditions, during the passage of the shaft of a large wave, the superheated liquid of the wall part of the film is captured by a large vortex and transferred to the wave crest, where it gives heat to the vapor flow in the mode of self-evaporation. After the passage of a large wave, the wall part of the film becomes cooled due to the replacement of superheated liquid with liquid from the outer part of the film. Before the arrival of the next large wave, the liquid warms up, changing the temperature gradients on the wall and the interfacial surface, due to which the heat flux densities on the wall and the interfacial surface are different until the steady state of heat exchange occurs. The rate of heating of the film depends on the degree of turbulence by the vortex swept under a large wave. Recently, a number of algebraic ratios have been proposed for the steady turbulent motion of a film, which take into account the specifics of the development of turbulence in films (Alhousseini et al., 1998, 2000; Asbik et al., 2005; Peterson et al., 1997). A number of other turbulence models have been proposed previously, an overview of which is given in (Mascarenhas et al., 2013). A convenient model for finding an analytical expression for temperature and velocity profiles in the film is one that reflects in one dependence the presence of a wall laminar layer with a gradual transition to a turbulent core, and takes into account the rapid drop in turbulence intensity within the interfacial surface. The specified model was proposed in (Petrenko et al., 2020, 2023) and was used to analyze heat transfer in a film with a developed system of low-frequency large waves.

The aim of the present research was to theoretically and experimentally determine the influence of periodic disturbances of the liquid film surface on the intensity of heat transfer during vaporization.

Materials and methods

The object of research is heat transfer processes during forced disruption of the ordered hydrodynamic structure of a flowing liquid film. The subject of research is thermal-

hydrodynamic processes in a flowing film of liquid, which is cyclically disturbed by surface large low-frequency waves or mechanical turbulators.

Methods

The theoretical results were obtained on the basis of mathematical modeling of heat transfer processes in flowing liquid films with disturbance of its surface by large waves generated in long heat exchange pipes of film evaporators. The solution of the equation of convective thermal conductivity was carried out by an approximate method with boundary conditions corresponding to the condition of vapor formation on the interfacial surface of the film.

Physical modeling was performed on an experimental stand, on which heat exchange processes in the film were reproduced in a 9-m-long pipe with a diameter of 30 mm. The model liquid is water saturated to the boiling point with a mass liquid flux of 0.16–0.72 kg/m·sec. Heating was carried out with dry saturated steam. The measurement of the heat flow was carried out by the volumetric method based on the amount of condensate formed on the sections of the heat exchange pipe with a height of 400 mm each.

Results and discussion

Heat exchange model

According to the proposed heat transfer model, it is postulated that after the passage of a large wave, the temperature profile "sags" due to the replacement of a part of the superheated liquid with one cooled from the interphase surface, and the depth of "sags" will be determined by the power of the central vortex. The limit curve to which the temperature profile "sags" depends on the degree of turbulence of the film at the moment of passage of the central vortex, and there is either no or a small temperature gradient on the interphase surface. The process of heat transfer per cycle is divided into two stages: first, there is a temperature profile, which is established after rapid cooling of the film as a result of removal of superheated liquid from the wall layer and its replacement with liquid from the area of the interfacial surface; then the process of restoring the temperature profile due to convective thermal conductivity to the previous level during the time interval between the passage of two large waves is considered. The temperature profile for both the first and second stages is found from the convective heat conduction equation, but under different boundary and initial conditions

$$u \frac{\partial t}{\partial x} = \frac{\partial}{\partial y} (a + a_t) \frac{\partial t}{\partial y}, \quad (1)$$

where t – temperature; y, x – transverse and longitudinal coordinates; a – temperature conductivity; a_t – turbulent temperature conductivity; u – velocity of the liquid in the film.

Given that $u = u_i \left(\frac{y}{\delta} \right)^{\frac{1}{5}} = \frac{6}{5} \bar{u} \left(\frac{y}{\delta} \right)^{\frac{1}{5}} = \frac{6}{5} \bar{u} \eta^{\frac{1}{5}}$, in the dimensionless form (1) we write as

$$\frac{6\delta}{5} \bar{u}(\eta)^{1/5} \frac{\partial \theta(\xi, \eta)}{\partial \xi} = \frac{\partial}{\partial \eta} (a + a_t) \frac{\partial \theta(\xi, \eta)}{\partial \eta}, \quad (2)$$

where $\theta(\eta, \xi) = \frac{t(\eta, \xi) - t_o}{t_{cm} - t_o}$ – dimensionless temperature; t_{cm} , t_o – wall temperature and

liquid saturation, respectively; $\eta = \frac{y}{\delta}$, $\xi = \frac{x}{\delta}$ – dimensionless transverse and longitudinal coordinates; δ – film thickness; \bar{u} – the average velocity of the liquid in the film; u_t – velocity of liquid at the interphase boundary of the film.

Let's solve equation (2) using Targa's approximate method, replacing the left part of (2) with the average value

$$\int_0^1 \frac{6\delta}{5} \bar{u}(\eta)^{1/5} \frac{\partial \theta(\xi, \eta)}{\partial \xi} \partial \eta = \delta \bar{u} \frac{\partial \theta_{av}(\xi)}{\partial \xi},$$

Then from (2) we get

$$\frac{Pe}{4} \frac{\partial \theta_{av}(\xi)}{\partial \xi} = \frac{\partial}{\partial \eta} \left(1 + \frac{a_t}{a} \right) \frac{\partial \theta(\xi, \eta)}{\partial \eta}, \quad (3)$$

where $Pe = \frac{4J_v}{a}$ the Peclet number; $J_v = \frac{G}{\rho \pi d}$ – volumetric liquid flux; G – mass flow rate; ρ – density; d – pipe diameter.

Since $\frac{a_t}{a} = \frac{\nu_t}{\nu} \frac{Pr}{Pr_t}$, expression (3) takes the form

$$\frac{Pe}{4} \frac{\partial \theta_{av}(\xi)}{\partial \xi} = \frac{\partial}{\partial \eta} \left(1 + \frac{\nu_t Pr}{\nu Pr_t} \right) \frac{\partial \theta(\xi, \eta)}{\partial \eta}. \quad (4)$$

where ν_t, ν – turbulent and molecular cinematic viscosity coefficient, respectively; Pr, Pr_t – Prandtl number and turbulent Prandtl number, respectively.

Temperature profile in the film at the first stage of the wave cycle

On the interfacial surface ($\eta = 1$) after the passage of a large wave, the temperature gradient is either too small or equal to zero, $\frac{\partial \theta}{\partial \eta} = 0$, and the temperature corresponds to the saturation temperature. Under this boundary condition, the solution of (4) is a curve that determines the degree of "sags" of the temperature profile for a certain value of turbulent viscosity. In the wall region ($\eta = 0$), the liquid temperature is equal to the wall temperature, and the initial conditions are formulated as $\xi = 0$, $\theta = 0$.

The first integration of (4) from the condition that at $\eta = 1$, $\frac{\partial \theta}{\partial \eta} = 0$, gives

$$\frac{Pe}{4} \frac{\partial \theta_{av}(\xi)}{\partial \xi} (\eta - 1) = \left(1 + \frac{\nu_t Pr}{\nu Pr_t} \right) \frac{\partial \theta(\xi, \eta)}{\partial \eta}. \quad (5)$$

The function of turbulence in the film, which most adequately reflects the dependence of the turbulent viscosity distribution in the cross section of the film, will be given as (Petrenko et al., 2020).

$$\frac{v_t}{\nu} = \varepsilon_m \eta^2 (1 - \eta^2), \quad (6)$$

where ε_m is the maximum value of the turbulence function in the film at the top of the deformed parabola (correlation parameter).

Taking $Pr_t = 1$, the general integral (5) taking into account (6) will be written as

$$\theta(\eta, \xi) = \frac{Pe}{4} \frac{\partial \theta_{av}(\xi)}{\partial \xi} \left[\int \frac{\eta d\eta}{(1 + \varepsilon_m (\eta^2 - \eta^4)) Pr} - \int \frac{d\eta}{(1 + \varepsilon_m (\eta^2 - \eta^4)) Pr} \right]. \quad (7)$$

Integrating (7) under the boundary conditions $\eta = 0, \theta = 1$, gives

$$\theta(\eta, \xi) = 1 + \frac{Pe}{4} \frac{\partial \theta_{av}(\xi)}{\partial \xi} \left[\frac{1}{H} \operatorname{atanh} \left(\frac{P(2\eta^2 - 1)}{H} \right) + \frac{\sqrt{2}H}{(4+P)A} \operatorname{atanh} \left(\frac{\sqrt{2}P}{A} \eta \right) - \right. \\ \left. - \frac{\sqrt{2}H}{(4+P)B} \operatorname{atanh} \left(\frac{\sqrt{2}P}{B} \eta \right) + \frac{1}{H} \operatorname{atanh} \left(\frac{P}{H} \right) \right], \quad (8)$$

where $P = \varepsilon_m Pr$; $H = \sqrt{4P + P^2}$; $A = \sqrt{P^2 - PH}$; $B = \sqrt{P^2 + PH}$.

The unknown derivative $\frac{\partial \theta_{av}(\xi)}{\partial \xi}$ is found from the relation for the average integral temperature of the film obtained from expression (8) under the initial condition $\xi = 0$, $\theta = 0$. Taking into account the fullness of the velocity profile for the turbulent film, with a certain approximation regarding the average temperature, we assume that

$$\theta_{cp}(\xi) = \int_0^1 \theta(\eta, \xi) \frac{u(\eta)}{\bar{u}} d\eta \approx \int_0^1 \theta(\eta, \xi) d\eta. \quad (9)$$

Integrating (8) gives:

$$\theta_{cp} = 1 + \frac{\partial \theta_{cp}}{\partial \xi} \frac{Pe}{4} \left[\frac{3\sqrt{2}P}{2H} \left(\frac{1}{A} \operatorname{atanh} \left(\frac{P\sqrt{2}}{A} \right) - \frac{1}{B} \operatorname{atanh} \left(\frac{P\sqrt{2}}{B} \right) \right) - \right. \\ \left. - \frac{\sqrt{2}}{2} \left(\frac{1}{A} \operatorname{atanh} \left(\frac{P\sqrt{2}}{A} \right) + \frac{1}{B} \operatorname{atanh} \left(\frac{P\sqrt{2}}{B} \right) \right) + \right. \\ \left. + \frac{2}{H} \ln \left(\frac{B}{C} \right) + \frac{2}{H} \left(\frac{P}{H} \right) \right], \quad (10)$$

where $C = \sqrt{PH - P^2}$.

Marking the expression in square brackets for S

$$S = \frac{Pe}{4} \left[\frac{3\sqrt{2}P}{2H} \left(\frac{1}{A} \operatorname{atanh} \left(\frac{P\sqrt{2}}{A} \right) - \frac{1}{B} \operatorname{atanh} \left(\frac{P\sqrt{2}}{B} \right) \right) - \frac{\sqrt{2}}{2} \left(\frac{1}{A} \left(\frac{P\sqrt{2}}{A} \right) + \frac{1}{B} \operatorname{atanh} \left(\frac{P\sqrt{2}}{B} \right) \right) \right] + \left[\frac{2}{H} \ln \left(\frac{B}{C} \right) + \frac{2}{H} \operatorname{atanh} \left(\frac{P}{H} \right) \right] \quad (11)$$

we obtain the differential equation $\theta_{cp} = 1 + S \frac{d\theta_{cp}}{d\xi}$, the solution of which, under the initial condition $\xi = 0; \theta = 0$, is an expression

$$\theta_{cp} = \left[1 - \exp \left(\frac{\xi}{S} \right) \right]. \quad (12)$$

It is substituted the derivative of (12) $\frac{d\theta_{cp}}{d\xi} = -\frac{1}{S} \exp \left(\frac{\xi}{S} \right)$ into (8)

$$\theta(\eta, \xi_m) = 1 - \frac{Pe}{4} \exp \left(\frac{\xi_m}{S} \right) \left[\frac{1}{H} \operatorname{atanh} \left(\frac{P(2\eta^2 - 1)}{H} \right) + \frac{\sqrt{2}H}{(4+P)A} \operatorname{atanh} \left(\frac{\sqrt{2}P}{A} \eta \right) - \frac{\sqrt{2}H}{(4+P)B} \operatorname{atanh} \left(\frac{\sqrt{2}P}{B} \eta \right) + \frac{1}{H} \operatorname{atanh} \left(\frac{P}{H} \right) \right]. \quad (13)$$

The obtained temperature profile (13) is valid only for one curve for a specific value of the longitudinal coordinate $\xi = \xi_m$, under which the condition is fulfilled $\frac{\partial \theta}{\partial \eta} = 0$. Formally, the depth of "sags" of the temperature profile (13) is determined by the parameter ξ_m , which is proportional to the degree of turbulence of the film at the moment of passage of the central vortex, Figure 1.

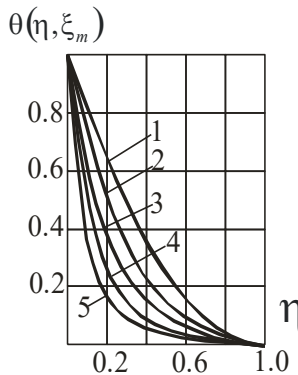


Figure 1. Limit temperature curve (13).
 1 – $\varepsilon_m = 0.01$; 2 – 3; 3 – 10; 4 – 30; 5 – 80.

The coordinate ξ_m , at which $\frac{\partial \theta}{\partial \eta} = 0$, is found from the condition $\eta = 1$, $\theta(1, \xi_m) = 0$ from equation (13)

$$\xi_m = S \ln \left(\frac{4S}{PeK} \right), \quad (14)$$

where $K = \left[\begin{array}{l} \frac{2}{H} \operatorname{atanh} \left(\frac{P}{H} \right) + \frac{\sqrt{2}H}{(4+P)A} \operatorname{atanh} \left(\frac{\sqrt{2}P}{A} \right) - \\ - \frac{\sqrt{2}H}{(4+P)B} \operatorname{atanh} \left(\frac{\sqrt{2}P}{B} \right) \end{array} \right]$.

Temperature profiles in the film at the stage of equalization of the temperature field in the second stage of the wave cycle

In the region $\xi \geq \xi_m$, the temperature of the interfacial surface of the film due to evaporation remains constant along the longitudinal coordinate ξ , and the temperature profile develops from the limit curve (13) to a straight line (in the flat setting) at $\xi \rightarrow \infty$. Since the temperature of the interfacial surface in the region $\xi \geq \xi_m$ remains constant, we will determine the temperature field from equation (4) under boundary conditions

$$\eta = 0, \theta = 1; \quad \eta = 1, \theta = 0. \quad (15)$$

The initial condition is the limiting curve (13), with $\xi = \xi_m$.

Double integration (4) with the turbulent viscosity distribution function (6) and boundary conditions (15) gives

$$\begin{aligned} \theta(\eta, \xi) = & \frac{Pe}{4} \frac{\partial \theta_{cp}}{\partial \xi} \left[\frac{1}{H} \operatorname{atanh} \left(\frac{2P\eta^2 - P}{H} \right) \right] + \\ & + \left[\frac{-H\sqrt{2}}{(4+P)A} \operatorname{atanh} \left(\frac{P\sqrt{2}}{A} \eta \right) + \frac{H\sqrt{2}}{(4+P)B} \operatorname{atanh} \left(\frac{P\sqrt{2}}{B} \eta \right) \right] \times \\ & \times \frac{\frac{-Pe}{2H} \frac{\partial \theta_{cp}}{\partial \xi} \operatorname{atanh} \left(\frac{P}{H} \right) - 1}{\frac{H}{4+P} \left(\frac{\sqrt{2}}{B} \operatorname{atanh} \left(\frac{P\sqrt{2}}{B} \right) - \frac{\sqrt{2}}{A} \operatorname{atanh} \left(\frac{P\sqrt{2}}{A} \right) \right)} + \frac{Pe}{4H} \frac{\partial \theta_{cp}}{\partial \xi} \operatorname{atanh} \left(\frac{P}{H} \right) + 1. \end{aligned} \quad (16)$$

It is found the unknown derivative $\frac{\partial \theta_{av}(\xi)}{\partial \xi}$ from (16) using the initial condition (13).

Let's substitute in (16) the average value of the temperature, which will be found by integration $\theta_{cp}(\xi) = \int_0^1 \theta(\eta, \xi) \frac{u(\eta)}{\bar{u}} d\eta \approx \int_0^1 \theta(\xi, \eta) d\eta$

$$\theta_{cp} = W \frac{\partial \theta_{cp}}{\partial \xi} + Z, \quad (17)$$

where

$$W = \frac{Pe\sqrt{2}}{N} \left\{ \left[\left(\frac{1}{8c} - \frac{P}{8cH} \right) \operatorname{atanh} \left(\frac{P\sqrt{2}}{c} \right) \left(\operatorname{atanh} \left(\frac{P\sqrt{2}}{A} \right) B - \operatorname{atanh} \left(\frac{P\sqrt{2}}{B} \right) A \right) \right] + \left[\frac{1}{8B} + \frac{P}{8BH} \right] \operatorname{atanh} \left(\frac{P\sqrt{2}}{B} \right) \left(\operatorname{atanh} \left(\frac{P\sqrt{2}}{A} \right) B - \operatorname{atanh} \left(\frac{P\sqrt{2}}{B} \right) A \right) + \frac{AB}{8PH} \operatorname{atanh} \left(\frac{P}{H} \right) \ln \left[\frac{(A^2 - 2P^2)B^2}{(B^2 - 2P^2)A^2} \right] \right\}, \quad (18)$$

$$Z = \frac{\sqrt{2}AB}{4NP} \ln \left[\frac{(A^2 - 2P^2)B^2}{(B^2 - 2P^2)A^2} \right], \quad (19)$$

$$c = \sqrt{P^2 - PH}; \quad N = A \operatorname{atanh} \left(\frac{P\sqrt{2}}{B} \right) - B \operatorname{atanh} \left(\frac{P\sqrt{2}}{A} \right).$$

The solution of (17) is

$$\theta_{cp} = Z + c_3 \exp \left(\frac{\xi}{W} \right). \quad (20)$$

The constant of integration c_3 is found from the initial condition (13), from which we determine the average value $\theta_{cp,m} = \int_0^1 \theta(\eta, \xi_m) d\eta$ by integration when $\xi = \xi_m$.

$$\theta_{cp,m} = 1 + \left[\frac{Pe \exp\left(\frac{\xi_m}{S}\right)}{S(P+4)} \right] \times \left[\frac{H\sqrt{2}}{4} \left(\frac{1}{B} \operatorname{atanh}\left(\frac{P\sqrt{2}}{B}\right) - \frac{1}{A} \operatorname{atanh}\left(\frac{P\sqrt{2}}{A}\right) \right) + \sqrt{2} \operatorname{atanh}\left(\frac{P\sqrt{2}}{B}\right) \right] \times \left[\frac{1}{2B} + \frac{P}{8B} + \frac{P}{2HB} + \frac{P^2}{8HB} \right] + \left(\frac{H}{8P} \right) \left[\ln \left(\frac{(B^2 - 2P^2)A^2}{(A^2 - 2P^2)B^2} \right) \right] + \sqrt{2} \operatorname{atanh}\left(\frac{P\sqrt{2}}{A}\right) \left[\frac{1}{2A} + \frac{P}{8A} - \frac{P}{2Ha} - \frac{P^2}{8HA} \right] - \operatorname{atanh}\left(\frac{P}{H}\right) \left(\frac{2}{H} + \frac{P}{2H} \right) \right] \quad (21)$$

Then (20) will be rewritten as $\theta_{cp,m} = Z + c_3 \exp\left(\frac{\xi_m}{W}\right)$, where is the constant of integration

$$c_3 = (\theta_{cp,m} - Z) \exp\left(\frac{-\xi_m}{W}\right).$$

By substituting c_3 in (20), we get the average temperature in the film along the coordinate ξ

$$\theta_{cp}(\xi) = Z + (\theta_{cp,m} - Z) \exp\left(\frac{\xi - \xi_m}{W}\right). \quad (22)$$

Derivative of θ_{cp} by ξ

$$\frac{\partial \theta_{cp}}{\partial \xi} = \left(\frac{\theta_{cp,m} - Z}{W} \right) \exp\left(\frac{\xi - \xi_m}{W}\right). \quad (23)$$

Substitute the resulting derivative into (16) and obtain the final expression for the temperature field in the film in the region $\xi \geq \xi_m$

$$\theta(\eta, \xi) = \frac{Pe}{4H} \left(\frac{\theta_{cp,m} - Z}{W} \right) \exp\left(\frac{\xi - \xi_m}{W}\right) \operatorname{atanh}\left(\frac{2P\eta^2 - P}{H}\right) + \left(\frac{H\sqrt{2}}{4+P} \left(\frac{1}{B} \operatorname{atanh}\left(\frac{P\sqrt{2}}{B}\right)\eta - \frac{1}{A} \operatorname{atanh}\left(\frac{P\sqrt{2}}{A}\right)\eta \right) \right) \times \left[\frac{-Pe}{2H} \left(\frac{\theta_{cp,m} - Z}{W} \right) \exp\left(\frac{\xi - \xi_m}{W}\right) \operatorname{atanh}\left(\frac{P}{H}\right) - 1 \right] + \frac{Pe}{4H} \left[\left(\frac{\theta_{cp,m} - Z}{W} \right) \exp\left(\frac{\xi - \xi_m}{W}\right) \operatorname{atanh}\left(\frac{P}{H}\right) + 1 \right] \times \left[\frac{H\sqrt{2}}{(4+P)} \left[\frac{1}{B} \operatorname{atanh}\left(\frac{P\sqrt{2}}{B}\right) - \frac{1}{A} \operatorname{atanh}\left(\frac{P\sqrt{2}}{A}\right) \right] \right] \quad (24)$$

The graphic interpretation of the development of the temperature field according to (24) at different distances from ξ_m and with different degrees of film turbulence ε_m is shown in Figure 2.

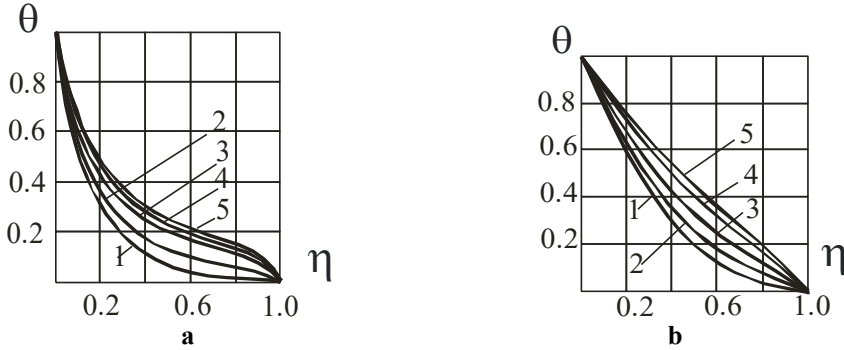


Figure 2. Leveling of the temperature profile after perturbation of the film by a large wave at

$$Pe = 7000; Pr = 2.$$

- a. $\varepsilon_m = 20; \xi_m = 51.9; 1 - \xi = \xi_m; 2 - \xi = 70; 3 - 110; 4 - 160; 5 - 800.$
- b. $\varepsilon_m = 2; \xi_m = 187.1; 1 - \xi = \xi_m; 2 - \xi = 220; 3 - 280; 4 - 400; 5 - 800.$

Heat flux on the heat exchange surface and heat transfer coefficient

The temperature gradient on the wall $\left. \frac{d\theta(\eta, \xi)}{d\eta} \right|_{\eta=0}$ changes from the maximum at the time of passage of the vortex of a large wave at $\xi = \xi_m$ to the minimum asymptotic at $\xi = \infty$. The derivative of (24) on the wall is equal to

$$\left. \frac{d\theta(\eta, \xi)}{d\eta} \right|_{\eta=0} = \frac{2HP}{4+P} \left(\frac{1}{B^2} - \frac{1}{A_2} \right) \frac{-Pe \left(\frac{\theta_{cp,m} - Z}{W} \right) \exp \left(\frac{\xi - \xi_m}{W} \right) \operatorname{atanh} \left(\frac{P}{H} \right) - 1}{\frac{H\sqrt{2}}{4+P} \left[\frac{1}{B} \operatorname{atanh} \left(\frac{P\sqrt{2}}{B} \right) - \frac{1}{A} \operatorname{atanh} \left(\frac{P\sqrt{2}}{A} \right) \right]}. \quad (25)$$

From the expression $q(\xi)_{\eta=0} = -\lambda \frac{t_w - t_{sat}}{\delta} \left. \frac{d\theta}{d\eta} \right|_{\eta=0}$, we find the heat flux density on the wall

$$q(\xi)_{\eta=0} = -\lambda \frac{t_w - t_{sat}}{\delta} \frac{2HP}{4+P} \left(\frac{1}{B^2} - \frac{1}{A_2} \right) \frac{-Pe \left(\frac{\theta_{cp,m} - Z}{W} \right) \exp \left(\frac{\xi - \xi_m}{W} \right) \operatorname{atanh} \left(\frac{P}{H} \right) - 1}{\frac{H\sqrt{2}}{4+P} \left[\frac{1}{B} \operatorname{atanh} \left(\frac{P\sqrt{2}}{B} \right) - \frac{1}{A} \operatorname{atanh} \left(\frac{P\sqrt{2}}{A} \right) \right]}, \quad (26)$$

where λ – heat conduction of liquid.

The average heat flux on the wall in the interval between the passage of two large waves

$$q_{cp} = \frac{1}{\xi_v - \xi_m} \int_{\xi_m}^{\xi_v} q(\xi)_{\eta=0} d\xi = -\frac{\lambda}{\delta} \frac{t_w - t_{sat}}{\xi_v - \xi_m} \left[\frac{P}{ABH} \frac{\sqrt{2}(A^2 - B^2)}{B \cdot \operatorname{atanh}\left(\frac{P\sqrt{2}}{A}\right) - A \cdot \operatorname{atanh}\left(\frac{P\sqrt{2}}{B}\right)} \right] \times$$

$$\times \left[\frac{Pe}{2} \operatorname{atanh}\left(\frac{P}{H}\right) (\theta_{cp,m} - Z) \left(\exp\left(\frac{\xi_v - \xi_m}{W}\right) - 1 \right) + H(\xi_v - \xi_m) \right] \quad (27)$$

Heat transfer coefficient

$$\alpha = \frac{q_{cp}}{t_w - t_{sat}} = -\frac{\lambda}{\delta} \frac{1}{\xi_v - \xi_m} \left[\frac{P}{ABH} \frac{\sqrt{2}(A^2 - B^2)}{B \cdot \operatorname{atanh}\left(\frac{P\sqrt{2}}{A}\right) - A \cdot \operatorname{atanh}\left(\frac{P\sqrt{2}}{B}\right)} \right] \times$$

$$\times \left[\frac{Pe}{2} \operatorname{atanh}\left(\frac{P}{H}\right) (\theta_{cp,m} - Z) \left(\exp\left(\frac{\xi_v - \xi_m}{W}\right) - 1 \right) + H(\xi_v - \xi_m) \right] \quad (28)$$

The thickness of the film, which is included in expression (28), is found from the equation of motion of a freely flowing film using the turbulence function (6).

$$\frac{g\delta^2}{\nu} (1 - \eta) = \left[1 + \varepsilon_m (\eta^2 - \eta^4) \right] \frac{du}{d\eta} \quad (29)$$

where g – acceleration of gravity.

The solution of (29) under the boundary condition $y = 0, u = 0$ is the velocity profile

$$u = \left(\frac{g\delta^2}{\nu} \right) \frac{\sqrt{2}h}{(4 + \varepsilon_m)} \left[\frac{1}{b} \operatorname{atanh}\left(\frac{\sqrt{2}\varepsilon_m}{b} \eta\right) - \frac{1}{r} \operatorname{atanh}\left(\frac{\sqrt{2}\varepsilon_m}{r} \eta\right) \right] -$$

$$- \frac{g\delta^2}{\nu h} \left[\operatorname{atanh}\left(\frac{\varepsilon_m(2\eta^2 - 1)}{h}\right) + \operatorname{atanh}\left(\frac{\varepsilon_m}{h}\right) \right]$$

Average speed in the film

$$\bar{u} = \left(\frac{g\delta^2}{\nu} \right) \frac{\sqrt{2}h}{(4 + \varepsilon_m)} \left[n - \frac{\sqrt{2}}{4\varepsilon_m} \ln\left(\frac{r^2 - 2\varepsilon_m^2}{b^2 - 2\varepsilon_m^2}\right) - \frac{\sqrt{2}}{2\varepsilon_m} \ln\left(\frac{b}{r}\right) \right] -$$

$$- \frac{g\delta^2}{\nu h} \left[2 \operatorname{atanh}\left(\frac{\varepsilon_m}{h}\right) - \frac{\sqrt{2}h}{2} \left(\frac{1}{b} \operatorname{atanh}\left(\frac{\sqrt{2}\varepsilon_m}{b}\right) + \frac{1}{r} \operatorname{atanh}\left(\frac{\sqrt{2}\varepsilon_m}{r}\right) \right) - \frac{\sqrt{2}\varepsilon_m}{2} n \right]$$

Where do we get the thickness of the film, given that the mass liquid flux $J = \rho \bar{u} \delta$,

$$\delta = \sqrt[3]{\frac{J \nu h}{\rho g (Dh - R)}} \quad , \quad (30)$$

where $R = \left[2 \operatorname{atanh} \left(\frac{\varepsilon_m}{h} \right) - \frac{\sqrt{2} h}{2} \left(\frac{1}{b} \operatorname{atanh} \left(\frac{\sqrt{2} \varepsilon_m}{b} \right) + \frac{1}{r} \operatorname{atanh} \left(\frac{\sqrt{2} \varepsilon_m}{r} \right) \right) - \frac{\sqrt{2} \varepsilon_m}{2} n \right]$,

$$D = \frac{\sqrt{2} h}{(4 + \varepsilon_m)} \left[n - \frac{\sqrt{2}}{4 \varepsilon_m} \ln \left(\frac{r^2 - 2 \varepsilon_m^2}{b^2 - 2 \varepsilon_m^2} \right) - \frac{\sqrt{2}}{2 \varepsilon_m} \ln \left(\frac{b}{r} \right) \right]$$

$$h = \sqrt{4 \varepsilon_m + \varepsilon_m^2} \quad , \quad r = \sqrt{\varepsilon_m^2 - \varepsilon_m h} \quad , \quad b = \sqrt{\varepsilon_m^2 + \varepsilon_m h} \quad ;$$

$$n = \left[\frac{1}{b} \operatorname{atanh} \left(\frac{\sqrt{2} \varepsilon_m}{b} \right) - \frac{1}{r} \operatorname{atanh} \left(\frac{\sqrt{2} \varepsilon_m}{r} \right) \right]$$

The intensity of heat transfer, as can be seen from (28), is inversely proportional to the distance $\xi_v - \xi_m$, which is interpreted as the dimensionless distance between the crests of large waves, in the case of a flow with a developed wave structure, or the distance between mechanical turbulators, in the case of their application. The results of calculating the heat transfer coefficient according to the ratio (28) depending on the distance between the heat exchange intensifiers L at the value of the parameter $\varepsilon_m = 10.4$ are shown in Figure 3.

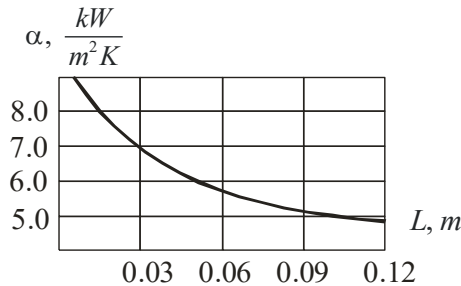


Figure 3. Dependence $\alpha = f(L)$ according to relation (28) at $\varepsilon_m = 10.4$, $J = 0.3 \frac{kg}{m \cdot sec}$

The degree of film turbulence is determined by the power of the vortex of a large wave, in the case of a flow with a developed wave structure, or the height of a mechanical turbulator, in the case of their application. The distance between the crests of large waves for pipes with a diameter of 25–35 mm is about 0.12 m. The results of calculating the heat transfer coefficient according to the ratio (28) depending on the degree of film turbulence are shown in Figure 4.

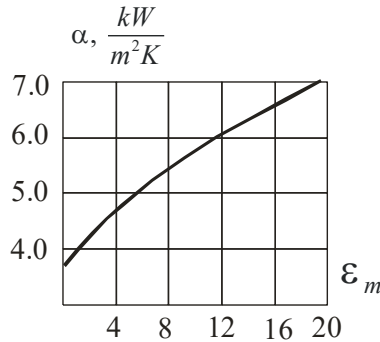


Figure 4. Dependence according to relation (28) at $L = 0.12 \text{ m}$, $J = 0.3 \frac{\text{kg}}{\text{m} \cdot \text{sec}}$

Thus, the obtained ratios adequately reflect the dependence of the heat transfer coefficient to the flowing liquid films during vaporization with heat exchange intensifiers on the turbulence parameters. The data of experimental studies of heat transfer to flowing films of water in the mode of evaporation from a free surface under atmospheric pressure in a pipe 9 m long with a diameter of 30 mm, where a developed structure of large waves with a length of 0.12 m is formed at a distance of 2 m, correspond to the theoretical results obtained, calculated by relation (28). A comparison of experimental and calculated results on the intensity of heat exchange established that their correspondence takes place under the condition of dependence ϵ_m on the mass liquid flux J in the form:

$$\epsilon_m = 0.634 - 4.348J + 158.175J^2 + 394.98J^3 - 2844J^4 + 4823J^5 - 2645J^6 \quad (31).$$

Note that the obtained dependence (31) cannot be considered as a turbulence parameter, since it was obtained as a correlation parameter of heat transfer data, and not because of direct measurements of turbulent pulsations. Graphical interpretation of dependence (31) is shown in Figure 5.

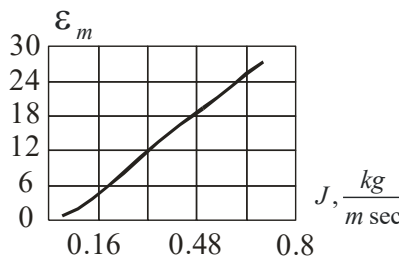


Figure 5. Dependence $\epsilon_m = f(J)$ according to ratio (31)

As can be seen from the graph in fig. 5, in the turbulent region with a mass liquid flux greater than 0.16 kg/m sec, which corresponds to a Reynolds number of 2200, the dependence $\epsilon_m = f(J)$ is almost linear. A comparison of the experimental results with those calculated using the ratios (28, 31) is shown in Figure 6.

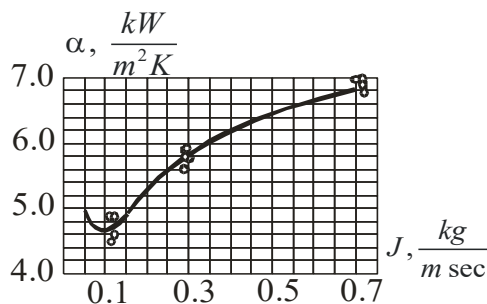


Figure 6. Dependence $\alpha = f(J)$ for water at atmospheric pressure in the region of the developed structure of large waves in the mode of evaporation from the interfacial surface in a pipe with a diameter of 30 mm. Line – calculation according to (28, 31).

Conclusions

1. An approximate analytical solution of the convective heat conduction equation for a turbulent film flowing down a vertical heat exchange surface was performed, and an analytical expression for the temperature field in the film, which develops in the transverse and longitudinal directions, was obtained.
2. The developed mathematical model of heat transfer in a film of liquid flowing down a vertical surface, in which the cyclic mixing of the film by low-frequency waves of large amplitude is considered, allows modeling the processes of heat transfer in a film of liquid during vaporization under the condition of periodic forced disruption of its structure.
3. The ratios obtained because of the approximate solution of the equations of convective heat conduction reflect the regularities of heat transfer in flowing films in the regime of both its periodic mixing by large waves and the system of passive ring intensifiers located with different densities.

References

- Alhousseini A.A., Chen J.C. (2000), Transport phenomena in turbulent falling film, *Industrial Engineering Chemistry Research*, 39, pp. 2091–2100, <https://doi.org/10.1021/ie9906013>
- Alhousseini A.A., Tuzla K., Chen J.C. (1998), Falling film evaporation of single component liquid, *International Journal of Heat and Mass Transfer*, 41, pp. 1623–1632, [https://doi.org/10.1016/S0017-9310\(97\)00308-6](https://doi.org/10.1016/S0017-9310(97)00308-6)
- Asbik M., Ansari O., Zeghmati B. (2005), Numerical study of boundary layer transition in falling film evaporation on horizontal elliptical cylinder, *Numerical Heat Transfer*, 48, pp. 645–669, <https://doi.org/10.1080/10407780590967467>
- Choudhury A., Samanta A. (2023), Thermocapillary instability for a shear-imposed falling film, *Physical Review Fluids*, 8(9), 94006, <https://doi.org/10.1103/PhysRevFluids.8.094006>
- Gourdon M., Karlsson E., Innings A., Vamling L. (2015), Heat transfer for falling film evaporation of industrially relevant fluids up to very high Prandtl numbers, *Heat and Mass Transfer*, 52(2), pp. 379–391, <https://doi.org/10.1007/s00231-015-1556-9>

- Kostoglou M., Samaras K., Karapantsios T.D. (2010), Large wave characteristics and their downstream evolution at high Reynolds number falling film, *American Institute of Chemical Engineers Journal*, 56(1), pp. 11–23, <https://doi.org/10.1002/aic.11992>
- Malamatairis N.A., Balakotaiah V. (2008), Flow structure underneath the large amplitude waves of a vertically falling film, *American Institute of Chemical Engineers Journal*, 54(7), pp. 1725–1740, <https://doi.org/10.1002/aic.11506>
- Mascarenhas N., Mudawar J. (2013), Investigation of eddy diffusivity and heat transfer coefficient for free-falling turbulent liquid films subjected to sensible heating, *International Journal of Heat and Mass Transfer*, 64, pp. 647–668, <https://doi.org/10.1016/j.ijheatmasstransfer.2013.04.061>
- Mascarenhas N., Mudawar J. (2013), Study of influential waves on heat transfer in turbulent falling films, *International Journal of Heat and Mass Transfer*, 67, pp. 1106–1121, <https://doi.org/10.1016/j.ijheatmasstransfer.2013.08.100>
- Peterson P.F., Schrock V.E., Kuhn S.Z. (1997), Recent experiments laminar and turbulent film heat transfer in vertical tubes, *Nuclear Engineering and Design*, 175, pp. 157–166, [https://doi.org/10.1016/S0029-5493\(97\)00171-4](https://doi.org/10.1016/S0029-5493(97)00171-4)
- Petrenko V., Pryadko M., Ryabchuk O. (2020), Modeling heat transfer in down flowing annular weakly turbulent vapor-liquid flows during evaporation, *Ukrainian Food Journal*, 9(4), pp. 901–916, <https://doi.org/10.24263/2304-974X-2020-9-4-14>
- Petrenko V., Pylypenko O., Ryabchuk O., Nalyvaiko M. (2023), Determining to parameters of demarcation of heat exchange model in the film during vaporization, *Ukrainian Food Journal*, 12(1), pp. 113–129, <https://doi.org/10.24263/2304-974X-2023-12-1-9>
- Ruyer-Quil C., Manneville P. (2005), On the speed of solitary waves running down a vertical wall, *Journal of Fluid Mechanics*, 531, pp. 181–190, <https://doi.org/10.1017/S0022112005003885>

Cite:

UFJ Style

Petrenko V., Ardashev V., Maksymenko D., Pustovoi O. (2024), Modeling of heat transfer processes by periodic perturbation of freely flowing liquid film flowing along vertical surface with large-amplitude waves, *Ukrainian Food Journal*, 13(2), pp. 351–365, <https://doi.org/10.24263/2304-974X-2024-13-2-11>

APA Style

Petrenko, V., Ardashev, V., Maksymenko, D., & Pustovoi, O. (2024). Modeling of heat transfer processes by periodic perturbation of freely flowing liquid film flowing along vertical surface with large-amplitude waves. *Ukrainian Food Journal*, 13(2), 351–365. <https://doi.org/10.24263/2304-974X-2024-13-2-11>

Change of crystallization process attributes in a vacuum pan of automation systems

Viktor Sidletskyi, Oleksandr Kukhar

National University of Food Technologies, Kyiv, Ukraine

Abstract

Keywords:

Sugar
Crystallization
Vacuum pan
Automation

Article history:

Received
10.11.2023
Received in
revised form
27.05.2024
Accepted
2.07.2024

Corresponding author:

Viktor Sidletskyi
E-mail:
vmsidletskyi@
gmail.com

DOI:

10.24263/2304-
974X-2024-13-2-
12

Introduction. The process of sugar crystallization is complex and non-linear, necessitating automatic control and management. However, the lack of instruments for directly measuring solution supersaturation and crystal growth highlights the need for improvements in the control system.

Materials and methods. The automation system for the process of sugar crystallization in a vacuum apparatus consists of sensors, converters of actuators, regulatory bodies, a microprocessor controller and an operator station with a SCADA program. The automation system algorithms are implemented in software in the controller and operator station.

Results and Discussion. The amount of initial syrup in the vacuum apparatus significantly affects the dry substance content in the massecuite. A high dry substance content ensures high-quality massecuite and promotes efficient crystallization. The optimal initial syrup concentration for achieving the standard dry matter content in massecuite 92% is 33%, but it can vary between 25% and 35%. An increase in the initial syrup concentration raises the average temperature of the massecuite during crystallization, which can negatively impact the final product quality. Therefore, temperature control by adjusting the initial syrup amount is crucial for optimal crystallization and producing a high-quality product.

The deformation gradient, constructed based on dry substance content and temperature parameters, reflects changes in the crystallization process. These parameters directly influence system properties, which is vital for optimizing the vacuum apparatus process. The obtained surfaces with first-rank strain tensors at 25% and 35% initial syrup values indicate changes in the strain gradient during crystallization. Key aspects such as volume change, strain tensor divergence, velocity, and acceleration are essential for calculating and analyzing the gain, time constant, and delay time in the vacuum sugar crystallization process.

Conclusions. Attributes of the crystallization process such as the amplification factor, time constant, and delay time are crucial for configuring and enhancing automated system operations, as precise calculations allow for improving control in automation systems.

Introduction

The peculiarity of the crystallization process lies in maintaining the necessary level of supersaturation of the solution, which ensures the formation and growth of crystals (Barrett et al., 2010). The supersaturation of the solution along the crystallizer determines its efficiency and requires a detailed mathematical model for control (Mazaeda et al., 2012). Due to the complexity of the process and the lack of reliable devices for direct measurement (Hassani et al., 2001), understanding the kinetics of crystal nucleation and growth, including physical mechanisms like aggregation, is crucial (Eggleston et al., 2011). Consequently, sugar crystallization is a non-linear and unstable process where key parameters such as mother liquor purity and supersaturation cannot be measured by existing sensors (Meng et al., 2019).

Studies have shown that impurities in the solution and massecuite suppress the crystallization process by specific mechanisms of inclusion on different faces of the growing crystal. These mechanisms include adsorption on the crystal surface, inclusion of liquid impurities, and co-crystallization (Azevedo et al., 1989, Schlumbach et al., 2017). A characteristic feature of the crystallization process in a vacuum apparatus is the interaction between continuous and periodic processes (Cutz et al., 2014). The main feature is that sugar crystallization is carried out in a mode that requires precise control of temperature, pressure, and steam flow, with constant adjustment in the control system (Garcia et al., 2002; Ibis, 2024; Zhang et al., 2020). This process involves cyclic heating and cooling, which affects the efficiency of evaporation (Castro et al., 2022).

Due to the lack of a reliable model describing the crystallization process, automatic crystallization control is often based on indirect measurements (Grondin-Perez et al., 2006; Lauret et al., 2000). Key parameters such as solution purity, supersaturation, crystal size, and content are difficult to measure directly (Suárez et al., 2011). The primary task of management is to monitor the supersaturation of the solution, which can be calculated through indirect measurements (Morales et al., 2023). The control process requires the use of indirect methods and mathematical models to estimate the saturation of the solution and adjust the control system settings (Bonnecaze et al., 2004; Mkwanzani et al., 2019; Prada et al., 2015).

The complexity of the crystallization process model and the adjustment of model parameters limit the possibility of its implementation in control systems (Meng et al., 2019; Villani et al., 2004). Control of the crystallization process in a vacuum apparatus has unique features due to its dynamic nature (Alvarado et al., 2024; Simoglou et al., 2005; Suárez et al., 2011). An important aspect is the effect of changing the operating mode on the transfer coefficient and the time constant of each control loop, which determine the system's response speed (Merino et al., 2018). The non-linearity of the processes means that changes in input parameters do not lead to proportional changes in output parameters, complicating the control system's operation (Zamarreño et al., 2000). The system must adapt to different phases of crystallization, fluctuations in external conditions, and wear of system components to maintain stable conditions and ensure high-quality final products (Georgieva et al., 2003; Ohara et al., 2012). This requires operators to constantly monitor and adjust settings, making the process of automating crystallization complex but necessary to achieve optimal results.

To control and analyze the quality of the crystallization process, pH measurement, dynamic light scattering, mechanical spectroscopy, and image processing methods using neural networks for automated monitoring are used (Grondin-Perez et al., 2005; Lauret et al., 2000; Meng et al., 2019). Traditional image processing methods analyze features such as

shape, color, and texture but often have poor pattern generalization capabilities. In sugar crystallization, neural networks enable the creation of high-precision models for the classification of crystal images, optimizing production processes in the food industry (Grondin-Perez et al., 2005; Lauret et al., 2000; Meng et al., 2019). Accordingly, the automated system should be flexible enough to quickly respond to changes and provide effective regulation and optimal crystallization conditions (Merino et al., 2018). Furthermore, an intuitive graphical interface is essential for allowing operators to easily interact with the system (Cutz et al., 2014; Georgieva et al., 2003; Suárez et al., 2011).

Considering the measurable and non-measurable parameters of technological processes, the hierarchical and distributed nature of production inherent in food industry processes (Santos et al., 2008; Sidletsykyi et al., 2019), and the specific process of sugar crystallization in a vacuum apparatus remain unresolved challenges. To address the challenges of processing large volumes of information, particularly for neural networks and artificial intelligence methods, data is presented in tensor form (Che et al., 2017; Karagoz et al., 2020). Tensor and finite element methods are already employed in electrodynamics, mechanics, gravitational field theory, elementary particle physics, the study of crystal properties, and differential geometry (Döhler et al., 2012; Hu et al., 2015). These methods were similarly used in developing a reliable regulator for aircraft (Kuntanapreeda, 2018). However, in that work, the construction of the regulator involved processing an already developed classical model in the state space using tensor analysis methods.

Given that the crystallization process is non-linear and non-stationary, and is part of the hierarchical and distributed sugar production chain, this work proposes investigating changes in the attributes of the crystallization process that affect the automation system settings. These attributes are derived from continuity equations and are presented in tensor form.

Materials and methods

The process of sugar crystallization was studied to enhance quality and reduce costs. Technical means are employed to control temperature and other parameters, followed by data analysis. Based on this analysis, trends in process parameter changes were calculated, enabling adjustments to automated control systems.

The research focuses on the crystallization of sugar in a vacuum apparatus, specifically the methods and approaches for controlling automated systems. The objective is to identify trends in the parameters of the crystallization process that influence the settings of automated control systems.

Equipment and technical means of the automation system

The automation system of the vacuum apparatus employs various technical means (Wilson et al., 1991), including sensors, converters, actuators, control bodies, a microprocessor controller (PLC – Programmable Logic Controller), and an operator station (AW) with SCADA (Supervisory Control and Data Acquisition) software (Behary et al., 2004). A fragment of the automation system, specifically the temperature and viscosity control circuits, is illustrated in Figure 1.

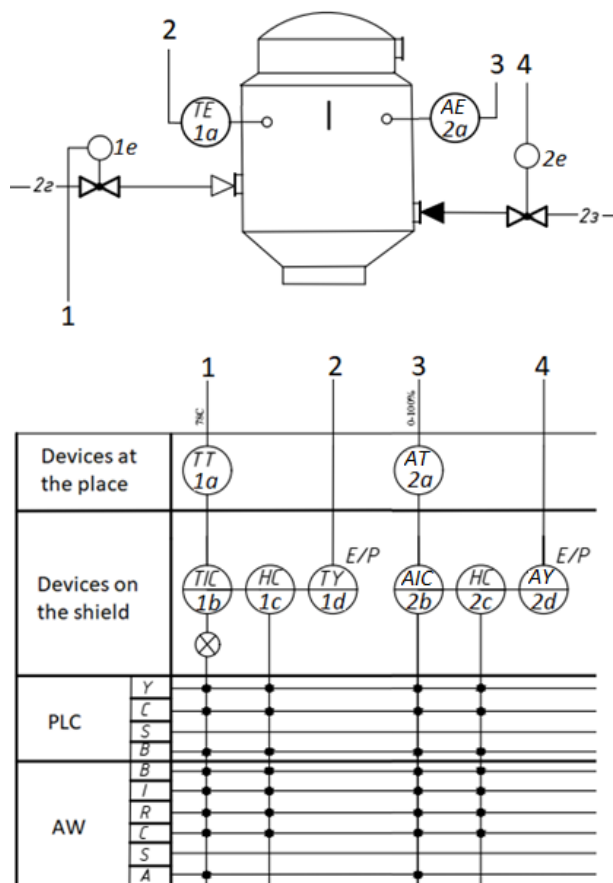


Figure 1. Fragment of vacuum apparatus automation system

TE- Temperature Element, TT – Temperature Transmitter, TIC – Temperature Indicator Controller, HC – Hand Controller, TY – Electropneumatic Converter, AE- Analytical Element, AT – Analytical Transmitter, AIC – Analytical Indicator Controller, AY – Electropneumatic Converter.

Temperature is measured using a resistance thermocouple (1a). The primary converter in device (1a), along with the converter (1a) at the site, converts the temperature value into a standardized direct current signal of 4-20 mA. The nominal supply voltage (direct current) is 24V. Since the normalizing converter is directly mounted in the measuring head of the sensor, two conductors are used to connect the converter. The standardized current signal, according to the "current loop" scheme, is sent from the normalizing converter to the secondary indicating and regulating device – the microprocessor PID regulator (1b) and to channel 4 of the controller's analog input module. The local regulator operates in manual mode when the system is started.

The control action from the analog output of the regulator, through the normally closed relay contact, or from the analog output module of the controller, through the normally open contact, is sent to the manual control unit (1c). The manual control unit is used to switch control circuits of executive devices. In automatic mode, the control action goes directly to the actuator from an external analog regulator (if manual control is necessary) or the

controller. In manual mode, the control action on the actuator is formed using the built-in potentiometer (1c). The control signal from the output (1c) is sent to the electro-pneumatic converter (1d), which converts the continuous electrical DC (Direct Current) signal in the range of 4-20mA into the corresponding output analog pneumatic signal (20-100kPa). The analog pneumatic signal is fed to the integral pneumatic positioner, which is used with the pneumatic 2-way control valve (1e) to provide an accurate valve stem position proportional to the input signal received from the control device. Information about the regulator's operation is stored in the PC memory.

The high-frequency concentration analyzer is a sensor used to measure the solids in solution and massecuite (2a). The unified current signal, following the "current loop" scheme, is supplied from the normalizing converter (2a) to the secondary indicating and regulating device (11b) and to the input of the analog input module of the PLC. The control action from the analog output of the regulator is sent to the manual control unit 2b), and then to the electro-pneumatic converter (2d), which converts a continuous electrical DC in the range from 4 to 20 mA into a corresponding output analog pneumatic signal (20 – 100 kPa). This pneumatic signal is supplied to an integral pneumatic positioner, which is used with the SAMSON 3278 (2e) pneumatic 2-way control valve to ensure precise valve stem positioning proportional to the input signal from the control device.

Processing of incoming information

Data on the operation of the crystallization process and the control system are stored in the operator station (AW) with the SCADA program. The stored data consists of a set of time-stamped parameter values (Dogbe et al., 2018).

Based on the saved data, attributes (amplification factor, time constant, delay time) of the crystallization process necessary for calculating the settings of the vacuum apparatus automation system are determined. To evaluate changes in gain, time constant, and delay time, factors such as strain gradient, volume, divergence, velocity, and acceleration are considered.

Results and discussion

Representation of the technological process of crystallization in tensor form

The importance of the initial syrup amount in the vacuum apparatus is determined by its effect on the dry substance content in massecuite. Studies have shown that to achieve the normative dry substance content in massecuite ($CP_{\text{massecuite}} = 92\%$) the optimal initial syrup value is $G_{\text{beginning}} = 33\%$ (Kotcubansky et al., 2012). High dry substance content ensures high-quality massecuite and contributes to an efficient crystallization process. Thus, controlling the initial syrup amount is crucial to obtaining a product of the required quality and avoiding issues associated with excessive massecuite viscosity, which can negatively impact crystallization. The initial syrup amount also significantly affects the dry substance content in the intercrystalline solution. An increase in the dry substance content in the solution worsens crystallization conditions due to higher sugar solution viscosity, which complicates heat transfer and raises the solution's average temperature (Kotcubansky et al., 2012). This leads to increased sucrose solubility and thermal decomposition, adversely affecting the final product. Therefore, maintaining the optimal initial syrup amount is critical for the stability

and efficiency of the crystallization process.

Temperature also varies significantly with the initial syrup amount. A higher initial syrup concentration leads to an increased average massecuite temperature during crystallization, which can negatively affect the final product quality (Kotcubansky et al., 2012). Elevated temperatures contribute to sucrose decomposition, reducing crystalline sugar yield and quality. Thus, temperature control by adjusting the initial syrup amount is vital for ensuring an optimal crystallization process and achieving a high-quality product.

Considering the above, the values $[C_{ut}, C_r, T]$, were formed based on the dry substance content in the solution and massecuite, accounting for temperature regimes for different initial syrup values, where (C_{ut}) – is the dry substance content in massecuite, (C_r) – is the dry substance content in the solution, and (T) – is the temperature. The vector $X_i = [x_{1i}, x_{2i}, x_{3i}]^T$ represents the initial syrup value, and vector $Y_i = [y_{1i}, y_{2i}, y_{3i}]^T$ represents the changed technological mode. Vector multiplication results in a surface in local spatial coordinates (Sidletskyi, 2019). Figure 2 illustrates the transition to spatial local coordinates.

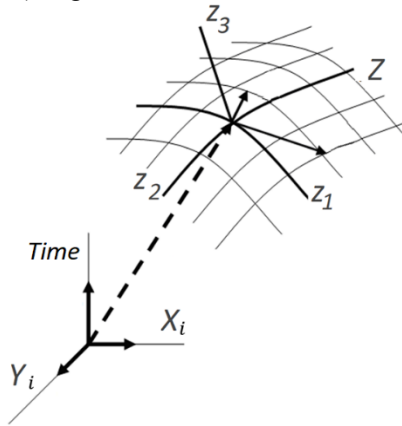


Figure 2. Transition from one technological regime to another depicted in local spatial coordinates

The deformation tensor is defined as the derivative of the displacement vector along spatial coordinates, describing how material points move relative to each other in space (Sperling et al., 2023). The strain gradient F describes changes in the position of a material point in space, encompassing linear transformations such as rotation and stretching, and is a rank 2 tensor (Baár et al., 2020; Horák et al., 2019, Sidletskyi et al., 2020):

$$F = \begin{pmatrix} \frac{\partial x}{\partial X} & \frac{\partial x}{\partial Y} & \frac{\partial x}{\partial Z} \\ \frac{\partial y}{\partial X} & \frac{\partial y}{\partial Y} & \frac{\partial y}{\partial Z} \\ \frac{\partial z}{\partial X} & \frac{\partial z}{\partial Y} & \frac{\partial z}{\partial Z} \end{pmatrix} \quad (1)$$

where x, y, z are the current coordinates of the point, and X, Y, Z are the initial coordinates.

The deformation tensor E is a symmetric tensor of the 2nd rank, describing quadratic deformations without considering rotation. It is related to internal deformations and the deformation energy of the material, defined through the deformation gradient F :

$$E = \frac{1}{2}(F^T F - I) \quad (2)$$

where I is the identity matrix.

For a general description of the energy balance (Loubser, 2004; Petrenko et al., 2020; Singh, 2019) of the thermal crystallization process, the thermal conductivity equations were used:

$$\rho c_p \left(\frac{\partial T}{\partial t} + \mathbf{v} \cdot \nabla T \right) = \nabla \cdot (k \nabla T) + Q \quad (3)$$

where:

- T is temperature, (K)
- c_p is specific heat capacity, (J/(kg·K))
- k is thermal conductivity, (W/(m·K))
- Q represents heat sources, (W)
- ρ is the density (concentration of dry substances), (kg/m³)
- ∇ denotes divergence (vector operator)
- \mathbf{v} is the velocity of the material (m/s)

To describe the mass balance (Hassani et al., 2001; Hrama et al., 2019; Pohorilyi, 2023; Suárez et al., 2011), which accounts for the change in dry substance concentration in the massecuite and solution, the equation is:

$$\frac{\partial \rho}{\partial t} + \nabla \cdot (\rho \mathbf{v}) = 0 \quad (4)$$

where:

- ρ is the density (concentration of dry substances),
- \mathbf{v} is the velocity of the material.

By combining these equations, we get:

For mass balance:

$$\frac{\partial \rho}{\partial t} + \nabla \cdot (\rho \mathbf{v}) + \rho (\nabla \cdot \mathbf{F}) = 0 \quad (5)$$

For heat balance:

$$\rho c_p \left(\frac{\partial T}{\partial t} + \mathbf{v} \cdot \nabla T \right) = \nabla \cdot (k \nabla T) + Q + \rho c_p (\nabla \cdot \mathbf{F}) T \quad (6)$$

For concentration change:

$$\frac{\partial C}{\partial t} + \nabla \cdot (C \mathbf{v}) = D \nabla^2 C + C (\nabla \cdot \mathbf{F}) \quad (7)$$

where:

- C is the concentration of dry substances, (kg/m³),
- D is the diffusion coefficient (m²/s).

The additional terms $\rho (\nabla \cdot \mathbf{F})$ i $\rho c_p (\nabla \cdot \mathbf{F}) T$ B account for volume change due to the strain gradient.

The divergence of the deformation tensor $\nabla \cdot \mathbf{F}$ characterizes the volume change in the system (Wang et al., 2020). Divergence of the deformation gradient:

$$\nabla \cdot \mathbf{F} = \frac{\partial F}{\partial x} + \frac{\partial F_{22}}{\partial y} + \frac{\partial F_{33}}{\partial z} \quad (8)$$

Considering the deformation gradient and its divergence in the continuity equations for mass and heat allows for the accurate description of mass and energy transfer processes in the crystallization system, including volume change, dry substance concentration, and temperature distribution. Therefore, the divergence of the deformation gradient $\nabla \cdot \mathbf{F}$ can be considered an indicator of changes in the internal state of the system, which can be used as an amplification factor in the automated control system.

Control system parameters as components of the deformation gradient of the technological process

In our case, the divergence of the deformation gradient shows how quickly the system parameters (solids content and temperature) change in space. This can be interpreted as a measure of the sensitivity or gain that the system applies to its internal parameters (Chowdhury et al., 2022; Pedersen et al., 2015; Tabassum et al., 2024; Tuttle et al., 2021). If the divergence of the strain gradient is large, it may indicate high concentration and temperature gradients, suggesting rapid changes in the system. Thus:

$$K_p = \nabla \cdot F \quad (9)$$

where K_p is the amplification factor determined by the divergence of the deformation gradient.

The speed and acceleration of the deformation gradient can be interpreted as dynamic characteristics of the system. Accordingly, the time constant τ is a characteristic of a dynamic system that determines how quickly the system responds to changes in the input signal. In first-order systems, this is the time it takes for the system response to reach approximately 63% of its final value after a disturbance. The delay time T_d is the time delay between the application of a disturbance to the system and the start of its response.

To determine the time constant and delay time of the system, consider a simplified model of a first-order system with a delay:

$$G(s) = \frac{Ke^{-T_d s}}{\tau s + 1} \quad (10)$$

where $G(s)$ is the transfer function of the system, K is the gain factor, τ is the time constant, and T_d is the delay time.

The rate of change of parameters (such as the concentration of dry substances or temperature) can be linked to the time constant of the system. A high rate indicates a fast response to changes, suggesting a smaller time constant.

Acceleration, representing the change in velocity over time, is related to the dynamic response characteristics of the system. However, additional aspects must be considered to determine the delay time accurately.

As previously mentioned, it is assumed that the deformation gradient F describes the change in the concentration of dry substances and temperature. Thus, the rate of change of the deformation gradient can be expressed as:

$$v = \frac{\partial F}{\partial t} \quad (11)$$

Acceleration characterizes the change in speed over time, aiding in the evaluation of the system's dynamic behavior and potential delays:

$$a = \frac{\partial^2 F}{\partial t^2} \quad (12)$$

The time constant τ can be estimated as the inverse of the system response rate:

$$\tau \approx \frac{1}{|v|} \quad (13)$$

An analysis of the system's response to a disturbance can estimate the delay time. If there is a known delay before the system begins to change parameters, this delay time can be estimated as:

$$T_d \approx \frac{1}{|a|} \quad (14)$$

Deformation gradient in local spatial coordinates

When studying the crystallization process in the vacuum apparatus, 25% initial loading and 35% final loading were used. According to (Kotcubansky et al., 2012), this approach allows for a comprehensive understanding of the crystallization process at different loading levels. This choice enables the analysis of a wide range of syrup concentrations, which helps to investigate how concentration changes affect the crystallization process. Analyzing the range of possible changes in the technological process is necessary to obtain optimal process conditions. The resulting parameter changes, from the initial to the final stage, reflect the dynamics of the process. This approach facilitates understanding how heat is effectively transferred at different syrup concentrations, which is crucial for maintaining a stable crystallization process and avoiding overheating or underheating (Kotcubansky et al., 2012, Petrenko et al., 2020, Pohorilyi, 2023). This comprehensive analysis of the crystallization process allows for the optimization of technological parameters and ensures high quality of the final product. Figures 3 and 4 present simplified graphs of the content of dry substances in massecuite, the content of dry substances in the solution, and temperature. The graphs were constructed by interpolating the points given in (Kotcubansky et al., 2012).

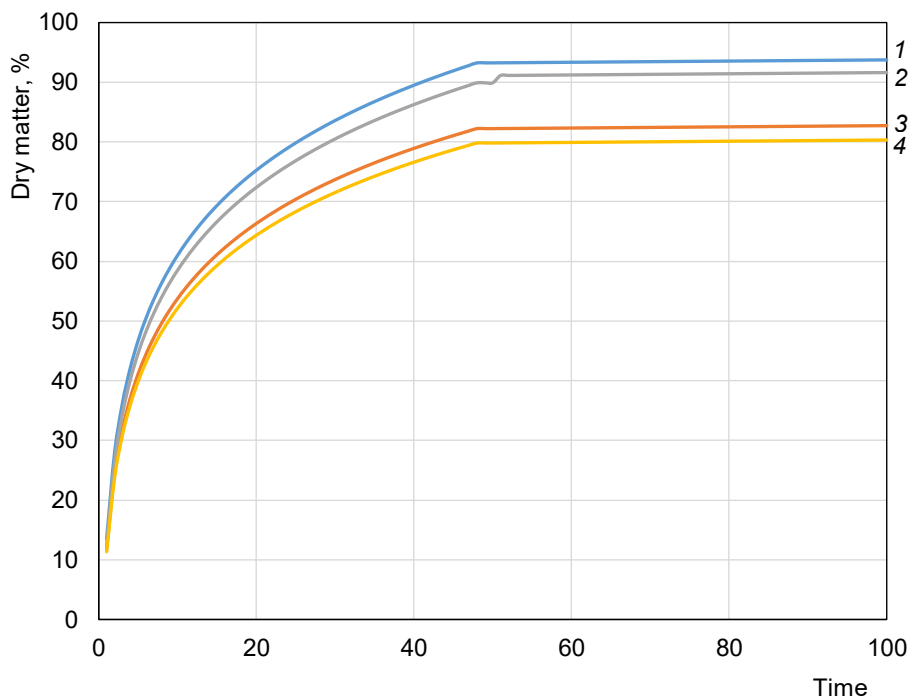


Figure 3. Simplified graphs of changes in dry matter at 25 and 35% initial loading of the apparatus:

- 1 – Dry matter in massecuite for 25% from initial loading of the apparatus;
- 2 – Dry matter in syrup for 25% from initial loading of the apparatus;
- 3 – Dry matter in massecuite for 35% from initial loading of the apparatus;
- 4 – Dry matter in syrup for 35% from initial loading of the apparatus;

*Time – dimensionless time, calculated as the ratio of the current time to the total crystallization time.

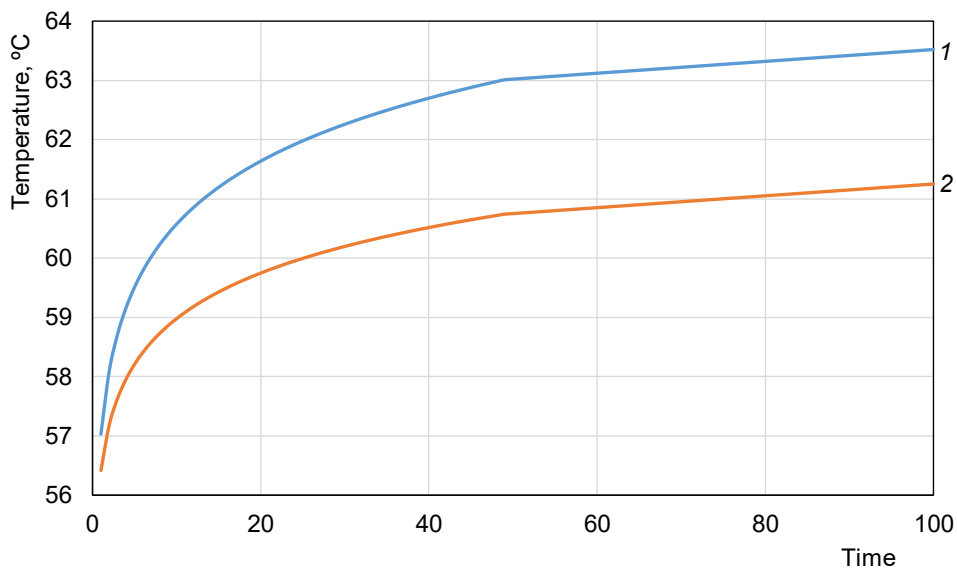


Figure 4. Simplified graphs of temperature changes at 25% and 35% from initial loading of the apparatus:

1 – Temperature mode for 25% from initial loading of the apparatus;

2 – Temperature mode for 35% from initial loading of the apparatus.

*Time – dimensionless time, calculated as the ratio of the current time to the total crystallization time.

Based on the data shown in Figures 3 and 4, and the dependencies in Section 2.3, the surfaces of the deformation gradient of the crystallization process in spatial coordinates were obtained. For analysis, the data were modified as follows:

- Figure 5a: The surface is constructed at 25% and 35% from initial loading of the device using the data shown in Figures 3 and 4.
- Figure 5b: The surface is constructed at 25% and 35% from initial loading of the device, but for the 25% mode, the temperature is considered constant with the initial value.
- Figure 5c: The surface is constructed at 25% and 35% from initial loading of the device, but for the 35% mode, the temperature is considered constant with the initial value.
- Figure 5d: The surface is constructed at 25% and 35% from initial loading of the apparatus, with temperatures considered constant with the initial value.

After analyzing the obtained surfaces, we found that surfaces a and d have the most significant changes. Therefore, for further calculations and research, the corresponding deformation gradients of the crystallization process were taken. The deformation gradient constructed according to the parameters of dry substance content and temperature reflects changes in the crystallization process. These parameters directly affect the system properties, which is crucial for optimizing the process in a vacuum apparatus.

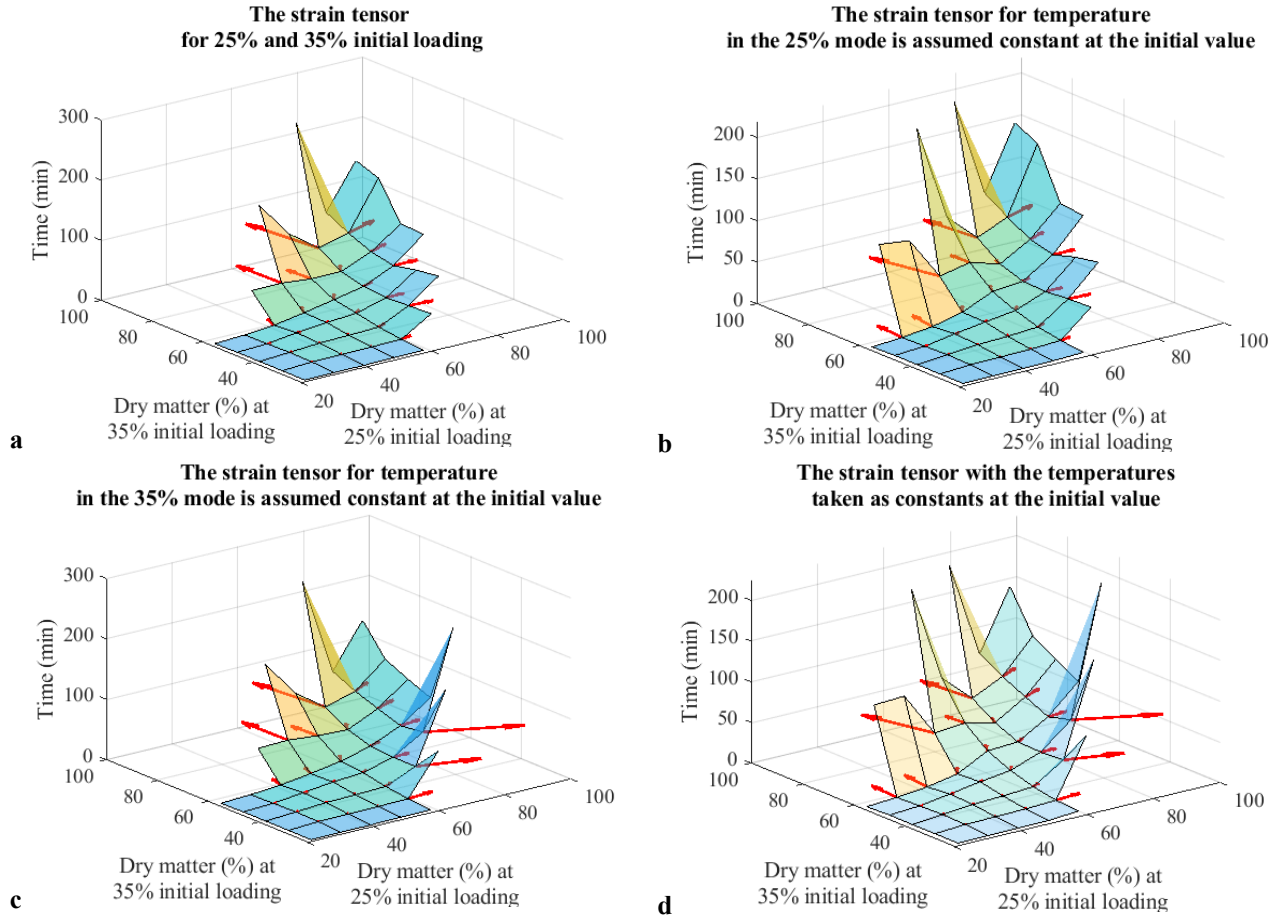


Figure 5. The strain tensors constructed at 25% and 35% from initial loading of the device and the data shown in Figures 3 and 4

Amplification factor for the vacuum apparatus at different loading values

Figures 6 and 7 show the changes in the volume of the deformation gradient and the divergence of the deformation tensor at 25% and 35% from initial loading of the apparatus. These are key aspects for calculating and analyzing the amplification factor in the crystallization process of sugar in a vacuum apparatus.

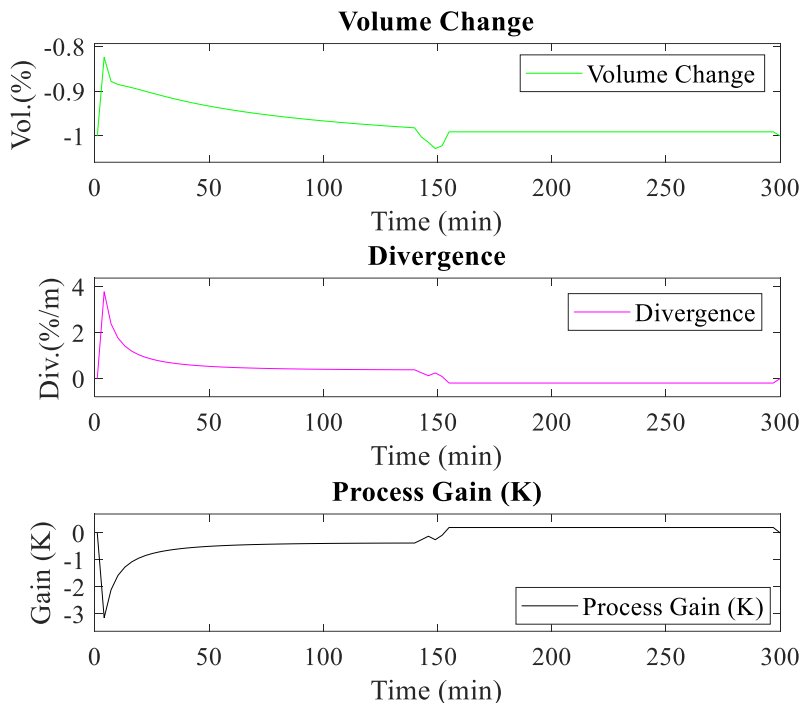


Figure 6. Volume, divergence, and amplification factor at 25% and 35% from initial loading of the device and the data shown in Figures 3 and 4.

The change in the volume of the deformation gradient reflects the interaction between the thermal and mechanical properties of sugar during crystallization. Considering these changes allows for accurate modeling of heat transfer and mechanical stresses affecting the crystallization rate. The divergence of the deformation gradient, which shows the spatial distribution of deformations, helps identify areas with the highest concentration of mechanical influences. This provides a more detailed process analysis, enabling the determination of optimal conditions for achieving the desired gain.

By analyzing changes in the volume and divergence of the deformation gradient, it is possible to accurately determine the parameters affecting the efficiency of the crystallization process. For example, changes in the volume of the deformation gradient help assess the influence of pressure and temperature on sugar crystal formation. Divergence shows how changes in mechanical stress affect the uniformity and size of crystals. This allows for the optimization of conditions in the vacuum apparatus to achieve the maximum amplification factor, critical for industrial process efficiency. Consequently, using these parameters provides a deeper understanding of the crystallization mechanisms, improving the quality of the final product

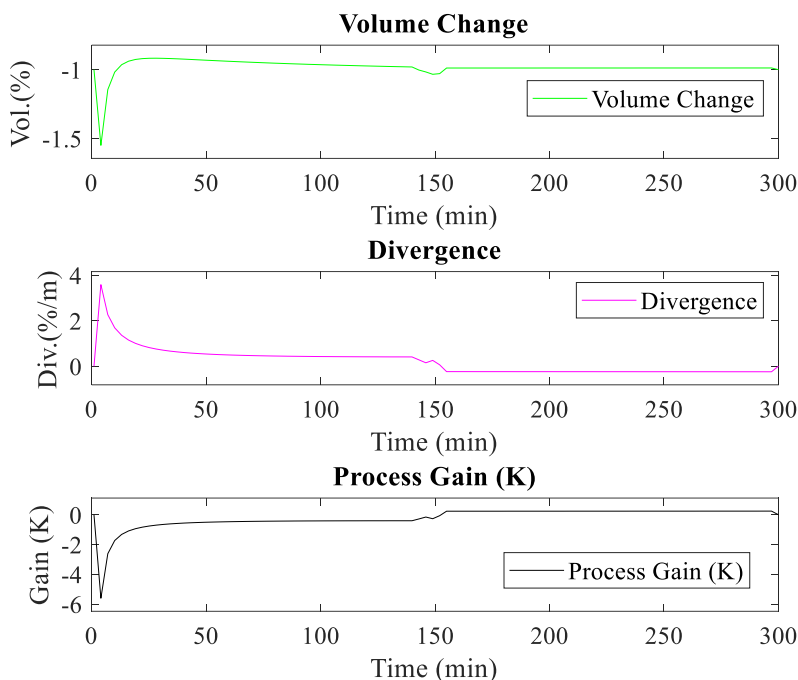


Figure 7. Volume, divergence, and amplification factor at 25% and 35% from initial loading of the device and the data shown in Figures 3 and 4 with constant process temperatures.

Changes in speed and acceleration as components of the constant time and delay time for the vacuum apparatus at different loading values

The change in the volume of the deformation gradient and the divergence of the deformation gradient allow for the calculation and analysis of the rate of change in velocity and acceleration during the sugar crystallization process in a vacuum apparatus. By analyzing these parameters, we can determine how quickly crystallization conditions respond to changes in thermal and mechanical conditions. This, in turn, allows us to calculate the time constant, which characterizes the speed of the process's reaction to changing conditions. Measuring acceleration, as the second derivative of the deformation gradient, helps assess the system's dynamic properties and identify potential instabilities. These parameters thus assist in precisely regulating the process to achieve optimal crystallization conditions.

Furthermore, the divergence of the deformation gradient helps determine the delay time, which is crucial for controlling the crystallization process. Divergence indicates moments when changes in one part of the system affect other parts, which is essential for accurately predicting the system's behavior. Considering the delay time helps adjust the control system to compensate for these delays and ensure stable operation of the vacuum apparatus. Overall, analyzing changes in velocity and acceleration based on the deformation gradient provides a deeper understanding of the dynamic characteristics of the process. This allows for the optimization of control parameters and improves the efficiency of sugar crystallization.

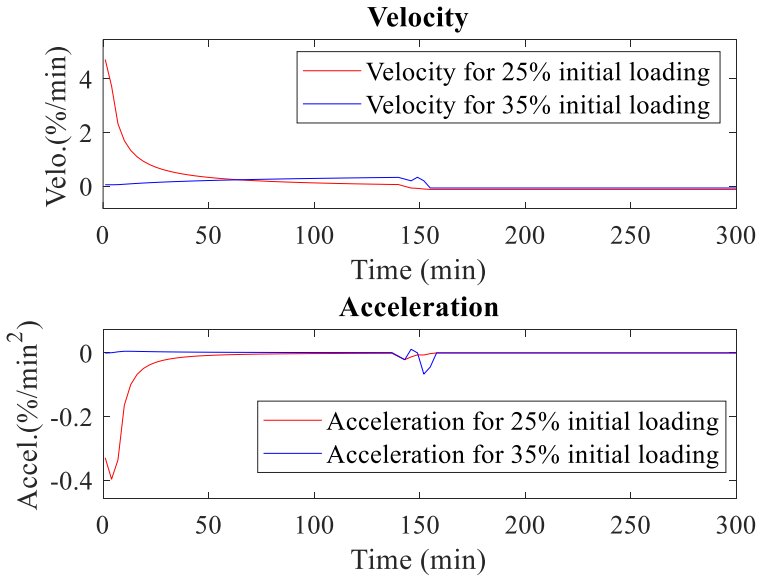


Figure 8. Speed and acceleration as components of the time constant and delay time for the deformation gradient at 25% and 35% from initial loading of the apparatus, based on data presented in Figures 3 and 4.

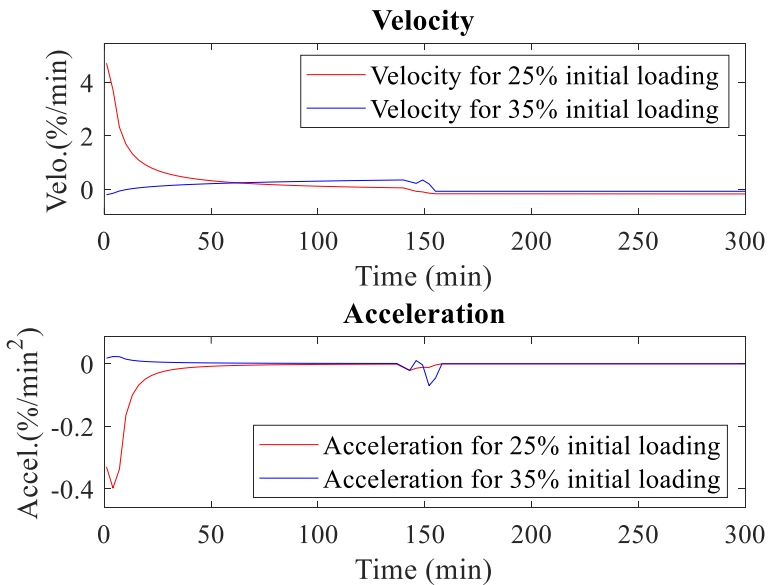


Figure 9. Speed and acceleration for 25% and 35% from initial loading of the apparatus, based on data presented in Figures 3 and 4 and constant process temperature values.

Thus, the velocity and acceleration of the deformation gradient can provide insights into the time constant and delay time of an object in an automated control system. The rate of change of parameters indicates the time constant, as it characterizes the system's response speed, while acceleration can highlight dynamic aspects related to delays in the system's response. However, accurately defining these characteristics requires a more detailed analysis of the system and its dynamic properties.

Using the deformation gradient and tensor, continuity equations, and balance equations allows for more precise modeling of complex physical processes. This is particularly important for the crystallization process, where it is necessary to consider thermodynamic and physicochemical features. These advantages in calculating parameters such as the time constant, amplification factor, and delay time provide better regulator settings to maintain the desired technological process in sugar crystallization. This is mainly due to accounting for temperature changes and the crystallization kinetics of dry substance content in the solution and massecuite.

However, models based on continuity equations and deformation gradients are much more complex and require more computational resources to solve. This can be problematic in real-world applications, especially for large systems. This complexity explains the use of tensor approaches for description and calculation, which allow processing significant amounts of data and information.

Conclusions

1. Strain gradients constructed on the basis of vectors including information on dry matter content and temperature can provide a complete picture of the crystallization process in a vacuum apparatus. This allows to model and control the process more accurately, providing effective management and optimization of the process.
2. The obtained values of the divergence of the deformation gradient as input parameters for the controller make it possible to evaluate and respond to changes in concentrations and temperature, regulating the processes to achieve the desired crystallization conditions. In an automated control system, such an indicator can be used to adjust control algorithms in order to stabilize the process or optimize crystallization conditions.
3. The divergence of the deformation gradient $\nabla \cdot \mathbf{F}$ can be used as an indicator of changes in the internal state of the system and considered as a gain factor in an automated control system. This allows taking into account the rate of change of system parameters, such as solids content and temperature, and adjusting control mechanisms accordingly for optimal control of the crystallization process.
4. Velocity and acceleration, as position-time derivative and velocity-time derivative, respectively, allow real-time process control and correction, which is critical for achieving a stable and efficient crystallization process.
5. The rate and acceleration of the deformation gradient, constructed on the basis of data on the content of solids in the massecuite, the content of solids in the solution and the temperature of the crystallization process, are information about the time constant and the delay time of the object in the automated control system.

References

- Alvarado J.P., Palma H.H., Ramos C.G., Moreno-Ríos A.L., Osio E.M., Horta R.G., Caraveo G.I., Moreno S.E. (2024), Evaporation automation at the Central de Mielles de Útica, Colombia, for non-centrifugal sugar cane production: Sustainable optimization strategies, *Bioresource Technology Reports*, 26, 101850, <https://doi.org/10.1016/j.biteb.2024.101850>
- Azevedo S.F., Gonçalves M.J., Ruiz V., Najim K. (1989), Generalized Predictive Control of a Batch Evaporative Crystallizer, *IFAC Proceedings Volumes*, 22, pp. 93–98, [https://doi.org/10.1016/S1474-6670\(17\)53342-X](https://doi.org/10.1016/S1474-6670(17)53342-X)
- Baár T., Bauer P.H., Luspay T. (2020), Decoupling of discrete-time dynamical systems through input-output blending, *IFAC-PapersOnLine*, 53, pp. 921–926, <https://doi.org/10.1016/j.ifacol.2020.12.856>
- Barrett M., McNamara M., Hao, H., Barrett P., Glennon B. (2010), Supersaturation tracking for the development, optimization and control of crystallization processes, *Chemical Engineering Research & Design*, 88, pp. 1108–1119, <https://doi.org/10.1016/j.cherd.2010.02.010>
- Behary M.S., Ah King R.T., Rughooputh H.C. (2004), Automation of sugar boiling process in batch vacuum pans using ABB-Freelance PLC (AC 800F) and conductor NT SCADA, *2004 IEEE International Conference on Industrial Technology, 2004 IEEE ICIT '04*, 2, pp. 853–858, <https://doi.org/10.1109/ICIT.2004.1490186>
- Castro R.E., Alves R.M., Nascimento, C.A. (2022), Dynamic Simulation of Multiple-Effect Evaporation, *SSRN Electronic Journal*, 34, pp. 1–14, <http://dx.doi.org/10.2139/ssrn.4021873>
- Che M., Cichocki A., Wei Y. (2017), Neural networks for computing best rank-one approximations of tensors and its applications, *Neurocomputing*, 267, pp. 114–133, <https://doi.org/10.1016/j.neucom.2017.04.058>
- Chowdhury M.A., Lu Q. (2022), A novel entropy-maximizing TD3-based reinforcement learning for automatic PID Tuning, *2023 American Control Conference (ACC)*, pp. 2763–2768, <https://doi.org/10.23919/ACC55779.2023.10156246>
- Cutz L., Santana D. (2014), Techno-economic analysis of integrating sweet sorghum into sugar mills: The Central American case, *Biomass and Bioenergy*, 68, pp. 195–214, <https://doi.org/10.1016/j.biombioe.2014.06.011>
- Dogbe E.S., Mandegari M., Görgens J.F. (2018), Exergetic diagnosis and performance analysis of a typical sugar mill based on Aspen Plus® simulation of the process, *Energy*, 145, pp. 614–625, <https://doi.org/10.1016/j.energy.2017.12.134>
- Döhler M., Mevel L. (2012), Fast multi-order computation of system matrices in subspace-based system identification, *Control Engineering Practice*, 20, pp. 882–894, <https://doi.org/10.1016/j.conengprac.2012.05.005>
- Eggleston G., Côté G.L., Santee C.J. (2011), New insights on the hard-to-boil massecuite phenomenon in raw sugar manufacture, *Food Chemistry*, 126, pp. 21–30, <https://doi.org/10.1016/j.foodchem.2010.10.038>
- Garcia A., Acebes L., Prada C.D. (2002), Modelling and simulation of batch processes: a case study, *IFAC Proceedings*, 35, pp. 169–174, <https://doi.org/10.3182/20020721-6-ES-1901.01014>
- Georgieva P., Meireles M., Azevedo S.F. (2003), Knowledge-based hybrid modelling of a batch crystallisation when accounting for nucleation, growth and agglomeration phenomena, *Chemical Engineering Science*, 58, pp. 3699–3713, [https://doi.org/10.1016/S0009-2509\(03\)00260-4](https://doi.org/10.1016/S0009-2509(03)00260-4)
- Grondin-Perez B., Benne M., Bonnecaze C., Chabriat J. (2005), Industrial multi-step forward predictor of mother liquor purity of the final stage of a cane sugar crystallisation plant,

- Journal of Food Engineering*, 66, 361–367, <https://doi.org/10.1016/j.jfoodeng.2004.04.002>
- Grondin-Perez B., Benne M., Chabriat J. (2006), Supervision of C crystallisation in Bois Rouge sugar mill using on-line crystal content estimation using synchronous microwave and refractometric brix measurements, *Journal of Food Engineering*, 76, pp. 639–645, <https://doi.org/10.1016/j.jfoodeng.2005.06.014>
- Hassani N.S., Saidi K., Bounahmidi T. (2001), Steady state modeling and simulation of an industrial sugar continuous crystallizer, *Computers & Chemical Engineering*, 25, pp. 1351–1370, [https://doi.org/10.1016/S0098-1354\(01\)00705-0](https://doi.org/10.1016/S0098-1354(01)00705-0)
- Horák M., Kružík M. (2019), Gradient polyconvex material models and their numerical treatment, *International Journal of Solids and Structures*, 195, pp. 57–65, <https://doi.org/10.1016/j.ijsolstr.2020.03.006>
- Hu Y., Li T., Fan C., Wang D., Li J. (2015), Three-dimensional tensor controlled-source electromagnetic modeling based on the vector finite-element method, *Applied Geophysics*, 12, pp. 35–46, <https://doi.org/10.1007/s11770-014-0469-1>
- Ibis O.I., Bugday Y.B., Aljurf B.N., Goksu A.O., Solmaz H., Oztop M.H., Sumnu, G. (2023), Crystallization of sucrose by using microwave vacuum evaporation, *Journal of Food Engineering*, 365(10), 111847, <https://doi.org/10.1016/j.jfoodeng.2023.111847>
- Karagoz R., Batselier K. (2020), Nonlinear system identification with regularized Tensor Network B-splines, *Automatica*, 122, 109300, <https://doi.org/10.1016/j.automatica.2020.109300>
- Kotcubansky A.M., Mironchuk V.H., (2012), Efficient by initial syrups vacuum pan for boiling restorative sugar solution, *Ukrainian Food Journal*, 1, pp 81-85.
- Kuntanapreeda S. (2018). Control of shimmy vibration in aircraft landing gears based on tensor product model transformation and twisting sliding mode algorithm, *MATEC Web of Conferences*, 161, 02001, <https://doi.org/10.1051/mateconf/201816102001>
- Lauret A.J., Boyer H., Gatina J.C. (2000), Hybrid modelling of a sugar boiling process, *Control Engineering Practice*, 8, 299–310, [https://doi.org/10.1016/S0967-0661\(99\)00151-3](https://doi.org/10.1016/S0967-0661(99)00151-3)
- Loubser R.C. (2004), Heat and mass balance using constraint equations, a spreadsheet, and the newton-raphson technique, *Proceedings of the 78th Annual Congress of South African Sugar Technologists' Association, held at Kwa-Shukela, Mount Edgecombe, South Africa, 27-30 July 2004*, 78, pp. 457–471.
- Mazaeda R., Gómez A.M., Moraga C.D., Arconada L.F. (2012), Hybrid modelling of batch centrifuges as part of a generic object oriented beet Sugar Mill library, *Simulation Modelling Practice and Theory*, 22, pp. 123–145, <https://doi.org/10.1016/j.simpat.2011.12.003>
- Meng Y., Yu S., Zhang J., Qin J., Dong Z., Lu G., Pang H.F. (2019), Hybrid modeling based on mechanistic and data-driven approaches for cane sugar crystallization, *Journal of Food Engineering*, 257, pp. 44–55, <https://doi.org/10.1016/j.jfoodeng.2019.03.026>
- Merino A., Acebes L., Alves R., Prada C.D. (2018), Real Time Optimization for steam management in an evaporation section, *Control Engineering Practice*, 79, pp. 91–104, <https://doi.org/10.1016/j.conengprac.2018.07.010>
- Mkwananzi T., Mandegari M., Görgens J.F. (2019), Disturbance modelling through steady-state value deviations: The determination of suitable energy indicators and parameters for energy consumption monitoring in a typical sugar mill, *Energy*, 176, pp. 211–223, <https://doi.org/10.1016/j.energy.2019.03.191>
- Morales H., Sciascio F.D., Aguirre-Zapata, E., Amicarelli A.N. (2023), A model-based supersaturation estimator (inferential or soft-sensor) for industrial sugar crystallization process, *Journal of Process Control*, 129, pp. 839–844, <https://doi.org/10.1016/j.jprocont.2023.103065>
- Ohara S., Fukushima Y., Sugimoto A., Terajima Y., Ishida T., & Sakoda, A. (2012), Rethinking the cane sugar mill by using selective fermentation of reducing sugars by *Saccharomyces*

- dairensis*, prior to sugar crystallization, *Biomass and Bioenergy*, 42, pp. 78–85, <https://doi.org/10.1016/j.biombioe.2012.03.024>
- Pedersen T., Godhavn J., Schubert J.J. (2015), Supervisory control for underbalanced drilling operations, *IFAC-PapersOnLine*, 48, pp. 120–127, <https://doi.org/10.1016/j.ifacol.2015.08.019>
- Petrenko V., Zasyadko Y., Pryadko M. (2020), Modeling of heat transfer deterioration regimes when concentrating solutions in industrial film evaporators, *Ukrainian Food Journal*, 9(4), pp. 901–916, <https://doi.org/10.24263/2304-974x-2019-8-2-12>
- Pohorilyi T. (2023), Modeling of non-stationary processes heat and mass transfer according to the cellular model of sucrose mass crystallization, *Ukrainian Food Journal*, 12(1), pp. 80–113, <https://doi.org/10.24263/2304-974x-2023-12-1-8>
- Prada C.D., Cristea S., Mazaeda R. (2015), Hierarchical optimal operation of continuous-batch processes, *IFAC-PapersOnLine*, 48, pp. 294–301, <https://doi.org/10.1016/j.ifacol.2015.11.298>
- Santos R.A., Normey-Rico J.E., Gómez A.M., Arconada L.F., Moraga C.D. (2008), Distributed continuous process simulation: An industrial case study, *Computers & Chemical Engineering*, 32, pp. 1195–1205, <https://doi.org/10.1016/j.compchemeng.2007.04.022>
- Schlumbach K., Pautov A., Flöter E. (2017), Crystallization and analysis of beet and cane sugar blends, *Journal of Food Engineering*, 196, pp. 159–169, <https://doi.org/10.1016/j.jfoodeng.2016.10.026>
- Sidletskiy V. (2019), Steam boiler control system using tensor analysis methods, *International Journal of Computing*, 18(2), pp. 147–154, <https://doi.org/10.47839/ijc.18.2.1413>
- Sidletskiy V., Elperin I., (2019), Integrated control system of the thermal power complex using the tensor analysis methods, *Naukovyi Visnyk Natsionalnoho Hirnychoho Universytetu*, 5, pp. 137–142, <https://doi.org/10.29202/nvngu/2019-5/20>
- Sidletskiy V., Korobiichuk I., Ladaniuk A., Elperin I., Rzeplińska-Rykała K. (2020), Development of the structure of an automated control system using tensor techniques for a diffusion station, *Advances in Intelligent Systems and Computing*, 920, pp. 175–185, https://doi.org/10.1007/978-3-030-13273-6_18
- Simoglou A., Georgieva P., Martin E.B., Morris A.J., Azevedo S.F. (2005), A time varying state space approach for sugar crystallization process modelling and monitoring, *IFAC Proceedings*, 38, pp. 27–32, <https://doi.org/10.3182/20050703-6-CZ-1902.01580>
- Singh O. (2019), Exergy analysis of a grid-connected bagasse-based cogeneration plant of sugar factory and exhaust heat utilization for running a cold storage, *Renewable Energy*, 143, pp. 149–163, <https://doi.org/10.1016/j.renene.2019.05.012>
- Sperling S., Hoefnagels J.P., van den Broek K., & Geers M. (2023), A continuum particle model for micro-scratch simulations of crystalline silicon, *Journal of the Mechanics and Physics of Solids*, 182, 105469 <https://doi.org/10.1016/j.jmps.2023.105469>
- Suárez L.A., Georgieva P., Azevedo S.F. (2011), Nonlinear MPC for fed-batch multiple stages sugar crystallization, *Chemical Engineering Research and Design*, 89, pp. 753–767, <https://doi.org/10.1016/j.cherd.2010.10.010>
- Tabassum T., Lim S., Khalghani M.R. (2024), Artificial intelligence-based detection and mitigation of cyber disruptions in microgrid control, *Electric Power Systems Research*, 226, 109925, <https://doi.org/10.1016/j.epr.2023.109925>
- Tuttle J.F., Blackburn L.D., Andersson K., Powell K.M. (2021), A systematic comparison of machine learning methods for modeling of dynamic processes applied to combustion emission rate modeling, *Applied Energy*, 292, 116886, <https://doi.org/10.1016/j.apenergy.2021.116886>
- Villani E., Pascal J., Miyagi P.E., Valette R. (2004), Object oriented approach for cane sugar production: modelling and analysis, *Control Engineering Practice*, 12, pp. 1279–1289, <https://doi.org/10.1016/j.conengprac.2004.04.011>

- Wang J., Peng X., Huang Z., Zhou H., (2020), A temperature-dependent 3D anisotropic visco-hyperelastic constitutive model for jute woven fabric reinforced poly (butylene succinate) biocomposite in thermoforming, *Composites Part B-engineering*, 208, 108584, <https://doi.org/10.1016/j.compositesb.2020.108584>
- Wilson D.I., Lee P.L., White E.T., Newell R.B. (1991), Advanced control of a sugar crystallizer, *Journal of Process Control*, 1, pp. 197–206, [https://doi.org/10.1016/0959-1524\(91\)85009-8](https://doi.org/10.1016/0959-1524(91)85009-8)
- Zamarreño J.M., Vega P.I., Garcia L., Francisco M. (2000), State-space neural network for modelling, prediction and control, *Control Engineering Practice*, 8, pp. 1063–1075, [https://doi.org/10.1016/S0967-0661\(00\)00045-9](https://doi.org/10.1016/S0967-0661(00)00045-9)
- Zhang J., Meng Y., Wu J., Qin J., Wang H., Yao T., Yu S. (2020), Monitoring sugar crystallization with deep neural networks, *Journal of Food Engineering*, 280, 109965, <https://doi.org/10.1016/j.jfoodeng.2020.109965>

Cite:

UFJ Style

Sidletskyi V., Kukhar O. (2024), Change of crystallization process attributes in a vacuum pan of automation systems, *Ukrainian Food Journal*, 13(2), pp. 366–384, <https://doi.org/10.24263/2304-974X-2024-13-2-12>

APA Style

Sidletskyi, V., & Kukhar, O. (2024). Change of crystallization process attributes in a vacuum pan of automation systems, *Ukrainian Food Journal*, 13(2), 366–384. <https://doi.org/10.24263/2304-974X-2024-13-2-12>

Risk assessment in target market selection by bread baking enterprises

Nataliya Skopenko¹, Iryna Fedulova², Tetiana Mostenska³,
Iryna Severyna⁴, Larysa Kapinus¹

1 – National University of Food Technologies, Kyiv, Ukraine

2 – State Trade and Economic University, Kyiv, Ukraine

3 – National University of Life and Environmental Sciences of Ukraine, Kyiv, Ukraine

4 – Taras Shevchenko National University of Kyiv, Kyiv, Ukraine

Abstract

Keywords:

Uncertainty
Bread
Bakery
Risk
Management
Target market

Introduction. The aim of research is to justify a comprehensive approach to enterprise risk management, which includes analysis of risk factors at the stages of target market selection by enterprise.

Materials and methods. Statistical and financial reporting of 26 Ukrainian bakery enterprises was carried out. For expert evaluation of the likelihood of risk events and the occurrence of each risk factor, a rating scale is employed, which includes five possible states ranging from 0 – Improbable to 1 – Likely. The scale for expert assessment of possible losses includes six ranges from 0 – no loss to 0.91–1 – catastrophic loss.

Results and discussion. The issue of minimizing or neutralizing risks is particularly pertinent when enterprises are selecting target markets. Seven stages of target market selection are proposed: assessment of enterprise level capabilities; identification of segmentation principles and factors; development of matrix models (functional maps); collection and analysis of information about the bakery market; selection and evaluation of market segments; collection and analysis of information about competitors; and target segments selection and making optimal managerial decisions.

The assessment of risk factors and possible consequences at the stages of target market selection by bread baking enterprises has led to the following conclusions: the probability of the risk of profit shortfall is 0.69, while the probability of the risk due to uneven output of finished products is 0.66. The probability of risk is 0.59 if the products do not meet the consumers requirements, the product features are worse in comparison with competitors, or if the marketing strategy is insufficiently developed.

The overall risk in selecting a target market for bread baking enterprises is 0.21, signifying a low probability of risk situations, but the total possible losses are at a moderate (acceptable) level of 0.6.

Conclusions. The proposed approach allows to prevent risks or at least to minimize the possible losses in the emergence of risk in target market selection and can be extended to other enterprises taking into account the branch specifics of their activity.

Article history:

Received
02.09.2023
Received in revised
form 25.05.2024
Accepted 2.07.2024

Corresponding author:

Nataliya Skopenko
E-mail:
skopnata67@
gmail.com

DOI:

10.24263/2304-
974X-2024-13-2-13

Introduction

Challenges of enterprise risk management (ERM) has been the subject of research by many scientists in recent years. Researchers developed a variety of approaches to the identification and managing risks. The scientific literature has provided certain types of risks which emerge from business operations and comprehensive approaches to enterprise risk management.

The publications are devoted to theoretical approaches to risk management. In addition, the attention has focused on the effectiveness of risk identification, assessment and control systems implementation. Therefore, the ways of the uncertainty reduction and risk neutralization are determined.

According to Anton et al. (2020), «the empirical literature on ERM can be divided into four broad categories: the ERM implementation; the determinants of the ERM adoption; the effectiveness of the ERM process; other aspects of ERM, such as ERM across domains, ERM strategies, ERM maturity, the impact of institutional context on ERM adoption, ERM adoption in family firms, and ERM as a moderating factor between different variables».

This are considered the theoretical approaches to the definition of risks, their classification, a comparative analysis of integrated and traditional approaches to risk management, the risk management process (Spikin, 2013; Vitlinskiy et al., 2004).

Investigation of a combination of mechanisms that solve the agency and information problems in enterprise risk management is presented in Jankensgard (Jankensggrd, 2016).

It is identified the most significant factors affecting the implementation of risk management in enterprise activities and characterize risk management processes focused on three theoretical perspectives: the sociotechnical, the mutual adaptation and the dynamic capabilities (Jean-Jules et al., 2021).

From our point of view, the broadest list and risk characterization is presented in the paper of Harland et al. (2003), in which strategic, operational, competitive, reputational, financial, fiscal, regulatory, legal, supply, customer, asset depreciation risks are defined.

A number of publications are devoted to identifying risks of certain types of activities. McShane (2018) illustrates the role of ERM in enhancing the resilience of the organization and identifying factors which reduce employee resistance to change in the process of implementation a risk management system.

Relevant issues are the emergence and reduction of the negative impacts of financial risks. It was examine the impact of risk management on the financial performance of the enterprise and its non-financial activities, determine the impact of risk management on the productivity and the relationship between risk management and the quality of intellectual capital (Saeidi et al., 2021). Alviniussen and Jankensgård (2009) consider the problem of risk budgeting, which allows to monitor the financial indicators of the enterprise and overall risk profile. They identify the impact of corporate policies taking into account the capital expenditures, dividend payments and hedging on risks.

Effective risk management contributes to enhance competitiveness (Ennouri, 2013; Noccoand, 2006), while implementation of risk management system in strategic planning (Gates, 2006; Viscelli et al., 2017; Treadway Commission, 2016) ensures the achievement of strategic objectives.

Thus, Ennouri (2013) considers the systematic review of policies, procedures and practices in management to assess and manage risks in strategic planning. It is presented the proactive and reactive approaches to risk management. In this case, the proactive strategy allows to predict risks and implement measures to prevent adverse effects, while the reactive strategy helps to respond to emerging risks.

It is considered enterprise risk management framework as the basis for a more holistic and integrated risk management, including the internal control (Posch, 2020). The issue of balancing the strict control system and the broad authority in the establishing of the enterprise risk management framework. It is noted that an excessive control of results restricts flexibility of employees, instead of this, the lack of control in risk management may lead to an increasing of risky situations and has a negative impact on enterprise. However, a combination of risk management control, information sharing for risk assessment, and a proactive growth provide a broader set of alternatives for the enterprise.

Despite the widespread considering of risk management issues, lack of attention has been given to the identification of risks in the selection of target markets by enterprises. In addition, specific risks determine the branch specifics of enterprises activities.

The aim of the article is to justify a comprehensive approach to enterprise risk management, which includes analysis of risk factors at the stages of target market selection by enterprise.

Materials and methods

Materials

Assessing the risk of target market selection, the research was conducted on the basis of statistical and financial reports of 26 Ukrainian bread baking enterprises.

Methods

In the process of analytical risk assessment, the methods of observation and comparison, formalization, generalization, systematization, classification, analysis and synthesis, methods of qualitative and abstract-logical analysis were used.

Risk factor analysis was applied during a comprehensive assessment of risks for bread baking enterprises.

There are some issues of quantifying the impact of external and internal environmental factors on a risk degree. Environmental impact is always a likelihood and, therefore, it is impossible to predict the results accurately. The effect of different factors is controversial; moreover, it is difficult to take into account a wide variety of external and internal environmental factors. Thus, when assessing risks in conditions of incomplete and inaccurate information, it is advisable to use expert judgment to make adequate decisions (Qazi et al., 2021; Wehrspohn, et al., 2021).

A high degree of uncertainty in the strategic development of an enterprise requires acting appropriately to reduce it. In this case, it is important to estimate possible losses, possibility of their occurrence and impact of individual factors on the overall risk of the enterprises activities (Peljhan et al., 2021; Puia et al., 2021; Singh, et al., 2020).

The multifactorial risk assessment ensures making decisions under conditions of vague assessment of individual risk factors impact (Abergel et al., 2022; Lai et al., 2011; Vermeulen, et al., 1996).

It was proposed to consider the main elements of a multifactorial risk assessment as follows (Ilyashenko, 1997):

- risk of each alternative directions of development is considered as a complex of the elemental risks;

- necessary to distinguish consistent (can be implemented simultaneously, increasing a potential total loss) and inconsistent factors, sources of risk (the occurrence of one undesirable event eliminates another);
- elemental risks should be allocated according to the following scheme: nature of risk → possible consequences → risk factors. A structure (a model) is formed for each of the elemental risks that combines risk factors and possible effects of their different combinations. These models can be implemented in the form of a decision tree, a table, a set of inference rules;
- elemental risks (consistent and inconsistent) are recommended to be calculated as counterbalancing risk factors, which can confirm or deny the possibility of an undesirable event;
- it is recommended to use probability to evaluate the impact of specific risk factors.

The use of Bayes' formula in risk assessment is studied by the authors (Machado et al., 2023; Tchangani, et al., 2022).

If the judgment is evaluated with probability interpretations, we will use the Bayes' formula. $i+1$ judgment ($i+1$ risk factor) is calculated on the basis of i -previous judgment. In this way, the judgment will be combined, if it is independent. Each next judgment clarifies the integral assessment of elemental risk. For this purpose, after the combination of several judgments, the estimation is combined with the next judgment – until their entire set came to an end (Bakaev et al., 1992).

The proposed approach provides an opportunity to determine a structure of risk factors and possible negative consequences of their impact, to identify different types of risk that are typical for any enterprise. Estimation of risk factors is recommended to be implemented by means of expert judgment.

Overall risk can be defined as the probability of independent negative events that can occur or as a calculation of consistent and inconsistent risks in the money flow indicators (risk of losing money).

To sum up different points of view, it is necessary to illustrate a risk assessment scheme (Figure 1).

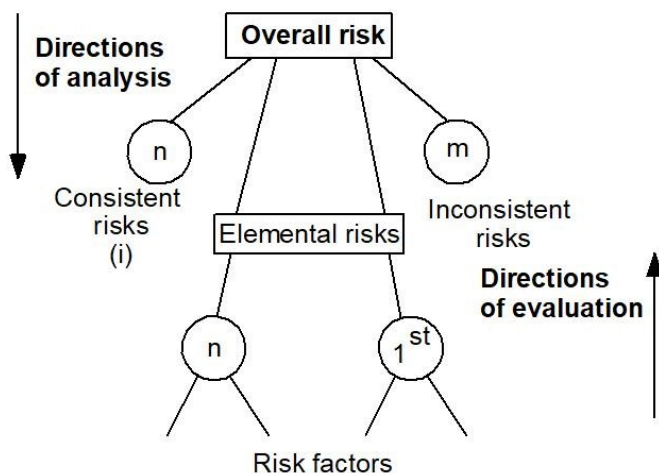


Figure 1. Risk assessment scheme

At first stage, it is important to perform a risk decomposition taking into account the enterprise' strategic development. Elemental risks are divided into consistent and inconsistent risks. Then, it is necessary to identify factors which can cause each risk situation. After that, in the reverse order, the quantitative risk evaluation is accomplished. For this reason, it is vital to estimate the degree of factors impact. Next step is a calculation of elemental risks to estimate a possible loss and probability of undesirable events occurrence. Finally, an overall risk assessment is calculated.

The uncertainty of risk factor assessment is characterised by inaccurate and incomplete data and is taken into account by probabilities.

The overall risk structure begins with the risk factors identification. It can be used for a forecasting and investigation of possible negative effects of different risk factors combinations on the business entities activity results. Each risk factor can increase or decrease (depending on the situation) the probability of negative consequences occurrence. Probability of risk factors impact on the outcome is different.

Probability of a negative result occurrence should include the effect of a whole complex of risk factors (independent judgment) and can be determined using causal models. These models help to explain the origins and estimate losses in the implementation of business processes using methods of probability theory. The basis of this approach is explained that causes and effects are related to conditional probability. The relative probability of a risk event occurring is calculated using Bayes' formula. According to the causal models, the degree of uncertainty for every event can be estimated by means of a probability.

Bayes' formula allows us to determine the probability of hypothesis (factor) F , in case of event H occurred, that is, the conditional probability of any hypothesis (Joyce, 2021):

$$P(F_j / H) = \frac{P(F_j) \cdot P(H / F_j)}{\sum_{i=1}^n P(F_i) \cdot P(H / F_i)} \sqrt{a^2 + b^2} \quad (j = 1, n), \quad (1)$$

where $P(F_j/H)$ – the probability that the hypothesis F_j occurs if H conclusion is true;

$P(F_j)$ - the probability of the hypothesis F_j ;

$P(H/F_j)$ – the posterior probability of H conclusion if the hypothesis F_j is known.

Formula of total probability is presented below:

$$P(H) = \sum_{i=1}^n P(F_i) \cdot P(H / F_i), \quad (2)$$

where $P(H)$ – a posterior probability of H conclusion.

If we take into account that any risk factor is a hypothesis, then the Bayesian method allows us to determine relative probability of conclusions (events) (Baka]:

$$P(H / F_j) = \frac{P(F_j / H) \cdot P(H)}{P(F_j)} \quad (3)$$

Thus, receiving of new evidence can increase or decrease the probability of a conclusion.

Bayesian network is shown in Figure 2.

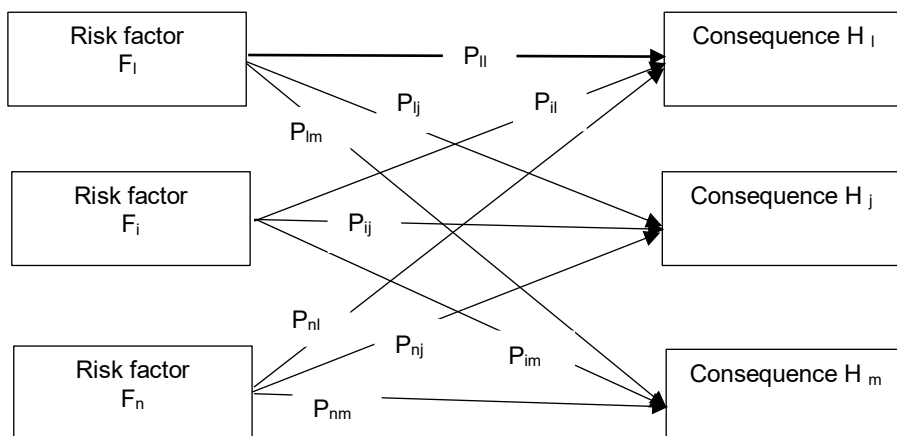


Figure 2. Bayesian network
Source: (Giarratano et al., 2004).

The casual model helps to identify a negative consequence or risk situation occurrence with probability accuracy measurement.

Results and discussion

Identification of the target market based on the risk profile

One of the most significant trends of corporate risk management in recent times is the development of enterprise risk management (ERM), which characterized a holistic approach to risk management for the enterprise and the centralized data aggregation on various types of risks (Alviniussen et al., 2009).

Rational decisions to determine the target market is based on the risk profile, which will allow to respond to changes in the external environment and make the most informed strategic and operational decisions.

To ensure the effectiveness of risk management, it is advisable to implement the method proposed in (Spikin, 2013), where the risk management process is considered as a sequence of steps (Figure 3). This approach can be used in the implementation of risk assessment, estimating the target market of the enterprise.

In the risk management process, assessing the probability of risk event occurrence plays an important role.

To apply expert judgment of a risk event occurrence and each risk factor appearance, it is necessary to develop an appropriate assessment scale. The authors proposes to use the following values of probabilistic factors assessment for expert conclusion (Table 1).

Authors propose to estimate the level of possible losses using loss coefficient. Loss coefficient is the ratio of maximum losses to the amount of the company's own funds for a certain economic operation (project). It is distinguished such zones of risk, according to the amount of loss ($K_z = 0$ – no losses; $K_z \leq 0.1$ – zone of the minimum risk; $0.1 < K_z \leq 0.3$ – zone of acceptable risk; $0.3 < K_z \leq 0.6$ zone of acceptable risk; $0.6 < K_z \leq 0.9$ zone of critical risk; $0.9 < K_z \leq 1$ zone of catastrophic risk) (Ilyashenko, 1997; Lototska et al., 2012).



Figure 3. The risk management process (Spikin, 2013).

Table 1

Rating scale

Evaluation factor	Expert judgment	Values
Probability of each risk factor occurrence and certain risk situation occurrence	Improbable (so unlikely that probability is close to zero)	0
	Remote- unlikely, although conceivable	0.25
	Possible – could occur sometime	0.5
	Probable – not surprised, will occur several times	0.75
	Likely – occur repeatedly / event only to be expected	1
Level of possible loss (Loss coefficient)	No losses	0
	Trivial loss	≤ 0.1
	Minor loss	0.11–0.3
	Acceptable loss	0.31–0.6
	Critical loss	0.61–0.9
	Catastrophic loss	0.91–1

Source: Own study based on the peculiarities of activity and financing of Ukrainian bread baking enterprises

Risk, as the expected possible losses, is determined by the formula (Ilyashenko, 2003):

$$R = \sum_{i=1}^n R_i , \tag{4}$$

where: R is an overall risk; R_i – risk of i -stage of their total number n .

Such approach allows us to predict and quantify the risk of *various* areas of the enterprise activities taking into account the factors influence and to observe the impact of each individual risk factor. The results of the analysis make it possible to reasonably develop a set of risk mitigation measures.

The need to extend products to new markets is determined by a decrease in demand caused by the rivalry among competitors, low purchasing power, changes in consumption patterns, poor quality of goods, an increase in prices, etc. Launching products into new markets require a reasonable approach to identifying target segments and minimizing the risk of poor performance. While the risk factors caused by changes in the external environment (macro-level) cannot be influenced by the enterprise, there are a number of micro-level risk factors that can be managed by business entities.

The risk can be significantly reduced if we analyze the influence of factors, quantify risks (possible losses), develop and implement measures to prevent and reduce them.

It should be emphasized that the right market targeting decision of a business entity provides almost all parameters of the enterprise activity: volume of supply, price policy, growth opportunities, competitiveness. Therefore, optimal target segment selection gives an opportunity to avoid most types of risks (Ilyashenko, 2003; Kotler et al., 2016, 2017).

In the conditions of changeable environment, lack of resources and crisis phenomena, it is necessary for enterprises to analyze the consumer market, envisage the origin of new consumers' necessities and produce the innovative products (Mostenska et al., 2015).

One of the major methods of consumer market analysis is segmentation. Market segmentation is one of the most efficient tools for identification of market development. Selecting target markets helps to improve the competitive positioning and avoid unnecessary competition. Market segmentation can enable to better serve and retain customers. Segmenting and reaching customers will help enterprises grow and remain focused on serving customers the way they would like to be served. Thus, choosing the right market segment can help create an improved and sustainable market positioning for an enterprise. It also helps strategically choose a competitive arena to operate in.

Steps to identifying the target market are:

- assessment of enterprise level capabilities;
- identifying the principles and factors of segmentation;
- development of matrix models (functional maps);
- gathering and analyzing information about markets;
- selecting and evaluating the market segments;
- collecting and analyzing information about competitors;
- target market selection.

Decision-making process of reorientation in a new product development, new sale markets (their segments or niches), is associated with risk acceptance. Therefore, making decisions based on market research, it is necessary to analyze the impact of internal and external risk factors.

It is important to estimate risk of finding the target market by segmentation. Taking into account the results of risk assessment we can make a decision about selection of different market segments and develop measures to reduce the degree of risk and enhance efficiency of bread baking enterprises.

It is not always possible to use the traditional approaches to quantify the degree of risk when the probabilities of undesirable events and possible outcomes (losses due to market changes, incorrect choice of market segment, lack of statistical information) are known. The necessity to take into account the whole complex of risk factors cause difficulties in quantitative risk assessment.

It is advisable to use approaches that allow us to quantify risk in the situation of incomplete and inaccurate information. This methodological approach is based on the elements of factor analysis and fuzzy logic (Markowski et al., 2009; Shang et al., 2013).

Risk analysis of the process of identifying the target market for new products will be carried out in stages: nature of risk → possible consequences → risk factors (conditions that increase or decrease the likelihood of undesirable events).

A factorial risk assessment should be conducted by considering the main stages of the target market selection. It gives us an opportunity to identify and analyze risk factors and assess the degree of risk at each stage of target market selection. The obtained results can be integrated in quantitative risk assessment.

The authors analyzed the main types of risks at the stages of target market selection by bread baking enterprises.

Elemental risks and the main factors that cause them at the stages of the target market selection are highlighted. An analysis of each elemental risk is given in Table 2.

A list of the main types of risk, factors that cause them and the possible consequences make it possible to apply the quantitative risk assessment methods and achieve optimal characteristics of the target market.

Risk factors assessment in selecting a target market by bread baking enterprises

Qualitative analysis will be a basis for the quantitative assessment of business entities risk activity. To calculate the overall risk of target market selection, each type of elemental risk should be structured into the risk factors and the possible consequences of their different combinations. These structures can be presented in the form of decision trees, tables or inference rules.

The analysis of advantages and disadvantages of existing methods of a risk degree estimation allowed us to choose a rational and adequate methodology based on risk factor assessment in the conditions of uncertainty. This methodology gives us an opportunity, taking into account branch specific of the enterprises, to quantify the degree of risk assessment for the appropriate enterprise in a target market selection.

It is necessary to use the method of expert assessments to identify risks of bakery enterprises. For the risk degree estimation, we conducted questioning with bringing of highly skilled specialists. They estimated different risks for medium-sized baking enterprises of Kyiv and Kyiv region. An expert group included five specialists approximately identical competence, each of them carried out an independent estimation. For determination of group estimations, the arithmetic average value of experts' estimations who participated in examination was used.

Consistency assessment of experts' opinions was carried out using the coefficient of concordance.

Experts had the list of risks that can take place on the enterprise and risk factors. It was suggested to estimate such indicators:

- probability of each risk factor appearance;
- probability of risk situation appearance (certain type of risk);
- degree of negative elemental risk influence on the activity of the enterprise (estimation of possible losses' size from undesirable event realization).

Probability of concrete risk situation appearance and probability of each risk factor appearance in the process of the enterprise economic activity was determined in parts of unit, according to the methodology given above (Table 1).

Components for each elemental risk have also been identified, combining risk factors and the potential impact of their different combinations. Experts' assessment of risk activity of bread baking enterprises is given in Table 3.

Table 2

Main types of risks at the stages of target market selection by bread baking enterprises

Essence of risk	Possible consequences	Risk factors
Stage 1. Assessment of enterprise level capabilities		
Inadequate production capability assessment and drawbacks in sales of new products	Difficulty or inability to produce the appropriate assortment of high quality products in quantities needed; difficulties in launching new products to target consumers	Insufficient analysis; underestimating or overestimating of production capability; A lack of qualified staff; Resources and goods distribution mistakes; Technical difficulties
Stage 2. Identification of principles and factors of segmentation		
Difference in predictable indicators of a structure, size and behavior of the target market; <i>insufficient</i> strategy for launching new products	Wrong target market segments (niches) selection; products are not selling; products do not meet the consumers requirements; additional costs for the right market research	A lack of qualified staff; making decisions based on incorrect or inaccurate information; Lack of awareness; underestimation of competitors; ignoring local conditions and traditions of consumption in different regions
Stage 3. Development of matrix models (functional maps)		
Inconsistency of the developed models with a structure, size, and behavior of the target market	Matrix models do not provide a clear information about the consumer market structure; it is necessary to do additional market research for selecting the target market segments	Inconsistent work of employees from different departments; lack of awareness; A lack of qualified staff; false information
Stage 4. Collection and analysis of information about the bakery market		
Making decisions based on incorrect or inaccurate information about market development perspectives	Non-competitive products; Production of bakery products that do not meet the market requirements; <i>insufficient</i> strategy for launching new products	The wrong method of collecting and analyzing information; insufficient analysis; lack of information; inaccurate information; a lack of qualified staff;

Table 2 (continue)

Essence of risk	Possible consequences	Risk factors
Stage 5. Selection and evaluation of market segments		
Difference in predictable indicators of a structure, size and behavior of the target market; <i>insufficient</i> market entry strategy	Wrong target market segments selection; products are not selling; products do not meet the consumers requirements; increasing costs for the right market research And re-segmentation	A lack of qualified staff; making decisions based on inaccurate information; Wrong target market segments selection; wrong choice of principles and factors of market segmentation; Insufficient accuracy of market segments evaluation and selection
Stage 6. Collection and analysis of information about competitors		
Inadequate production capability assessment and drawbacks in sales of competitors' products	Increasing competition (quality; price); Inability to sell a new product; The decrease in sales volumes; <i>Insufficient</i> sales profit	Insufficient analysis; underestimating or overestimating of production capability of competitors; underestimating the capability of production of competitors; Insufficient competence of experts; competitors' mistakes in distribution of goods
Stage 7. Target segments selection and making optimal managerial decisions		
Rejection of a new product; slow deployment of mass production or the impossibility of its deployment	The decrease in sales volumes; A profit shortfall; Bankruptcy risk	Making decisions based on inaccurate information; unpredictable changes in the external environment

Source: Own study based on expert assessment

Table 3
Risk factors assessment and possible consequences in selecting a target market by bread baking enterprises

Risk factors (Fi)	Possible consequences (negative result Hj)	Conditional probability P (Fi / Hj)
A lack of qualified staff	Production volume is lower than possible	0.1
	Disruption in production terms of finished products	0.2
	Products do not meet the consumers requirements	0.2
	Product features are worse in comparison with competitors	0.3
	Reducing sales	0.2
	<i>Insufficient</i> marketing strategy	0.1
	$\Sigma =$	1.0
Inadequate production capability assessment	Insufficient quantity of production volume	0.4
	Disruption in production terms of finished products	0.2
	Profit shortfall	0.4
	$\Sigma =$	1.0
Resources and goods distribution mistakes	Insufficient quantity of production volume	0.4
	Disruption in production terms of finished products	0.2
	Reducing sales	0.4
	$\Sigma =$	1.0
Insufficient analysis	Increasing competition	0.2
	Reducing sales	0.2
	Products do not meet the consumers requirements	0.1
	Product features are worse in comparison with competitors	0.1
	<i>Insufficient</i> marketing strategy	0.1
	Additional costs for the right market research	0.1
	Profit shortfall	0.2
	$\Sigma =$	1.0

<i>Table 3 (continue)</i>		
Risk factors (Fi)	Possible consequences (negative result Hj)	Conditional probability P (Fi / Hj)
Insufficient competence of experts	Reducing sales	0.3
	<i>Insufficient</i> information about market structure	0.2
	Additional costs for the right market research	0.2
	Increasing competition	0.2
	Profit shortfall	0.2
	$\Sigma =$	1.0
Insufficient and inaccurate information	<i>Insufficient</i> information about market structure	0.3
	Products do not meet the consumers requirements	0.3
	<i>Insufficient</i> marketing strategy	0.3
	Additional costs for the right market research	0.2
	$\Sigma =$	1.0
Ignoring local conditions and traditions of consumption in different regions	<i>Insufficient</i> information about market structure	0.4
	Products do not meet the consumers requirements	0.6
	$\Sigma =$	1.0
Underestimating the capability of production of competitors	Quality of product doesn't develop the competitive advantages	0.3
	Additional costs for the right market research	0.1
	Increasing competition	0.2
	Profit shortfall	0.4
	$\Sigma =$	1.0
Wrong method of collecting and analyzing information	Product features are worse in comparison with competitors	0.7
	Additional costs for the right market research	0.3
	$\Sigma =$	1.0
Change of inflation rate	Bankruptcy of an enterprise	0.2
	Profit shortfall	0.8
	$\Sigma =$	1.0
Unpredictable political and legislation changes	Bankruptcy of an enterprise	0.3
	Profit shortfall	0.7
	$\Sigma =$	1.0

Source: Own study based on expert assessment

Table 4

Risk factors assessment and possible consequences at the stages of target market selection by bread baking enterprises

Risk factors (Fi) and possible consequences (Hj)	Probability of risk factor appearance P (Fi)	Conditional probability of consequences appearance P (Fi / H)	Probability of risk P (H)	Conditional probability of risk occurrence P (H / Fi)
lack of skills and / or experience of employees	0.60	0.13	x	0.14
inadequate production capability assessment	0.60	0.40	x	0.42
resources and goods distribution mistakes	0.60	0.43	x	0.45
Insufficient output of finished products			0.63	0.34
lack of skills and / or experience of employees	0.60	0.17	x	0.18
inadequate production capability assessment	0.63	0.23	x	0.25
resources and goods distribution mistakes	0.60	0.20	x	0.22
Uneven output of finished products			0.66	0.22
insufficient analysis	0.63	0.17	x	0.13
insufficient competence of experts	0.58	0.27	x	0.23
resources and goods distribution mistakes	0.60	0.37	x	0.31
Reducing sales			0.50	0.22
wrong target market segments selection	0.55	0.30	x	0.24
insufficient competence of experts	0.58	0.20	x	0.15
insufficient and inaccurate information	0.68	0.27	x	0.17
ignoring local conditions and traditions of consumption in different regions	0.60	0.37	x	0.27
Insufficient information about market structure			0.44	0.21
insufficient analysis	0.63	0.13	x	0.13
lack of skills and / or experience of employees	0.60	0.17	x	0.16
ignoring local conditions and traditions of consumption in different regions	0.60	0.63	x	0.63
insufficient and inaccurate information	0.68	0.27	x	0.23

Risk factors (F_i) and possible consequences (H_j)	Probability of risk factor appearance $P (F_i)$	Conditional probability of consequences appearance $P (F_i / H)$	Probability of risk $P (H)$	Conditional probability of risk occurrence $P (H / F_i)$
Products do not meet the consumers requirements			0.59	0.29
insufficient analysis	0.63	0.10	x	0.06
insufficient competence of experts	0.58	0.20	x	0.13
Underestimating the capability of production of competitors	0.60	0.13	x	0.08
insufficient and inaccurate information	0.68	0.17	x	0.09
Additional costs for the right market research			0.38	0.09
Wrong method of collecting and analyzing information	0.58	0.70	x	0.72
insufficient analysis	0.63	0.13	x	0.13
lack of skills and / or experience of employees	0.60	0.27	x	0.26
Product features are worse in comparison with competitors			0.59	0.37
insufficient analysis	0.63	0.10	x	0.10
lack of skills and / or experience of employees	0.60	0.10	x	0.10
insufficient information	0.68	0.10	x	0.09
Insufficient marketing strategy			0.59	0.09
wrong target market segments selection	0.58	0.17	x	0.14
insufficient analysis	0.63	0.17	x	0.13
lack of skills and / or experience of employees	0.60	0.17	x	0.14
Reducing sales			0.50	0.14
insufficient analysis	0.63	0.20	x	0.16
underestimating the capability of production of competitors	0.60	0.20	x	0.17
insufficient competence of experts	0.58	0.17	x	0.14
resources and goods distribution mistakes	0.60	0.20	x	0.17

Risk factors (F_i) and possible consequences (H_j)	Probability of risk factor appearance $P (F_i)$	Conditional probability of consequences appearance $P (F_i / H)$	Probability of risk $P (H)$	Conditional probability of risk occurrence $P (H / F_i)$
Increasing competition			0.5	0.16
insufficient analysis	0.63	0.17	x	0.18
underestimating the capability of production of competitors	0.63	0.37	x	0.40
insufficient competence of experts	0.58	0.17	x	0.20
Profit shortfall			0.69	0.26
change of inflation rate	0.50	0.17	x	0.11
unpredictable political and legislation changes	0.60	0.30	x	0.25
Bankruptcy of an enterprise			0.34	0.18

Source: Own study based on expert assessment

Table 5

Risk assessment in selecting a target market by bread baking enterprises

Possible negative consequences	Conditional probability of risk occurrence	Probabilistic losses estimation
Insufficient output of finished products	0.34	0.59
Uneven output of finished products	0.22	0.61
Reducing sales	0.22	0.71
<i>Insufficient</i> information about market structure	0.21	0.33
Products do not meet the consumers requirements	0.29	0.61
Additional costs for the right market research	0.09	0.38
Product features are worse in comparison with competitors	0.37	0.57
<i>Insufficient</i> marketing strategy	0.09	0.49
Reducing sales	0.14	0.71
Increasing competition	0.16	0.40
Profit shortfall	0.26	0.81
Bankruptcy of an enterprise	0.18	1.00
Total risk	0.21	0.60

Source: Own study based on expert assessment

The same risk factor can cause both positive and negative situations. Therefore, it is possible to identify the impact of each risk factor on the possible outcomes. Probability of risk situation appearance (negative result H_j) and probability of each risk factor appearance (F_i) were determined by experts estimation. A generalized assessment of risk factors impact and possible consequences in selecting a target market for the bread baking enterprises are given in table 3. It was taken into account that the sum of the probabilities of possible consequences for each risk factor equals to one.

Qualitative analysis has shown that risk events may be a result of a poor performance of the various stages of target market selection. Negative situations can be caused by different risk factors. In this case, each of the undesirable situations is considered at one stage and excluded from consideration at other stage. This avoids the double counting of possible losses due to the occurrence of the same risk event.

Risk factors at the stages of target market selection, possible negative consequences of their influence and their probabilistic estimation, generalized probabilistic estimation of the result are given in Table 4.

Based on the data of the table 4, we calculated all possible losses of undesirable event appearance and found the overall risk in selecting a target market by bread baking enterprises (Table 5).

Estimation of conditional probability of risk appearance arising from the selection of new target markets by bread baking enterprises is shown in Figure 4 and Figure 5.

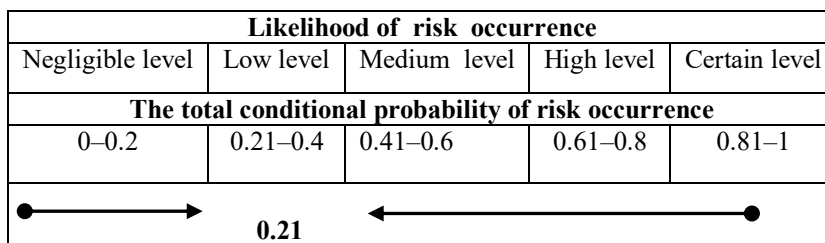


Figure 4. Conditional probability estimation of the micro risk occurrence at the target market selection by bread baking enterprises
Source: Own study based on expert assessment

Thus, for instance, the overall risk at the target market selection of the bread baking enterprises equals to 0.21, which means that there is a low probability of risk situation appearance, but the total possible losses will be on medium level (0.6).

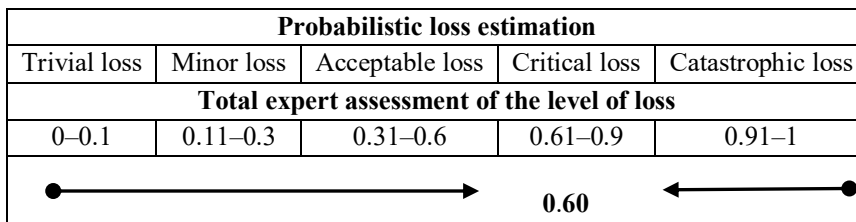


Figure 5. Probabilistic loss estimation of the influence of risk at the target market selection by bread baking enterprises
Source: Own study based on expert assessment

Discussion

Enterprise effectiveness management in the condition of uncertainty implies the importance of risk assessment to divide all the alternatives to reasonable, unjustified and risky ones.

Reasonable risk is a necessary attribute of strategy and management tactics in modern economic systems. In each risk situation, it is important to measure the level of risk (from acceptable level to the catastrophic risk). Thus, it is possible to calculate the level of optimal risk, the quantitative and qualitative assessment of concrete risk decisions. The degree of risk is the likelihood of risk occurrence and the level of possible losses.

To determine an effective way of risk management, it is necessary to design a matrix of "probability of losses occurrence" / "level of losses" according to the selected framework of probability and magnitude of losses estimation. This methodological approach helps us to design a matrix for the best choice of influence direction on risk of medium-sized bread baking industry enterprises of Kyiv and Kyiv region (Table 6).

Table 6
Decision matrix of a rational choice of influence on risk of bread baking enterprises

		Likelihood of risk occurrence				
		Negligible level	Low level	Medium level	High level	Certain level
		0–0.2	0.21–0.4	0.41–0.6	0.61–0.8	0.81–1.0
Level of loss		The degree of risk impact				
		Weak level	Moderate level	Medium level	High level	Immoderate level
Trivial loss	0.00–0.10	Risk acceptance			Risk acceptance or allocation, risk reduction	
Minor loss	0.11–0.30	Risk allocation or risk reduction	Risk transfer or allocation, risk reduction			Risk avoidance
Acceptable loss	0.31–0.60	Risk transfer or allocation, risk reduction			Risk avoidance	
Critical loss	0.61–0.90	Risk transfer or allocation, risk reduction		Risk avoidance		
Catastrophic loss	0.91–1.00	Risk transfer or allocation, risk reduction	Risk avoidance			

Source: Own study

Thus, on our point of view, the best choice for risk reduction is a combination of several methods and the main criterion for selection should be the optimal correlation between the degree of risk reduction achieved and all necessary costs.

Conclusions

1. Undertaken research gave an opportunity to develop an algorithm of factor analysis of risk types in the conditions of uncertainty, which including the following stages:
 - elemental risks allocation according to the following scheme: nature of risk → possible consequences → risk factors;
 - selection of experts;
 - risk factors assessment is carried out by method of expert judgement;
 - identification of the impact of certain risk factors assessment using probabilities;
 - development a structure for each of elemental risks that combines risk factors and the possible effects of their different combinations. These structures can be presented in the form of a decision tree, a table or a set of inference rules;
 - calculation of elemental risks (consistent and inconsistent) as counterbalancing risk factors;
 - experts' assessment of risks taking into account the probability of risk situation appearance and the degree of negative risk influence on the activity of enterprise;
 - *consistency assessment of experts' opinions*;
 - identification of the total level for each type of risk.
2. The main advantages of the proposed approach outlined above are the ability to calculate magnitude of risk in the conditions of uncertainty. It is possible to calculate the impact of each risk factor and estimate its share in total loss.
3. The considered approach can be used to estimate risks and choose the right ways for enterprise development. Based on the results of risk assessment, it is possible to determine the amount of funds that will be needed to prevent, reduce or avoid potential losses. Based on this assessment, a risk management system can be developed.

References

- Abergel F., Bellone B., Soupé F. (2022). A factor-based risk model for multifactor investment strategies, *Journal of Risk*, 24(4), pp. 1–22, <https://doi.org/10.21314/JOR.2022.027>
- Alviniussen A., Jankensgård H. (2009), Enterprise risk budgeting: Bringing risk management into the financial planning process, *Journal of Applied Finance*, 19, pp. 178–192.
- Anton S.G., Nucu A.E.A. (2020), Enterprise risk management: a literature review and agenda for future research, *Journal of Risk Financial Manag.*, 13, 281, <https://doi.org/10.3390/jrfm13110281>
- Bakaev A.A., Gritsenko V.I., Kozlov D.N. (1992), *Expert systems and logical programming*, Naukova Dumka, Kyiv.
- Committee of Sponsoring Organizations of the Treadway Commission (2016), Enterprise risk management – Aligning Risk Management with Strategy and Performance. June Edition.
- Ennouri W. (2013). Risks management: new literature review, *Polish Journal of Management Studies*, 8, pp. 288–297. <https://oaji.net/articles/2014/1384-1416476647.pdf>
- Etges A.P., Cortimiglia M. (2017), A systematic review of risk management in innovation-oriented firms. *Journal of Risk Research*. 22(3), pp. 1–18, <https://doi.org/10.1080/13669877.2017.1382558>

- Gates S. (2006). Incorporating strategic risk into enterprise risk management: a survey of current corporate practice, *Journal of Applied Corporate Finance*, 18(4), pp. 81–90. <https://doi.org/10.1111/j.1745-6622.2006.00114.x>.
- Giarratano J., Riley G.D. (2004), *Expert systems: principles and programming*, 4-th ed., Course Technology.
- Harland, C., Brenchley, R., Walker, H. (2003). Risk in supply networks. *Journal of Purchasing and Supply Management*, 9, pp. 51–62, [https://doi.org/10.1016/S1478-4092\(03\)00004-9](https://doi.org/10.1016/S1478-4092(03)00004-9).
- Ilyashenko S. (2003), *Management of innovative development: problems, concepts, methods*, VTD "University Book", Sumy.
- Ilyashenko S.N. (1997), *Economic aspects of target markets selection: segmentation, risk assessment, economic tools*, VTD "University Book", Sumy.
- Jankensgrd H. (2016), A theory of enterprise risk management, *SSRN Electronic Journal*. <https://doi.org/10.2139/ssrn.2753106>
- Jean-Jules J., Vicente R. (2021), Rethinking the implementation of enterprise risk management (ERM) as a socio-technical challenge, *Journal of Risk Research*, 24(2), pp. 247–266, <https://doi.org/10.1080/13669877.2020.1750462>
- Joyce J. (2021), Bayes' Theorem, In E.N. Zalta (Ed.), *The Stanford encyclopedia of philosophy*, Available at: <https://plato.stanford.edu/archives/fall2021/entries/bayes-theorem/>
- Kotler P., Keller. K.L. (2016), *Marketing Management*, 15 Global Edition. United States of America: Pearson Education Limited. Available at: <https://www.edugonist.com/wp-content/uploads/2021/09/Marketing-Management-by-Philip-Kotler-15th-Edition.pdf>
- Kotler Ph., Berger R., Bickhoff N. (2010), *The quintessence of strategic management: what you really need to know to survive in business*, Springer Heidelberg Dordrecht, London-New York.
- Lai F.W., Fazilah A.S.M., Azlinna A. (2011), Multifactor model of risk and return through enterprise risk management framework. 3rd International Conference on Information and Financial Engineering, 19-21 Aug 2011, Shanghai, China, Available at: <http://eprints.um.edu.my/id/eprint/12803>
- Lototska M.R., Kondur O.S. (2012), *Economic risk*, PNU, Ivano-Frankivsk.
- Machado P.G., de Oliveira R.C., do Nascimento O., Augusto C. (2023). Risk analysis in energy projects using Bayesian networks: a systematic review, *Energy Strategy Reviews*, 47, Available at: <https://www.sciencedirect.com/science/article/pii/S2211467X23000470>
- Markowski A.S., Mannan M.S., Bigoszevska A. (2009), Fuzzy logic for process safety analysis, *Journal of Loss Prevention in the Process Industries*, 22(6), pp. 695–702. <https://doi.org/10.1016/j.jlp.2008.11.011>
- McShane M. (2018), Enterprise risk management: history and a design science proposal, *The Journal of Risk Finance*, 19(2), pp. 137–153, <https://doi.org/10.1108/JRF-03-2017-0048>
- Mostenska T.L., Bilan, Y.V., Mostenska T.G. (2015), Risk management as a factor ensuring enterprises' economic security, *Actual Problems of Economics*, 170(8), pp. 193–203.
- Nocco B., Stulz R. (2006), Enterprise risk management: theory and practice, *Journal of Applied Corporate Finance*, 18, pp. 8–20. <https://doi.org/10.1111/i.1745-6622.2006.00106.x>
- Peljhan D., Marc M. (2021). Risk management and strategy alignment: influence on new product development performance, *Technology Analysis, Strategic Management*, 35(12), pp. 1547–1559, <https://doi.org/10.1080/09537325.2021.2011192>
- Posch A. (2020), A management-control perspective on risk management: the complementarity between risk-focused results controls and risk-focused information sharing, *Accounting, Organizations and Society*. <https://doi.org/10.2139/ssrn.2792169>.
- Puia G., Potts M. (2021). Risk in strategic management. *Oxford Research Encyclopedia of Business and Management*. Available at: <https://ssrn.com/abstract=4032672>
- Qazi A., Simsekler M. C. E. (2021). Quality assessment of enterprise risk management programs. *Journal of Risk Research*, 25(1), pp. 92–112. <https://doi.org/10.1080/13669877.2021.1913633>
- Rehacek P., Bazsova B. (2018), Risk management methods in projects, *Journal of Eastern Europe Research in Business and Economics*, Available at: <http://ibimapublishing.com/articles/JEERBE/2018/790198>

- Saeidi P., Saeidib S.P., Gutierrez L., Streimikiene D., Alrasheedihhttps M., Saeidi S.P., Mardanig A. (2021), The influence of enterprise risk management on firm performance with the moderating effect of intellectual capital dimensions, *Economic Research-Ekonomiska Istraživanja*, 34(1), pp. 122–151 <https://doi.org/10.1080/1331677X.2020.1776140>
- Shang K., Hossen Z. (2013), *Applying Fuzzy Logic to Risk Assessment and Decision-Making*, Available at: <https://www.soa.org/globalassets/assets/files/research/projects/research-2013-fuzzy-logic.pdf>
- Singh N.P., Hong P.C. (2020). Impact of strategic and operational risk management practices on firm performance: An empirical investigation. *European Management Journal*, 38(5), pp. 723–735, <https://doi.org/10.1016/j.emj.2020.03.003>
- Spikin I.C. (2013). Risk Management theory: the integrated perspective and its application in the public sector, *Estado, Gobierno Y Gestión Pública*, 11(21), pp. 89–126, <https://doi.org/10.5354/0717-8980.2013.29402>
- Tchangani A. (2022). Decision support system for complex systems risk assessment with bayesian networks. In: Kim Phuc Tran. *Machine Learning and Probabilistic Graphical Models for Decision Support Systems*, Francis & Taylor; CRC Press, Available at: <https://hal.science/hal-04109742>
- Vermeulen E.M., Spronk J., van der Wiist N. (1996). Analyzing risk and performance using the multi-factor concept, *European Journal of Operational Research*, 93(5), pp. 173–184, [https://doi.org/10.1016/0377-2217\(95\)00157-3](https://doi.org/10.1016/0377-2217(95)00157-3)
- Viscelli T.R., Hermanson D.R., Beasley M.S. (2017). The integration of ERM and strategy: implications for corporate governance, *Accounting Horizons*, 31(2), pp. 69–82, <https://doi.org/10.2308/acch-51692>
- Wehrspohn U. (2023), *Early Warning Indicators for Problematic Expert Assessments*, <http://dx.doi.org/10.2139/ssrn.4583955>

Cite:

UFJ Style

Skopenko N., Fedulova I., Mostenska T., Severyna I., Kapinus L. (2024), Risk assessment in target market selection by bread baking enterprises, *Ukrainian Food Journal*, 13(2), pp. 385–405, <https://doi.org/10.24263/2304-974X-2024-13-2-13>

APA Style

Skopenko, N., Fedulova, I., Mostenska, T., Severyna, I., & Kapinus L. (2024). Risk assessment in target market selection by bread baking enterprises. *Ukrainian Food Journal*, 13(2), 385–405. <https://doi.org/10.24263/2304-974X-2024-13-2-13>

Instructions for authors



Dear colleagues!

The Editorial Board of scientific periodical
“Ukrainian Food Journal”
invites you for publication of your research results.

A manuscript should describe the research work that has not been published before and is not under consideration for publication anywhere else. Submission of the manuscript implies that its publication has been approved by all co-authors as well as by the responsible authorities at the institute where the work has been carried out.

It is mandatory to include a covering letter to the editor which includes short information about the subject of the research, its novelty and significance; state that all the authors agree to submit this paper to Ukrainian Food Journal; that it is the original work of the authors.

Manuscript requirements

Authors must prepare the manuscript according to the guide for authors. Editors reserve the right to adjust the style to certain standards of uniformity.

Language – English

Manuscripts should be submitted in Word.

Use 1.0 spacing and 2 cm margins.

Use a normal font 14-point Times New Roman for text, tables, and signs on figures, 1.0 line intervals.

Present tables and figures in the text of manuscript.

Consult a recent issue of the journal for a style check.

Number all pages consecutively.

Abbreviations should be defined on first appearance in text and used consistently thereafter. No abbreviation should be used in title and section headings.

Please submit math equations as editable text and not as images (It is recommend software application MathType or Microsoft Equation Editor)

Minimal size of the article (without the Abstract and References) is 10 pages. For review article is 25 pages (without the Abstract and References).

Manuscript should include:

Title (should be concise and informative). Avoid abbreviations in it.

Authors' information: the name(s) of the author(s); the affiliation(s) of the author(s), city, country. One author has been designated as the corresponding author with e-mail address. If available, the 16-digit ORCID of the author(s).

Declaration of interest

Author contributions

Abstract. The **abstract** should contain the following mandatory parts:

Introduction provides a rationale for the study (2–3 lines).

Materials and methods briefly describe the materials and methods used in the study (3–5 lines).

Results and discussion describe the main findings (20–26 lines).

Conclusion provides the main conclusions (2–3 lines).

The abstract should not contain any undefined abbreviations or references to the articles.

Keywords. Immediately after the abstract provide 4 to 6 keywords.

Text of manuscript

References

Manuscripts should be divided into the following sections:

- **Introduction**
- **Materials and methods**
- **Results and discussion**
- **Conclusions**
- **References**

Introduction. Provide a background avoiding a detailed review of literature and declare the aim of the present research. Identify unexplored questions, prove the relevance of the topic. This should be not more than 1.5 pages.

Materials and methods. Describe sufficient details to allow an independent researcher to repeat the work. Indicate the reference for methods that are already published and just summarize them. Only new techniques need be described. Give description to modifications of existing methods.

Results and discussion. Results should be presented clearly and concisely with tables and/or figures, and the significance of the findings should be discussed with comparison with existing in literature data.

Conclusions. The main conclusions should be drawn from results and be presented in a short Conclusions section.

Acknowledgments(if necessary). Acknowledgments of people, grants, or funds should be placed in a separate section. List here those persons who provided help during the research. The names of funding organizations should be written in full.

Divide your article into sections and into subsections if necessary. Any subsection should have a brief heading.

References

Please, check references carefully.

The list of references should include works that are cited in the text and that have been published or accepted for publication.

All references mentioned in the reference list are cited in the text, and vice versa.

Cite references in the text by name and year in parentheses. Some examples:

(Drobot, 2008); (Qi and Zhou, 2012); (Bolarinwa et al., 2019; Rabie et al., 2020; Sengev et al., 2013).

Reference list should be alphabetized by the last name of the first author of each work. If available, please always include DOI links in the reference list.

Reference style

Journal article

Please follow this style and order: author's surname, initial(s), year of publication (in brackets), paper title, *journal title (in italic)*, volume number (issue), first and last page numbers, DOI. e.g.:

Popovici C., Gitin L., Alexe P. (2013), Characterization of walnut (*Juglans regia* L.) green husk extract obtained by supercritical carbon dioxide fluid extraction, *Journal of Food and Packaging Science, Technique and Technologies*, 2(2), pp. 104-108, <https://doi.org/11.1016/22-33-85>

Journal names should not be abbreviated.

Book

Deegan C. (2000), *Financial Accounting Theory*, McGraw-Hill Book Company, Sydney.

Book chapter in an edited book

Fordyce F.M. (2013), Selenium deficiency and toxicity in the environment. In: O. Selinus (Ed.), *Essentials of Medical Geology*, Springer, pp. 375–416, https://doi.org/10.14453/10.1007/978-94-007-4375-5_16

Online document

Mendeley J.A., Thomson, M., Coyne R.P. (2017), *How and When to Reference*, Available at: <https://www.howandwhentoreference.com>

Conference paper

Arych M. (2018), Insurance's impact on food safety and food security, *Resource and Energy Saving Technologies of Production and Packing of Food Products as the Main Fundamentals of Their Competitiveness: Proceedings of the 7th International Specialized Scientific and Practical Conference, September 13, 2018*, NUFT, Kyiv, pp. 52–57, <https://doi.org/11.1016/22-33-85>

Figures

All figures should be made in graphic editor using a font Arial.

The font size on the figures and the text of the article should be the same.

Black and white graphic with no shading should be used.

The figure elements (lines, grid, and text) should be presented in black (not gray) colour.

Figure parts should be denoted by lowercase letters (a, b, etc.).

All figures are to be numbered using Arabic numerals.

Figures should be cited in text in consecutive numerical order.

Place figure after its first mentioned in the text.

Figure captions begin with the term **Figure** in bold type, followed by the figure number, also in bold type.

Each figure should have a caption describing what the figure depicts in bold type.

Supply all figures and EXCEL format files with graphs additionally as separate files.

Photos are not advisable to be used.

If you include figures that have already been published elsewhere, you must obtain permission from the copyright owner(s).

Tables

Number tables consecutively in accordance with their appearance in the text.

Place footnotes to tables below the table body and indicate them with superscript lowercase letters.

Place table after its first mentioned in the text.

Ensure that the data presented in tables do not duplicate results described elsewhere in the article.

Suggesting / excluding reviewers

Authors are welcome to suggest reviewers and/or request the exclusion of certain individuals when they submit their manuscripts.

When suggesting reviewers, authors should make sure they are totally independent and not connected to the work in any way. When suggesting reviewers, the Corresponding Author must provide an institutional email address for each suggested reviewer. Please note that the Journal may not use the suggestions, but suggestions are appreciated and may help facilitate the peer review process.

Submission

Email for all submissions and other inquiries:

ufj_nuft@meta.ua

Шановні колеги!

Редакційна колегія наукового періодичного видання «**Ukrainian Food Journal**» запрошує Вас до публікації результатів наукових досліджень.

Вимоги до оформлення статей

Мова статей – англійська.

Мінімальний обсяг статті – **10 сторінок** формату А4 (без врахування анотацій і списку літератури).

Для всіх елементів статті шрифт – **Times New Roman**, кегль – **14**, інтервал – 1.

Всі поля сторінки – по 2 см.

Структура статті:

1. УДК.
2. **Назва статті.**
3. Автори статті (ім'я та прізвище повністю, приклад: Денис Озеряно).
4. *Установа, в якій виконана робота.*
5. Анотація. **Обов'язкова** структура анотації:
 - Вступ (2–3 рядки).
 - Матеріали та методи (до 5 рядків)
 - Результати та обговорення (пів сторінки).
 - Висновки (2–3 рядки).
6. Ключові слова (3–5 слів, але не словосполучень).

Пункти 2–6 виконати англійською і українською мовами.

7. Основний текст статті. Має включати такі обов'язкові розділи:
 - Вступ
 - Матеріали та методи
 - Результати та обговорення
 - Висновки
 - Література.

За необхідності можна додавати інші розділи та розбивати їх на підрозділи.

8. Авторська довідка (Прізвище, ім'я та по батькові, вчений ступінь та звання, місце роботи, електронна адреса або телефон).
9. Контактні дані автора, до якого за необхідності буде звертатись редакція журналу.

Рисунки виконуються якісно. Скановані рисунки не приймаються. Розмір тексту на рисунках повинен бути **співрозмірним (!)** тексту статті. **Фотографії можна використовувати лише за їх значної наукової цінності.**

Фон графіків, діаграм – лише білий. Колір елементів рисунку (лінії, сітка, текст) – чорний (не сірий).

Рисунки та графіки EXCEL з графіками додатково подаються в окремих файлах.

Скорочені назви фізичних величин в тексті та на графіках позначаються латинськими літерами відповідно до системи СІ.

У списку літератури повинні переважати англомовні статті та монографії, які опубліковані після 2010 року.

Оформлення цитат у тексті статті:

Кількість авторів статті	Приклад цитування у тексті
1 автор	(Arych, 2019)
2 автора	(Kuievda and Bront, 2020)
3 і більше авторів	(Bazopol et al., 2022)

Приклад тексту із цитуванням: It is known (Arych, 2019; Bazopol et al., 2022), the product yield depends on temperature, but, there are some exceptions (Kuievda and Bront, 2020).

У цитуваннях необхідно вказувати одне джерело, звідки взято інформацію.

Список літератури сортується за алфавітом, літературні джерела не нумеруються.

Правила оформлення списку літератури

В Ukrainian Food Journal взято за основу загальноприйняте в світі спрощене оформлення списку літератури згідно стандарту Garvard. Всі елементи посилання розділяються **лише комами**.

1. Посилання на статтю:

Автори А.А. (рік видання), Назва статті, Назва журналу (курсивом), Том (номер), сторінки, DOI.

Ініціали пишуться після прізвища.

Всі елементи посилання розділяються комами.

Приклад:

Popovici C., Gitin L., Alexe P. (2013), Characterization of walnut (*Juglans regia* L.) green husk extract obtained by supercritical carbon dioxide fluid extraction, *Journal of Food and Packaging Science, Technique and Technologies*, 2(2), pp. 104–108, <https://doi.org/5533.935-3>.

2. Посилання на книгу:

Автори (рік), Назва книги (курсивом), Видавництво, Місто.

Ініціали пишуться після прізвища.

Всі елементи посилання розділяються комами.

Приклад:

Deegan C. (2000), *Financial Accounting Theory*, McGraw-Hill Book Company, Sydney.

3. Посилання на розділ у редактованій книзі:

Автори (рік), Назва глави, In: Редактори, Назва книги (курсивом), Видавництво, Місто, сторінки.

Приклад:

Fordyce F.M. (2013), Selenium deficiency and toxicity in the environment. In: O. Selinus (Ed.), *Essentials of Medical Geology*, Springer, pp. 375–416, https://doi.org/10.14453/10.1007/978-94-007-4375-5_16

4. Тези доповідей конференції:

Arych M. (2018), Insurance's impact on food safety and food security, *Resource and Energy Saving Technologies of Production and Packing of Food Products as the Main Fundamentals of Their Competitiveness: Proceedings of the 7th International Specialized Scientific and Practical Conference, September 13, 2018*, NUFT, Kyiv, pp. 52–57, <https://doi.org/5533.935-3>.

5. Посилання на електронний ресурс:

Виконується аналогічно посиланню на книгу або статтю. Після оформлення даних про публікацію пишуться слова **Available at:** та вказується електронна адреса.

Приклад:

Cheung T. (2011), *World's 50 most delicious drinks*, Available at: <http://travel.cnn.com/explorations/drink/worlds-50-most-delicious-drinks-883542>

Список літератури оформлюється лише латиницею. Елементи списку українською та російською мовою потрібно транслітерувати. Для транслітерації з українською мови використовується паспортний стандарт.

Зручний сайт для транслітерації з української мови: <http://translit.kh.ua/#lat/passport>

Стаття надсилається за електронною адресою:

ufj_nuft@meta.ua

Ukrainian Food Journal публікує оригінальні наукові статті, короткі повідомлення, оглядові статті, новини та огляди літератури.

Тематика публікацій в **Ukrainian Food Journal**:

Харчова інженерія	Процеси та обладнання
Харчова хімія	Нанотехнології
Мікробіологія	Економіка та управління
Фізичні властивості харчових продуктів	Автоматизація процесів
Якість та безпека харчових продуктів	Упаковка для харчових продуктів

Періодичність виходу журналу 4 номери на рік.

Результати досліджень, представлені в журналі, повинні бути новими, мати чіткий зв'язок з харчовою наукою і представляти інтерес для міжнародного наукового співтовариства.

Ukrainian Food Journal індексується наукометричними базами:

- Index Copernicus (2012)
- EBSCO (2013)
- Google Scholar (2013)
- UlrichsWeb (2013)
- CABI full text (2014)
- Online Library of University of Southern Denmark (2014)
- Directory of Open Access scholarly Resources (ROAD) (2014)
- European Reference Index for the Humanities and the Social Sciences (ERIH PLUS) (2014)
- Directory of Open Access Journals (DOAJ) (2015)
- InfoBase Index (2015)
- Chemical Abstracts Service Source Index (CASSI) (2016)
- FSTA (Food Science and Technology Abstracts) (2018)
- Web of Science (Emerging Sources Citation Index) (2018)
- Scopus (2022)

Рецензія рукопису статті. Матеріали, представлені для публікування в «Ukrainian Food Journal», проходять «Подвійне сліпе рецензування» двома вченими, призначеними редакційною колегією: один є членом редколегії і один незалежний учений.

Авторське право. Автори статей гарантують, що робота не є порушенням будь-яких авторських прав, та відшкодовують видавцю порушення даної гарантії. Опубліковані матеріали є правовою власністю видавця «Ukrainian Food Journal», якщо не узгоджено інше.

Детальна інформація про Журнал, інструкції авторам, приклади оформлення статті та анотацій розміщені на сайті:

<http://ufj.nuft.edu.ua>

Редакційна колегія

Головний редактор:

Олена Стабнікова, д-р., *Національний університет харчових технологій, Україна*

Члени міжнародної редакційної колегії:

Агота Гедре Райшене, д-р., *Литовський інститут аграрної економіки, Литва*
В. І. Вернадського НАН України

Бао Тхи Вуронг, д-р., *Університет Меконгу, В'єтнам*

Віктор Стабніков, д.т.н., проф., *Національний університет харчових технологій, Україна*

Годвін Д. Ндоссі, професор, *Меморіальний університет Хуберта Кайрукі, Дар-ес-Салам, Танзанія*

Дора Марінова, професор, *Університет Кертіна, Австралія*

Егон Шніцлер, д-р, професор, *Державний університет Понта Гросси, Бразилія*

Ейрін Марі Скійондал Бар, д-р., професор, *Норвезький університет науки і техніки, Тронхейм, Норвегія*

Йорданка Стефанова, д-р, *Пловдивський університет "Паїсій Хілендарскі", Болгарія*

Кірстен Брандт, професор, *Університет Ньюкасла, Великобританія*

Крістіна Луїза Міранда Сілва, д-р., професор, *Португальський католицький університет – Біотехнологічний коледж, Португалія*

Крістіна Попович, д-р., доцент, *Технічний університет Молдови*

Лелівельд Хуб, асоціація «Міжнародна гармонізаційна ініціатива», *Нідерланди*

Марія С. Тапіа, професор, *Центральний університет Венесуели, Каракас, Венесуела*

Мойзес Бурачик, д-р., *Інститут сільськогосподарської біотехнології Покапіо (INDEAR), Покапіо, Аргентина*

Марк Шамцян, д-р., доцент, *Чорноморська асоціація з харчової науки та технології, Румунія*

Нур Зафіра Нур Хаснан, доктор філософії, *Університет Путра Малайзії, Селангор, Малайзія*

Октавіо Паредес Лопес, д-р., проф., *Центр перспективних досліджень Національного політехнічного інституту, Мексика*

Олександр Шевченко, д.т.н., проф., *Національний університет харчових технологій, Україна*

Рана Мустафа, д-р., *Глобальний інститут продовольчої безпеки, Університет Саскачевана, Канада*

Семіх Отлес, д-р., проф., *Університет Еге, Туреччина*

Соня Амарей, д-р., проф., *Університет «Штефан чел Маре», Сучава, Румунія*

Станка Дам'янова, д.т.н., проф., *Русенський університет «Ангел Канчев», філія Разград, Болгарія*

Стефан Стефанов, д.т.н., проф., *Університет харчових технологій, Болгарія*

Тетяна Пирог, д.б.н., проф., *Національний університет харчових технологій, Україна*

Умезуруйке Лінус Опара, професор, *Стелленбошський університет, Кейптаун, Південна Африка*

Шейла Кілонзі, *Університет Каратіна, Кенія*
Юлія Дзязько, д-р. хім. наук, с.н.с., *Інститут загальної та неорганічної хімії імені Юн-Хва Пеггі Хсі*, д-р, професор, *Університет Флориди, США*
Юрій Білан, д-р., проф., *Університет Томаша Баті в Зліні, Чехія*
Ясмiна Лукiнак, д.т.н., професор, *Університет Осієка, Хорватія*
Ясмiна Лукiнак, д-р, проф., *Осієкський університет, Хорватія.*

Члени редакційної колегії:

Агота Гедре Райшене, д-р., *Литовський інститут аграрної економіки, Литва*
Бао Тхи Вуронг, д-р., *Університет Меконгу, В'єтнам*
Валерій Мирончук, д-р. техн. наук, проф., *Національний університет харчових технологій, Україна*
Віктор Стабніков, д.т.н., проф., *Національний університет харчових технологій, Україна*
Володимир Ковбаса, д-р. техн. наук, проф., *Національний університет харчових технологій, Україна*
Галина Сімахіна, д-р. техн. наук, проф., *Національний університет харчових технологій, Україна*
Годвін Д. Ндоссі, професор, *Меморіальний університет Хуберта Кайрукі, Дар-ес-Салам, Танзанія*
Дора Марінова, професор, *Університет Кертіна, Австралія*
Егон Шніцлер, д-р, професор, *Державний університет Понта Гросси, Бразилія*
Ейрін Марі Скійондал Бар, д-р., професор, *Норвезький університет науки і техніки, Тронхейм, Норвегія*
Йорданка Стефанова, д-р, *Пловдивський університет "Паїсій Хілендарскі", Болгарія*
Кірстен Брандт, професор, *Університет Ньюкасла, Великобританія*
Крістіна Луїза Міранда Сілва, д-р., професор, *Португальський католицький університет – Біотехнологічний коледж, Португалія*
Крістіна Попович, д-р., доцент, *Технічний університет Молдови*
Лада Шерінян, д-р. екон. наук, професор., *Національний університет харчових технологій, Україна*
Лелівельд Хуб, асоціація «Міжнародна гармонізаційна ініціатива», *Нідерланди*
Марія С. Тапіа, професор, *Центральний університет Венесуели, Каракас, Венесуела*
Мойзес Бурачик, д-р., *Інститут сільськогосподарської біотехнології Покапіо (INDEAR), Покапіо, Аргентина*
Марк Шамцяня, д-р., доцент, *Чорноморська асоціація з харчової науки та технології, Румунія*
Нур Зафіра Нур Хаснан, доктор філософії, *Університет Путра Малайзії, Селангор, Малайзія*
Октавіо Паредес Лопес, д-р., проф, *Центр перспективних досліджень Національного політехнічного інституту, Мексика.*
Олександр Шевченко, д.т.н., проф., *Національний університет харчових технологій, Україна*
Ольга Рибак, канд. техн. наук, доц., *Тернопільський національний технічний університет імені Івана Пулюя, Україна*
Рана Мустафа, д-р., *Глобальний інститут продовольчої безпеки, Університет Саскачевана, Канада*
Семіх Отлес, д-р., проф, *Університет Еге, Туреччина*

Соня Амарей, д-р., проф., *Університет «Штефан чел Маре», Сучава, Румунія*
Станка Дам'янова, д.т.н., проф., *Русенський університет «Ангел Канчев», філія Разград, Болгарія*
Стефан Стефанов, д.т.н., проф., *Університет харчових технологій, Болгарія*
Тетяна Пирог, д-р. біол. наук, проф., *Національний університет харчових технологій, Україна*
Умезуруйке Лінус Опара, професор, *Стелленбошський університет, Кейптаун, Південна Африка*
Шейла Кілонзі, *Університет Каратіна, Кенія*
Юлія Дзязько, д-р. хім. наук, с.н.с., *Інститут загальної та неорганічної хімії імені В. І. Вернадського НАН України*
Юн-Хва Пеггі Хсі, д-р, професор, *Університет Флориди, США*
Ясмiна Лукiнак, д-р, проф., *Осікський університет, Хорватія.*

Олексій Губеня (відповідальний секретар), канд. техн. наук, доц., *Національний університет харчових технологій, Україна.*

Наукове видання

Ukrainian Food Journal

**Volume 13, Issue 2
2024**

**Том 13, № 2
2024**

Підп. до друку 30.08.2024 р. Формат 70x100/16.
Обл.-вид. арк. 13.42. Ум. друк. арк. 13.54.
Гарнітура Times New Roman. Друк офсетний.
Наклад 100 прим. Вид. № 21н/24.

НУХТ. 01601 Київ–33, вул. Володимирська, 68

Свідоцтво про державну реєстрацію
друкованого засобу масової інформації
КВ 18964–7754Р
видане 26 березня 2012 року.